AD_____

Award Number: DAMD17-03-1-0343

TITLE: Breast Cancer Gene Therapy: Development of Novel Non-Invasive Magnetic Resonance Assay to Optimize Efficacy

PRINCIPAL INVESTIGATOR: Ralph P. Mason, Ph.D.

CONTRACTING ORGANIZATION: University of Texas Southwestern Medical Center
Dallas, TX 75390-9105

REPORT DATE: May 2005

TYPE OF REPORT: Annual

PREPARED FOR: U.S. Army Medical Research and Materiel Command
Fort Detrick, Maryland 21702-5012

REPORT DOCUMENTATION PAGE

Form Approved
OMB No. 074-0188

1. AGENCY USE ONLY (Leave blank)	2. REPORT DATE	3. REPORT TYPE AND DATES COVERED
	May 2005	Annual (1 May 2004 - 30 Apr 2005)

4. TITLE AND SUBTITLE
Breast Cancer Gene Therapy: Development of Novel Non-Invasive Magnetic Resonance Assay to Optimize Efficacy

5. FUNDING NUMBERS
DAMD17-03-1-0343

6. AUTHOR(S)
Ralph P. Mason, Ph.D.

7. PERFORMING ORGANIZATION NAME(S) AND ADDRESS(ES)
University of Texas Southwestern Medical Center
Dallas, TX 75390-9105

E-Mail: Ralph.mason@UTSouthwestern.edu

8. PERFORMING ORGANIZATION REPORT NUMBER

9. SPONSORING / MONITORING AGENCY NAME(S) AND ADDRESS(ES)
U.S. Army Medical Research and Materiel Command
Fort Detrick, Maryland 21702-5012

10. SPONSORING / MONITORING AGENCY REPORT NUMBER

11. SUPPLEMENTARY NOTES

12a. DISTRIBUTION / AVAILABILITY STATEMENT
Approved for Public Release; Distribution Unlimited

12b. DISTRIBUTION CODE

13. ABSTRACT (Maximum 200 Words)

Gene therapy holds great promise for treatment of breast cancer. In particular, clinical trials are underway to apply therapeutic genes related to pro-drug activation or to modulate the activity of oncogenes by blocking promoter sites. However, there are major problems in terms of assessing the delivery to target tissue, assessing the uniformity (versus heterogeneity) of biodistribution and determining whether the genes are expressed.

We propose to design, evaluate and apply a novel approach to gene activity detection- specifically, using fluorinated substrates of β-galactosidase to reveal gene activity. Our prototype molecule PFONPG (para- fluoro- ortho- nitro- phenyl β-D-galactopyranoside) is a direct analog of the traditional "yellow' biochemical indicator ONPG (ortho- nitro- phenyl β-D-galactopyranoside). This shows useful MR characteristics, sensitivity to enzyme activity and ability to enter cells. We will synthesize analogs of this prototype to optimize MR and biological characteristics and explore the feasibility of tailoring the reporter to specific applications, *e.g.*, exploiting β-gal activity to deliver specific physiological reporter molecules such as pH and potentially specific cytotoxic agents. The agents will be rigorously tested in solution, applied to cultured breast cancer cells and ultimately used to examine β-gal activity *in vivo* in transfected breast tumors in mice and rats.

14. SUBJECT TERMS
Gene therapy, fluorine NMR, β-galactosidase, pH

15. NUMBER OF PAGES
127

16. PRICE CODE

17. SECURITY CLASSIFICATION OF REPORT	18. SECURITY CLASSIFICATION OF THIS PAGE	19. SECURITY CLASSIFICATION OF ABSTRACT	20. LIMITATION OF ABSTRACT
Unclassified	Unclassified	Unclassified	Unlimited

Table of Contents

Introduction

Gene therapy holds great promise for treatment of breast cancer (1, 2). In particular, clinical trials are underway to apply therapeutic genes related to pro-drug activation or modulation of the activity of oncogenes by blocking promoter sites. However, there are major problems in terms of assessing the delivery to target tissue, assessing the uniformity (versus heterogeneity) of biodistribution and determining whether the genes are expressed. We propose to design, evaluate and apply a novel approach to gene activity detection- specifically, using fluorinated substrates of β-galactosidase to reveal gene activity. Our prototype molecule PFONPG (para- fluoro- ortho- nitro- phenyl β-D-galactopyranoside) is a direct analog of the traditional "yellow' biochemical indicator ONPG (ortho- nitro- phenyl β-D-galactopyranoside). This shows useful MR characteristics, sensitivity to enzyme activity and ability to enter cells. We will synthesize analogs of this prototype to optimize MR and biological characteristics and explore the feasibility of tailoring the reporter to specific applications, *e.g.*, exploiting β-gal activity to deliver specific physiological reporter molecules such as pH and potentially specific cytotoxic agents. The agents will be rigorously tested in solution, applied to cultured breast cancer cells and ultimately used to examine β-gal activity *in vivo* in transfected breast tumors in mice and rats.

Statement of Work

Year 1

Task 1 Synthesize novel molecules to report activity of the β-galactosidase gene- minimum 8 novel agents (**Completed in Year 1**)

Task 2 Characterize novel agents (NMR, mass spec, colorimetric analysis) (**Completed in Year 1**)

Task 3 Test agents for enzyme activity in solution (**Completed in Year 1**)

Task 4 Test initial indicators in cultured breast cancer cells (control + transfected) (Months 6-12) (**Completed in Year 2**)

Year 2

Task 5 Scale up synthesis of most promising indicator for animal investigations (Months 13-15) (**Completed in Year 2**)

Task 6 Evaluate in mice (constitutively expressing β-gal ROSA animals); test dosing protocols, timing, MR detection protocols- (20 mice) (Months 13-18) (**Ongoing**)

Task 7 Evaluate in rodents with stably transfected tumors and compare with traditional assays- (20 mice + 20 rats) (Months 15-24) (**Ongoing**)

Task 8 Synthesize second generation "smart" β-gal substrates as reporters of physical parameters such as pH or as cytotoxic agents (Months 15-24) (**Ongoing**)

Year 3

Task 9 Apply optimal β-gal reporters to assess transfection efficiency, gene expression (spatial and temporal) in tumors *in vivo* (20 mice + 20 rats) (Months 25-34) (**Ongoing**)

Task 10 Evaluate "smart agents" *in vitro* (Months 25-34) (**Ongoing**)

Task 11 Evaluate "smart agents" *in vivo* (Months 25-34) (**Year 3**)

Task 12 Prepare manuscripts and final report (Months 34-36) (**Year 3**)

Progress

While we have not completed all tasks proposed for year 2, we have already initiated some tasks set for year 3, and we believe our progress is on schedule.

Task 4 Completed during Year 2.

We had expected to be able to acquire β-gal expressing breast tumor cells readily from tissue banks or colleagues, but they were found to exhibit very low expression. Thus, in year 1 we were forced to undertake tests in PC3, LNCaP, Mat-Lu, and 9L glioma cells expressing β-gal. Establishing high expressing lacZ (β-gal) breast cancer cell lines became a high priority and Dr. Liu has now established several tumors in our laboratory (*e.g.*, MTLn3-lacZ, MCF7-LacZ). Results using these cells have been presented at several conferences, have been included in papers published in Bioconjugate Chemistry (appendix item 1), Medicinal Chemistry (appendix item 2) and form the basis for two submitted manuscripts (appendix items 4 and 5).

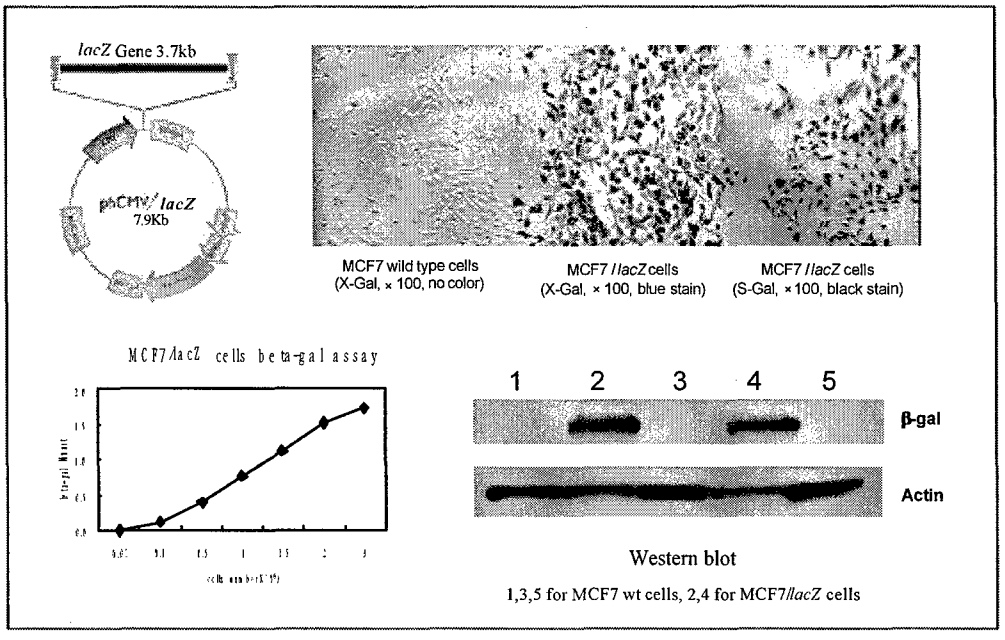

Figure 1. Stable expression of β-gal MCF7 cell lines. The phCMV/*lacZ* plasmid map is top left, MCF7/*lacZ* cells were stained by X-Gal (blue) and S-Gal (black), MCF7 wild type cell did not stain (no color). More than 90% MCF7/*lacZ* cells were stained after passage 30 generations. *lacZ* gene expression in stably MCF7/*lacZ* cells were confirmed by β-gal assay and western blot. The definition of β-gal unit is that one unit will hydrolyze 1.0 μmol of o-nitrophenyl β-D-galactoside (OFPNPG) to o-nitrophenol and D galactose per min.

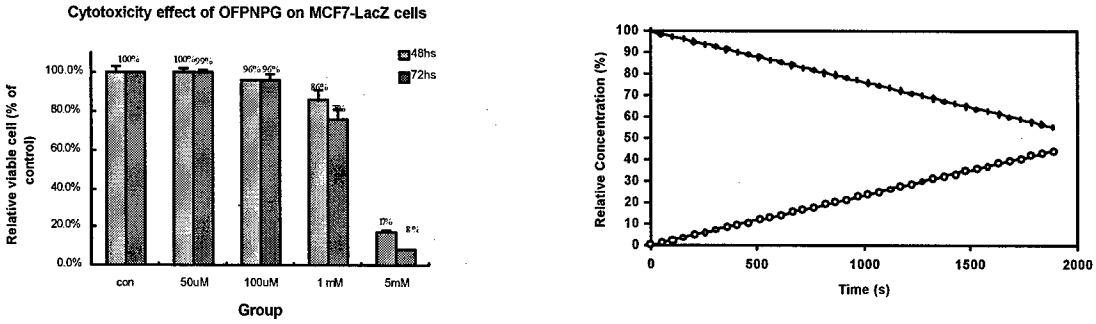

Figure 2. left: **Cytotoxicity of OFPNPG** to MCF-7-*lacZ* breast cancer cells in culture. Right: Hydrolysis of 2-Nitro-4-trifluoromethylphenyl β-D-galactopyranoside (5.0 mmol) by stably transfected MCF-7-*lacZ* breast cancer cells (1.75×10^6) in PBS buffer at 37 °C.

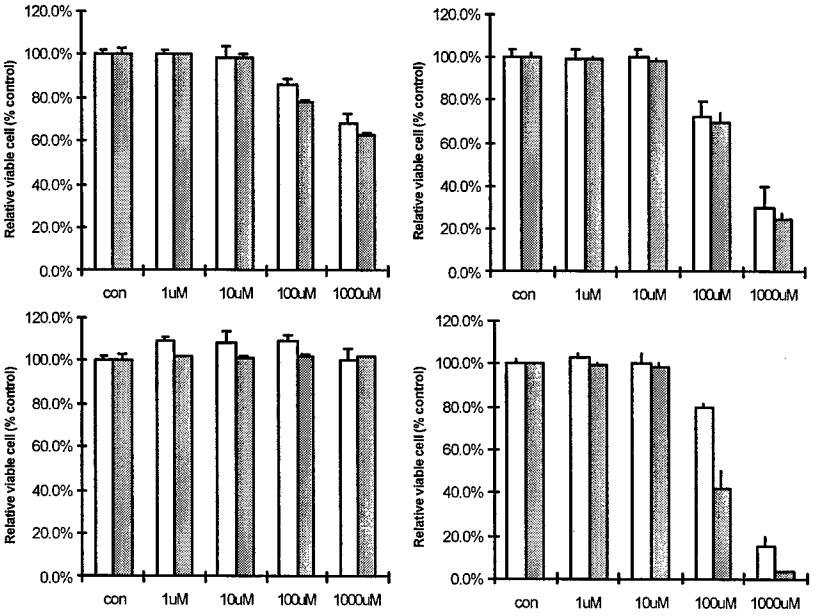

Figure 3. Viability of human breast cancer cells with respect to exposure to substrate 2-Nitro-4-trifluoromethyl phenyl β-D-galactopyranoside (left panels) or aglycone (2-Nitro-4-trifluoromethylphenol) (right panels). Upper panels MCF-7-lacZ cells; lower panels MCF-7-WT. Open bars 48 h exposure; hatched bars 96 h exposure.

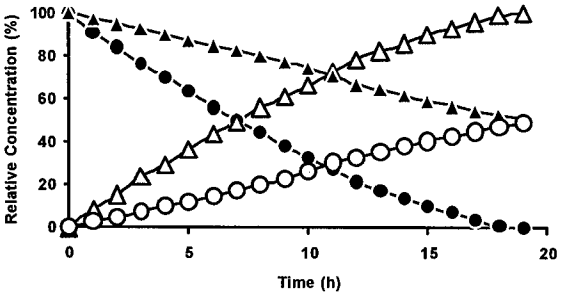

Figure 4 Hydrolysis of 2-fluoro-4-nitrophenyl-β-D-galactopyranoside (open symbols) to 2-fluoro-4-nitrophenol (solid symbols) by stably transfected MAT-Lu-*lacZ* cells (Δ 92×10^6) and rat breast tumor MTLn3-*lacZ* (O 9.8×10^6) in PBS at 37 °C.

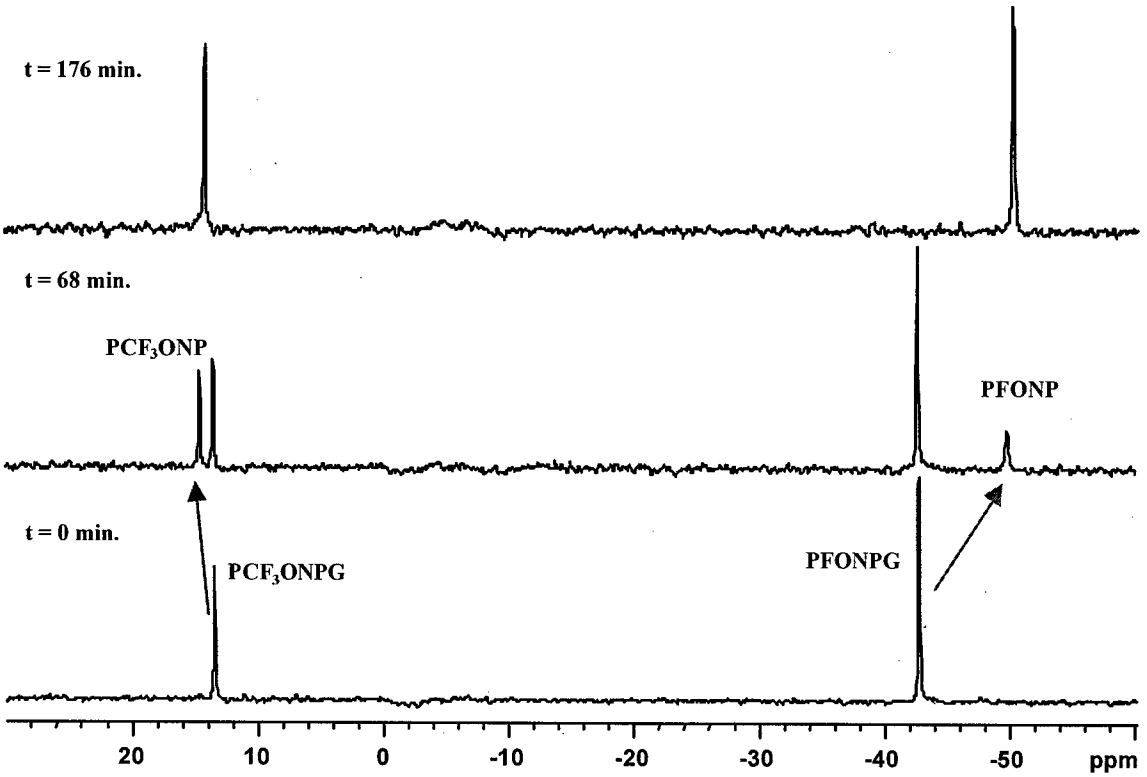

Figure 5. ^{19}F NMR spectra of PCF_3ONPG (1.4 mg, 4.5 mmol) and **PFONPG** (6.0 mg, 18.8 mmol) showing simultaneous hydrolysis by stably transfected MCF-7-*lacZ* cells (1.75×10^6) in PBS (0.1M, pH=7.4, 600μL) at 37 °C. Each spectrum acquired in 51 s.

Ideal NMR gene reporters will exhibit minimal toxicity. We have found some toxicity associated with the nitrophenol aglycones. This does set a foundation for gene activated broad spectrum chemotherapy. In figure 3, lower panel, we find that the toxicity of the aglycone is

masked in the conjugate substrate for wild type cells, but toxicity occurs in β-gal expressing cells. Thus, we are pursuing cytotoxic agents, while also establishing agents with minimal toxicity as part of Task 8.

Task 5 Synthesis of reporter molecules has been scaled up to provide materials for *in vivo* evaluation. In particular, Dr. Yu has developed novel synthetic strategies, which give higher yields and fewer synthetic steps, as described in appendix item 2. In a synthesis of **GFPOL** the overall yield for the original five-step route was ~3% (scheme 1). A revised strategy gave 68% overall yield (scheme 2) and direct galactopyranosylation using 2, 3, 4, 6-tetra-*O*-acetyl-α-D-galactopyranosyl bromide and phase-transfer catalysis gave (88%) (scheme 3).

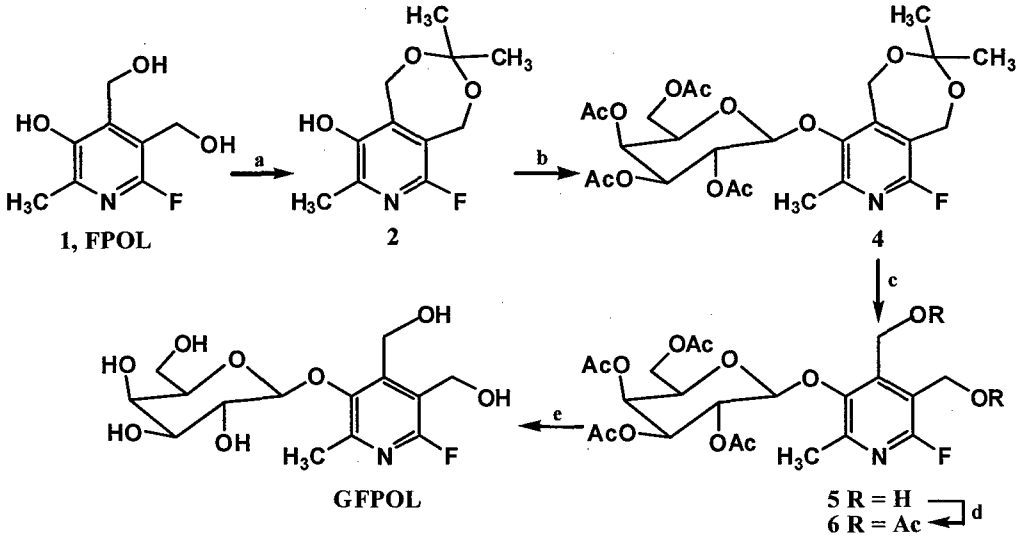

Scheme 1

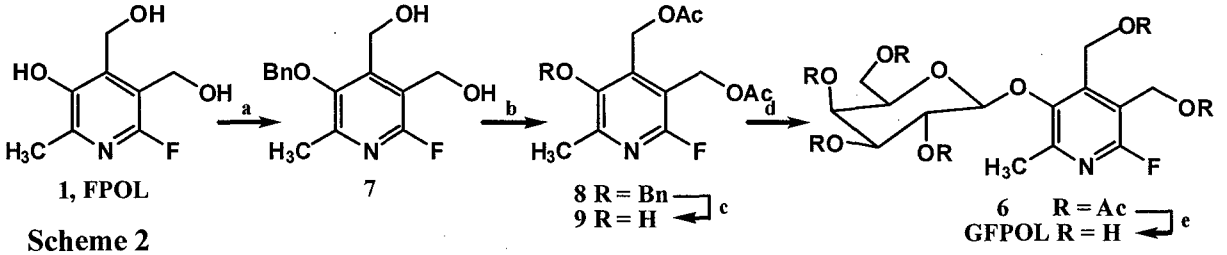

Scheme 2

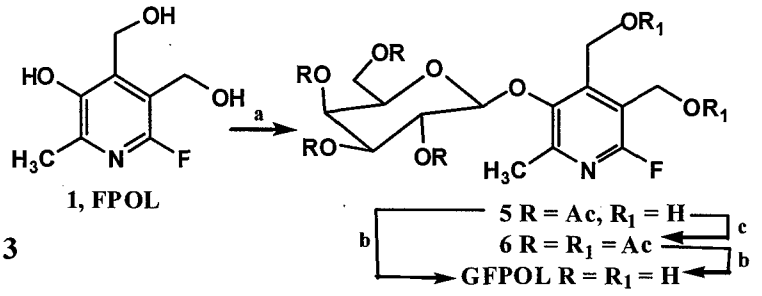

Scheme 3

Figure 6 Synthetic approaches to GFPOL

Task 6

Dr. Cui found that administration of PFONPG to ROSA mice caused rapid death. We believe this is due to release of toxic aglycone (nitrophenol) causing rapid depolarization of the heart. Indeed, perfusion of a heart with PFONP caused immediate cardiac arrest. However, we were able to show effective conversion of reporter molecules by tissues (heart, liver and muscle) excised from ROSA mice, but not wild type mice. We have temporarily suspended this Task, but will resume if less toxic reporter molecules are identified.

Dr. Kodibagkar has developed NMR methods to enhance detection of reporter molecules, particularly to allow chemical shift selective imaging to reveal substrate and product by imaging. In phantom studies the techniques are effective and they will be tested in tumors, as soon as sufficient signal to noise is observed.

Figure 7

Selective imaging of substrate and aglycone product. Two vials containing TFA and substrate or product as aqueous solutions.

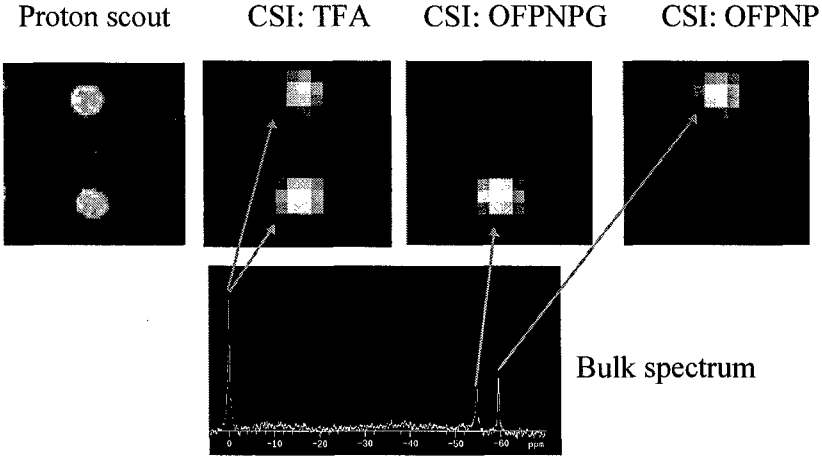

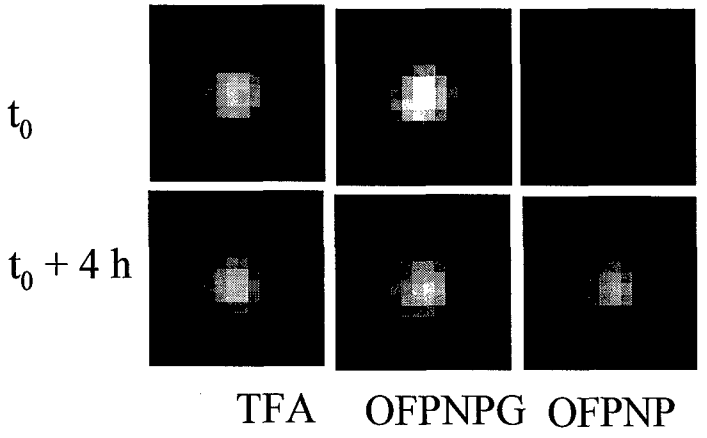

Figure 8 A vial containing OFPNPG was imaged at t_0. 10^7 lacZ transfected MCF7 cells were added to the vial and imaged. ^{19}F CSI detects the conversion of OFPNPG to OFPNP by the MCF7-LacZ cells.

Task 7

We have undertaken tests in mice with wild type or lacZ expressing tumors. Administration of reporter molecule IV is not ideal for initial agents, since many are poorly soluble in water and require addition of DMSO for effective solvation. While DMSO can be administered IV, we prefer IP. Following IP administration, we have detected substrate in tumors, though to date, no conversion of substrate to product has been detected. Direct injection of substrate into breast tumors has shown conversion over 30 mins using ^{19}F NMR spectroscopy.

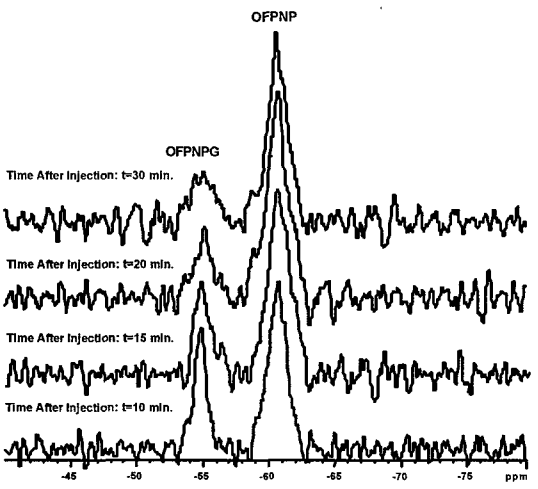

Figure 9. The ^{19}F MRS and the kinetic hydrolysis time courses of **OFPNPG** DMSO/PBS (V/V' 1:1) solution (0.24 M, 100 μL) injected intra-tumorally in MCF7-lacZ tumor bearing mouse, tumor size = 0.8×1.1×1.2 cm^3, at 4.7 T acquisition time 5 min. per spectrum.

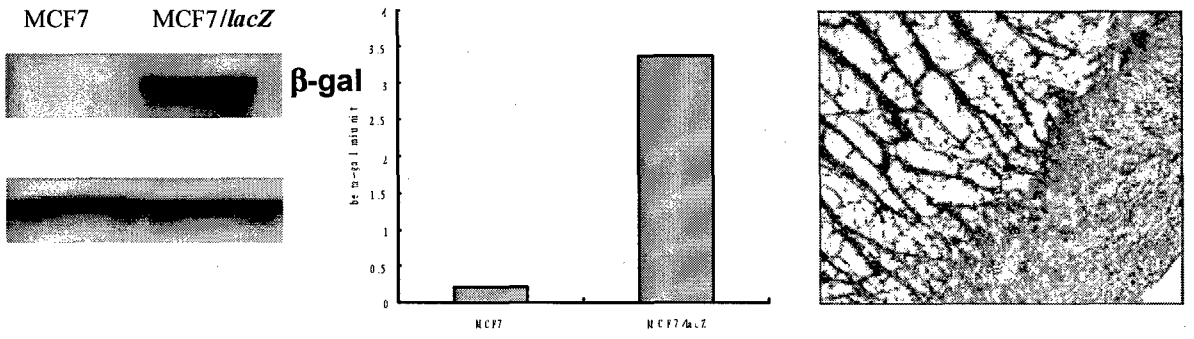

Figure 10 Verification of β-gal expression in tumors groping in mice using Western blot and enzyme activity analysis. Post mortem histology of MCF7/*lacZ* tumor showed intense stain in the tumor periphery with central tumor necrosis. Wild type tumors showed essentially no activity.

Task 8

Several "second" generation gene reporters have now been synthesized. GFPOL uses the fluorinated vitamin B6 as the aglycone to reduce toxicity of product. GDUFPOL and GDMFPOL each include additional sugar moieties to enhance water solubility. OFPNMG is designed to be highly toxic upon β-gal cleave releasing a nitrogen mustard.

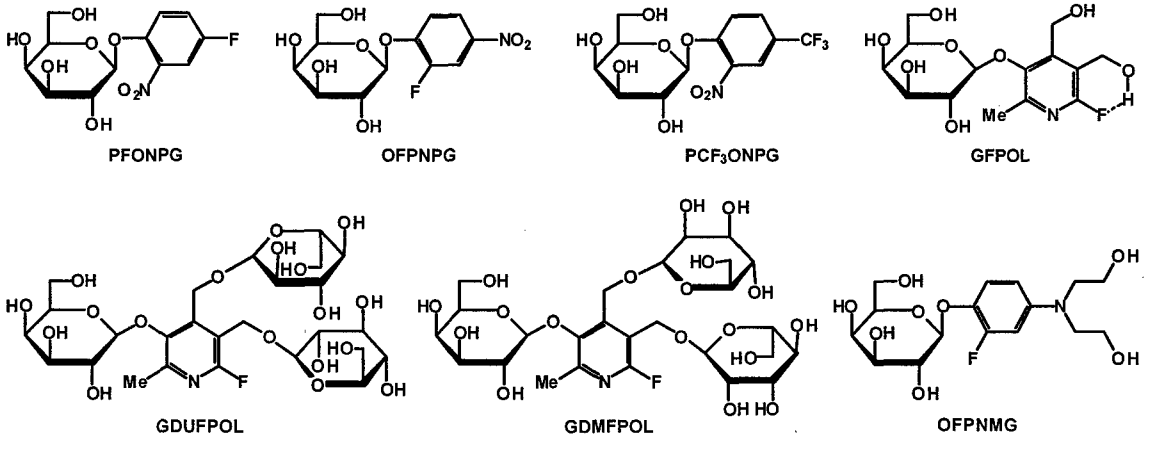

Figure 11 Second generation gene reporter molecules. Each has been successfully synthesized.

Task 9 Apply optimal β-gal reporters to assess transfection efficiency, gene expression (spatial and temporal) in tumors *in vivo* (20 mice + 20 rats) (Months 25-34)

Task 10 Evaluate "smart agents" *in vitro* (Months 25-34)

Aspects of Task 10 have been initiated ahead of schedule in year 2, and will continue.

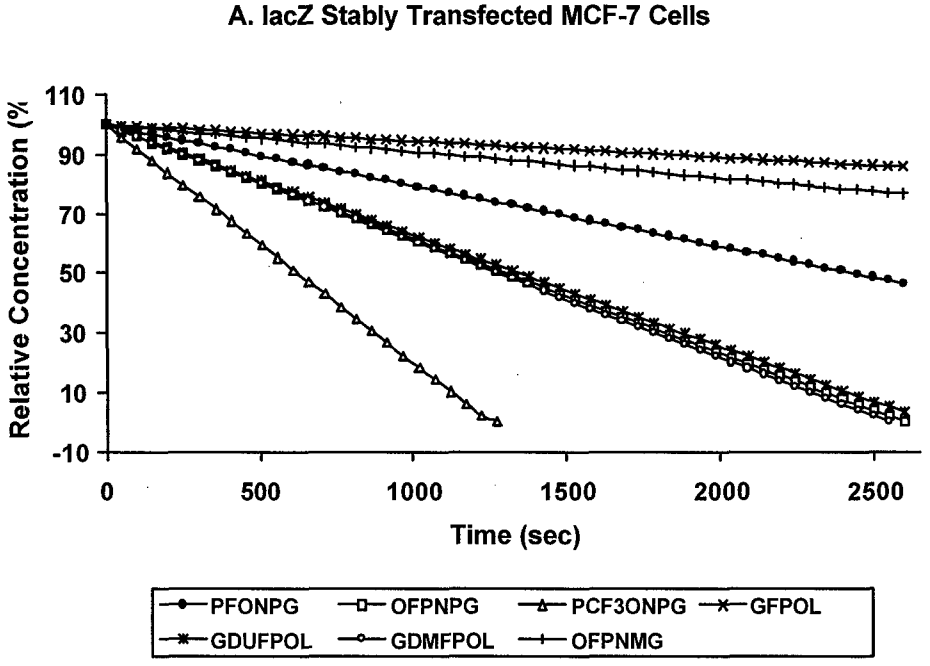

Figure 12. The relative cleavage rates of **PFONPG**, **OFPNPG**, **PCF_3ONPG**, **GFPOL**, **GDUFPOL**, **GDMFPOL** and **OFPNMG** (5.0 mmol) by MCF7-*lacZ* cells in culture.

KEY RESEARCH ACCOMPLISHMENTS:

- We have generated breast tumor cell lines stably expressing high activity of β-galactosidase. We have demonstrated ^{19}F NMR detection of β-gal activity in breast tumor cells *in vitro* and in tumors growing in mice. Meanwhile no activity was found in wild type cells and tumors.
- We have successfully synthesized a series of novel fluorine substituted phenylgalactosides as

potential ^{19}F NMR reporter molecules for β-galactosidase activity.

- The fluorophenyl β-D-galactopyranosides are stable in saline, but are rapidly cleaved by the enzyme β-galactosidase.
- The fluorophenyl β-D-galactopyranosides provide a single ^{19}F NMR signal, which is invariant with pH. Enzyme cleavage produces a new signal well removed from the parent compound.
- Preliminary data show that the fluorophenyl β-D-galactopyranosides enter breast tumor cells. In wild type cells, the substrate is stable, but in cells transfected to express β-gal. there is cleavage releasing aglycone product as revealed by chemically shifted signal.
- Incorporation of trifluoromethyl groups enhances NMR signal to noise, though there is a smaller chemical shift response to cleavage.
- Prototype "smart" β-gal substrates have been synthesized using the pH reporter molecule 6-fluoropyridoxol in place of fluorophenol aglycones.

REPORTABLE OUTCOMES:

Published manuscripts

Year 1- one manuscript

Year 2

1. "A Novel NMR Platform for Detecting Gene Transfection: Synthesis and Evaluation of Fluorinated Phenyl β-D-Galactosides with Potential Application for Assessing LacZ Gene Expression", J. Yu, P. Otten, Z. Ma, W. Cui, L. Liu, R. P. Mason, *Bioconjug. Chem*. 15 (6): 1334-1341 (2004)
2. "Synthesis and Evaluation of a Novel Gene Reporter Molecule: Detection of β-galactosidase

activity Using ^{19}F NMR of a Fluorinated Vitamin B_6 conjugate" J. Yu, Z. Ma, Y. Li, K. S. Koeneman, L. Liu, R. P. Mason, *Med. Chem.* 1(3) 255-262 (2005)

3. "^{19}F: a versatile reporter for non-invasive physiology and pharmacology using magnetic resonance", J. Yu, V. D. Kodibagkar, W. Cui, R. P. Mason, *Curr. Med. Chem.* 12 (7) 819-848 (2005) + cover figure and editorial

Conference presentations

Year 1- 3 presentations

Year 2

1. "Synthesis and Characterization of Novel Probes for *in vivo* Detection of LacZ Gene Expression", J. Yu, V. Kodibagkar, L. Liu, R. P. Mason, *Third Meeting of the Society for Molecular Imaging*, St. Louis, MO, September 2004
2. "Magnetic resonance chemical shift imaging of gene-reporter molecule OFPNPG", V. Kodibagkar, J. Yu, L. Liu, H. P. Hetherington and R. P. Mason, *Third Meeting of the Society for Molecular Imaging*, St. Louis, MO, September 2004
3. "*Novel Magnetic resonance Assays of Gene Imaging Constructs (MAGIC)*" R. P. Mason, J. Yu, L. Liu, W. Cui and V. Kodibagkar, Molecular Medicine Symposium, Houston, Feb. 2005
4. "*In vivo* detection of lacZ gene expression in a human prostate xenograft tumor by ^{19}F NMR using OFPNPG", L. Liu, V. Kodibagkar, J. Yu, R. P. Mason, Molecular Medicine Symposium, Houston, Feb. 2005
5. "^{19}F CSI of gene-reporter molecule OFPNPG", V. Kodibagkar, J. Yu, L. Liu, S. Brown, H. P. Hetherington, R. D. Gerard, and R. P. Mason, ISMRM 13th Scientific Meeting in

Miami Beach, Florida, USA May 2005.

6. "Breast cancer gene therapy: development of novel non-invasive magnetic resonance assay to optimize efficacy", R. P. Mason, J. Yu., L. Liu, V. D. Kodibagkar, W Cui, and S. L. Brown, Era of Hope, accepted as poster and oral, Philadelphia June 2005

CONCLUSIONS:

Gene therapy holds great promise for tracing breast cancer. A major current obstacle to implementation is assessment of gene expression in terms of heterogeneity and longevity in tissues. Reporter genes and associated molecules should allow assessment of gene expressions. To date successful reporters have been developed for nuclear imaging, but radionuclides can be difficult to handle and decay limiting shelf life detectability (3). Optical techniques are favored for gene assessment in small animals, but light penetration can limit utility (4). NMR facilitates assessment of deep tissues without radiation exposure. We have now demonstrated the feasibility of synthesizing an NMR reporter molecule to reveal activity of β-galactosidase, the primary tool of molecular biologists to assess gene transfection. Significantly the molecules enter cells and are effective substrates. Moreover the ^{19}F NMR chemical shift unequivocally reveals enzyme activity. Differences in chemical shift associated with small molecular changes may further allow multiple substrates to be interrogated simultaneously allowing for several genes to be interrogated simultaneously. Appropriate NMR pulse sequences allow distribution of substrate and product to be observed by imaging in phantoms. Second generation agents exhibit enhanced sensitivity to enzyme activity, accompanied by modified toxicity.

REFERENCES:

1. Zwiebel, J. A. Cancer gene and oncolytic virus therapy. [Review], Semin. Oncol. *28:* 336-43, 2001.

2. Vlachaki, M. T., Chhikara, M., Aguilar, L., Zhu, X., Chiu, K. J., Woo, S., Teh, B. S., Thompson, T. C., Butler, E. B., and Aguilar-Cordova, E. Enhanced therapeutic effect of multiple injections of HSV-TK + GCV gene therapy in combination with ionizing radiation in a mouse mammary tumor model, Int J Radiat Oncol Biol Phys. *51:* 1008-17, 2001.

3. Berger, F. and Gambhir, S. S. Recent advances in imaging endogenous or transferred gene expression utilizing radionuclide technologies in living subjects: applications to breast cancer. [Review], Breast Cancer Res. *3:* 28-35, 2001.

4. Contag, C. H. and Ross, B. D. It's not just about anatomy: In vivo bioluminescence imaging as an eyepiece into biology, JMRI. *16:* 378-87, 2002.

APPENDICES:

1 "A Novel NMR Platform for Detecting Gene Transfection: Synthesis and Evaluation of Fluorinated Phenyl β-D-Galactosides with Potential Application for Assessing LacZ Gene Expression", J. Yu, P. Otten, Z. Ma, W. Cui, L. Liu, R. P. Mason, *Bioconjug. Chem*. 15 (6): 1334-1341 (2004)

2 "Synthesis and Evaluation of a Novel Gene Reporter Molecule: Detection of β-galactosidase activity Using ^{19}F NMR of a Fluorinated Vitamin B_6 conjugate" J. Yu, Z. Ma, Y. Li, K. S. Koeneman, L. Liu, R. P. Mason, *Med. Chem.* 1(3) 255-262 (2005)

3 "^{19}F: a versatile reporter for non-invasive physiology and pharmacology using magnetic resonance", J. Yu, V. D. Kodibagkar, W. Cui, R. P. Mason, *Curr. Med. Chem.* 12 (7) 819-848 (2005) + cover figure and editorial

4 "Synthesis and Characterization of Novel *lacZ* Gene Reporter Molecules: Detection of β-Galactosidase Activity Using ^{19}F NMR of Polyglycosylated Fluorinated Vitamin B_6 as ^{19}F NMR Indicator" J. Yu and R. P. Mason *Letters in Drug Discovery and Design*, submitted 2005

5 "Synthesis and Evaluation of Novel Enhanced Gene Reporter Molecules: Detection of β-Galactosidase Activity Using ^{19}F NMR of Trifluoromethylated Aryl β-D-Galactopyranosides", J. Yu, L. Liu, W. Cui, R. P. Mason, Biorg. Med. Chem., submitted 2005

Novel NMR Platform for Detecting Gene Transfection: Synthesis and Evaluation of Fluorinated Phenyl β-D-Galactosides with Potential Application for Assessing LacZ Gene Expression†

Jianxin Yu, Pieter Otten, Zhenyi Ma, Weina Cui, Li Liu, and Ralph P. Mason*

Department Radiology, The University of Texas Southwestern Medical Center at Dallas, Dallas, Texas 75390-9058. Received March 12, 2004; Revised Manuscript Received October 1, 2004

Gene therapy holds great promise for the treatment of diverse diseases, but widespread implementation is hindered by difficulties in assessing the success of transfection. The development of noninvasive reporter techniques based on appropriate molecules and imaging modalities may help to assay gene expression. Fluorophenyl-β-D-galactopyranosides provide a novel class of NMR active molecules, which are highly responsive to the action of β-galactosidase (β-gal), the product of the lacZ gene. The reporter molecules are stable in solution and with respect to wild-type cells, but the enzyme causes liberation of the aglycon, a fluorophenol, accompanied by distinct color formation and a ^{19}F NMR chemical shift of 5−10 ppm, depending on pH. Synthetic strategy, experimental methods, and molecular and ^{19}F NMR characteristics are reported for a series of molecules in solution, blood, and tumor cells. This class of molecules presents a new strategy for assaying gene expression with a highly versatile molecular structural platform.

INTRODUCTION

Gene therapy holds great promise for the treatment of diseases including cancer, cystic fibrosis, and immunodeficiency. However, a major hurdle to widespread successful implementation is the need to verify successful transfection, in particular, the spatial distribution of gene expression in the target tissue, together with assays of the longevity of expression. An image-based assay could greatly facilitate optimal gene therapy vector dosing, in a precise temporal and spatial manner.

Two approaches are gaining popularity for reporter genes. One method favors the use of genes producing reporter molecules such as green fluorescent protein, which are directly detectable by physical methods such as fluorescence. The second approach uses genes to produce enzymes, which act upon substrates administered to specifically interrogate gene expression. A critical criterion is that the reporter gene not be normally present or expressed in the cells of interest. The most popular reporter genes today are associated with optical imaging, because this is a cheap modality and is highly sensitive and the results are rapidly available (*1*, *2*). Thus, fluorescent imaging of green fluorescent protein [GFP[1] and longer wavelength variants (*3*)] and bioluminescent imaging (BLI) of luciferase activity on administered D-luciferin (*4*) are popular. These techniques are useful only in superficial tissues and have extensive applications in mice, but application to larger bodies is limited by shallow light penetration.

Several nuclear medicine approaches have been demonstrated by exploiting the action of thymidine kinase on a variety of substrates including iodo- and fluoronucleosides, such as FIAU and gancyclovir, and various radionuclide labels including ^{123}I, ^{124}I, ^{125}I, and ^{18}F (*5*, *6*). For cancer, thymidine kinase has the advantage that not only does the gene serve as a reporter, but the gene products can themselves have therapeutic value. An alternative approach uses the sodium iodine symporter (hNIS), which works well with both iodide and pertechnetate substrates (*7*).

NMR has been applied to cells transfected to express melanin or transferrin resulting in iron accumulation, which produces proton MRI contrast (*8*, *9*). ^{19}F NMR has been used to detect conversion of 5-fluorocytosine to 5-fluorouracil following introduction of cytosine deaminase (*10*).

Historically, the bacterial *lac*Z gene, encoding the enzyme β-galactosidase (β-gal, EC 3.2.1.23), has been the most popular reporter gene. The lac operon was the first gene expression system to be well characterized, some 40 years ago by Jacob and Monod (*11*), and it is a recognized tool for the study of problems in cell and molecular biology and the recently emerging fields of genomics and proteomics (*12*). Its induction has become a standard means of assaying clonal insertion and transcriptional activation (*13*). The long-established tests for β-gal based on colorimetric assay of *o*- and *p*-nitrophenyl-β-galactopyranoside hydrolysis to release yellow *o*- or *p*-nitrophenols remain popular (*14*). However, because of the broad substrate specificity of the enzyme, alternate reporter substrates have been proposed (*15*–*19*), and many are commercially available. Fluorogenic galactosides based on fluorescein and resorufin, such as *p*-naphtholbenzein, 1,2-dihydroxyanthraquinone, 4-methylumbeliferone, 5-bromo-4-chloro-3-indoxyl-β-galactopyranoside (X-Gal), and 3,4-cyclohexenoesculetin-β-galactopyranoside (S-Gal) are well established (*16*, *20*–

†Presented in part at the 16th International NMR Spectroscopy Conference, Cambridge, U.K., July 2003.

* Address correspondence to this author at the Department of Radiology, The University of Texas Southwestern Medical Center at Dallas, 5323 Harry Hines Blvd., Dallas, TX 75390-9058 [telephone (214) 648-8926; fax (214) 648-2991; e-mail Ralph.Mason@UTSouthwestern.edu].

[1] Abbreviations: β-gal, β-galactosidase; BLI, bioluminescent imaging; GFP, green fluorescent protein; ONPG, *o*-nitrophenyl-β-galactopyranoside; PFONPG, 4-fluoro-2-nitrophenyl-β-D-galactopyranoside; S-Gal, 3,4-cyclohexenoesculetin-β-galactopyranoside; X-Gal, 5-bromo-4-chloro-3-indoxyl-β-galactopyranoside.

10.1021/bc049936d CCC: $27.50
Published on Web 10/23/2004

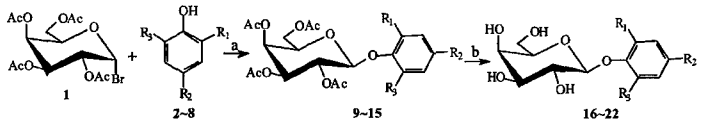

Reaction conditions: (a) CH_2Cl_2-H_2O, pH 8~9, 50 °C, TBAB, ~1 hr, near quantitative yield; (b) NH_3-MeOH, 0 °C→r.t., 24 hr, quantitative yields.

Compounds	R_1	R_2	R_3
2, 9, 16	NO_2	F	H
3, 10, 17	F	NO_2	H
4, 11, 18	F	H	NO_2
5, 12, 19	F	H	H
6, 13, 20	H	F	H
7, 14, 21	Cl	F	H
8, 15, 22	Br	F	H

Figure 1. Reactions and structures of **1**–**22**.

23). The staining methodologies described above are effective for histological specimens and in vitro, but in vivo capabilities would promise new applications to study, and clinically evaluate, gene transfection.

Recently, Louie et al. (*24*) demonstrated an elegant MRI assessment of β-gal activity based on 1-[2-(β-D-galactopyranosyloxy)propyl]-4,7,10-tris(carboxymethyl)-1,4,7,10-tetraazacyclododecane)gadolinium(III) (EgadMe). Access of water to the first coordination sphere of the paramagnetic Gd^{3+} is blocked by a galactopyranose bridge, but β-gal cleaves the bridge, yielding a 20% increase in relaxivity. Whereas EgadMe is a poor substrate for the enzyme (several orders of magnitude less efficient than the colorimetric biochemical agent ONPG) and does not penetrate cells, it facilitated effective investigation of cell lineage following direct intracellular microinjections (*24*). These studies prompted us to consider other NMR active analogues, and it appeared that introduction of a fluorine atom into the popular colorimetric biochemical indicator ONPG could produce a strong candidate molecule. Diverse fluorinated reporter molecules have been successfully applied previously to metabolic and physiological studies (*25*, *26*). ^{19}F-labeled molecules exploit the high NMR visibility of fluorine, the great NMR sensitivity of ^{19}F to the environmental milieu, and the lack of background signal. We recently reported the successful synthesis of a prototype reporter molecule, *p*-fluoro-*o*-nitrophenyl β-D-galactopyranoside (PFONPG; **16**), and demonstrated initial NMR applications (*27*). We have now synthesized and evaluated a series of analogues and provide structural characterization, together with evaluation of their activity in solution and in cell culture, and compare the relative merits of the substrates.

EXPERIMENTAL SECTION

General Methods. NMR spectra were recorded on Varian Inova spectrometers (400 or 600 MHz for ^1H, 100 or 150 MHz for ^{13}C) with $CDCl_3$ (for **9**–**15**) or DMSO-d_6 (for **16**–**22**) as solvents, and ^1H and ^{13}C chemical shifts were referenced to TMS, as internal standard. Compounds were characterized by acquisition of ^1H, ^{13}C, DEPT, ^1H–^1H COSY, or NOESY experiments at 25 °C. ^{19}F NMR (376 MHz) measurements were performed at 25–37 °C in aqueous solution with ^{19}F signals referenced to dilute sodium trifluoroacetate (NaTFA) in a capillary, as an external standard. High-resolution mass spectra were obtained on an ABI Voyager STR MALDI-TOF mass spectrometer in reflector mode (service provided by Dr. Tichy, Department of Chemistry, Texas A&M University).

Reactions requiring anhydrous conditions were performed under nitrogen or argon. Solutions in organic solvents were dried with anhydrous sodium sulfate and concentrated in vacuo below 45 °C. Column chromatography was performed on silica gel (200–300 mesh) with cyclohexane–EtOAc. Analytical TLC (silica gel GF_{254}; Aldrich Chemical Co.) used detection by UV or staining with 5% ethanolic H_2SO_4 at 110 °C for 10 min.

Although many nitrophenol glycosides have been described (*28*, *29*) including nitrophenyl fluorogalactoside (*30*), to our knowledge there have been no published syntheses of the β-D-galactosides **16**–**22**. For the construction of *O*-glycosidic linkages, many strategies are available using anhydrous zinc chloride (for the α anomer) or *p*-toluenesulfonic acid (for the β anomer), but the *p*-nitrophenyl glycosides were usually obtained in low yield (*31*–*33*).

We initially tested the method of Yoon et al. (*30*), which involves the reaction of a potassium salt of an acidic phenol with an α-D-galactopyranosyl bromide. Aryl β-D-galactopyranosides **16** and **17** were prepared by a nucleophilic substitution reaction of a phenolate ion on acetobromo-α-D-galactose **1** followed by saponification of the acetyl groups. We applied two different procedures for generating the phenolate ion, depending on the acidity of the phenol. The brightly colored solid potassium salts of fluoronitrophenols **2** and **3** could be isolated by lyophilizing an aqueous solution of phenol with a slight excess of aqueous KOH. The salts were subsequently used directly in excess for the synthesis of the corresponding fluoronitrophenyl tetra-*O*-acetyl β-D galactopyranosides **9** and **10**. Compounds **9** and **10** were isolated pure in moderate yields (58–77%) after basic extractive workup and flash chromatography. A different strategy had to be applied for the less acidic 2-fluorophenol **5**. The phenolate was generated in situ with K_2CO_3 in refluxing acetone in the presence of a catalytic amount of 18-crown-6 (*34*).

However, given the reported high yields, mild reaction conditions, and high stereospecificity, we ultimately explored phase-transfer catalysis for the synthesis of our desired glycosides (Figure 1) (*30*, *34*).

Fluorophenyl β-D-Galactopyranoside Tetraacetates 9–15. *General Procedure (Figure 1).* A solution of **1** (1 mmol; 2,3,4,6-tetra-*O*-acetyl-α-D-galactopyranosyl bromide, Sigma) in CH_2Cl_2 (5 mL) was added dropwise

to a vigorously stirred solution of fluorophenol **2**–**8** (1.2 mmol) and tetrabutylammonium bromide (0.48 g, 1.5 mmol) in H_2O (5 mL; pH 8–9) at 50 °C in a three-neck round-bottom flask equipped with a condenser and thermometer. After TLC showed complete reaction (~1 h), the organic layer was separated, washed, dried, evaporated under reduced pressure, and recrystallized (EtOH–H_2O) or purified by column chromatography on silica gel to give fluorinated aryl β-D-galactopyranoside tetraacetates **9**–**15**, as white crystals.

2-Nitro-4-fluorophenyl 2,3,4,6-tetra-O-acetyl-β-D-galactopyranoside ***9:*** 0.5 g, 99%; R_f 0.31 (3:2 cyclohexane–EtOAc); δ_H 7.55 (1H, dd, J = 3.0, 8.4 Hz, Ar–H), 7.42 (1H, dd, J = 4.8, 9.0 Hz, Ar–H), 7.27 (1H, m, Ar–H), 5.04 (1H, d, $J_{1,2}$ = 7.8 Hz, H-1), 5.52 (1H, dd, $J_{2,3}$ = 8.4 Hz, H-2), 5.11 (1H, dd, $J_{3,4}$ = 3.0 Hz, H-3), 5.47 (1H, d, $J_{4,5}$ = 2.6 Hz, H-4), 4.07 (1H, m, H-5), 4.26 (1H, dd, $J_{5,6a}$ = 4.2 Hz, $J_{6a,6b}$ = 11.4 Hz, H-6a), 4.17 (1H, dd, $J_{5,6b}$ = 5.4 Hz, H-6b), 2.20, 2.14, 2.07, 2.02 (12H, 4s, 4 × CH_3-CO); δ_C 170.43, 170.31, 170.24, 169.62 (4 × CH_3CO), 157.70 (d, J_{F-C} = 164.8 Hz, Ar–C), 145.66 (Ar–C), 141.86 (d, J_{F-C} = 5.7 Hz, Ar–C), 122.68 (d, J_{F-C} = 4.9 Hz, Ar–C), 120.77 (d, J_{F-C} = 15.2 Hz, Ar–C), 112.60 (d, J_{F-C} = 18.3 Hz, Ar–C), 101.40 (C-1), 68.01 (C-2), 70.63 (C-3), 66.86 (C-4), 71.58 (C-5), 61.45 (C-6), 21.25, 21.10, 20.38, 20.25 (4 × $\mathbf{C}H_3CO$); HRMS, $[M + Na]^+$, $C_{20}H_{22}NO_{12}FNa$, calcd 510.1024, found 510.1014; $[M + K]^+$, $C_{20}H_{22}NO_{12}$-FK, calcd 526.0763, found 526.0751.

2-Fluoro-4-nitrophenyl 2,3,4,6-tetra-O-acetyl-β-D-galactopyranoside ***10:*** 0.5 g, 99%; R_f 0.35(3:2 cyclohexane–EtOAc); δ_H 8.03 (2H, m, Ar–H), 7.32 (1H, m, Ar–H), 5.13 (1H, d, $J_{1,2}$ = 7.8 Hz, H-1), 5.58 (1H, dd, $J_{2,3}$ = 10.2 Hz, H-2), 5.15 (1H, dd, $J_{3,4}$ = 3.6 Hz, H-3), 5.40 (1H, dd, $J_{4,5}$ = 3.6 Hz, H-4), 4.10 (1H, ddd, $J_{5,6a}$ = 4.5 Hz, $J_{5,6b}$ = 5.0 Hz, H-5), 4.26 (1H, dd, $J_{6a,6b}$ = 11.0 Hz, H-6a), 4.19 (1H, dd, H-6b), 2.21, 2.11, 2.08, 2.04 (12H, 4s, 4 × CH_3CO); δ_C 170.45, 170.26, 170.21, 169.44 (4 × CH_3CO), 152.23 (d, J_{F-C} = 252.0 Hz, Ar–C), 150.07 (d, J_{F-C} = 10.6 Hz, Ar–C), 120.51 (d, J_{F-C} = 9.2 Hz, Ar–C), 118.53 (d, J_{F-C} = 11.7 Hz, Ar–C), 113.11 (d, J_{F-C} = 23.7 Hz, Ar–C), 100.28 (d, J_{F-C} = 3.1 Hz, C-1), 68.34 (C-2), 70.57 (C-3), 66.81 (C-4), 71.83 (C-5), 61.45 (C-6), 20.80, 20.77, 20.72, 20.33 (4 × $\mathbf{C}H_3CO$); HRMS, $[M + Na]^+$, $C_{20}H_{22}NO_{12}FNa$, calcd 510.1010, found 510.1014; $[M + K]^+$, $C_{20}H_{22}NO_{12}$-FK, calcd 526.0763, found 526.0751.

2-Nitro-6-fluorophenyl 2,3,4,6-tetra-O-acetyl-β-D-galactopyranoside ***11:*** 0.49 g, 98%; R_f 0.30 (3:2 cyclohexane–EtOAc); δ_H 7.58 (1H, ddd, J = 1.2, 1.4, 8.8 Hz, Ar–H), 7.39 (1H, ddd, J = 1.8, 8.4, 9.8 Hz, Ar–H), 7.29 (1H, m, Ar–H), 5.02 (1H, d, $J_{1,2}$ = 8.0 Hz, H-1), 5.48 (1H, dd, $J_{2,3}$ = 10.4 Hz, H-2), 5.08 (1H, dd, $J_{3,4}$ = 5.4 Hz, H-3), 5.41 (1H, dd, $J_{4,5}$ = 3.6 Hz, H-4), 3.90 (1H, m, H-5), 4.11 (1H, dd, $J_{5,6a}$ = 7.8 Hz, $J_{6a,6b}$ = 10.2 Hz, H-6a), 4.08 (1H, dd, $J_{5,6b}$ = 7.2 Hz, H-6b), 2.20, 2.14, 2.01, 2.00 (12H, 4s, 4 × CH_3CO); δ_C 170.45, 170.19, 169.61 (4 × CH_3CO), 155.84 (d, J_{F-C} = 251.8 Hz, Ar–C), 146.01 (Ar–C), 137.17 (d, J_{F-C} = 15.3 Hz, Ar–C), 125.66 (d, J_{F-C} = 7.6 Hz, Ar–C), 121.11 (d, J_{F-C} = 20.6 Hz, Ar–C), 120.22 (d, J_{F-C} = 3.8 Hz, Ar–C), 102.84 (d, J_{F-C} = 2.3 Hz, C-1), 68.75 (C-2), 70.76 (C-3), 66.74 (C-4), 71.41 (C-5), 61.02 (C-6), 20.82, 20.79, 20.70, 20.66 (4 × $\mathbf{C}H_3CO$); HRMS, $[M + Na]^+$, $C_{20}H_{22}NO_{12}FNa$, calcd 510.1024, found 510.1011; $[M + K]^+$, $C_{20}H_{22}NO_{12}FK$, calcd 526.0763, found 526.0750.

2-Fluorophenyl 2,3,4,6-tetra-O-acetyl-β-D-galactopyranoside ***12:*** 0.45 g, 98%; R_f 0.40 (3:2 cyclohexane–EtOAc); δ_H 7.48 (1H, dd, J = 2.0, 10 Hz, Ar–H), 7.36 (1H, m, Ar–H), 7.30 (1H, m, Ar–H), 7.22 (1H, m, Ar–H), 5.54 (1H, d, $J_{1,2}$ = 8.4 Hz, H-1), 5.48 (1H, dd, $J_{2,3}$ = 10.0 Hz, H-2), 5.09 (1H, dd, $J_{3,4}$ = 4.4 Hz, H-3), 5.40 (1H, d, $J_{4,5}$ = 3.0 Hz, H-4), 4.24 (1H, m, H-5), 4.18 (1H, dd, $J_{5,6a}$ = 7.5 Hz, $J_{6a,6b}$ = 10.4 Hz, H-6a), 4.08 (1H, dd, $J_{5,6b}$ = 7.0 Hz, H-6b), 2.19, 2.10, 2.04, 2.02 (12H, 4s, 4 × CH_3CO); δ_C 170.66, 170.23, 170.10, 169.58 (4 × CH_3CO), 156.14 (Ar–C), 146.01 (d, J_{F-C} = 245.9 Hz, Ar–C), 136.58 (d, J_{F-C} = 14.8 Hz, Ar–C), 126.08 (d, J_{F-C} = 7.9 Hz, Ar–C), 122.33 (d, J_{F-C} = 26.3 Hz, Ar–C), 121.33 (d, J_{F-C} = 6.8 Hz, Ar–C), 101.89 (d, J_{F-C} = 2.6 Hz, C-1), 68.85 (C-2), 70.58 (C-3), 66.79 (C-4), 71.56 (C-5), 61.33 (C-6), 20.77, 20.70, 20.60, 20.58 (4 × $\mathbf{C}H_3CO$); HRMS, $[M + Na]^+$, $C_{20}H_{23}NO_{10}FNa$, calcd 465.1173, found 465.1169; $[M + K]^+$, $C_{20}H_{23}NO_{10}$-FK, calcd 481.0912, found 481.0907.

4-Fluorophenyl 2,3,4,6-tetra-O-acetyl-β-D-galactopyranoside ***13:*** 0.42 g, 95%; R_f 0.45 (3:2 cyclohexane–EtOAc); δ_H 6.99 (4H, m, Ar–H), 4.98 (1H, d, $J_{1,2}$ = 8.0 Hz, H-1), 5.48 (1H, dd, $J_{2,3}$ = 10.0 Hz, H-2), 5.11 (1H, dd, $J_{3,4}$ = 4.2 Hz, H-3), 5.45 (1H, d, $J_{4,5}$ = 2.4 Hz, H-4), 4.06 (1H, m, H-5), 4.24 (1H, dd, $J_{5,6a}$ = 7.2 Hz, $J_{6a,6b}$ = 10.4 Hz, H-6a), 4.16 (1H, dd, $J_{5,6b}$ = 6.4 Hz, H-6b), 2.19, 2.09, 2.06, 2.02 (12H, 4s, 4 × CH_3CO); δ_C 170.45, 170.36, 170.28, 169.48 (4 × CH_3CO), 160.08 (Ar–C), 157.69 (Ar–C), 153.10 (d, J_{F-C} = 20.0 Hz, Ar–C), 118.82–115.97 (m, Ar–C), 100.62 (C-1), 68.68 (C-2), 70.71 (C-3), 66.90 (C-4), 71.06 (C-5), 61.44 (C-6), 20.79, 20.72, 20.68, 20.64 (4 × $\mathbf{C}H_3CO$); HRMS, $[M + Na]^+$, $C_{20}H_{23}NO_{10}FNa$, calcd 465.1173, found 465.1170; $[M + K]^+$, $C_{20}H_{23}NO_{10}FK$, calcd 481.0912, found 481.1014.

2-Bromo-4-fluorophenyl 2,3,4,6-tetra-O-acetyl-β-D-galactopyranoside ***14:*** 0.50 g, 97%; R_f 0.48 (3:2 cyclohexane–EtOAc); δ_H 7.28 (1H, ddd, J = 3.2, 2.8, 3.2 Hz, Ar–H), 7.16 (1H, dd, J = 4.8, 9.2 Hz, Ar–H), 6.97 (1H, m, Ar–H), 4.91 (1H, d, $J_{1,2}$ = 8.0 Hz, H-1), 5.56 (1H, dd, $J_{2,3}$ = 10.8 Hz, H-2), 5.10 (1H, dd, $J_{3,4}$ = 3.6 Hz, H-3), 5.46 (1H, d, $J_{4,5}$ = 4.0 Hz, H-4), 4.24 (1H, m, H-5), 4.25 (1H, dd, $J_{5,6a}$ = 7.2 Hz, $J_{6a,6b}$ = 11.4 Hz, H-6a), 4.08 (1H, dd, $J_{5,6b}$ = 6.0 Hz, H-6b), 2.19, 2.11, 2.06, 2.02 (12H, 4s, 4 × CH_3-CO); δ_C 170.52, 170.43, 170.34, 169.57 (4 × CH_3CO), 159.80 (Ar–C), 157.35 (Ar–C), 150.22 (Ar–C), 120.91–13.93 (m, Ar–C), 101.36 (C-1), 68.33 (C-2), 70.66 (C-3), 67.03 (C-4), 71.49 (C-5), 61.51 (C-6), 21.28, 21.15, 21.10, 20.91 (4 × $\mathbf{C}H_3CO$); HRMS, $[M + Na]^+$, $C_{20}H_{22}O_{10}F^{79}$-BrNa, calcd 543.0279, found 543.0266; $C_{20}H_{22}O_{10}F^{81}BrNa$, calcd 545.0259, found 545.0205; $[M + K]^+$, $C_{20}H_{22}O_{10}F^{79}$-BrK, calcd 559.0043, found 559.0043; $C_{20}H_{22}O_{10}F^{81}BrNa$, calcd 560.9997, found 560.9892.

2-Chloro-4-fluorophenyl 2,3,4,6-tetra-O-acetyl-β-D-galactopyranoside ***15:*** 0.48 g, 99%; R_f 0.46 (3:2 cyclohexane–EtOAc); δ_H 7.21 (1H, dd, J = 4.8, 8.8 Hz, Ar–H), 7.13 (1H, dd, J = 3.2, 8.0 Hz, Ar–H), 6.92 (1H, m, Ar–H), 4.90 (1H, d, $J_{1,2}$ = 8.0 Hz, H-1), 5.54 (1H, dd, $J_{2,3}$ = 10.8 Hz, H-2), 5.12 (1H, dd, $J_{3,4}$ = 3.2 Hz, H-3), 5.46 (1H, d, $J_{4,5}$ = 3.6 Hz, H-4), 4.04 (1H, m, H-5), 4.26 (1H, dd, $J_{5,6a}$ = 6.8 Hz, $J_{6a,6b}$ = 11.4 Hz, H-6a), 4.16 (1H, dd, $J_{5,6b}$ = 6.4 Hz, H-6b), 2.19, 2.11, 2.06, 2.02 (12H, 4s, 4 × CH_3-CO); δ_C 170.40, 170.32, 170.21, 169.49 (4 × CH_3CO), 159.72 (Ar–C), 157.25 (Ar–C), 149.14 (d, J_{F-C} = 3.1 Hz, Ar–C), 125.55 (d, J_{F-C} = 9.9 Hz, Ar–C), 120.62–114.34 (m, Ar–C), 101.46 (C-1), 68.29 (C-2), 70.51 (C-3), 66.97 (C-4), 71.38 (C-5), 61.40 (C-6), 20.99, 20.87, 20.77, 20.66 (4 × $\mathbf{C}H_3CO$); HRMS, $[M + Na]^+$, $C_{20}H_{22}O_{10}F^{35}ClNa$, calcd 499.0783, found 499.0761; $C_{20}H_{22}O_{10}F^{37}ClNa$, calcd 501.0754, found 501.0701; $[M + K]^+$, $C_{20}H_{22}O_{10}F^{35}ClK$, calcd 515.0523, found 515.0495; $C_{20}H_{22}O_{10}F^{37}ClK$, calcd 517.0494, found 517.0488.

Fluoroaryl β-D-Galactopyranosides 16–22. *General Procedure.* A solution of fluorophenyl 2,3,4,6-tetra-*O*-acetyl-β-D-galactopyranoside (**9**–**15**) (0.4 g) in anhydrous MeOH (15 mL) containing 0.5 M NH_3 was vigorously stirred from 0 °C to room temperature overnight until

TLC showed complete reaction. Following solvent removal in vacuo, chromatography on silica gel (EtOAc/MeOH) afforded the free galactopyranosides **16**–**22** in nearly quantitative yield, as white crystalline materials.

2-Nitro-4-fluorophenyl β-D-galactopyranoside ***16****:* R_f 0.40 (1:9 MeOH–EtOAc), δ_H 7.84 (1H, dd, J = 2.8, 8.0 Hz, Ar–H), 7.53 (1H, ddd, J = 1.6, 1.0, 2.8 Hz, Ar–H), 7.43 (1H, dd, J = 4.4, 9.2 Hz, Ar–H), 4.96 (1H, d, $J_{1,2}$ = 7.6 Hz, H-1), 3.60 (1H, dd, $J_{2,3}$ = 10.6 Hz, H-2), 3.51 (1H, dd, $J_{3,4}$ = 5.2 Hz, H-3), 3.47 (1H, d, $J_{4,5}$ = 5.6 Hz, H-4), 3.43 (1H, m, H-5), 3.67 (2H, m, H-6), 5.16 (1H, d, $J_{H-2,OH-2}$ = 5.2 Hz, HO-2), 4.67 (1H, d, $J_{H-3,OH-3}$ = 4.4 Hz, HO-3), 4.90 (1H, d, $J_{H-4,OH-4}$ = 6.0 Hz, HO-4), 4.67 (1H, t, $J_{H-6,OH-6}$ = 5.2, 5.4 Hz, HO-6); δ_C 155.41 (d, J_{F-C} = 239.6 Hz, Ar–C), 146.19 (d, J_{F-C} = 3.1 Hz, Ar–C), 140.17 (d, J_{F-C} = 9.1 Hz, Ar–C), 120.91 (d, J_{F-C} = 22.1 Hz, Ar–C), 119.03 (d, J_{F-C} = 7.7 Hz, Ar–C), 111.89 (d, J_{F-C} = 27.5 Hz, Ar–C), 101.65 (C-1), 70.07 (C-2), 73.37 (C-3), 68.06 (C-4), 75.87 (C-5), 60.33 (C-6); HRMS, $[M + Na]^+$, $C_{12}H_{14}NO_8FNa$, calcd 342.0601, found 342.0589; $[M + K]^+$, $C_{12}H_{14}NO_8FK$, calcd 358.0341, found 358.0328.

2-Fluorine-4-nitrophenyl β-D-galactopyranoside ***17****:* R_f 0.45 (1:9 MeOH–EtOAc); δ_H 7.58 (1H, dd, J = 3.3, 8.0 Hz, Ar–H), 7.42 (1H, dd, J = 4.2, 8.7 Hz, Ar–H), 7.28 (1H, m, Ar–H), 5.16 (1H, d, $J_{1,2}$ = 7.8 Hz, H-1), 4.60 (1H, dd, $J_{2,3}$ = 8.8 Hz, H-2), 3.70 (1H, dd, $J_{3,4}$ = 3.2 Hz, H-3), 3.63 (1H, d, $J_{4,5}$ = 3.1 Hz, H-4), 3.60 (1H, m, H-5), 3.50 (2H, m, H-6), 4.98 (1H, d, $J_{H-2,OH-2}$ = 7.2 Hz, HO-2), 4.66 (1H, d, $J_{H-3,OH-3}$ = 4.0 Hz, HO-3), 4.80 (1H, d, $J_{H-4,OH-4}$ = 5.0 Hz, HO-4), 4.90 (1H, t, $J_{H-6,OH-6}$ = 5.5, 5.8 Hz, HO-6); δ_C 156.80 (d, J = 160.4 Hz, Ar–C), 146.55 (Ar–C), 140.68 (d, J = 5.5 Hz, Ar–C), 123.44 (d, J = 4.2 Hz, Ar–C), 121.33 (d, J = 18.2 Hz, Ar–C), 114.80 (d, J = 17.9 Hz, Ar–C), 101.73 (C-1), 68.33 (C-2), 70.86 (C-3), 66.90 (C-4), 71.47 (C-5), 61.77 (C-6); HRMS, $[M + Na]^+$, $C_{12}H_{14}NO_8FNa$, calcd 342.0601, found 342.0585; $[M + K]^+$, $C_{12}H_{14}NO_8FK$, calcd 358.0341, found 358.0320.

2-Nitro-6-fluorophenyl β-D-galactopyranoside ***18A****:* R_f 0.40 (1:9 MeOH–EtOAc); δ_H 7.73 (1H, ddd, J = 1.6, 3.2, 8.4 Hz, Ar–H), 7.63 (1H, ddd, J_{HH} = 1.2, 4.0, 8.4 Hz, J_{HF} = 19.2 Hz, Ar–H), 7.46 (1H, ddd, J_{HH} = 5.2, 8.4 Hz, J_{HF} = 16.8 Hz, Ar–H), 5.00 (1H, d, $J_{1,2}$ = 7.6 Hz, H-1), 3.88 (1H, dd, $J_{2,3}$ = 9.2 Hz, H-2), 3.82 (1H, dd, $J_{3,4}$ = 4.0 Hz, H-3), 3.70 (1H, dd, $J_{4,5}$ = 3.2 Hz, H-4), 3.66 (1H, m, H-5), 4.00 (2H, m, H-6), 3.80 (1H, d, $J_{H-2,OH-2}$ = 4.2 Hz, HO-2), 3.69 (1H, d, $J_{H-3,OH-3}$ = 3.0 Hz, HO-3), 3.86 (1H, d, $J_{H-4,OH-4}$ = 1.6 Hz, HO-4), 3.62 (1H, dd, $J_{H-6,OH-6}$ = 4.6, 5.0 Hz, HO-6); δ_C 156.66 (d, J_{F-C} = 246.2 Hz, Ar–C), 145.78 (Ar–C), 138.54 (d, J_{F-C} = 12.2 Hz, Ar–C), 125.83 (d, J_{F-C} = 8.4 Hz, Ar–C), 121.65 (d, J_{F-C} = 19.9 Hz, Ar–C), 120.80 (d, J_{F-C} = 3.8 Hz, Ar–C), 106.06 (d, J_{F-C} = 3.8 Hz, C-1), 70.59 (C-2), 74.48 (C-3), 69.30 (C-4), 77.00 (C-5), 61.73 (C-6); HRMS, $[M + Na]^+$, $C_{12}H_{14}NO_8FNa$, calcd 342.0601, found 342.0599; $[M + K]^+$, $C_{12}H_{14}NO_8FK$, calcd 358.0341, found 358.0337.

2-Nitro-6-fluorophenyl α-D-galactopyranoside ***18B****:* R_f 0.47 (1:9 MeOH–EtOAc); δ_H 7.76 (1H, ddd, J = 1.6, 2.8, 8.4 Hz, Ar–H), 7.62 (1H, ddd, J_{HH} = 0.4, 4.8, 8.4 Hz, J_{HF} = 12.0 Hz, Ar–H), 7.40 (1H, ddd, J_{HH} = 4.8, 8.4 Hz, J_{HF} = 13.2 Hz, Ar–H), 5.85 (1H, d, $J_{1,2}$ = 3.2 Hz, H-1), 4.01 (1H, dd, $J_{2,3}$ = 8.9 Hz, H-2), 4.03 (1H, dd, $J_{3,4}$ = 3.6 Hz, H-3), 4.11 (1H, dd, $J_{4,5}$ = 3.6 Hz, H-4), 3.74 (1H, m, H-5), 3.63 (2H, m, H-6), 3.92 (1H, d, $J_{H-2,OH-2}$ = 3.2 Hz, HO-2), 3.74 (1H, d, $J_{H-3,OH-3}$ = 3.6 Hz, HO-3), 3.83 (1H, d, $J_{H-4,OH-4}$ = 2.0 Hz, HO-4), 3.80 (1H, t, $J_{H-6,OH-6}$ = 5.6, 6.0 Hz, HO-6); δ_C 157.06 (d, J_{F-C} = 248.7 Hz, Ar–C), 146.05 (Ar–C), 139.20 (d, J_{F-C} = 13.8 Hz, Ar–C), 124.59 (d, J_{F-C} = 8.4 Hz, Ar–C), 122.05 (d, J_{F-C} = 19.9 Hz, Ar–C), 121.37 (d, J_{F-C} = 3.0 Hz, Ar–C), 104.14 (d, J_{F-C} = 7.6 Hz, C-1), 70.23 (C-2), 70.59 (C-3), 69.94 (C-4), 74.21 (C-5), 62.03 (C-6); HRMS, $[M + Na]^+$, $C_{12}H_{14}NO_8FNa$, calcd 342.0601, fouz342.0590; $[M + K]^+$, $C_{12}H_{14}NO_8FK$, calcd 358.0341, found 358.0333.

2-Fluorophenyl β-D-galactopyranoside ***19****:* R_f 0.48 (1:9 MeOH–EtOAc); δ_H 7.26 (1H, m, Ar–H), 7.21 (1H, ddd, J = 1.2, 3.6, 8.0 Hz, Ar–H), 7.11 (1H, ddd, J_{HH} = 1.2, 7.2, J_{HF} = 14.4 Hz, Ar–H), 6.98 (1H, m, Ar–H), 4.91 (1H, d, $J_{1,2}$ = 7.6 Hz, H-1), 3.41 (1H, dd, $J_{2,3}$ = 9.6 Hz, H-2), 3.47 (1H, dd, $J_{3,4}$ = 4.0 Hz, H-3), 3.71 (1H, d, $J_{4,5}$ = 3.2 Hz, H-4), 3.54 (1H, m, H-5), 3.60 (2H, m, H-6), 3.58 (1H, d, $J_{H-2,OH-2}$ = 4.0 Hz, HO-2), 3.48 (1H, d, $J_{H-3,OH-3}$ = 3.1 Hz, HO-3), 3.57 (1H, d, $J_{H-4,OH-4}$ = 2.2 Hz, HO-4), 3.54 (1H, t, $J_{H-6,OH-6}$ = 4.0, 5.2 Hz, HO-6); δ_C 152.28 (d, J_{F-C} = 242.7 Hz, Ar–C), 145.50 (d, J_{F-C} = 9.9 Hz, Ar–C), 125.10 (d, J_{F-C} = 3.8 Hz, Ar–C), 122.60 (d, J_{F-C} = 6.9 Hz, Ar–C), 117.73 (Ar–C), 116.66 (d, J_{F-C} = 18.3 Hz, Ar–C), 101.53 (C-1), 70.59 (C-2), 73.81 (C-3), 68.52 (C-4), 76.04 (C-5), 60.74 (C-6); HRMS, $[M + Na]^+$, $C_{12}H_{15}O_6FNa$, calcd 297.0750, found 297.0739; $[M + K]^+$, $C_{12}H_{15}O_6FK$, calcd 313.0490, found 313.0486.

4-Fluorophenyl β-D-galactopyranoside ***20****:* R_f 0.40 (1:9 MeOH–EtOAc); δ_H 7.14–7.03 (4H, m, Ar–H), 4.74 (1H, d, $J_{1,2}$ = 7.6 Hz, H-1), 3.54 (1H, dd, $J_{2,3}$ = 10.6 Hz, H-2), 3.50 (1H, dd, $J_{3,4}$ = 3.6 Hz, H-3), 3.72 (1H, d, $J_{4,5}$ = 3.2 Hz, H-4), 3.43 (1H, m, H-5), 3.58 (2H, m, H-6), 5.30–4.4 (4H, br, HO-2,3,4,6); δ_C 157.25 (d, J_{F-C} = 235 Hz, Ar–C), 153.98 (Ar–C), 117.93–115.69 (Ar–C), 101.88 (C-1), 70.40 (C-2), 73.32 (C-3), 68.30 (C-4), 75.60 (C-5), 60.46 (C-6); HRMS, $[M + Na]^+$, $C_{12}H_{15}O_6FNa$, calcd 297.0750, found 297.0731.

2-Bromo-4-fluorophenyl β-D-galactopyranoside ***21****:* R_f 0.52 (1:9 MeOH–EtOAc); δ_H 7.54 (1H, dd, J = 2.4, 8.0 Hz, Ar–H), 7.22 (2H, m, Ar–H), 4.90 (1H, d, $J_{1,2}$ = 7.6 Hz, H-1), 3.41 (1H, dd, $J_{2,3}$ = 9.6 Hz, H-2), 3.47 (1H, dd, $J_{3,4}$ = 4.0 Hz, H-3), 3.71 (1H, d, $J_{4,5}$ = 3.2 Hz, H-4), 3.54 (1H, m, H-5), 3.60 (2H, m, H-6), 5.11 (1H, d, $J_{H-2,OH-2}$ = 5.6 Hz, HO-2), 4.58 (1H, d, $J_{H-3,OH-3}$ =4.8 Hz, HO-3), 4.89 (1H, d, $J_{H-4,OH-4}$ = 5.2 Hz, HO-4), 4.67 (1H, t, $J_{H-6,OH-6}$ = 5.2, 5.2 Hz, HO-6); δ_C 157.38 (d, J_{F-C} = 240.4 Hz, Ar–C), 151.09 (Ar–C), 120.79–121.32 (m, Ar–C), 101.96 (C-1), 70.87 (C-2), 73.78 (C-3), 68.84 (C-4), 76.13 (C-5), 61.13 (C-6); HRMS, $[M + Na]^+$, $C_{12}H_{14}O_6F^{79}BrNa$, calcd 374.9855, found 374.9851; $C_{12}H_{14}O_6F^{81}BrNa$, calcd 376.9835, found 376.9665; $[M+K]^+$, $C_{12}H_{14}O_6F^{79}BrK$, calcd 390.9595, found 390.9803; $C_{12}H_{14}O_6F^{81}BrK$, calcd 392.9575, found 392.9687.

2-Chloro-4-fluorophenyl β-D-galactopyranoside ***22****:* R_f 0.45 (1:9 MeOH–EtOAc); δ_H 7.42 (1H, dd, J = 2.8, 8.4 Hz, Ar–H), 7.28 (1H, dd, J = 5.2, 9.6 Hz, Ar–H), 7.17 (1H, m, Ar–H), 4.90 (1H, d, $J_{1,2}$ = 7.6 Hz, H-1), 3.57 (1H, dd, $J_{2,3}$ = 11.6 Hz, H-2), 3.52 (1H, dd, $J_{3,4}$ = 5.2 Hz, H-3), 3.72 (1H, m, H-4), 3.17 (1H, m, H-5), 3.60 (1H, dd, $J_{5,6a}$ = 8.8 Hz, $J_{6a,6b}$ = 12.4 Hz, H-6a), 3.45 (1H, dd, $J_{5,6b}$ = 6.0 Hz, H-6b), 5.17 (1H, d, $J_{H-2,OH-2}$ = 4.0 Hz, HO-2), 4.59 (1H, d, $J_{H-3,OH-3}$ = 3.2 Hz, HO-3), 4.89 (1H, d, $J_{H-4,OH-4}$ = 7.0 Hz, HO-4), 4.69 (1H, br, HO-6); δ_C 156.38 (d, J_{F-C} = 238.80 Hz, Ar–C), 149.62 (Ar–C), 122.55 (d, J_{F-C} = 10.7 Hz, Ar–C), 117.45–114.54 (m, Ar–C), 101.45 (C-1), 70.25 (C-2), 73.47 (C-3), 68.23 (C-4), 75.75 (C-5), 60.39 (C-6); HRMS, $[M+Na]^+$, $C_{12}H_{14}O_6F^{35}ClNa$, calcd 331.0361, found 331.0349; $C_{12}H_{14}O_6F^{37}ClNa$, calcd 333.0331, found 333.0249.

Kinetic Experiments. Relative substrate efficacies of **16**–**22** were compared using ^{19}F NMR. Enzyme reactions were conducted at 37 °C in PBS (0.1 M, pH 7.4) using β-gal (E801A, Promega, Madison, WI). Fluorophenyl β-D-galactopyranosides **16**–**22** (15 mmol) were dissolved in PBS (600 μL, pH 7.4) and β-gal (20 μL, 1 unit/

μL E801A in PBS) was added, followed by immediate ^{19}F NMR data acquisition at 37 °C with subsequent spectra every 101 s providing a kinetic curve over 51 min.

Substrate efficacy relative to traditional indicators was assessed by spectrophotometry. PFONPG **16** and ONPG (2.5 μmol/mL), respectively, were dissolved in buffer (pH 4.5, 10 mM sodium hydrogen phosphate, 5 mM citric acid). A solution of β-gal [G5160 from *Aspergillus oryzae* (Aldrich), 95 μg in 10 μL of buffer] was added and the absorption ($\lambda = 420$ nm) measured every 30 s for 10 min at room temperature.

Cell Culture and Cell Proliferation Assay. Dunning R3327-MAT-Lu rat prostate cancer cells (isolated for growth in culture by us from solid tumor tissues originally provided by Dr. Peter Peschke of the DKFZ, Heidelberg, Germany) and MTLn3 rat breast cancer cells (ATCC, Manassas, VA) were maintained in RPMI-1640 medium supplemented with 100 units/mL penicillin, 100 μg/mL streptomycin, and 10% fetal bovine serum (FBS) at 37 °C, with 5% CO_2 and 95% humidified air. Using TransFast transfection reagent (Promega), MAT-Lu and MTLn3 cells were cotransfected with pCMVβ (Clontech, Palo Alto, CA) comprising the *Escherichia coli lacZ* gene located under the human cytomegalovirus (CMV) immediate-early enhancer/promoter region and pCI-neo (Promega) carrying the neomycin phosphotransferase gene and were selected in growth medium containing 400 μg/mL G418 (Cellgro, Merndon, VA). Cells were harvested, trypsinized and resuspended in PBS, pH 7.4. **17** (1.9 mg, 100 μL) was added to cell suspension in PBS (10^8 cells in 600 μL), and ^{19}F NMR spectra were acquired immediately at 37 °C and again at various times up to 72 h. The β-gal activity of MAT-Lu-LacZ cells was 196 milliunits/10^7 cells and that for MTLn3-LacZ cells, 67 milliunits/10^7 cells.

The toxicity of aglycons and conjugates was assessed in both wild-type and LacZ-transfected MAT-Lu cells using a colorimetric CellTiter 96 Aqueous Nonradioactive MTS Cell Proliferation Assay (Promega). Assays were performed in triplicate using 24-well plates seeded with 10^3 cells per well in 500 μL of RPMI-1640 without phenol red and supplemented with 10% FCS and 2 mM glutamine. After 24 h of incubation, the medium was replaced with fresh medium. To determine IC_{50}, cells were incubated (72 h) with molecules **2**–**8** (0–1.6 mM) and **16**–**22** (0–4.5 mM), followed by the MTS assay. In each case successive dilutions were 2-fold. In some cases maximum tested doses were lower because some molecules showed poor solubility.

RESULTS

The methodology presented by Yoon et al. (*30*) to synthesize phenyl fluorogalactoside tetraacetates using potassium salts of the phenol produced mediocre yields for the fluorophenyl analogues **9** and **10**. By contrast, the phase-transfer approach using TBAB produced fluorophenyl β-D-galactopyranoside tetraacetates **9**–**15** in nearly quantitative yields. The anomeric β-D-configuration of compounds **9**–**15** in the $^4C_1$ chair conformation was unambiguously established on the basis of the observed ^1H NMR chemical shifts (δ_H 5.00–5.25) of the anomeric protons and the $J_{1,2}$ ($J \sim 8$ Hz) and $J_{2,3}$ ($J \sim 10$ Hz) coupling constants (*34*). The signals of the ^{13}C NMR spectra of **9**–**15** were assigned by comparison with the chemical shifts of *p*-nitrophenyl β-D-galactopyranoside (*30*). As expected, the anomeric carbon resonances appeared at ~100 ppm in accord with the β-D-configuration.

Deacetylation of **9**–**15** gave the free galactopyranosides **16**–**22** in nearly quantitative yields. ^1H NMR spectra of

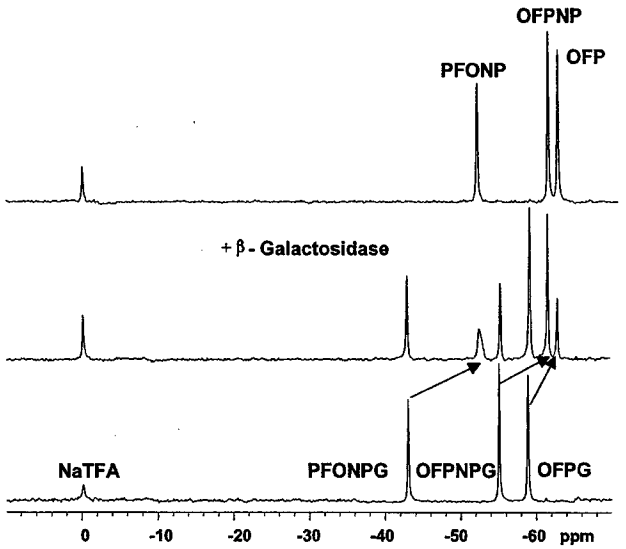

Figure 2. ^{19}F NMR spectra of β-D-galactopyranosides **16** (PFONPG), **17** (OFPNPG), and **19** (OFPG) in PBS at 37 °C (a) and following addition of β-gal [2 min) (b) and 34 min (c)].

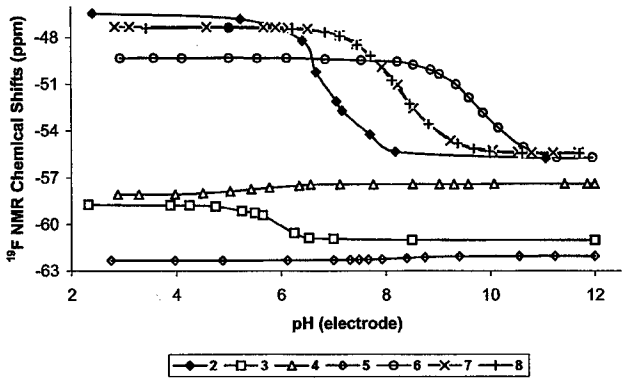

Figure 3. ^{19}F NMR chemical shift pH titration curves of **2**–**8** in saline at 25 °C.

16–**22** were assigned by ^1H–^1H COSY spectra and D_2O exchange. The ^1H NMR chemical shifts (δ_H 4.91–5.85) of the anomeric protons and the coupling constants ($J_{1,2} \sim 8$ Hz; $J_{2,3} \sim 10$ Hz) showed that the free galactopyranosides **16**–**22** (except **18**) retained the anomeric β-D-configuration with the $^4C_1$ chair conformation. The synthesis of **18** was more complex with the isolation of two distinct and separable isomers **18A** and **18B** in a 1:1 ratio, which also gave distinct ^{19}F NMR spectra. The downfield shifts of **18B** δ_{H1} at 5.85 with $J_{1,2} = 3.2$ Hz and δ_C at 104.14 compared to those of **18A** at 5.00 ppm with $J_{1,2} = 7.6$ Hz and δ_C at 106.06 suggest α and β isomers, respectively (*35*–*38*). Further evidence supporting the structural assignment of **18B** is that the α anomer resists activity of β-gal (Figure 4). Epimerization likely occurs during removal of the acetyl groups, possibly via a carbocation pathway due to the excellent leaving group ability of the 2-fluoro-6-nitrophenol anion group.

All except **18A** were stable in saline (0.9%), PBS (0.1 M), and fresh whole rabbit blood, at 25 and 37 °C, for extended periods showing no breakdown by ^{19}F NMR even after 1 week. **18A** hydrolyzed completely within 2 h in 0.1 M PBS buffer solution (pH 7.4) at 25 °C. By contrast, **18B** was stable even at 60 or 100 °C. As expected, the more polar substituted phenyl β-D-galactopyranosides **16**–**18** were most soluble and **19**–**21** quite

Table 1. ^{19}F Chemical Shifts (Parts per Million) of 16–22 before and after Hydrolysis by β-gal[a]

	compound							
	16	**17**	**18A**	**18B**	**19**	**20**	**21**	**22**
$\delta_{F(substrate)}$	−42.87	−54.93	−50.67	−49.37	−58.74	−45.87	−43.56	−43.82
$\delta_{F(product)}$	−52.71	−61.04	−58.67	−58.67	−62.30	−49.59	−48.13	−48.24
observed $\Delta\delta_F$	9.84	6.11	8.00	9.30	3.56	3.72	4.57	4.42
min $\Delta\delta_F$	1.57	3.84	6.72	8.7	3.3	3.46	3.76	3.58
max $\Delta\delta_F$	12.89	6.11	8.1	9.4	3.59	11.85	11.84	11.63

[a] β-gal (E801A, 20 units at 37 °C in 0.1 M PBS, pH 7.4).

Table 2. ^{19}F NMR pH Characterization of Aglycons at 25 °C

	compound						
	2	**3**	**4**	**5**	**6**	**7**	**8**
pK_a	6.87	6.03	5.44	8.33	9.80	8.31	8.28
$\delta_{(acid)}$	−46.44	−58.77	−58.07	−62.33	−49.33	−47.32	−47.40
$\delta_{(base)}$	−55.76	−61.01	−57.39	−62.04	−57.72	−55.40	−55.45
$\Delta\delta$	9.3	2.24	0.68	0.29	6.39	8.08	8.05

soluble in water, buffer, and whole blood, but 2-bromo-4-fluorophenyl β-D-galactopyranoside **22** was poorly soluble.

^{19}F NMR. Compounds **16–22** each gave a single, narrow ^{19}F NMR signal essentially invariant ($\Delta\delta \leq 0.03$) in rabbit whole blood, 0.9% saline, and PBS in the pH range 3–12 and at various temperatures ranging from 25 to 37 °C. The liberated aglycons display a chemical shift range of ~16 ppm (Table 1; Figure 2). Addition of β-galactosidase (E801A) in PBS (0.1 M, pH 7.4) at 37 °C caused each substrate to hydrolyze, releasing the pH sensitive aglycons **2–8** appearing also as a single narrow ^{19}F NMR signal (Figure 2; Table 1), consistent with the titration curves of **2–8** (Figure 3; Table 2). The minimum ^{19}F NMR chemical shift response observed was 3.56 ppm for **19** and maximum was 9.84 ppm for **16** at pH 7.4 (Table 1).

The various substrates **16–22** exhibited differential sensitivity to β-galactosidase in PBS (pH 7.4), and kinetics were monitored by changes in the integration of the ^{19}F NMR signals (Figures 2 and 4). The shapes of the kinetic curves suggest straightforward first-order kinetics for all substrates. The best substrate was **18A**, with an initial rate of 0.74 mM/min/unit, although this molecule hydrolyzed spontaneously within 2 h. **16**, **17**, and **19** also showed rapid cleavage, whereas **20–22** were somewhat slower and **18B** resisted enzyme action (as expected for an α anomer). By colorimetric assay **16** was essentially equivalent to ONPG as a substrate (Figure 5).

Several of the aglycons (**2**, **3**, **6–8**) exhibit a large ^{19}F NMR chemical shift in response to pH with $\Delta\delta$ reaching 9.3. However, **4** and **5** showed little response (Figure 3). The observed pK_a values were found to be in the range of 5.4–9.8 (Table 2). There was a strong linear correlation between initial rate of enzymatic hydrolysis of the substrates and pK_a of the aglycon (Figure 6).

When **17** was incubated with wild-type MAT-Lu rat prostate cancer cells (4 h, PBS, 37 °C under air–5% CO_2 with 95% humidity), ^{19}F NMR spectra showed no changes. When **17** was incubated with MAT-Lu-LacZ cells (92 ×

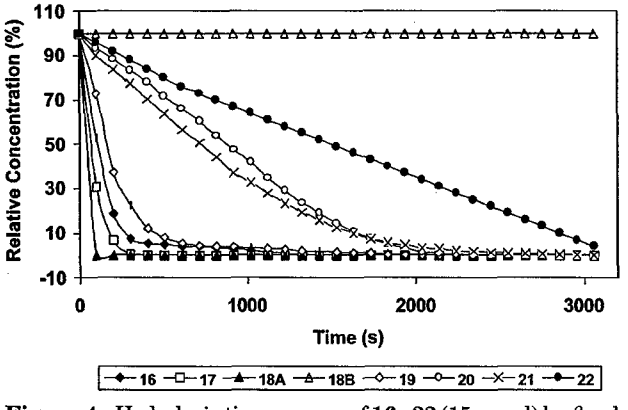

Figure 4. Hydrolysis time courses of **16–22** (15 mmol) by β-gal (E801A, 20 units) in PBS (0.1 M, 0.6 mL) at 37 °C.

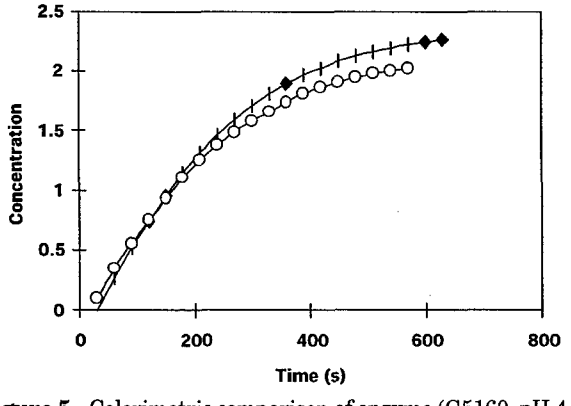

Figure 5. Colorimetric comparison of enzyme (G5160, pH 4.5) sensitivity for **16** and ONPG.

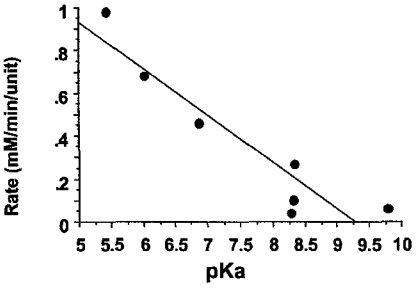

Figure 6. Brønsted plot of substrate susceptibility to β-gal (E801A, pH 7.4) versus of pK_a of liberated aglycon ($r^2 > 0.85$).

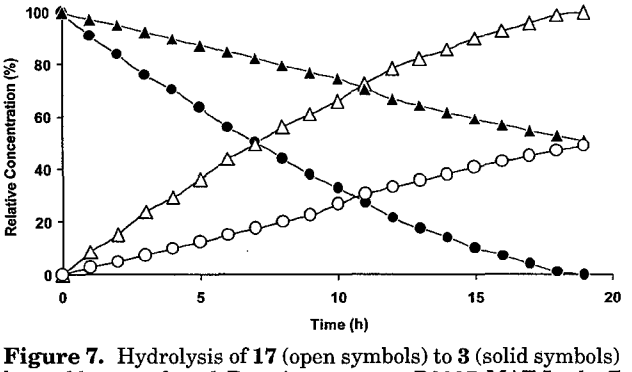

Figure 7. Hydrolysis of **17** (open symbols) to **3** (solid symbols) by stably transfected Dunning prostate R3327 MAT-Lu-*lacZ* cells (△, 92 × 10^6) and MTLn3-*lacZ* (○, 9.8 × 10^6) suspended in PBS at 37 °C.

Table 3. Toxicity of 2–8 and 16–22 to MAT-Lu -WT and -*LacZ* Cells (PBS, pH 7.4)

		molecule													
		2	**3**	**4**	**5**	**6**	**7**	**8**	**16**	**17**	**18A/B**	**19**	**20**	**21**	**22**
IC_{50} mM	MAT-Lu	<0.4	>1.6[a]	>1.3	<0.003	<1.6	<0.003	>0.9	>3.6[a]	<3	<4.5	>4.5	>4.5	>4.5[a]	>0.3[a]
	MAT-Lu-LacZ	<0.8	>1.6[a]	>1.3[a]	<0.003	< 0.8	<0.003	>0.9	>3.6[a]	>6	>4.5	>4.5	>4.5	>4.5[a]	>0.3[a]

[a] Greater than 90% survival at the highest dose tested.

10^6, 1803 milliunits of β-gal) in PBS, cleavage proceeded in a smooth monotonic manner with hydrolysis complete after 19 h (Figure 7). MTLn3-*LacZ* breast cancer cells (9.8×10^6, 67 milliunits of β-gal) hydrolyzed ~50% of **17** in 19 h.

Toxicity was evaluated for both aglycons and conjugates using both wild-type and lacZ expressing MAT-Lu cells (Table 3). **5** and **7** were severely cytotoxic, **2** was somewhat toxic (IC_{50} < 0.4 mM), and the other aglycons, **3**, **4**, **6**, and **8**, were less toxic (IC_{50} > 1 mM), making them more suitable for in vivo NMR investigations. Most conjugates were much less toxic; in particular, the toxicity of the aglycons was masked in **19** and **21**.

DISCUSSION

We have presented a method to efficiently and stereoselectively synthesize a series of fluorophenyl β-D-galactopyranosides **16**–**22** as potential ^{19}F NMR-based gene reporter molecules. We previously demonstrated that **16** could be used to assess β-gal activity in transiently transfected human prostate cancer cells (*27*). We have now assessed the relative substrate efficacy of a series of analogues and demonstrated the utility of **17** to assess β-gal activity in stably transfected rat breast and prostate tumor cells.

^{19}F NMR provides a large chemical shift response to small changes in molecular structure or microenvironment (*25*, *26*). Here, hydrolysis provided a minimum $\Delta\delta$ 3.56 between the substrate and the aglycon at pH 7.4, although depending on the pH, it could range from 1.6 to 12.9 ppm. Significantly, because of the chemical shift range of the ^{19}F signals of the aglycons **2**–**8** (up to 9.3 ppm), several substrates and aglycons can be detected simultaneously, allowing direct comparison of substrate efficacy (Figure 2). Preliminary data suggest that the approach used here could also be applied to glucosidases and glucoronides. Indeed, Schmidt and Monneret (*39*) presented ^{19}F NMR analysis of a fluorine-tagged nitrogen mustard pro-drug activated by glucuronidase. ^{19}F NMR spectroscopy lacks the spatial resolution of ^1H MRI, but the chemical shift accompanying substrate cleavage by β-gal unequivocally reveals enzyme activity. Comparing the substrates shows a 10-fold range in rate of substrate reaction at pH 7.4, the optimal pH for activity of β-gal derived from *Escherichia coli*. The observed initial rates were found to have a strong linear correlation with the pK_a of the aglycon (Figure 6), consistent with previous work by Richard et al. (*40*), who examined a series of alkyl β-galactosides. At pH 4.5—the optimal pH for β-gal derived from *Aspergillus oryzae*—**16** showed very similar activity in comparison with the traditional colorimetric indicator ONPG.

Substrates **16** and **17** share many attributes with similar sensitivity to β-gal at pH 7.4 (Figure 4), a large chemical shift range, and effective response to cells expressing β-gal (Figure 7) (*27*). All of the aglycons are electronically similar to the classic biochemical uncoupler dinitrophenol, raising potential concerns of toxicity. We have found extensive cell lysis upon direct exposure to the product aglycon **2** (IC_{50} < 0.4 mM), but **16** has allowed us to assess β-gal expression in culture (*27*). Other aglycons, **3**, **4**, **6**, and **8**, are less toxic, making them more suitable for in vivo NMR investigations, although **5** and **7** are severely cytotoxic. The conjugates are generally much less toxic, and indeed **19** and **21** showed essentially no toxicity up to the highest concentrations tested in wild-type or lacZ-expressing cells. Intriguingly, the conjugate **17** was more toxic that its aglycon. Similar toxicity was observed for all materials in wild-type or LacZ cells. Release of the less toxic, pH-sensitive aglycons suggests a novel approach to measuring pH at the site of enzyme activity. Moreover, noting the broad specificity of β-gal, we have synthesized an alternative galactoside with the ^{19}F NMR pH indicator fluoropyridoxol (*25*), as the aglycon and preliminary data show that it is also sensitive to enzyme activity (*41*).

We believe that noninvasive detection of gene reporter molecules will become increasingly important in biomedicine. It will be important to have diverse agents, genes, and modalities for specific applications. Fluorophenyl β-D-galactosides offer a novel approach for addressing β-gal activity. Moreover, we believe the concept of using ^{19}F NMR to monitor gene transfection, together with the molecular approach presented here, can serve as a platform technology with widespread application to many diverse genes and enzymes.

ACKNOWLEDGMENT

Supported in part by DOD Breast Cancer Initiative IDEA Award BC022001 DAMD17-03-1-0343-01, a DOD Prostate Cancer Initiative Postdoctoral Award W81XWH-04-10331 (L.L.), and the Cancer Imaging Program, NCI Pre-ICMIC P20 CA086354. NMR experiments were conducted at the Mary Nell and Ralph B. Rogers NMR Center, an NIH BTRP facility (P41-RR02584).

LITERATURE CITED

(1) Bronstein, I., Fortin, J., Stanley, P. E., Stewart, G. S., and Kricka, L. J. (1994) Chemiluminescent and bioluminescent reporter gene assays. *Anal. Biochem. 219*, 169–181.

(2) Contag, C. H., Jenkins, D., Contag, P. R., and Negrin, R. S. (2000) Use of reporter genes for optical measurements of neoplastic disease in vivo. *Neoplasia 2*, 41–52.

(3) Hoffman, R. (2002) Green fluorescent protein imaging of tumour growth, metastasis, and angiogenesis in mouse models. *Lancet Oncol. 3*, 546–556.

(4) Contag, C. H., and Ross, B. D. (2002) It's not just about anatomy: In vivo bioluminescence imaging as an eyepiece into biology. *J. Magn. Reson. Imag. 16*, 378–387.

(5) Herschman, H. R. (2002) Non-invasive imaging of reporter genes. *J. Cell. Biochem. 39*, 36–44.

(6) Tjuvajev, J. G., Doubrovin, M., Akhurst, T., Cai, S., Balatoni, J., Alauddin, M. M., Finn, R., Bornmann, W., Thaler, H., Conti, P. S., and Blasberg, R. G. (2002) Comparison of radiolabeled nucleoside probes (FIAU, FHBG, and FHPG) for PET imaging of HSV1-tk gene expression. *J. Nucl. Med. 43*, 1072–1083.

(7) Haberkorn, U., Altmann, A., Jiang, S., Morr, I., Mahmut, M., and Eisenhut, M. (2001) Iodide uptake in human anaplastic thyroid carcinoma cells after transfer of the human thyroid peroxidase gene. *Eur. J. Nucl. Med. 28*, 633–638.

(8) Weissleder, R., Simonova, M., Bogdanova, A., Bredow, S., Enochs, W. S., and Bogdanov, A. J. (1997) MR imaging and

scintigraphy of gene expression through melanin induction. *Radiology 204*, 425−429.
(9) Moore, A., Josephson, L., Bhorade, R. M., Basilion, J. P., and Weissleder, R. (2001) Human transferrin receptor gene as a marker gene for MR imaging. *Radiology 221*, 244−250.
(10) Stegman, L. D., Rehemtulla, A., Beattie, B., Kievit, E., Lawrence, T. S., Blasberg, R. G., Tjuvajev, J. G., and Ross, B. D. (1999) Noninvasive quantitation of cytosine deaminase transgene expression in human tumor xenografts with in vivo magnetic resonance spectroscopy. *Proc. Natl. Acad. Sci. U.S.A. 96*, 9821−9826.
(11) Beckwith, J. R., and Zipser, D. (1970) in *The Lactose Operon*, Cold Spring Harbor, Cold Spring Harbor, NY.
(12) Serebriiskii, I. G., and Golemis, E. A. (2000) Uses of lacZ to study gene function: evaluation of β-galactosidase assays employed in the yeast two-hybrid system. *Anal. Biochem. 285*, 1−15.
(13) Kruger, A., Schirrmacher, V., and Khokha, R. (1999) The bacterial lacZ gene: An important tool for metastasis research and evaluation if new cancer therapies. *Cancer Metastasis Rev. 17*, 285−294.
(14) Pulvin, S., Friboulet, A., and Thomas, D. (1990) Substrate inhibition or activation kinetics of the β-galactosidase from the extreme thermoacidophile archaebacterium *Caldariella acidophila*. *Biochim. Biophys. Acta 1041*, 97−100.
(15) Pocsi, I., Taylor, S. A., Richardson, A. C., Smith, B. V., and Price, R. G. (1993) Comparison of several new chromogenic galactosides as substrates for various β-D-galactosidases. *Biochim. Biophys. Acta 1163*, 54−60.
(16) James, A. L., Perry, J. D., Ford, M., Armstrong, L., and Gould, F. K. (1996) Evaluation of cyclohexenoesculetin-β-D-galactoside and -hydroxyquinoline-β-D-galactoside as substrates for the detection of β-galactosidase. *Appl. Environ. Microbiol. 62*, 3868−3870.
(17) James, A. L., Perry, J. D., Chilvers, K., Robson, I. S., Armstrong, L., and Orr, K. E. (2000) Alizarin-β-D-galactoside: a new substrate for the detection of bacterial β-galactosidase. *Lett. Appl. Microbiol. 30*, 336−340.
(18) Manafi, M., Kneifel, W., and Bascomb, S. (1991) Fluorogenic and chromogenic substrates used in bacterial diagnostics. *Microbiol. Rev. 55*, 335−348.
(19) Buller, C. J., Zang, X. P., Howard, E. W., and Pento, J. T. (2003) Measurement of β-galactosidase tissue levels in a tumor cell xenograft model. *Methods Findings Exp. Clin. Pharmacol. 25*, 713−716.
(20) Youngman, P., Zuber, P., Perkins, J. B., Sandman, K., Igo, M., and Losick, R. (1985) New ways to study developmental genes in spore-forming bacteria. *Science 228*, 285−290.
(21) Alam, J., and Cook, J. L. (1990) Reporter genes: Application to the study of mammalian gene transcription. *Anal. Biochem. 188*, 245−254.
(22) Horwitz, J. P., Chua, J., Curby, R. J., Tomson, A. J., DaRooge, M. A., Fisher, B. E., Mauricio, J., and Klundt, I. (1964) Substrates for cytochemical demonstration of enzyme activity. I. Some substituted 3-indolyl-β-D-glycopyranosides. *J. Med. Chem. 7*, 574−575.
(23) Heuermann, K., and Cosgrove, J. (2001) S-Gal: an autoclavable dye for color selection of cloned DNA inserts. *Biotechniques 30*, 1142−1147.
(24) Louie, A. Y., Huber, M. M., Ahrens, E. T., Rothbacher, U., Moats, R., Jacobs, R. E., Fraser, S. E., and Meade, T. J. (2000) In vivo visualization of gene expression using magnetic resonance imaging. *Nat. Biotechnol. 18*, 321−325.
(25) Mason, R. P. (1999) Transmembrane pH gradients in vivo: measurements using fluorinated vitamin B6 derivatives. *Curr. Med. Chem. 6*, 481−499.
(26) Mason, R. P., Ran, S., and Thorpe, P. E. (2002) Quantitative assessment of tumor oxygen dynamics: molecular imaging for prognostic radiology. *J. Cell. Biochem. 87S*, 45−53.
(27) Cui, W., Otten, P., Li, Y., Koeneman, K., Yu, J., and Mason, R. P. (2004) A novel NMR approach to assessing gene transfection: 4-fluoro-2-nitrophenyl-β-D-galactopyranoside as a prototype reporter molecule for β-galactosidase. *Magn. Reson. Med. 51*, 616−620.
(28) Hwang, D. R., and Scott, M. E. A. (1988) Chromogenic Substrates for β-Galactosidase, Eur. Pat. Appl. EP 88-304173 19880509.
(29) Guder, H. J., Herrmann, R. Z., and Zdunek, D. (1992) Preparation of Nitrophenyl β-D-Galactopyranosides as β-Galactosidase Substrates for Cloned Enzyme Donor Immunoassay (CEDIA), DE 4021063 A1 19920109; assignee: Boehringer Mannheim G.m.b.H.
(30) Yoon, S., Kim, H. G., Chun, K. H., and Shin, J. E. N. (1996) 4-deoxy-analogs of *p*-nitrophenyl β-D-galactopyranosides for specificity study with β-galactosidase from *Escherichia coli*. *Bull. Korean Chem. Soc. 17*, 599−604.
(31) Garegg, P. I. (1997) Thioglycosides as glycosyl donors in oligosaccharide synthesis. *Adv. Carbohydr. Chem. Biochem. 52*, 179−205.
(32) Ernst, B., Hart, G. W., and Sinäy, P. (2000) in *Chemistry of Saccharides; Chemical Syntheses of Glycosides and Glycomimetics*, Wiley-VCH, Weinheim, Germany.
(33) Lam, S. N., and Gervay-Hague, J. (2002) Solution-phase hexasaccharide synthesis using glucosyl iodides. *Org. Lett. 4*, 2039−2042.
(34) Dushin, R. G., and Danishefsky, S. J. (1992) Stereospecific synthesis of aryl β-glucosides: an application to the synthesis of a prototype corresponding to the aryloxy carbohydrate domain of vancomycin. *J. Am. Chem. Soc 114*, 3471−3475.
(35) Ding, Y. L., and Liu, Y. T. (1991) Stereoselective syntheses of acetylated *o*-tolyl 1-thioglycosides. *Carbohydr. Res. 209*, 306−310.
(36) Mizutani, K., Kasai, R., and Tanaka, O. (1980) 13C-NMR spectroscopy of α- and β-anomeric series of alkyl L-arabinopyranosides. *Carbohydr. Res. 87*, 19−26.
(37) Kasai, R., Okihara, M., Asakawa, J., Mizutani, K., and Tanaka, O. (1979) 13C-NMR study of a- and b-anomeric pairs of D-mannopyranosides and L-rhamnopyranosides. *Tetrahedron 35*, 1427−1432.
(38) Duus, J. O., Gotfredsen, C. H., and Bock, K. (2000) Carbohydrate structural determination by NMR spectroscopy: modern methods and limitations. *Chem. Rev. 100*, 4589−4614.
(39) Schmidt, F., and Monneret, C. (2002) In vitro fluorine-19 nuclear magnetic resonance study of the liberation of antitumor nitrogen mustard from prodrugs. *J. Chem. Soc., Perkin Trans 1* 1302−1308.
(40) Richard, J. P., Westerfeld, J. G., and Lin, S. (1995) Structure−reactivity relationships for β-galactosidase (*Escherichia coli*, lac Z). 1. Bronsted parameters for cleavage of alkyl β-D-galactopyranosides. *Biochemistry 34*, 11703−11712.
(41) Yu, X., and Mason, R. P. (2003) Novel in vivo gene reporter molecule using fluorinated vitamin B6 as ^{19}F NMR indicator. In *Proceedings of the International Society for Magnetic Resonance in Medicine*, Toronto, Canada, p 675 ISMRM, Berkeley, CA.

BC049936D

Synthesis and Evaluation of a Novel Gene Reporter Molecule: Detection of β-galactosidase Activity Using ^{19}F NMR of a Fluorinated Vitamin B_6 Conjugate+

FINAL

Jianxin Yu[1], Zhenyi Ma[1], Yingming Li[2,$], Kenneth S. Koeneman[2,$], Li Liu[1], Ralph P. Mason[1,*]

Departments of Radiology[1] and Urology[2], UT Southwestern Medical Center, Dallas, TX, USA

Abstract: Gene therapy has emerged as a promising strategy for treatment of various diseases. However, widespread implementation is hampered by difficulties in assessing the success of transfection, in particular, the spatial extent of expression in the target tissue and the longevity of expression. Thus, the development of non-invasive reporter techniques based on appropriate molecules and imaging modalities may help to assay gene expression. We now report the design, synthesis and evaluation of a novel *in vivo* gene transfection reporter molecule 3-*O*-(β-D-galactopyranosyl)-6-fluoropyridoxol (GFPOL) using fluorinated vitamin B_6 as the ^{19}F NMR sensitive aglycone. GFPOL exhibits the following strengths as an *in vivo* ^{19}F NMR gene expression reporter: (a) large chemical shift response to enzyme cleavage ($\Delta\delta$=8.00 ppm); (b) minimal toxicity for substrate or aglycone; (c) good water solubility; (d) good blood stability; (e) pH responsiveness of aglycone.

Key Words: β-galactosidase, ^{19}F NMR, gene reporter, pyridoxol, pH.

INTRODUCTION

Gene therapy shows promise for the treatment various disorders and clinical trials are underway. However, non-invasive detection of transgenes *in vivo* would be of considerable value for assessing the location, magnitude and persistence of expression. Generally, therapeutic genes are not readily detected, and thus, various reporter genes have been developed and are widely applied in molecular biology, *e.g.*, β-galactosidase (β-gal), β-glucuronidase, chloramphenicol acetyltransferase, and firefly luciferase [1]. Among these, the *lacZ* gene, encoding β-gal, is the most attractive reporter gene, because β-gal activity is readily assessed *in vitro* in hosts as evolutionarily diverse as bacteria, yeast, and mammals, and its introduction has become a standard means of assaying clonal insertion, transcriptional activation, protein expression, and protein interaction [2]. Many chromogenic or fluorogenic substrates are well-established, but they are generally limited to histology or *in vitro* assays [3-8].

Recently, Weissleder *et al.* [9] presented a near infrared approach based on 9H-(1, 3-dichloro-9, 9-dimethylacridin-2-one-7-yl) β-D-galactopyranoside (DDAOG), and Meade et al. [10] reported an NMR approach using 1-[2-(β-D-galactopyranosyloxy) propyl]-4, 7, 10-tris (carboxymethyl)-1, 4, 7, 10-tetraazacyclododecane) gadolinium (III) (EgadMe), to assess β-gal activity *in vivo*. These diverse substrates emphasize the promiscuity (lack of substrate specificity) of β-gal activity. However, EgadMe was found to be 500 times less sensitive to β-gal than the traditional "yellow" biochemical indicator *ortho*-nitrophenol-β-D-galactopyranoside (*ONPG*) and failed to enter cells, necessitating direct microinjection. We realized that introduction of a fluorine atom into the traditional nitrophenol aglycones could generate NMR indicator molecules with minimal perturbation to a well-established molecular structure. Indeed, we successfully demonstrated the use of *p-fluoro-o*-nitrophenyl β-D-galactopyranoside (*PFONPG*) to detect enzyme activity in solution and transfected tumor cells [11]. *PFONPG* exhibits virtually identical sensitivity to cleavage by β-gal as compared with *ONPG* [12]. However, the liberated aglycone p-fluoro-o-nitrophenol (*PFONP*) exhibits some cytotoxicity, likely by analogy to the well known uncoupler of oxidative phosphorylation 2, 4-dinitrophenol [13]. More recently, we showed that various analogs of the aglycone structure (halophenols) showed significant differences in rate of response to enzyme action and some of these alternate aglycones exhibit much lower toxicity [12]. We now report the design, synthesis, and evaluation of another novel *in vivo* gene transfection reporter molecule using fluorinated vitamin B_6 as a stable aglycone and sensitive ^{19}F NMR indicator.

RESULTS AND DISCUSSION

Design

^{19}F NMR signals are exquisitely sensitive to molecular changes and often also to the microenvironment, and thus, there are many reporter molecules exploiting fluorine atoms [14]. We have previously shown that 6-fluoropyridoxol (**1**, **FPOL**) exhibits exceptional sensitivity to changes in pH

*Address correspondence to this author at the Department of Radiology, The University of Texas Southwestern Medical Center at Dallas, 5323 Harry Hines Blvd, Dallas, Texas 75390-9058, USA; Tel: (214)-648-8926; Fax: (214)-648-4538; E-mail: Ralph.Mason@UTSouthwestern.edu

$Current address: Dept. of Urologic Surgery and Comprehensive Cancer Center, University of Minnesota, Minneapolis, MN, USA

+Presented in part at the 11th *ISMRM* in Toronto, Canada, 2003

1573-4064/05 $50.00+.00

with ~10 ppm acid/base ^{19}F NMR shift [15]. We recognized that **1** could serve as a replacement for fluorophenol aglycones offering similar steric and electrostatic properties. The fluorine atom located *para* to the phenolic group should provide sensitive response to enzyme induced cleavage of the substrate **GFPOL. FPOL** exhibits little toxicity and can reveal local pH in a similar manner to the prototype aglycone **PFONP.**

Synthesis

Condensation of **FPOL** and galactose has regioselectivity requirements and Scheme **1** outlines a synthetic route exploiting regioselective protection of the α^4, α^5- hydroxyl groups through ketal condensation. However, the ketal addition of **1** with acetone using standard conditions gave 6-fluoro-3, α^4-isopropylidenepyridoxol, as major product and the desired 6-fluoro-α^4, α^5-isopropylidenepyridoxol **2,** as minor by-product. Testing various acids as catalysts showed 2% H_2SO_4 acetone solution to provide the best yield of **2** (26%). The regioselectivity of the acetonation reaction was confirmed by analyzing ^{1}H-NMR spectra of **2** and 6-fluoro-3, α^4-isopropylidenepyridoxol, in which the 5-CH_2 signal of **2** appeared at 5.03 ppm as singlet and of 6-fluoro-3, α^4-isopropylidenepyridoxol at 4.97 ppm, but as doublet ($J_{H\text{-}5,\ HO\text{-}5}$=1.2 Hz) due to the coupling of the 5-OH. The inefficient reaction is presumably due to the unfavorable seven member ring, as opposed to alternate six member ring.

Treatment of **2** with 2, 3, 4, 6-tetra-*O*-acetyl-α-D-galactopyranosyl bromide **3** using the Koenigs-Knorr glycosylation method gave 3-*O*-(2, 3, 4, 6-tetra-*O*-acetyl-β-D-galactopyranosyl)-α^4, α^5-isopropylidene-6-fluoropyridoxol **4** in 85% yield. NMR verified that the galactose was in the β-configuration ($\delta_{H\text{-}1'}$ 4.64 ppm (doublet, $J_{1,2}$=8.0 Hz) and $\delta_{C\text{-}1'}$ 100.03 ppm). The correlation between 2-CH_3 and H-1' of sugar ring from the NOSEY spectrum of **4** verified that 2, 3, 4, 6-tetra-*O*-acetyl-β-D-galactopyranosyl residue connected at the 3 phenolic site provided further evidence that acetonation reaction did occur regioselectively on 4, 5 hydroxymethyl groups.

Cleavage of acetonide **4** for synthesis of 3-*O*-(2, 3, 4, 6-tetra-*O*-acetyl-β-D-galactopyranosyl)-6-fluoropyridoxol **5** was achieved, however, the yields were low (≤15%), based on several hydrolysis conditions, such as 80% AcOH, 1% HCl or 90% CF_3CO_2H in MeOH, CH_2Cl_2 or **1**, 4-dioxane at various temperatures (60~100 °C). A moderate amount of **1** was recoverable indicating that the β-D-galactopyranosyl $C_{1'(gal)}$-O_3 bond became weak and sensitive to acid hydrolysis presumably due to the presence of 6-fluorine atom. Acetylation of **5** to **6** facilitated purification and structural characterization by NMR. Finally, deacetylation of **6,** in NH_3/MeOH from 0°C to room temperature yielded the target molecule **GFPOL** in quantitative yield. The overall yield for **GFPOL** through this five-step route was ~3% with limiting steps in the α^4, α^5-isopropylidene group formation and hydrolysis procedures (a and c).

We thus considered alternate approaches, *e.g.*, Scheme **2.** Particularly, the acidic phenolic group *para* to the 6-fluorine atom should be ionized under mild base conditions to selectively react with benzyl bromide affording the expected 3-mono benzylated product under carefully controlled conditions. When benzyl bromide (1.1 equiv.) was added dropwise over a period of 4~5 h to the well-stirred reaction mixture of compound **1** in a biphasic dichloromethane-aqueous system (pH 10~11) using tetrabutylammonium bromide (TBAB) as the phase-transfer catalyst (PTC), 3-*O*-benzyl-6-fluoropyridoxol **7** was isolated as major product in 76% yield with small amounts of di-*O*-benzyl derivatives 3, α^4-di-*O*-benzyl-6-fluoropyridoxol (16%) and 3, α^5-di-*O*-benzyl-6-fluoropyridoxol (8%). The structure of **7** was established on the basis of the coupling characteristics of α^4, α^5-CH_2 as doublets ($J_{H\text{-}4,\ HO\text{-}4}$=6.0 Hz, $J_{H\text{-}5,\ HO\text{-}5}$=5.4 Hz) and α^4, α^5-OH as triplets in the ^{1}H-NMR spectrum. Treatment of **7** with acetic anhydride in pyridine from 0 °C to r.t. overnight gave 3-O-benzyl-α^4, α^5-di-*O*-acetyl-6-fluoropyridoxol **8** in

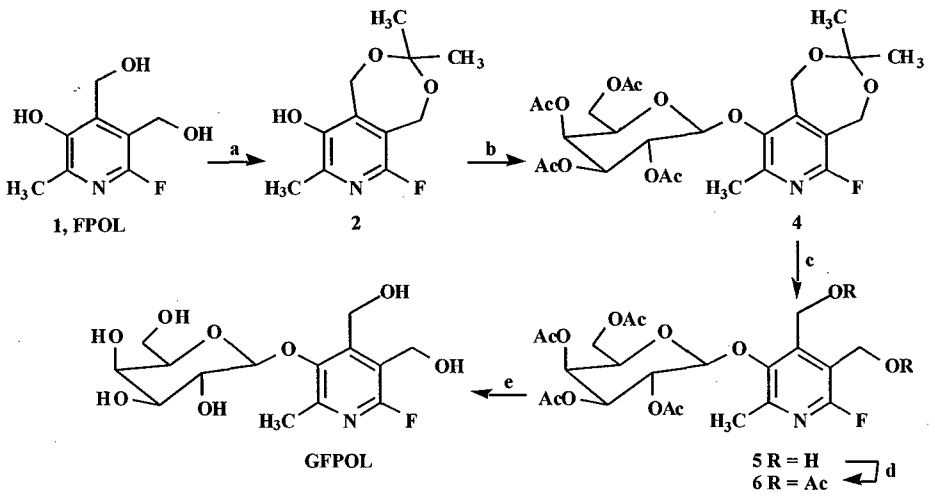

Scheme 1. Reagents and conditions: (a) 2% H_2SO_4, acetone, r.t. 4~5 h, 26%; (b) 2, 3, 4, 6-tetra-*O*-acetyl-α-D-galactopyranosyl bromide (**3**), $Hg(CN)_2$, 4Å M.S., CH_2Cl_2, r.t., 12 h, 85%; (c) 80% AcOH, 80 °C, 4~5 h, 15%; (d) Ac_2O-Pyridine, 0 °C→r.t., 24 h, quantitative yield; (e) NH_3-MeOH, 0 °C→r.t., 24 h, quantitative yield.

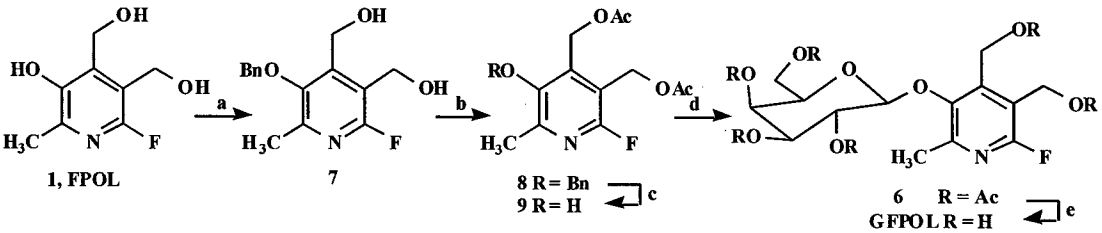

Scheme 2. Reagents and conditions: (a) benzyl bromide (1.1 equiv.), CH_2Cl_2-H_2O, pH 10~11, 50 °C, TBAB, 4~5 h, 76%; (b) Ac_2O-Pyridine, 0 °C→r.t., 24 h, quantitative yield; (c) H_2, Pd/C, r.t., 12 h, quantitative yields; (d) 2, 3, 4, 6-tetra-*O*-acetyl-α-D-galactopyranosyl bromide (**3**), $Hg(CN)_2$, 4Å M.S., CH_2Cl_2, r.t., 12 h, 90%; (e) NH_3-MeOH, 0 °C→r.t., 24 h, quantitative yield.

quantitative yield. The 3-benzyl protecting group was removed under 5% Pd/C hydrogenation overnight affording nucleophile α^4, α^5-di-*O*-acetyl-6-fluoropyridoxol **9** in quantitative yield. **9** was then subjected to a procedure similar to that described for the preparation of galactoside **4** giving 3-*O*-(2, 3, 4, 6-tetra-*O*-acetyl-β-D-galactopyranosyl)-α^4, α^5-di-*O*-acetyl-6-fluoropyridoxol **6** in 90% yield. After work up and deacetylation, the target compound **GFPOL** was obtained in 68% overall yield over five steps.

Recognizing the differential reactivity of the 3 phenolic group over the hydroxymethyl groups suggested a more direct synthesis. Direct galactopyranosylation of **1** with 2, 3, 4, 6-tetra-*O*-acetyl-α-D-galactopyranosyl bromide **3** failed as a result of the very low selectivity of the Koenigs-Knorr glycosylation reaction for the 3 phenolic group in the presence of the two free active hydroxymethyl groups. Product **5** could not be isolated, but using 2, 3, 4, 6-tetra-*O*-acetyl-α-D-galactopyranosyl bromide **3** phase-transfer catalysis gave **5** (88%) directly, and **GFPOL** (88%) through only two reaction steps (Scheme **3**).

In conclusion, Scheme **3** provided a very efficient and direct method to stereo- and regioselectively synthesize 3-*O*-(β-D-galactopyranosyl)-6-fluoropyridoxol **GFPOL** in high yields. Large-scale preparation of **GFPOL** can be performed by these PTC methods.

Characteristics

As expected, **GFPOL** readily dissolves in saline, whole blood, or PBS buffer, and is much more soluble than the aglycone **1**. **GFPOL** was stable in aqueous solutions in the pH range 3 to 12 at temperatures from 25 to 37 °C for at least 5 days. Cell viability assays [16] showed that neither **GFPOL** nor **FPOL** exhibited significant cytotoxicity (Fig. **1**). For **GFPOL** viability exceeded 98% at all concentrations tested and for **FPOL** survival was > 80% up to 2 mM.

Proton decoupling was applied to simplify ^{19}F NMR spectra and sodium trifluoroacetate (NaTFA) in a capillary was used as an external standard. **GFPOL** gave a single narrow ^{19}F NMR signal at δ -3.22 ppm essentially invariant ($\Delta\delta \leq 0.06$ ppm) with pH in the range 3 to 12 and temperatures from 25 to 37 °C. Addition of β-gal (E801A) in PBS buffer (0.1M, pH=7.4) at 37 °C caused hydrolysis releasing the pH indicator aglycone **FPOL** appearing also as a single narrow ^{19}F signal shifted up-field to δ -11.21 ppm (Fig. **2**), consistent with our previous titration curve of **FPOL** [15]. Sequential ^{19}F NMR spectra showed that **GFPOL** decreased monotonically, releasing free **FPOL** with an initial rate of 4.3 μmol/min/unit (Fig. **3**). For comparison **PFONPG** gave 19 μmol/min/unit and **OFPNPG** gave 32 μmol/min/unit [12]. **PFONPG** was previously shown to exhibit very similar substrate activity to the traditional yellow biochemical indicator **ONPG** [12]. When **GFPOL** was incubated with wild type human cancer cells (prostate PC-3 or C4-2 (LNCaP lineage derived androgen independent subline)) or (breast MCF-7) for 5 h in PBS buffer at 37 °C under 5% CO_2 in air with 95% humidity, no changes were observed in the ^{19}F NMR spectra. However, addition of **GFPOL** to cells from these lines, which had been transfected transiently or stably to express β-gal led to cleavage of **GFPOL**, as detected over a period of hours (Fig. **4**).

GFPOL provides further evidence for the ^{19}F NMR approach to assessing enzyme activity *in situ*. We are currently extending applications to imaging based on chemical shift selective excitation exploiting the large chemical shift difference between the substrate and product.

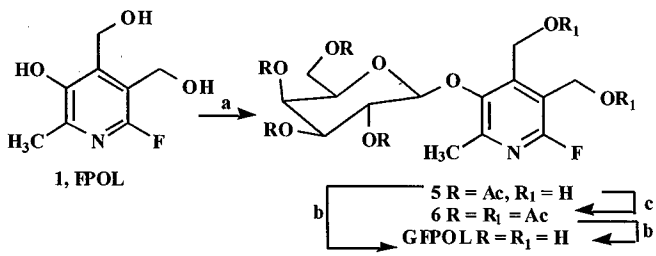

Scheme 3. Reagents and conditions: (a) 2, 3, 4, 6-tetra-O-acetyl-α-D-galactopyranosyl bromide (**3**), CH_2Cl_2-H_2O, pH 10~11, r.t., TBAB, 4~5 h, 88%; (b) NH_3-MeOH, 0 °C→r.t., 24 h, quantitative yield; (c) Ac_2O-Pyridine, 0 °C→r.t., 24 h, quantitative yield.

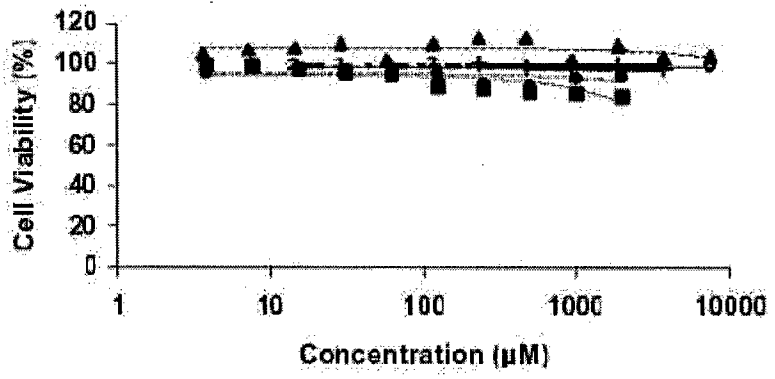

Fig. (1). Cellular toxicity of reporter molecules o C4-2 cells (GFPOL), + PC3 cells (GFPOL), • MAT-Lu cells (FPOL), ▲ MAT-Lu-LacZ cells (FPOL), ■ MAT-Lu-LacZ cells (GFPOL).

We are also initiating studies in living animals and exploring the utility of enzyme activated pH measurements.

EXPERIMENTAL

General Methods

NMR spectra were recorded on a Varian Inova 400 spectrometer (400 MHz for ^{1}H, 100 MHz for ^{13}C) with $CDCl_3$, acetone-d_6 or DMSO-d_6, as solvents, and chemical shifts referenced to TMS, as internal standard. ^{19}F NMR (376 MHz) signals are referenced to dil. sodium trifluoroacetate (NaTFA) in an external capillary. 2, 3, 4, 6-tetra-O-acetyl-α-D-galactopyranosyl bromide (**3**) was purchased from Sigma. Reactions requiring anhydrous conditions were performed under nitrogen or argon. $Hg(CN)_2$ was dried before use at 50 °C for 1 h, CH_2Cl_2 was dried over Drierite. Solutions in organic solvents were dried with anhydrous sodium sulfate, and concentrated *in vacuo* below 45 °C. Column chromatography was performed on silica gel (200~300 mesh) by elution with cyclohexane-EtOAc and silica gel GF_{254} used for analytical TLC (Aldrich). Detection was effected by spraying the plates with 5% $EtOH/H_2SO_4$ (followed by heating at 110 °C for 10 min.) or by direct UV. Microanalyses were performed on a Perkin-Elmer 2400 CHN microanalyser.

β-Gal (E801A) was purchased from Promega and enzymic reactions performed at 37 °C in PBS buffer (0.1M, pH 7.4). For enzyme kinetic experiments, **GFPOL** (5.25 mg) was dissolved in PBS buffer (600 μL, pH=7.4), a PBS solution of β-gal (20 μL, E801A, 1unit/μL) was added and NMR data were acquired immediately at 37 °C.

Both PC-3 and C4-2 were plated at 5 million cells per dish (P150) and grown for 24 h. Then PC-3 and C4-2 were transfected for 48 h with a first generation adenovirus vector encoding the lacZ gene driven by the CMV promoter. PC-3 was transfected with 50 moi and C4-2 with 10 moi of Ad-CMV-lacZ. After 48 h incubation and washing, cells were trypsinized and concentrated to 10 million cells per ml. for further use (NMR).

Human breast cancer cells MCF-7 were stably co-transfected with pCMVβ (Clontech, Palo Alto, CA, USA), using TransFast™ Transfection Reagent (Promega, Madison, WI, USA) comprising the *E.coli lacZ* gene located under the human cytomegalovirus (CMV) immediate-early enhancer/ promoter region and pCI-neo (Promega, Madison, WI, USA) carrying the neomycin phosphotransferase gene. For MCF-7 cells clonal selection was applied to identify those cells with highest β-gal expression.

Control wild type and transfected human prostate tumor cells (PC3 and C4-2 (LNCaP lineage derived androgen independent subline)) and human breast tumor cells MCF-7 were grown in culture dishes under standard conditions and harvested. **GFPOL** (1.84 mg) in PBS buffer (70 μL) was

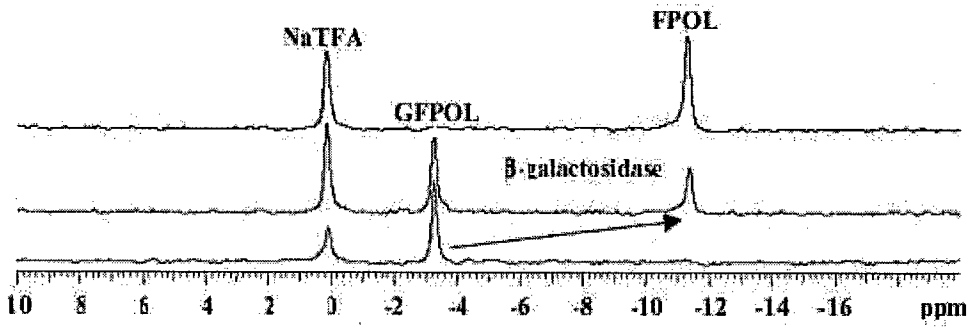

Fig. (2). ^{19}F NMR spectra of **GFPOL** during the hydrolysis by β-gal in PBS buffer at 37 °C.

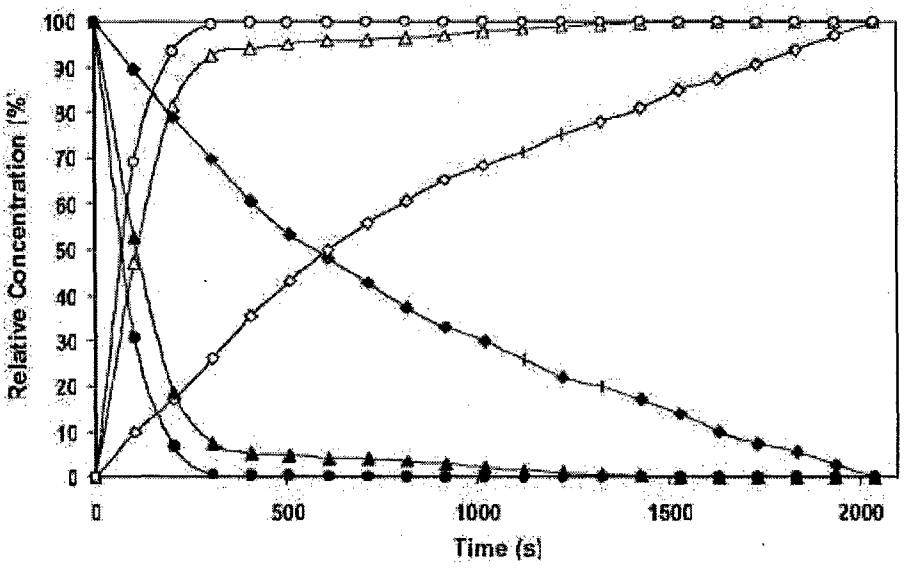

Fig. (3). Relative action of β-gal (E801A) on **GFPOL** (◆), PFONPG (Δ) and OFPNPG (O) in PBS buffer at 37 °C yielding **FPOL** (◇), PFONP (Δ) and OFPNP (O), respectivley . In each case 20 units of β-gal (E801A) were added to 15 mmol substrate in PBS at 37 °C.

added to suspension of 10^7 cells in PBS buffer (530 μL) and NMR data were acquired immediately, and again after incubation for various times up to 5 h at 37 °C (prostate tumor cells PC3 and C4-2) or at 22 °C (breast tumor cells MCF-7).

The sensitivities of human prostate cancer cells PC3, C4-2 and their LacZ transfected counterparts to **GFPOL** and **FPOL** were quantified using a colorimetric CellTiter 96 Aqueous Nonradioactive MTS Cell Proliferation Assay (Promega, Madison, WI, USA). The assays were performed in triplicate using 24-well plates seeded with 10^3 cells per well in 500 μL RPMI 1640 without phenol red and supplemented with 10% FCS and 2 mM glutamine. After 24 h incubation, the medium was replaced with fresh RPMI 1640 containing various concentrations of **GFPOL**. For the determination of IC_{50} drug concentrations, incubations with **GFPOL** (0~7.5 mM) and **FPOL** (0~2 mM) were performed for 72 h, followed by the MTS assay (Figure **1**).

Syntheses

α^4, α^5-O-isopropylidene-6-fluoropyridoxol 2

A suspension of 6-fluoropyridoxol **1** (0.50 g, 2.67 mmol) in anhydrous acetone (40 ml) containing 2% c.H_2SO_4 was stirred until TLC (4:1 cyclohexane-EtOAc) indicated complete reaction (4~5 h), then cold saturated Na_2CO_3 solution was added with vigorous stirring up to pH 8~9. The precipitate was filtered, the reaction mixture concentrated under reduced pressure followed by purification on flash silica gel column (4:1 cyclohexane-EtOAc) yielding the acetonide **2** (0.64 g, 26%) as a syrup, R_f 0.34(4:1 cyclohexane-EtOAc), Δ_H: 7.45(1H, s, HO-3), 5.03(2H, s,

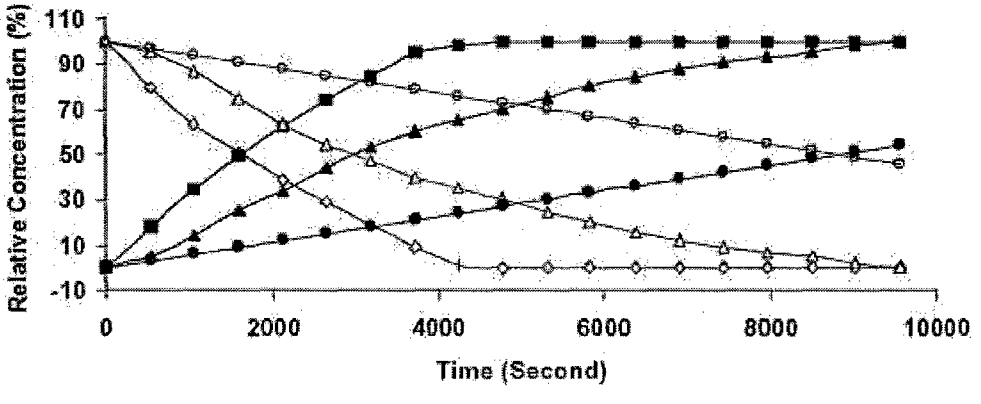

Fig. (4). Kinetic curves showing changes in **GFPOL** (open symbols) and **FPOL** (closed symbols) during incubation with human C4-2 (square) and PC-3 (triangle) prostate and MCF-7 breast (circle) cancer cells transfected to express β-gal. Prostate cells were investigated at 37 °C, while breast cells were examined at 22 °C in PBS buffer.

CH_2-5), 4.57(2H, s, CH_2-4), 2.33(3H, s, CH_3-2), 1.55(6H, s, 2×CH_3)ppm; Δ_C: 154.49(s, Py-C), 152.20(s, Py-C), 144.14(d, J_{F-C}=14.5 Hz, Py-C), 131.37(d, J_{F-C}=3.8 Hz, Py-C), 114.01(d, J_{F-C}=32.9 Hz, Py-C), 99.51(s, **C**Me_2), 59.04(d, J_{F-C}=3.8 Hz, CH_2-5), 54.51(s, CH_2-4), 31.62(s, C(**C**H_3)$_2$), 17.58(s, CH_3-2)ppm.

Anal. Calcd. for $C_{11}H_{14}NO_3F$(%): C, 58.13, H, 6.21, N, 6.17; Found: C, 58.08, H, 6.16, N, 6.11.

3-O-(2, 3, 4, 6-tetra-O-acetyl-β-D-galactopyranosyl)-α^4, α^5-O-isopropylidene-6-fluoropyridoxol 4

To a solution of α^4, α^5-*O*-isopropylidene-6-fluoropyridoxol **2** (0.62 g, 2.72mmol) and $Hg(CN)_2$ (0.88 g, 3.50 mmol) in dry CH_2Cl_2 (10 mL) containing freshly activated 4Å molecular sieve (2 g) was added dropwise **3** (1.23 g, 3.0 mmol, 1.1 equiv. in CH_2Cl_2). The mixture was stirred overnight in the dark at r.t. under N_2 until TLC indicated complete reaction. The mixture was diluted with CH_2Cl_2 (30 mL), filtered through Celite, washed, dried (Na_2SO_4) and concentrated *in vacuo*. The residue was purified on a silica gel column (2:3 cyclohexane-EtOAc) to yield **4** (1.29 g, 85%) as syrup, R_f 0.40(2:3 cyclohexane-EtOAc), Δ_H: 4.64(1H, d, $J_{1',2'}$=8.0 Hz, H-1'), 5.25(1H, dd, $J_{2',3'}$=10.0 Hz, H-2'), 5.02(1H, dd, $J_{3',4'}$=3.6 Hz, H-3'), 5.41(1H, dd, $J_{4',5'}$=3.2 Hz, H-4'), 3.97(1H, m, H-5'), 4.21(1H, dd, $J_{5',6a'}$=4.4 Hz, $J_{6a',6b'}$= 11.2 Hz, H-6a'), 4.13(1H, dd, $J_{5',6b'}$=7.2 Hz, H-6b'), 5.10(1H, d, $J_{CH2\text{-}4a,\ CH2\text{-}4b}$=8.0 Hz, CH_2-4a), 4.67(1H, d, $J_{CH2\text{-}4a,\ CH2\text{-}4b}$=8.0 Hz, CH_2-4b), 5.14 (1H, d, $J_{CH2\text{-}5a,\ CH2\text{-}5b}$=9.6 Hz, CH_2-5a), 5.12(1H, d, $J_{CH2\text{-}5a,\ CH2\text{-}5b}$=9.6 Hz, CH_2-5b), 2.42(3H, s, CH_3-2), 2.17, 2.09, 2.08, 1.99(12H, 4s, 4×CH_3CO), 1.61, 1.59(6H, 2s, 2×CH_3)ppm; Δ_C: 170.78, 170.39, 170.26, 170.11(4s, 4×CH_3**C**O), 155.44(s, Py-C), 153.15(s, Py-C), 145.48(d, J_{F-C}=15.2 Hz, Py-C), 133.16(d, J_{F-C}=4.0 Hz, Py-C), 116.95(d, J_{F-C}=32.1 Hz, Py-C), 101.41(s, **C**Me_2), 100.03(s, C-1'), 68.70(s, C-2'), 70.82(s, C-3'), 67.12(s, C-4'), 71.53(s, C-5'), 64.28(s, C-6'), 55.38(s, CH_2-4), 61.58(s, CH_2-5), 31.88(s, C(**C**H_3)$_2$), 20.90, 20.89, 20.82, 20.77(4s, 4×**C**H_3CO), 18.77(s, CH_3-2)ppm.

Anal. Calcd. for $C_{25}H_{32}NO_{12}F$(%): C, 53.84, H, 5.79, N, 2.51; Found: C, 53.79, H, 5.74, N, 2.49.

3-O-(2, 3, 4, 6-tetra-O-acetyl-β-D-galactopyranosyl)-6-fluoropyridoxol 5

A mixture of 3-*O*-(2, 3, 4, 6-tetra-*O*-acetyl-β-D-galactopyranosyl)-α^4, α^5-*O*-isopropylidene-6-fluoropyridoxol **4** (1.25 g, 2.50 mmol) in 80% AcOH (40 mL) was stirred at 80 °C for 4~5 h, until TLC (1:3 cyclohexane-EtOAc) showed complete reaction. The cooled mixture was neutralized with cold saturated Na_2CO_3, extracted (EtOAc, 4×30 mL), concentrated and purified by flash silica gel column (1:4 cyclohexane-EtOAc) yielding **5** (0.17 g, 15%) as a syrup, R_f 0.18(1:4 cyclohexane-EtOAc), δ_H: 4.79(1H, d, $J_{1',2'}$=8.0 Hz, H-1'), 5.55(1H, dd, $J_{2',3'}$=10.6 Hz, H-2'), 5.10(1H, dd, $J_{3',4'}$=3.6 Hz, H-3'), 5.41(1H, dd, $J_{4',5'}$=3.6 Hz, H-4'), 3.88(1H, m, H-5'), 4.24(1H, dd, $J_{5',6a'}$=4.4Hz, $J_{6a',6b'}$=12.0 Hz, H-6a'), 4.09(1H, dd, $J_{5',6b'}$=6.0 Hz, H-6b'), 5.01(2H, d, $J_{CH2\text{-}4a,\ CH2\text{-}4b}$=$J_{CH2\text{-}5a,\ CH2\text{-}5b}$=12.4 Hz, CH_2-4a, CH_2-5a), 4.62(1H, d, $J_{CH2\text{-}4a,\ CH2\text{-}4b}$=12.4Hz, CH_2-4b), 4.66(1H, d, $J_{CH2\text{-}5a,\ CH2\text{-}5b}$=12.4 Hz, CH_2-5b), 3.50(1H, m, HO-4, exchangeable with D_2O), 3.56(1H, m, HO-5, exchangeable with D_2O), 2.47(3H, s, CH_3-2), 2.23, 2.17, 2.02, 2.00(12H, 4s, 4×CH_3CO)ppm; Δ_C: 170.32, 170.28, 170.18, 169.48(4×CH_3**C**O), 158.78(s, Py-C), 156.42(s, Py-C), 150.33(d, J_{F-C}=15.2 Hz, Py-C), 147.62(d, J_{F-C}=4.6 Hz, Py-C), 120.17(d, J_{F-C}=32.0 Hz, Py-C), 102.39(s, C-1'), 68.91(s, C-2'), 70.74(s, C-3'), 67.19(s, C-4'), 71.93(s, C-5'), 61.98(s, C-6'), 55.91(s, **C**H_2-4), 59.60(s, **C**H_2-5), 20.99, 20.85, 20.70, 20.67(4s, 4×**C**H_3CO), 19.46(s, CH_3-2)ppm.

Anal. Calcd. for $C_{22}H_{28}NO_{12}F$(%): C, 51.05, H, 5.46, N, 2.71; Found: C, 51.00, H, 5.39, N, 2.68.

As an alternative, **5** was synthesized from **1** directly by phase transfer catalysis. To a well stirred CH_2Cl_2 (10 mL)-H_2O (10 mL) biphasic mixture (pH 10~11) of **1** (0.5 g, 2.67mmol) and tetrabutylammonium bromide (TBAB; 0.1 g, 0.31mmol) as the phase-transfer catalyst, a solution of 2, 3, 4, 6-tetra-*O*-acetyl-α-D-galactopyranosyl bromide (**3**)(1.21 g, 2.94 mmol, 1.1equiv.) in CH_2Cl_2 (10 mL) was added dropwise over a period of 4~5 h at r.t., and the stirring continued for an additional hour. The products were extracted (EtOAc, 4×20 mL), washed free of alkali, dried (Na_2SO_4), concentrated and the residue purified by column chromatography on silica gel (1:4 cyclohexane-EtOAc) to afford **5** (1.08 g, 88%) as a syrup, which was identical in all respects to the product obtained above.

3-O-(2, 3, 4, 6-tetra-O-acetyl-β-D-galactopyranosyl)-α^4, α^5-di-O-acetyl-6-fluoropyridoxol 6

A solution of **5** (1.20 g, 2.64mmol) in pyridine (30 mL) was treated with Ac_2O (15 mL). The reaction mixture was stirred from 0 °C to r.t., overnight, coevaporated with toluene under reduced pressure and the residue purified by flash silica gel column chromatography (1:1 cyclohexane-EtOAc) to give **6** (1.56 g, 100%) as a foamy solid, R_f 0.32(1:2 cyclohexane-EtOAc), δ_H: 5.15(1H, d, $J_{1',2'}$=7.8 Hz, H-1'), 5.18(1H, dd, $J_{2',3'}$=10.8 Hz, H-2'), 4.17(1H, dd, $J_{3',4'}$=6.0 Hz, H-3'), 5.41 (1H, dd, $J_{4',5'}$=5.6 Hz, H-4'), 5.31(1H, m, H-5'), 4.06(1H, dd, $J_{5',6a'}$=5.2 Hz, $J_{6a',6b'}$= 12.0 Hz, H-6a'), 4.01(1H, dd, $J_{5',6b'}$=6.8 Hz, H-6b'), 5.28(2H, m, CH_2-5), 5.12(2H, s, CH_2-4), 2.44(3H, s, CH_3-2), 2.17, 2.12, 2.03, 2.02, 1.99, 1.96(18H, 6s, 6×CH_3CO)ppm; δ_C: 170.42, 170.41, 170.29, 170.25, 170.00, 169.68(6×CH_3CO), 158.91(s, Py-C), 156.57(s, Py-C), 152.36(d, J_{F-C}=16.0 Hz, Py-C), 147.05(d, J_{F-C}=4.6 Hz, Py-C), 115.53(d, J_{F-C}=32.0 Hz, Py-C), 101.97 (s, C-1'), 69.10(s, C-2'), 70.51(s, C-3'), 67.63(s, C-4'), 70.84(s, C-5'), 60.20(s, C-6'), 57.13(s, **C**H_2-4), 61.44(s, **C**H_2-5), 21.15, 20.88, 20.86, 20.84, 20.80, 20.76(6s, 6×**C**H_3CO), 19.83(s, CH_3-2)ppm.

Anal. Calcd. for $C_{26}H_{32}NO_{14}F$(%): C, 51.90, H, 5.37, N, 2.33; Found: C, 51.88, H, 5.31, N, 2.29.

3-O-(β-D-galactopyranosyl)-6-fluoropyridoxol GFPOL

Compound **6** (1.25 g, 2.1 mmol) was deacetylated with 0.5M NH_3/MeOH (30 mL) from 0 °C to r.t., giving the free galactopyranoside **GFPOL** (0.75 g) as a foamy solid in quantitative yield, R_f 0.21 (1:9 MeOH-EtOAc), δ_H: 4.43(1H, d, $J_{1',2'}$= 8.0 Hz, H-1'), 3.63(1H, dd, $J_{2',3'}$=8.8 Hz, H-2'), 3.39(1H, dd, $J_{3',4'}$=3.2 Hz, H-3'), 4.54(1H, dd, $J_{4',5'}$=2.8 Hz, H-4'), 4.69(1H, m, H-5'), 3.45(1H, dd, $J_{5',6a'}$=4.4 Hz, $J_{6a'}$,

$_{6b'}$=10.8Hz, H-6a'), 3.07 (1H, dd, $J_{5',\ 6b'}$=6.0 Hz, H-6b'), 5.20~4.70(4H, br, HO-2', 3', 4', 6', exchangeable with D_2O), 4.53(2H, s, CH_2-4), 4.71(2H, s, CH_2-5), 3.39(2H, br, HO-4, 5, exchangeable with D_2O), 2.42(3H, s, CH_3-2)ppm; δ_C: 158.03(s, Py-C), 155.71(s, Py-C), 150.28(d, $J_{F\text{-}C}$=15.3 Hz, Py-C), 147.61(d, $J_{F\text{-}C}$=5.3 Hz, Py-C), 119.71 (d, $J_{F\text{-}C}$=31.3 Hz, Py-C), 105.62(s, C-1'), 70.90(s, C-2'), 73.06(s, C-3'), 68.14(s, C-4'), 75.47(s, C-5'), 60.58(s, C-6'), 53.79(s, CH_2-4), 54.65(s, CH_2-5), 19.40(s, CH_3-3)ppm.

Anal. Calcd. for $C_{14}H_{20}NO_8F$(%): C, 48.12, H, 5.77, N, 4.01; Found: C, 48.08, H, 5.75, N, 3.97.

3-O-Benzyl-6-fluoropyridoxol 7

To a well stirred CH_2Cl_2(15 mL)-H_2O(20 mL) biphasic mixture (pH 10~11) of **1** (1.0 g, 5.34 mmol) and TBAB (0.3 g, 0.93mmol), a solution of benzyl bromide (1.02 g, 5.88 mmol, 1.1 equiv.) in CH_2Cl_2 (15 mL) was added dropwise over a period of 4~5 h, while the reaction temperature was maintained at 50 °C, and the stirring continued for an additional hour. The products were extracted (CH_2Cl_2, 4×30 mL), washed free of alkali, dried (Na_2SO_4), concentrated and the residue purified by column chromatography on silica gel (1:2 cyclohexane-EtOAc) to afford major product **7** and small amounts of di-O-benzyl-6-fluoropyridoxol derivatives.

(1.12 g, 76%), white crystalline, R_f 0.38(1:2 cyclohexane-EtOAc), δ_H: 7.39(5H, m, Ar-H), 4.90(2H, s, $PhCH_2$), 4.75(2H, d, $J_{H\text{-}5,\ HO\text{-}5}$=5.4 Hz, CH_2-5), 4.72(2H, d, $J_{H\text{-}4,\ HO\text{-}4}$=6.0 Hz, CH_2-4), 3.57(1H, t, $J_{H\text{-}5,\ HO\text{-}5}$=5.4 Hz, HO-5, exchangeable with D_2O), 3.49(1H, t, $J_{H\text{-}4,\ HO\text{-}4}$=6.0 Hz, HO-4, exchangeable with D_2O), 2.44(3H, s, CH_3-2)ppm; δ_C: 157.38(s, Py-C), 155.82(s, Py-C), 149.55(d, $J_{F\text{-}C}$=4.7 Hz, Py-C), 146.97(d, $J_{F\text{-}C}$=4.0 Hz, Py-C), 119.09(d, $J_{F\text{-}C}$=31.2 Hz, Py-C), 136.33, 128.96, 128.88, 128.57(Ph-C), 55.99(s, $PhCH_2$, CH_2-4), 56.76(s, CH_2-5), 19.31(s, CH_3-2)ppm.

Anal. Calcd. for $C_{15}H_{16}NO_3F$(%): C, 64.96, H, 5.82, N, 5.05; Found: C, 64.95, H, 5.79, N, 5.04.

3, α^4-Di-O-benzyl-6-fluoropyridoxol

(0.30 g, 16%), syrup, R_f 0.30(1:2 cyclohexane-EtOAc), δ_H: 7.46~7.33(10H, m, Ar-H), 4.90(2H, s, $PhCH_2$-3), 4.69(2H, s, $PhCH_2$-4), 4.64(2H, d, $J_{H\text{-}5,\ HO\text{-}5}$=4.8 Hz, CH_2-5), 4.62(2H, s, CH_2-4), 3.37(1H, t, $J_{H\text{-}5,\ HO\text{-}5}$=4.8 Hz, HO-5, exchangeable with D_2O), 2.44(3H, s, CH_3-2)ppm; δ_C: 157.98(s, Py-C), 155.65(s, Py-C), 152.10(d, $J_{F\text{-}C}$=14.5 Hz, Py-C), 150.04(d, $J_{F\text{-}C}$=4.6 Hz, Py-C), 116.16(d, $J_{F\text{-}C}$=31.3 Hz, Py-C), 136.91, 136.59, 128.92, 128.76, 128.56, 128.48, 128.44(Ph-C), 77.21(s, $PhCH_2$-3), 73.48(s, $PhCH_2$-4), 56.73(s, CH_2-4), 63.30(s, CH_2-5), 19.65(s, CH_3-2)ppm.

Anal. Calcd. for $C_{22}H_{22}NO_3F$(%): C, 71.90, H, 6.04, N, 3.81; Found: C, 71.86, H, 5.99, N, 3.77.

3, α^5-Di-O-benzyl-6-fluoropyridoxol

(0.16 g, 8%), syrup, R_f 0.25(1:2 cyclohexane-EtOAc), δ_H: 7.39~7.30(10H, m, Ar-H), 4.77(2H, s, $PhCH_2$-3), 4.66(2H, d, $J_{H\text{-}4,\ HO\text{-}4}$=6.8 Hz, CH_2-4), 4.63(2H, s, CH_2-5), 4.58(2H, s, $PhCH_2$-5), 2.95(1H, t, $J_{H\text{-}4,\ HO\text{-}4}$=6.8 Hz, HO-5, exchangeable with D_2O), 2.46(3H, s, CH_3-2)ppm; δ_C: 158.39(s, Py-C), 156.04(s, Py-C), 151.04(d, $J_{F\text{-}C}$=14.5 Hz, Py-C), 149.72(d, $J_{F\text{-}C}$=4.6 Hz, Py-C), 120.36(d, $J_{F\text{-}C}$=32.8 Hz, Py-C), 136.78, 136.30, 128.92, 128.77, 128.60, 128.55, 128.27(Ph-C), 77.05(s, $PhCH_2$-3), 73.97(s, $PhCH_2$-5), 56.09(s, CH_2-4), 63.66(s, CH_2-5), 19.43(s, CH_3-2)ppm.

Anal. Calcd. for $C_{22}H_{22}NO_3F$(%): C, 71.90, H, 6.04, N, 3.81; Found: C, 71.88, H, 6.01, N, 3.78.

3-O-Benzyl-α^4, α^5-di-O-acetyl-6-fluoropyridoxol 8

Acetylation of **7** (1.10 g, 4.0 mmol) was carried out as described above for **6** to give **8** (1.43 g, 100%), white crystalline, R_f 0.44(3:2 cyclohexane-EtOAc), δ_H: 7.40(5H, m, Ar-H), 4.98(2H, s, CH_2-5), 4.92(2H, s, $PhCH_2$), 4.85(2H, s, CH_2-4), 2.46(3H, s, CH_3-2), 2.20, 2.17(6H, 2s, 2×CH_3CO)ppm; δ_C: 170.58, 170.46(2×CH_3**C**O), 158.48(s, Py-C), 155.98(s, Py-C), 150.35(d, $J_{F\text{-}C}$=5.0Hz, Py-C), 147.68(d, $J_{F\text{-}C}$=4.4 Hz, Py-C), 120.06(d, $J_{F\text{-}C}$=31.6 Hz, Py-C), 137.43, 129.66, 129.38, 128.88(Ph-C), 56.69(s, $PhCH_2$, CH_2-4), 57.66(s, CH_2-5), 21.45, 20.98(2s, 2×**C**H_3CO), 19.36(s, CH_3-2)ppm.

Anal. Calcd. for $C_{19}H_{20}NO_5F$(%): C, 63.13, H, 5.58, N, 3.88; Found: C, 63.09, H, 5.53, N, 3.86.

α^4, α^5-di-O-acetyl-6-fluoropyridoxol 9

A mixture of **8** (1.20 g, 3.32 mmol) and 5% Pd-C (500 mg) in MeOH (100 mL) was stirred for 24 h at r.t., under H_2 atmosphere. After filtration, the filtrate was evaporated to afford **9** in quantitative yields (white crystals), R_f 0.24(3:2 cyclohexane-EtOAc), δ_H: 7.56(1H, s, HO-3), 5.08(2H, s, CH_2-5), 4.91(2H, s, CH_2-4), 2.48(3H, s, CH_3-2), 2.22, 2.18(6H, 2s, 2×CH_3CO)ppm; δ_C: 170.56, 170.50(2×CH_3**C**O), 158.68(s, Py-C), 156.00(s, Py-C), 150.75(d, $J_{F\text{-}C}$=5.1 Hz, Py-C), 147.88(d, $J_{F\text{-}C}$=4.2 Hz, Py-C), 120.09(d, $J_{F\text{-}C}$=31.9 Hz, Py-C), 56.88(s, CH_2-4), 57.94(s, CH_2-5), 21.65, 20.89(2s, 2×**C**H_3CO), 19.44(s, CH_3-2)ppm.

Anal. Calcd. for $C_{12}H_{14}NO_5F$(%): C, 53.11, H, 5.20, N, 5.17; Found: C, 53.08, H, 5.17, N, 5.14.

ACKNOWLEDGEMENTS

Supported by grants from the Department of Defense Breast Cancer Initiative IDEA award DAMD 17-03-1-0343-01, Department of Defense Prostate Cancer Initiative IDEA awards DAMD 17-01-1-0107 (KSK) and DAMD17-02-1-0148 (KSK) and Prostate Cancer Consortium DAMD17-03-2-0033 (KSK), a post doc award from the DOD Prostate Cancer Initiative W81XWH-04-10331 (LL) and the Cancer Imaging Program, NIH P20 CA 86354 (pre-ICMIC). NMR experiments were conducted at the Mary Nell and Ralph B. Rogers NMR Center, an NIH BTRP facility #P41-RR02584.

REFERENCES

[1] Wood, K.V. *Curr. Opin. Biotechnol.* **1995**, *6*, 50.
[2] Serebriiskii, I.G.; Golemis, E.A. *Anal. Biochem.* **2000**, *285, 1.*
[3] Nolan, G.P.; Fiering, S.; Nicholas, J.-F.; Herzenberg, L.A. *Proc. Natl. Acad. Sci. USA* **1988**, *85*, 2603.
[4] James, A.L.; Perry, J.D.; Ford, M.; Armstrong, L.; Gould, F.K. *Appl. Environ. Microbiol.* **1996**, *62*, 3868.
[5] James, A.L.; Perry, J.D.; Chilvers, K.; Robson, I.S.; Armstrong, L.; Orr, K.E. *Letters in Applied Microbiol.* **2000**, *30*, 336.
[6] Heuermann, K.; Cosgrove, J. *Biotechniques* **2001**, *30*, 1142.

[7] Manafi, M.; Kneifel, W.; Bascomb, S. *Microbiol. Rev.* **1991**, *55*, 335.
[8] Perry, J.D.; Ford, M.; Taylor, J.; Jones, A.L.; Freeman, R.; Gould, F.K. *J. Clin. Microbiol.* **1999**, *37*, 766.
[9] Tung, C.H.; Zeng, Q.; Shah, K.; Kim, D.E.; Schellingerhout, D.; Weissleder, R. *Cancer Res.* **2004**, *64*, 1579.
[10] Louie, A.Y.; Huber, M.M.; Ahrens, E.T.; Rothbacher, U.; Moats, R.; Jacobs, R.E.; Fraser, S.E.; Meade, T.J. *Nature Biotechnol.* **2000**, *18*, 321.
[11] Cui, W.; Otten, P.; Li, Y.; Koeneman, K.; Yu, J.; Mason, R.P. *Magn. Reson. Med.* **2004**, *51*, 616.
[12] Yu, J.; Otten, P.; Ma, Z.; Cui, W.; Liu, L.; Mason, R.P. *Bioconj. Chem.* **2004**, *15*, 1334.
[13] Slater, E.C., In , S. P. Colowick and N. O. Kaplan, Ed.; Academic Press: New York, **1967** 48.
[14] Mason, R.P. *Curr. Med. Chem.* **1999**, *6*, 481.
[15] Mehta, V.D.; Kulkarni, P.V.; Mason, R.P.; Constantinescu, A.; Aravind, S.; Goomer, N.; Antich, P.P. *FEBS Letters* **1994**, *349*, 234.
[16] Mosmann, T. *Immunol. Methods* **1983**, *65*, 55.

Editorial

Scientific endeavor evolves based on developments in physics, chemistry, and biology. Progress in three critical disciplines promises new frontiers in biomedicine:

1. Fast, efficient, high resolution, high sensitivity imaging instrumentation;
2. An understanding of the genome for several species and associated genomics, proteomics, etc.;
3. Novel pharmaceuticals providing high target selectivity and specificity, including antibodies, RNAi's and many other drug platforms.

Many now realize that molecular imaging is the key to exploiting and integrating these developments. Tissue analysis needs to be non-invasive, three-dimensional and provide dynamic insight into pharmacokinetics and pharmacodynamics. Ideally, imaging would exploit endogenous molecules, and indeed, magnetic resonance imaging (MRI) provides exquisite anatomy based on water and fat signals, and water suppression techniques can reveal distribution of critical metabolites, such as N-acetyl aspartate (NAA), lactate, creatine, citrate, and glutathione. ^{31}P NMR can interrogate high energy phosphates and indicate pH, albeit at much lower spatial resolution. Near infrared spectroscopy or imaging can reveal oxy- to deoxy-hemoglobin ratios. On the physiological front, MRI can provide insight into blood flow, cellular integrity (diffusion), and temperature. Ultra-sound and CT provide other opportunities for imaging soft and hard tissues.

However, many critical components of molecular biology, pharmacology, and biomedicine occur at concentrations far below the detection thresholds of these modalities, or are associated with signals masked by more intense signals. Thus, there is a need for specific reporter molecules. In the USA, this need has been recognized by the establishment of a new National Institute of Health, the National Institute of Biomedical Imaging and Bioengineering (NIBIB) [1]. In addition, many of the other National Institutes of Health have developed programs to push the frontiers in molecular imaging, notably, the National Cancer Institute has established the ICMIC (*In vivo* Cellular and Molecular Imaging Centers) and SAIRP (Small Animal Imaging Research Program) initiatives [2]. Many conferences espouse imaging (International Society of Magnetic Resonance in Medicine [3], Imaging in 2020, Society of Molecular Imaging [4]) and new societies and journals aimed to promote interdisciplinary activities are centered on imaging.

Several journals have recently featured special issues devoted to imaging, but generally from a biological, biomedical or physics standpoint [5]. This Hot Topic Issue considers imaging agents and reporter molecules from a chemist's point of view. Papers are presented by leaders in the fields of radionuclide imaging, NMR, and optical imaging. Each presents novel chemistry and considers the design and application of reporter molecules, providing unique insight into cellular and molecular biology. In some cases, agents may be truly inspired to tackle novel issues. Often agents build on interdisciplinary experience, indeed, cross-fertilization between the sciences and engineering and medicine may provide the most rapid developments. Reagents developed for histology and pathology over the past 200 years can be modified to provide highly sensitive, non-invasive reporter molecules, *e.g.*, addition of a fluorine atom to the classic yellow stain for β-galactosidase provides a ^{19}F NMR reporter [6]. The black stain S-Gal™ generates a paramagnetic precipitate upon exposure to β-galactosidase and ferric ammonium citrate, which induces strong T_2* contrast in MRI [1].

---

[1] Cui, W.; Ma, Z.; Mason, R.P., Proc, ISMRM, Kyoto, Japan, 2004, p. 1712.

Many NMR investigations require millimolar concentrations of reporter molecules, whereas radionuclide and optical imaging can detect micromolar to picomolar concentrations opening opportunities to probe molecular events, but requiring novel chemistry. While many reporter molecules occur in the literature, wide-spread application can be hindered by lack of availability of materials for routine use. Certain speciality companies do exist, notably, Molecular Probes for optical agents [7], Nycomed Amersham specializing in radionuclides [8], and Macrocyclics providing specialized ligands for carrying metal ions [9] and increased demand is bound to stimulate new commerce.

In thanking the contributors to this special issue, I propose that reporter molecules for molecular imaging will revolutionize radiology from its structural background to a prognostic discipline. Moreover, the pharmaceutical industry and regulatory bodies will experience a paradigm shift, whereby imaging provides the foundation for drug development, evaluation, and application.

REFERENCES

1 http://www.nibib1.nih.gov/about/mission.html

2 http://www3.cancer.gov/bip/centers.htm

3 http://www.ismrm.org/

4 http://www.molecularimaging.org

5 *J. Cell. Biochem.* **2002**, 87S and **2003**, 90(6); *Methods Enzymol.* **2004** ,386; *JMRI* **2002**, 16; *Molec. Imaging Biol.* **2003**, 5(5)

6 Cui, W.; Otten, P.; Li, Y.; Koeneman, K.; Yu, J.; Mason, R.P. *Magn. Reson. Med.* **2004**, *51,* 616

7 http://www.amersham.com/

8 http://www.probes.com/

9 http://www.macrocyclics.com/about.html

Ralph P. Mason
Department Radiology
The University of Texas Southwestern Medical Center at Dallas
Texas
USA
E-mail: Ralph.Mason@UTSouthwestern.edu

^{19}F: A Versatile Reporter for Non-Invasive Physiology and Pharmacology Using Magnetic Resonance

Jian-xin Yu[+], Vikram D. Kodibagkar[+], Weina Cui and Ralph P. Mason*

Department Radiology, The University of Texas Southwestern Medical Center at Dallas, Texas, USA

Abstract: The fluorine atom provides an exciting tool for diverse spectroscopic and imaging applications using Magnetic Resonance. The organic chemistry of fluorine is widely established and it can provide a stable moiety for interrogating many aspects of physiology and pharmacology *in vivo*. Strong NMR signal, minimal background signal and exquisite sensitivity to changes in the microenvironment have been exploited to design and apply diverse reporter molecules. Classes of agents are presented to investigate gene activity, pH, metal ion concentrations (*e.g.*, Ca^{2+}, Mg^{2+}, Na^{+}), oxygen tension, hypoxia, vascular flow and vascular volume. In addition to interrogating speciality reporter molecules, ^{19}F NMR may be used to trace the fate of fluorinated drugs, such as chemotherapeutics (*e.g.*, 5-fluorouracil, gemcitabine), anesthetics (*e.g.*, isoflurane, methoxyflurane) and neuroleptics. NMR can provide useful information through multiple parameters, including chemical shift, scalar coupling, chemical exchange and relaxation processes (R1 and R2). Indeed, the large chemical shift range (~ 300 ppm) can allow multiple agents to be examined, simultaneously, using NMR spectroscopy or chemical shift selective imaging.

Keywords: Oxygen, pH, gene reporter, metal ions, 5FU, FDG, anesthetics.

1. INTRODUCTION

Nuclear magnetic resonance (NMR) was originally a curiosity for physicists, but its demonstration led to Nobel Prizes for Purcell and Bloch [1]. During the 1960's to 1980's NMR was embraced by the chemistry community for its power to discriminate chemical structures. Demand fed development with increasingly sophisticated instruments, including higher magnetic fields, faster and more precise electronics and more powerful computers, combined with innovations in data acquisition (*e.g.*, Fourier transform [2], echo planar imaging [2]) and radiofrequency coils (quadrature [3], SMASH [4], SENSE [5]). In biomedicine, the intense water signal (55 M H_2O) is exploited for high resolution, anatomical MR Imaging providing 3D tomography non-invasively in living systems. Millimeter resolution is routine and microscopy is feasible [6]). For many diseases, proton MRI has become the modality of choice for the radiologist. Increasingly, manipulation of the water signal through appropriate spin physics provides insight into physiology, such as, blood flow (arterial spin labeling (ASL) [7]), diffusion (diffusion tensor imaging (DTI) [8]), and oxygenation (Blood oxygen level dependent (BOLD) contrast [9]). Chemists have exploited NMR, but increasingly they also contribute in the form of contrast agents and reporter molecules, as described in this Hot Topics issue. Diagnostic value is added by applying paramagnetic contrast agents: several are in clinical use today, including Gd-DTPA (diethylenetriaminepentaacetic acid, Magnevist®) and Gd-DTPA-BMA (gadodiamide, OmniScan®), and Gd-HP-DO3A (1,4,7-tricarboxymethyl-1,4,7,10-tetraazacyclododecane, ProHance®) and Gd-DOTA (1,4,7,10-tetraazacyclododecane-1,4,7,10-tetraacetic acid, Dotarem®), and new generations of "smart" agents are being developed, as reviewed in the accompanying paper by McMurry, *et al.* [10].

Use of proton NMR to detect metabolites other than water is severely complicated by the relative signal intensity, since many metabolites occur at millimolar concentrations. Thus, hetero-nuclear approaches have been developed to explore other endogenous molecules and ^{31}P NMR has been widely applied in the pre-clinical setting, with limited clinical application, to assess metabolites such as phosphocreatine, ATP, and inorganic phosphate, providing insight into both bioenergetics and pH [11, 12]. ^{23}Na NMR is also very sensitive, but is essentially limited to the Na^{+} ion; though application of contrast agents may differentiate intra- and extra-cellular sodium ions and these can be sensitive to edema and potentially reveal tumors [13-15][1]. Tissues also have extensive carbon, though 98.9% exists as NMR invisible ^{12}C. ^{13}C may be detected directly, but more significantly provides an opportunity for the use of isotopically enriched substrates (*e.g.*, acetate, formaldehyde), which are readily available and detectable [16, 17]. Isotopic substitutions may also be applied to protons, with replacement by deuterium or tritium to examine metabolic pathways and kinetic isotope effects [18, 19].

An alternative approach is ^{19}F NMR, as described below. Some common drugs include a fluorine atom [20], and are obvious candidates for investigation (*e.g.*, 5FU [21, 22], flurbiprofen [23, 24], isoflurane [25], fluoxetine [26]). In other cases, a fluorine atom may be added as a simple tracking label, or by judicious placement in a carefully designed reporter molecule to interrogate some parameter, such as pO_2 [27], pH [28] or gene activity [29].

*Address correspondence to this author at the Laboratory of Prognostic Radiology, Department of Radiology, The University of Texas Southwestern Medical Center at Dallas, 5323 Harry Hines Blvd, Dallas, Texas 75390-9058, USA; Tel: (214)-648-8926, Fax: (214)-648-2991; E-mail: Ralph.Mason@UTSouthwestern.edu

[+]Contributed equally to this review.

[1] Kalyanapuram, R.; Winter, P.; Mason, R.P.; Bansal, N., Proc. 5th ISMRM, Vancouver, 1997, p. 2116.

0929-8673/05 $50.00+.00

NMR has many virtues compared with other modalities:

1 It is intrinsically non-invasive, though ^{19}F requires infusion of reporter molecules.

2 There is no radioactivity, so the substrates (reporter molecules) are inherently stable with a long shelf life and are not associated with problems of radioactive waste disposal.

3 Any tissues of arbitrary depth may be interrogated.

4 Multiple signals may be detected simultaneously from separate reporter molecules. By analogy, one may consider multi-wavelength fluorescent optical imaging or energy selective γ-ray detection in a gamma camera.

5 Clinical anatomical ^{1}H MRI is readily acquired together with ^{19}F-reporter molecule signals, providing context in terms of organs and tissue heterogeneity.

NMR is endowed with multiple characteristics including parameters such as signal intensity (SI), chemical shift (δ) and changes therein (Δδ), transverse dephasing rate (R_2^*), spin-spin relaxation rate (R_2) and longitudinal relaxation rate (R_1). This provides both a wealth of potential information and complexity in optimal experimental planning. The signal intensity of a particular peak (more specifically integral of area under the peak) in the NMR spectrum is proportional to the amount of the corresponding substance in the region excited by the NMR coil. This provides qualitative and often quantitative assessment of the dynamic changes in the concentration of endogenous or exogenous probes.

NMR has certain drawbacks in terms of cost of instrumentation (much higher than optical methods), sensitivity (typically, mM vs. μM for optical or radionuclide studies), and acquisition time. Acquisition time depends on substrate concentration, magnetic field, and volume of interrogation. Traditional NMR sensitivity is quoted in the mM range. There are indications that specific contrast agents may be effective at lower concentrations by manipulating spin thermodynamics [30, 31] or exploiting activatable paramagnetic magnetization transfer contrast agents (PARACEST) [32].

^{19}F NMR has been used since the eighties for *in vivo* studies. In the past, various reviewers have discussed diverse applications of *in vivo* ^{19}F NMR [21, 27, 28, 33-41]. Thomas [33], Selinsky and Burt [34], Prior *et al.* [35] and London [36] reviewed the contemporary state-of-the-art, covering the entire spectrum of *in vivo* applications. Mason reviewed the use of perfluorocarbons for measuring pO_2 [27, 37] and the use of fluorinated derivatives of vitamin B_6 as probes for measuring *in vivo* cellular transmembrane pH gradients [28]. McSheehy *et al.* [38] discussed applications of ^{19}F magnetic resonance spectroscopy (MRS) to oncology. Menon [39] focused on the studies involving fluorinated anesthetic agents. Passe *et al.* [40] reviewed neuropsychiatric applications of NMR, which included a discussion on ^{19}F NMR applications. Bachert [42], Martino *et al.* [41] and Wolf *et al.* [21] gave comprehensive reviews of pharmacokinetics of fluoropyrimidine drugs using ^{19}F NMR. The continuing appearance of reports of the use of ^{19}F NMR and development of novel reporter molecules justifies a current review. Moreover, ^{19}F NMR has made inroads into some new areas (Table **1**). The purpose of this article is to review the applications of ^{19}F NMR to *in vivo* studies especially from a chemical standpoint.

Table 1. Fluorinated Reporter Molecules

Parameter	Indicator (example)	References (representative)
Gene activity	PFONPG, 5FC	[29, 74]
pO_2	Fluorocarbons, *e.g.*, hexafluorobenzene	[27, 218]
Hypoxia	F-Misonidazoles	[150, 347]
pH	FPOL, ONPG, ZK 150471	[28, 29, 87, 105, 107, 348]
$[Na^+]$	F-cryp-1	[145]
$[Ca^{2+}]$	5F-BAPTA	[128, 130, 135]
$[Mg^{2+}]$	5F-APTRA	[36, 140]
Membrane/Chloride potential	TFA	[349, 350]
Temperature	PFCs	[33, 167, 351]
Blood flow	Freon FC-23	[292, 293]
Cell volume	TFM	[349]
Diffusion	FDG	[352]
Glycolysis	FDG	[302]
Drug metabolism	5-FU, gemcitabine	[21, 42]
Vascular volume	Fluorocarbon emulsion	[284, 285]
Protein catabolism	DLBA	[353]
Artherosclerotic plaques	nanoparticles	[354]
Lung function	PFC; SF_6	[269, 355]
GI function	PFC	[277, 278]

2. ^{19}F AS AN *IN VIVO* NMR PROBE

^{19}F has a nuclear spin 1/2 and a gyromagnetic ratio (γ) of 40.05 MHz/T. Being the only stable isotope of fluorine, it is 100 % naturally abundant. The NMR sensitivity of ^{19}F is 0.83 relative to ^{1}H. The high γ (only about 6% lower than protons) generally allows the use of existing proton NMR instrumentation with a minimum of component adjustments. While fluorine occurs in the body, it is present mostly in the form of solid fluorides in bones and teeth [43]. Endogenous fluorine has a very short T_2 relaxation time [43] and the resulting signal is below the limits of NMR detection in most biological systems of interest. Thus, exogenously administered fluorine containing compounds are observed without interference from background signals.

The ^{19}F NMR chemical shift is exquisitely sensitive to perturbations in the chemical microenvironment. The range of chemical shifts of ^{19}F is greater than 300 parts per million (ppm), as opposed to about 10 ppm for proton NMR [44]. The sensitivity and range of chemical shifts ensure that fluorinated probes and their metabolites, if any, are easily differentiated. While signals can be interpreted in isolation, it is often preferable to include a reference signal. There is no single fluorine-containing compound that is suitable as a universal chemical shift reference for *in vivo* studies. The IUPAC standard for ^{19}F chemical shift reference is fluorotrichloromethane ($CFCl_3$). The range of chemical shifts of most organic fluorinated compounds is about –50 ppm to +250 ppm relative to $CFCl_3$. However, $CFCl_3$ is not convenient for most biomedical applications, and hence, secondary reference materials are commonly used. Chemical shifts can be strongly solvent dependent and vary with dilution [44]. CF_3CO_2H is quoted as –76.530 ppm on the ϕ scale (extrapolated to infinite dilution). Many investigators favor aqueous sodium trifluoroacetate (NaTFA) as a chemical shift reference for biological studies [28, 45-47]. NaTFA has the advantage of being quite nontoxic, and hence, can be introduced together with a fluorinated probe, as an internal chemical shift reference *in vivo*. This is preferable to an external reference, if total signal quantification is not an issue, since susceptibility effects may cause errors in estimation of chemical shifts of *in vivo* probes relative to an external standard.

To obtain detectable signals, spectra, or images, sufficient fluorinated probe must be administered, though the concentration of probe in studies of living organisms should be as low as possible to avoid physiological perturbations or toxic side effects. Unlike ^{1}H and ^{13}C NMR, ^{19}F chemical shift can appear quite unpredictable though theoretical treatments have attempted to rationalize values [44, 48] (+ refs therein). Extensive tables of ^{19}F NMR chemical shifts and coupling constants have been published [49]. Molecules may include a single fluorine atom, in which case F-H coupling may be observed. For multiple F atoms, F-F coupling also occurs (Table **2**). Unlike ^{1}H or ^{13}C NMR, the coupling constants do not decrease monotonically with increasing separation, and negative coupling constants are sometimes observed [44, 50]. While C-F coupling is seen in ^{13}C NMR spectroscopy, the low natural abundance of ^{13}C is not generally apparent in ^{19}F NMR spectroscopy. F-H coupling can be removed by proton de-coupling, however, fluorine detection is often accomplished by retuning the proton NMR channel, and thus, proton de-coupling is often not practical. F-F coupling is often unresolved, particularly in the broader signals encountered *in vivo*, but it can, nonetheless, give rise to J modulation in echo acquisitions [51]. While this may distort signals, it has also been exploited for signal editing providing resonance selective imaging [52]. The easiest way to avoid J_{FF} coupling is to ensure symmetry, *e.g.*, CF_3 groups. Moreover, this avoids the potential toxicity associated with mono- and di-fluoroacetate groups [53]. In addition to chemical shift, relaxation rates are exploited in ^{19}F NMR. In particular, the ^{19}F spin-lattice relaxation rate ($R_1=1/T_1$) of many perfluorocarbons (PFCs) is linearly related to the partial pressure of oxygen (pO_2) [27].

Fluorine may be introduced in many forms, though chemical reaction conditions are often quite severe and reagents include HF [54], various metal halides [55], SeF_4 [56], WF_6 [57], XeF_2 [58], SbF_5 [59], F_2 [60, 61], S-ethyltrifluorothioacetate [62] and trifluoroacetic anhydride [63]. Thus, it may be preferable to incorporate a moiety into synthetic planning, which already includes the desired fluorine atoms, *e.g.*, trifluoromethyl. Typical reporter groups are shown in (Table **3**), together with reported syntheses and applications. For biological activity, the F atom has a similar size to a hydroxyl group, but exhibits a strong carbon-fluorine bond, and low chemical reactivity. Fluorine is highly electro-negative, causing potential charge redistribution. Some of the earliest biomedical applications of ^{19}F NMR used fluorine labeled substrates to explore enzyme activity and protein structures, *e.g.*, ribonuclease A, hemoglobin and lysozyme as reviewed by Dwek [64] and Gerig [65].

Table 2. Typical Values of Fluorine Coupling Constants Summarized From [44, 49]

$^{2}J_{FH}$	**45-90 Hz**
$^{3}J_{FH}$	0-53 Hz
$^{2}J_{FF}$	200-800 Hz
$^{3}J_{FF}$	< 1 Hz
$^{4}J_{FF}$	1-20 Hz
$^{5}J_{FF} - {}^{6}J_{FF}$	0-40 Hz
$^{1}J_{FC}$	>200-312 Hz
$^{2}J_{FC}$	(-25) 17-54 Hz

This review will consider three classes of molecular ^{19}F NMR based on i) "Active agents", specifically designed to interact with the environment and including ^{19}F atom(s), which respond to a specific parameter, such as enzyme activity, ion concentration or pO_2 (Section 3); ii) "Passive agents", which occupy space, thereby, revealing a tissue property, such as vascular volume based on NMR signal intensity, while remaining essentially inert (Section 4), iii) pharmaceuticals, which include a fluorine atom making them suitable for NMR investigations (Section 5).

3. ACTIVE AGENTS

Active agents typically fall into three categories; i) those which undergo irreversible interaction modifying their structure, as revealed by a change in chemical shift. These are represented by gene reporter molecules, where substrates are cleaved by specific enzyme activity (Section 3.1), and hypoxia agents (Section 3.4.2), which are modified by reductases and trapped. ii) Ligands designed to trap/bind specific entities, such as ions, specifically, but reversibly, *e.g.*, H^+ (pH) (Section 3.2), metal ions (Ca^{2+}, Mg^{2+}) (Section 3.3); iii) perfluorocarbons, which exhibit exceptional gas solubility and reveal oxygen tension based on modification of relaxation parameters (Section 3.4.1).

Table 3. Synthetic Approaches to Fluorochemistry

Name	Structure	Synthesis	Example
Alkyl Fluoride	RCHFR'	SeF_4 [56], $PhPF_4$ [356], HF[54],	$CH_3CH_2FCH_3$
Difluoroalkane	RCH_2CF_2R' or $RCHF(CH_2)_nCHFR'$	ClF [357], XeF_2 [58], KF [358], CF_2Br_2 [359],	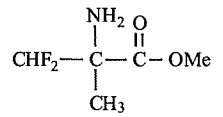
Trifluoroalkane	RCH_2CF_3	CoF_3 [360], Bu_4NBF_4	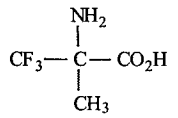
Tetrafluoroalkane	$RCF_2(CH_2)_nCF_2R'$	HF, SF_4 [361]	$MeCF_2CH_2CF_2Me$
Trifluoroacetic compounds	CF_3CO_2R	$EtSCOCF_3$ or Trifluoroacetamido-succinic anhydride [62]	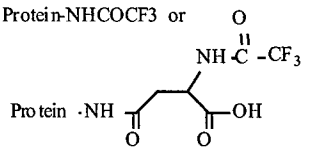
Monofluoro aromatic compounds	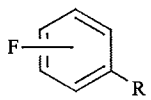	[362, 363]	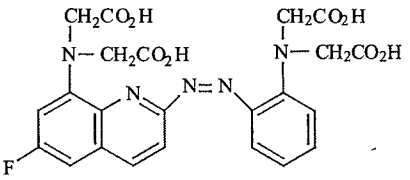
Trifluoromethyl aromatic compounds	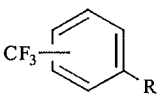	[362, 363]	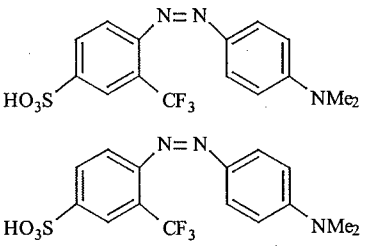
Trifluoromethyl Aromatic Compounds	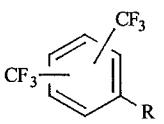	[65]	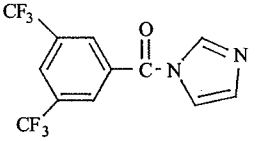
Trifluoroacetyl compounds	CF_3COR	Me_3SiCF_3, Bu_4NF [364]	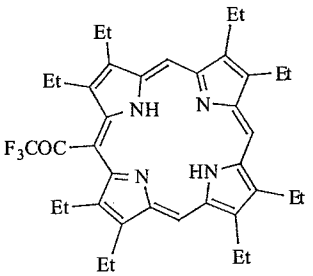
Di or tri-trifluoromethyl Derivatives		Me_3SiCF_3, Bu_4NF [364, 365]	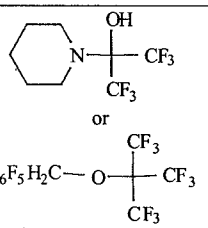

(Table 3). contd.....

Name	Structure		Example
CF_3S- Derivatives	CF_3SR	Me_3SiCF_3, Bu_4NF [364, 365]	$4\text{-}NO_2C_6H_4SCF_3$
CF_3SO- Derivatives	CF_3SOR	Me_3SiCF_3, Bu_4NF [364, 365]	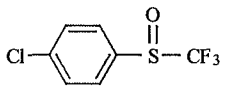
CF_3SO_2- Derivatives	CF_3SO_2R	Me_3SiCF_3, Bu_4NF [364, 365]	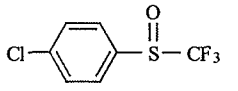
$(CF_3)_2N$- Derivatives	$(CF_3)_2NR$	Me_3SiCF_3, Bu_4NF [364, 365]	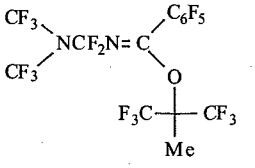

3.1 Gene Reporters

Gene therapy holds great promise for the treatment of diverse diseases. However, widespread implementation is hindered by difficulties in assessing the success of transfection in terms of spatial extent, gene expression, and longevity of expression. The development of non-invasive reporter techniques based on appropriate molecules and imaging modalities may help to assay gene expression and this is often achieved by including a reporter gene in tandem with the therapeutic gene [66-69]. A critical criterion is that the reporter gene not be normally present or expressed in the cells of interest. Popular reporter genes today are associated with optical imaging, since this is a cheap modality and highly sensitive results are rapidly available. Thus, bioluminescent imaging (BLI) of luciferase [66, 70] and fluorescent imaging of green fluorescent protein (GFP and longer wavelength variants [71]) are popular. These techniques are very useful in superficial tissues and have extensive applications in mice, but application to larger bodies is limited by depth of light penetration. Fluorescent imaging has been presented in a tomographic format, but to date BLI was limited to planar images. We have recently developed the first optical light emission tomography system (LETS) revealing luciferase expression in mice in 3D [2]. Nuclear medicine approaches (see Haberkorn *et al.* this issue) exploit thymidine kinase with a variety of substrates including iodo- and fluoro-nucleosides, such as FIAU and gancyclovir, and various radionuclide labels including 123-, 124-, 125-I, and ^{18}F [68, 72]. An alternative approach uses the sodium iodine symporter (hNIS), which works well with both iodide and pertechnetate substrates [67]. For cancer, thymidine kinase has the advantage that the gene serves not only as a reporter, but gene products can themselves have therapeutic value [73].

Gene activated drug therapy, often termed GDEPT (gene directed enzyme prodrug therapy) [74], has been demonstrated using the cytosine deaminase (CD) gene. Specifically, CD activates the minimally toxic 5-fluorocytosine (5-FC) to the highly toxic 5-fluorouracil (5-FU). This is being widely exploited in gene therapy trials, in the hope of mitigating the toxicity threshold associated with systemic 5-FU delivery [73, 74]. The conversion of 5-FC to 5-FU causes a ^{19}F NMR chemical shift ~1.5 ppm, hence, revealing gene activity, which has been demonstrated in a number of systems *in vivo* [74, 75]. NMR can be used to monitor conversion (gene activity) or conversely deduce lack of activity (Fig. **1**). It is also interesting to note that some of the major metabolic products of 5-FU exhibit chemical shift sensitivity to pH and these could provide an indication of local tissue pH [47].

LacZ, which produces β-galactosidase, has been the primary choice of reporter gene to verify effective transfection in biochemistry and molecular biology for many years [76-78]. Diverse reporter agents are commercially available with specific characteristics, such as developed color, thermal stability, and cellular retention (*e.g.*, X-gal, ONPG (o-nitrophenylgalactoside), S-Gal^{TM}, and S-Galacton-star^{TM}) for biological and histological analysis [79-81]. Representative agents (Fig. **2**) show the broad range of substrate structures consistent with enzyme promiscuity (lack of substrate specificity). However, β-galactosidase had been largely neglected for *in vivo* work, until the elegant studies of Meade *et al.* [82]. As reviewed by McMurry (this issue [10], Fig. **19**) the galactose bridged cyclic gadolinium contrast agent ((1-(2-(galactopyranosyloxy)propyl)-4,7,10-tris(carboxymethyl)-1,4,7,10–tetraazacyclo dodecane) gadolinium(III) (EgadMe) shows considerable change in water relaxivity upon exposure to β-galactosidase. While the molecule is a poor substrate for the enzyme (about 500 times less efficient than the colorimetric biochemical agent ONPG) and does not penetrate cells, it facilitated effective investigation of cell lineage following direct intra-cellular microinjections [82]. These studies prompted us to consider other NMR active analogs, and it appeared that introduction of a fluorine atom into the popular colorimetric biochemical indicator ONPG could produce a strong candidate molecule. Fluoro-nitrophenol galactosides had previously been reported by Yoon *et al.* [83], though they placed the fluorine atom on the sugar moiety, which provided much less chemical shift response to cleavage.

[2] Richer, E., Slavine, N., Lewis, M. A., Tsyganov, E., Gellert, G. C., Gunnur Dikmen, Z., Bhagwandin, V., Shay, J. W., Mason, R. P., and Antich, P. P., Proc. 3rd Soc. Molecular Imaging, St. Louis, September 2004

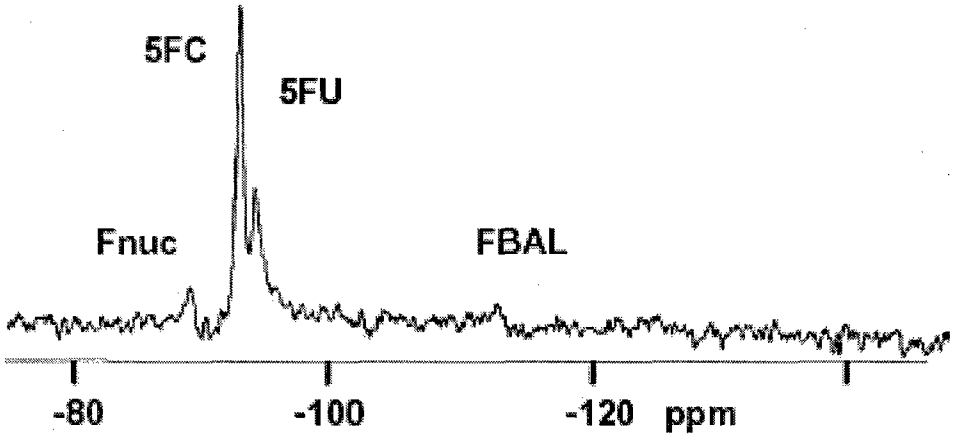

Fig. (1). Simultaneous detection of 5-fluorocytosine (5FC, prodrug) and 5-fluorouracil (5FU) by ^{19}F NMR in Dunning prostate R3327-AT1 cells. The tumor cells had been transfected in culture using adenovirus to express cytosine deaminase. However, following implantation into rat and growth, expression was lost and no conversion was detected *in vivo* following i.p. infusion of 5-FC. However, when 5-FU was administered in addition, both resonances could be resolved and metabolites of 5-FU were detectable. Thus, ^{19}F NMR can provide assay of gene expression (or lack thereof). (Data achieved in collaboration with Dr. Steven Brown, Henry Ford Hospital, Detroit).

We recently demonstrated 4-fluoro-2-nitrophenyl-β-D-galactopyranoside (PFONPG, (Fig. **3**) as an effective substrate for β-galactosidase [29]. This molecule is an excellent substrate for the enzyme and acts competitively with traditional biochemical indicators. It provides a single ^{19}F NMR signal with a narrow linewidth and good stability in solution. It is stable in normal wild type cells and whole blood, but exposure to the enzyme or cells transfected to express β- galactosidase causes rapid cleavage in line with anticipated levels of transfection [29]. As with the traditional indicator ONPG, a color change accompanies release of the aglycone, but this would be masked in tissue studies. Upon cleavage of the glycosidic bond a chemical shift difference $\Delta\delta > 3.6$ ppm is observed (Fig. **4**). However, the chemical shift of the product may have a range of about 9 ppm, since the released aglycone is pH sensitive and the pKa is in the physiological range. Significantly, there is no overlap between the chemical shift of the substrate and the product and the chemical shift difference is sufficient to permit chemical shift selective imaging to reveal distribution of each entity separately (Fig. **5**).

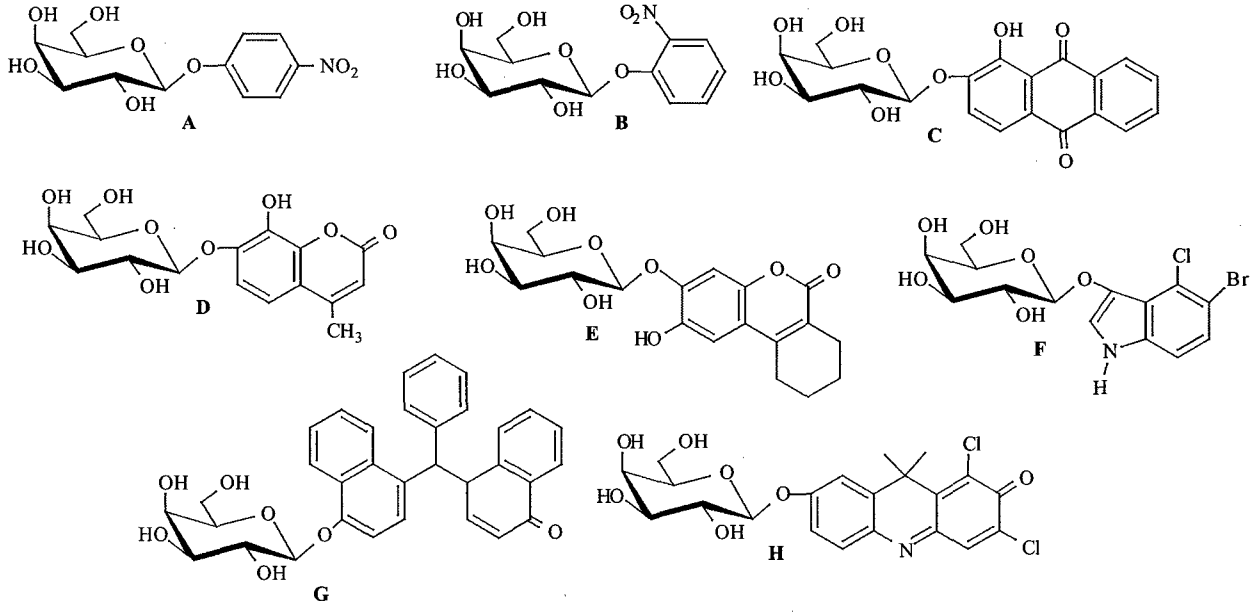

Fig. (2). Diverse substrates for β-galactosidase: 4-nitrophenyl β-D-galactopyranoside (A); 2-nitrophenyl β-D-galactopyranoside (B); p-naphtholbenzein β-D-galactopyranoside (C); 1,2-dihydroxyanthraquinone β-D-galactopyranoside (D); 4-methylumbeliferoneβ-D-galactopyranoside (E); 5-bromo-4-chloro-3-indoxylβ-D-galactopyranoside (X-gal) (F); 3,4-cyclohexenoesculetinβ-D-galactopyranoside (G); 1-[2-(β-D-galactopyranosyloxy)propyl]-4,7,10-tris(carboxymethyl)-1,4,7,10-tetraazacyclo-dodecane) gadolinium(III) (EgadMe, H) with 9H-(1,3-dichloro-9,9-dimethylacridin-2-one-7-yl)-α-D-galactopyranoside (DDAOG) (H).

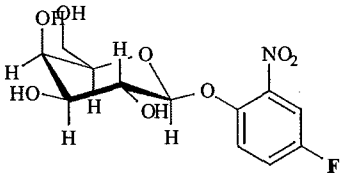

Fig. (3). 4-fluoro-2-nitrophenyl-β-D-galactopyranoside (PFONPG).

previously [84]. Although β-gal accepts a wide range of substrate structures, there was no activity on an alpha anomeric substrate. Ortho fluoro ortho nitrophenyl galactoside (OFONPG) was found to be substantially less toxic (preliminary studies Yu and Ma). Preliminary investigations also show the feasibility of conjugating other aglycones, such as the pH reporter 6-fluoropyridoxol [28] to galactose, generating an effective substrate for β-gal [4]. Given the different chemical shifts of individual substrates and

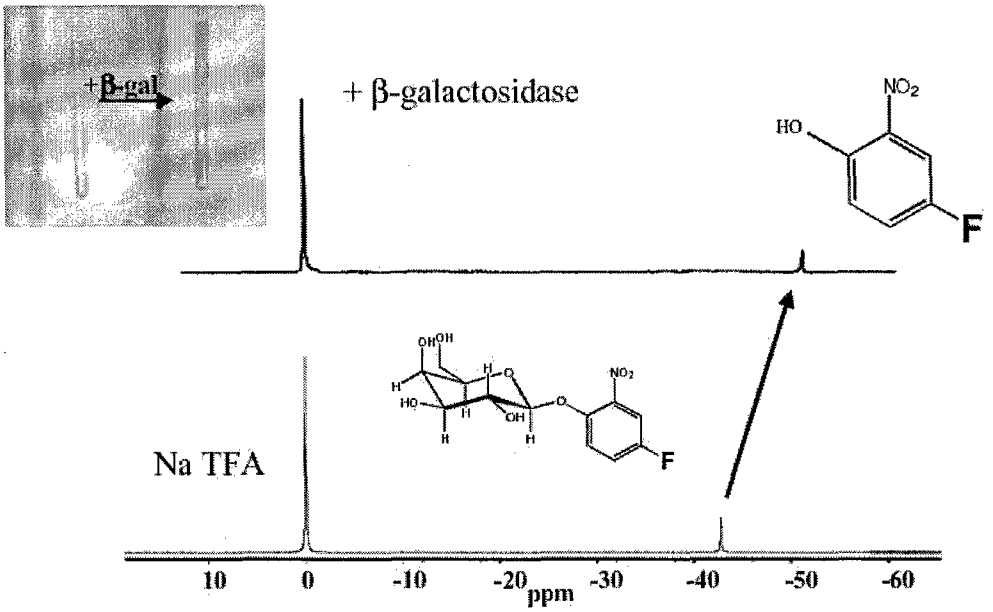

Fig. (4). Action of β-gal on PFONPG in saline. ^{19}F NMR showed a single narrow signal at δ -42.75 ppm and a chemical shift response Δδ > 5 ppm upon cleavage, which was also accompanied by a colorimetric change to yellow (inset). Sodium trifluoroacetate was used as a chemical shift reference (δ 0 ppm).

The pH sensitivity of the product aglycone presents the interesting possibility of selective determination of pH at the site of enzyme activity. In some cases, we have observed a split peak in cells transfected to express β-gal, which may indicate a transmembrane pH gradient (Fig. **6**). We have demonstrated that if the aglycone (PFONP) is added to a suspension of red blood cells, two signals are rapidly observed representing the intra and extra cellular pH [3]. However, PFONP is somewhat toxic and can cause lysis of less robust cells. Thus, PFONPG may be regarded as an interesting prototype molecule primarily representative of a new approach to NMR gene reporter molecules for use in association with β-galactosidase. We have synthesized series of analogues with the fluorine atom placed at various locations on the phenolic ring and incorporating alternate substituents, such as Cl and Br. Each adduct and aglycone provides a unique chemical shift allowing ready comparison of susceptibility to enzyme activity (manuscript in preparation). For the various substrates, the change in chemical shift ranged from a minimum of 1.57 ppm to a maximum of 12.89 ppm. The chemical shift accompanying cleavage depends strongly on the orientation of the F-atom with largest response for para-F and less for ortho-F. The rate of cleavage was closely related to the pKa of the aglycone commensurate with enzyme studies reported products, we believe there will be opportunities to establish optimized reporter molecules based on one-pot combinatorial approaches.

The chemical shift difference between substrate and aglycone product reveals unambiguous detection of enzyme activity. Signal to noise could be enhanced by introduction of a trifluoromethyl (CF_3) reporter group, as opposed to the single F-atom. However, a CF_3 group will likely perturb the water solubility to a greater extent and the chemical shift response is expected to be considerably smaller, due to transmission of the electron density redistribution through an additional carbon-carbon bond [5].

The concept of ^{19}F NMR reporter molecules for detecting gene activity is in its infancy, but we believe it has great promise for future development.

3.2 pH

Development of ^{19}F NMR pH indicators (Table **4**) has followed three strategies: i) development of molecules specifically designed for ^{19}F NMR, ii) fluorinated analogues of existing fluorescent indicators, iii) exploitation of the ^{19}F NMR chemical shift sensitivity inherent in cytotoxic drugs.

[3] Cui, W., Otten, P., Merritt, M., and Mason, R. P., Proc. 10th ISMRM, Honolulu, Hawai'i, USA, 2002, p. 385.

[4] Yu, X. and Mason, R. P., Proc. 11th ISMRM, Toronto, Canada, 2003, p. 675.

[5] Cui, W., Otten, P., Yu, J., Kodibagkar, V., and Mason, R. P., Proc. ISMRM, Toronto, Canada, 2003, p. 675.

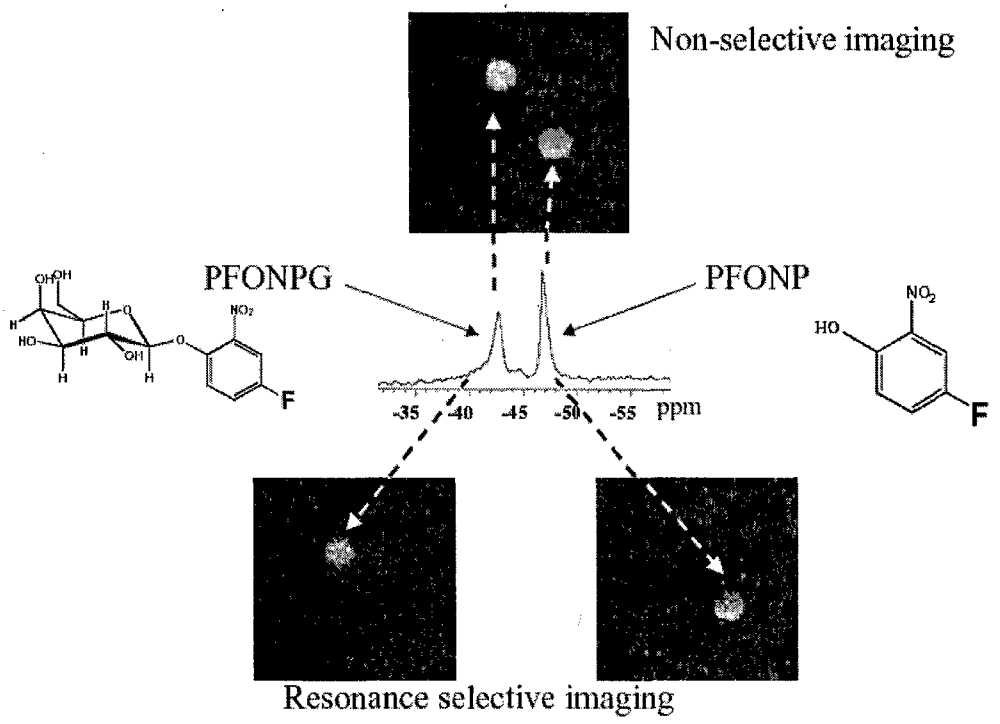

Fig. (5). ^{19}F MRI at 4.7 T of a phantom comprising vials of PFONPG and PFONP in buffer. Frequency selective excitation provides separate images of substrate (PFONPG) and aglycone product (PFONP).

The high sensitivity of ^{19}F NMR chemical shift to the microenvironment has prompted widespread application to pH indicators, as reviewed recently [28]. Many molecules exhibit chemical shift response to changes in pH, *e.g.,* the ^{19}F NMR resonance of 6-fluoropyridoxol. On the NMR time scale, protonated and deprotonated moieties are generally in fast exchange, so that a single signal is observed representing the amplitude weighted mean of acid and base forms. As such, measurements of chemical shift may be directly related to pH in the form of a titration curve. pH values are calculated from the spectra on the basis of chemical shift of δ_{obs} with respect to a standard. The pH is measured using the Henderson-Hasselbalch equation:

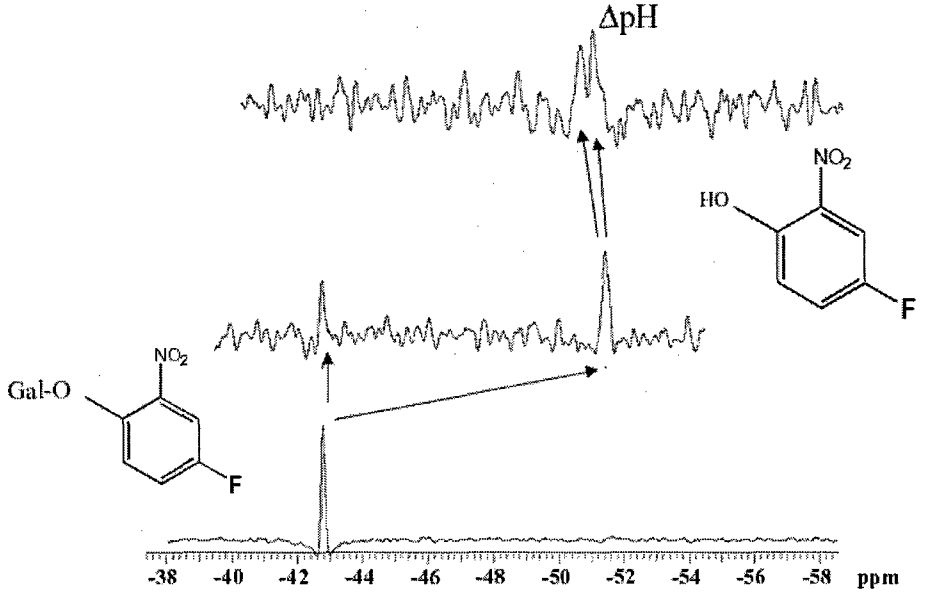

Fig. (6). Conversion of PFONPG by PC3 human prostate cancer cells transfected for 48 h using adenovirus to transiently express lacZ under CMV promoter. The split peak in the upper spectrum suggests a transmembrane pH gradient (Mason, Otten, Li and Koeneman, *Proc. ISMRM 10th Scientific Meeting*, 2002).

Table 4 ^{19}F NMR pH indicators

Reporter	Structure	pKa	Chemical Shift Response (Δδ ppm)	References
3-fluoro-2-methylalanine	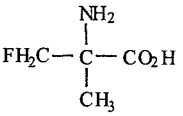	8.5	1.1	[86]
3,3-difluoro-2-methylalanine	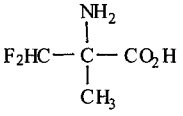	7.3	2	[86]
3,3,3-trifluoro-2-methylalanine	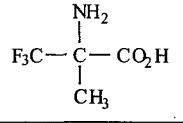	5.9	2	[86]
2-difluoromethyl ornithine	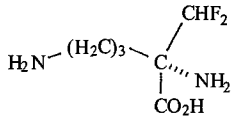	6.4	0.4	[103]
N,N-(methyl-2-carboxyisopropyl)-4-fluoroaniline	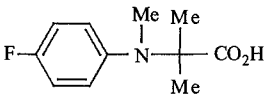	5.8	17	[105]
FQuene	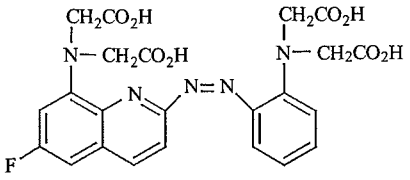	6.7	4.8	[102]
6-FPOL	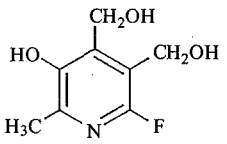	8.2	9.7	[28, 45, 94]
5F-NEAP-1	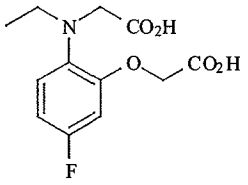	6.9	11	[106]
5F-NEAP-2	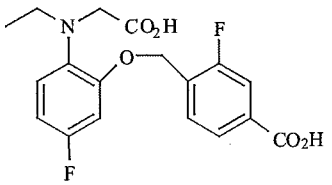	6.6	11	[106]
ZK 150471	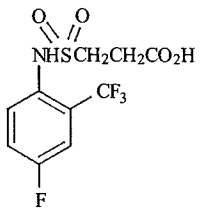	7.3	11	[109, 110]

(Table 4). contd.....

Reporter	Structure	pKa	Chemical Shift Response(Δδ ppm)	References
PFONP	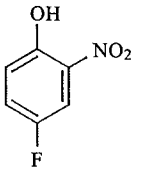	6.9	9.3	[29]
CF_3POL	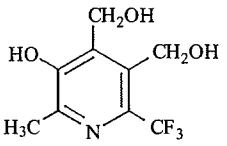	6.8	1.7	6

Due to the non-linear form of the equation, greatest sensitivity is found close to the pKa. If exchange is slow on the NMR time scale both protonated and deprotonated structures provide separate signals simultaneously. In this case, the ratio of signals provides an indication of pH. Such is often the case in reporter molecules for metal ions (section 3.3, below). Another critical time scale is movement of reporter molecules between compartments, which gives rise to signal averaging as encountered for trifluoroethylamine [85]. Should exchange fall into an intermediate exchange regimen signal may be severely broadened or lost altogether. Such exchange rates are strongly temperature and magnetic field dependent.

$$pH = pKa + \log 10 \left[\frac{\delta obs - \delta acid}{\delta base - \delta obs} \right] \quad (1)$$

3.2.1 Fluoro Amino Acids

Deutsch *et al.* [86, 87] championed the use of ^{19}F NMR of fluorinated indicators to measure intracellular pH. The first studies used trifluoroethylamine, which provided both intra- and extracellular signals in blood at 4 °C [85]. However, at room temperature transmembrane exchange accelerated and fell into the intermediate exchange regime causing severe line broadening. Based on this approach a series of fluorinated agents was developed, particularly, using mono-, di- and tri- D, L,- 2-amino- 3,3- difluoro-2-methyl propanoic acid (Table 4). These molecules have been successfully applied to pH measurements in peripheral blood lymphocytes [86, 88, 89], isolated hepatocytes [90], rabbit colon and frog skin [86]. Thoma and Ugurbil [91] used this approach in a perfused liver. Comparison of pH measurements determined using ^{31}P NMR of inorganic phosphate (P_i) or difluoromethyl alanine showed close similarity. Toxicity was low and the molecules were stable, but loading indicators into cells is problematic. Generally, methyl esters have been used, which are relatively stable in water, but undergo non-specific enzymatic hydrolysis intracellularly, liberating the pH-sensitive molecules [87]. This approach can lead to complex spectra including overlapping multi-line ester and liberated free acid resonances from both intra- and extracellular compartments [92]. For investigations in perfused organs or cell culture, extracellular indicator can be washed away with unlabeled perfusate, after loading the intracellular compartment, in order to simplify the NMR spectra. The mono- and trifluoro derivatives require an additional chemical shift reference standard, *e.g.*, sodium trifluoroacetate. An advantage of the difluoro derivative is that the relative chemical shifts of the resonances of the ^{19}F AB quartet are pH sensitive obviating the need for a standard. However, the multiple signals do cause decreased SNR and both mono and difluoro derivatives require ^{1}H-decoupling for efficient utilization. Widespread use of these molecules has been hindered by the problem of loading the indicators into cells and the relatively small chemical shift range ~ 2 ppm.

3.2.2 Fluorinated Vitamin B6 Derivatives

Analogs of vitamin B6, *e.g.*, 6-FPOL (2-fluoro-5-hydroxy-6-methyl-3,4-pyridinedimethanol) are highly sensitive to pH [45, 93-95]. Synthesis of 6-FPOL is achieved in three steps starting from pyridoxine hydrochloride [96]. Diazotization of pyridoxine with benzene diazonium chloride yields 6-phenazopyridoxol and dithionite reduction produces 6-aminopyridoxol. 6-FPOL is then obtained using a modified Schieman reaction. 6-FPOL readily enters cells and provides well resolved resonances reporting both intra- and extracellular pH (pHi and pHe), simultaneously, in whole blood [45] and the perfused rat heart, as confirmed by ^{31}P NMR and pH electrodes [93]. In contrast to other pH indicators, 6-FPOL readily enters certain cells without the need for loadable derivatives. For blood cells, this may be related to transport, since vitamin B6 is naturally stored, transported, and redistributed by erythrocytes [97]. *In vivo*, we have generally only observed a single signal from tumors implanted in rats or mice suggesting extra cellular signal only, and it is often broad suggesting tumor heterogeneity (Fig. 7). The molecule not only has a remarkable chemical shift range (~ 10 ppm), but in contrast to many pH indicators there is negligible response to changes in metal ion concentrations, the presence of proteins, or variations in temperature [93]. The somewhat basic pKa = 8.2 is appropriate for investigations of cellular alkalosis, but it is not ideal for studies in the normal physiological range (6.5-7.5).

[6] Cui, W.; Otten, P.; Yu, J.; Kodibagkar, V.; Mason, R.P., Proc. ISMRM, Toronto, Canada, 2003, p. 675.

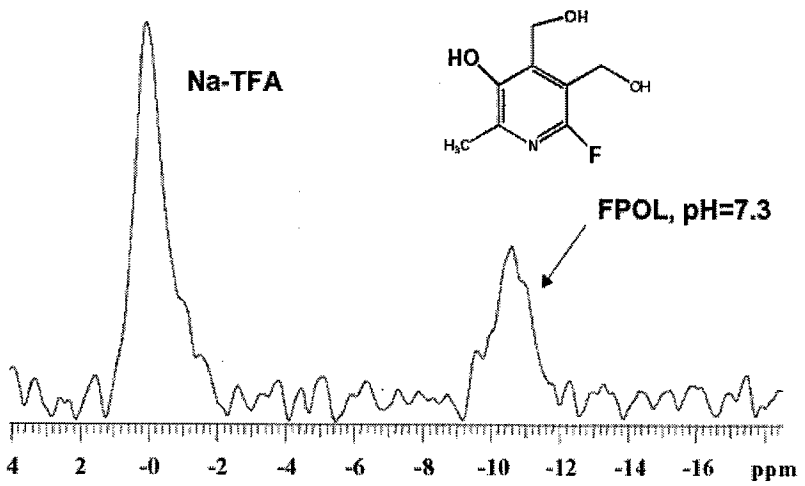

Fig. (7). 188 MHz ^{19}F NMR of rat pedicle breast tumor 13762NF following administration of 470 μmol FPOL i.p. together with NaTFA. The broad ^{19}F NMR signal indicates pH = 7.3.

The response of ^{19}F NMR chemical shift to pH in the physiological range in these molecules is considered to be mainly due to protonation and deprotonation of the 3-phenolic OH [96, 98]. This affects the electronic environment around fluorine at the 6-position, which is particularly pronounced due to the para location. Extensive literature on modifications of vitamin B_6 suggested that the introduction of electron donating or withdrawing groups at the 4 and 5 positions of the pyridoxol ring could significantly alter the pKa of the 3-phenolic group, and the NMR properties at the 6-position [95, 99, 100]. From a series of analogs 6-fluoropyridoxamine (6-FPAM) was identified as an enhanced pH indicator (pKa 7.05) [94]. Other analogs had pKa in the range 5.5 to 9.5 with chemical shift response of 7.5 to 12.1 ppm. 6-FPAM also has a single narrow resonance in solution with chemical shift independent of environment, other than pH. Like with 6FPOL, we have observed intra and extracellular signals in whole blood and perfused rat hearts [28, 94]. On rare occasions, we have seen evidence for intra and extra cellular signals in tumor cells (Fig. **8**) [7]. Given the large chemical shift range for ^{19}F, signal interference is rare. However, there can be conflict between signals from the popular anesthetic gas isoflurane (δ = 5 and 11 ppm) and the Vitamin B6 indicators (δ 9.8 - 20 ppm) (Fig. **9**). Such interference can be avoided by using alternate anesthetics.

To enhance SNR, or reduce the required dose, a pH sensitive CF_3 moiety could be introduced in place of the F-atom. The chemical shift range decreases (Δδ~ 1.64 ppm)[8], as expected since electronic sensing must be transmitted through an additional C-C bond. Importantly, the ^{19}F NMR signal occurs downfield from NaTFA and there is no longer any interference from the isoflurane signals [6] (Fig. **9**). While FPOL and FPAM provide both intra and extra cellular signals with varying ratios depending on cell type. CF_3POL is found to occur exclusively in the extra cellular compartment, and thus reports pHe, or interstitial pH.

3.2.3. Fluorophenols

Many fluorophenols are commercially available facilitating ready evaluation as physiological indicators (Aldrich, Lancaster). Based on our observations with the fluorophenol galactosides, we explored the use of the aglycones as pH indicators. As expected, o-fluorophenols have a smaller chemical shift range (~ 0.3 to 2.2 ppm), as opposed to p-fluorophenols, which exhibit Δδ 6.4 to 11.3 ppm. pKa was found in the range 5.4 to 9.8 ppm depending on substituents (Yu, Cui, Otten, unpublished observations). PFONP has Δδ 9.29 ppm and pKa 6.85 [29][3]. PFONP appears cytolytic for certain tumor cells and may act as an ionophore. However, we have obtained pH gradient measurements in whole blood, which were in agreement with FPOL and electrode measurements[3]. Trifluoromethyl-phenols also show titration response though typically, Δδ = 1.2 ppm (p-CF_3ArOH, pKa 8.5) to 0.4 ppm (o-CF_3-Ar, pKa 7.92) (Cui, Yu unpublished).

3.2.4. Other pH Reporters

By modifying known fluorescent pH indicators, Metcalfe *et al.* reported a series of fluorinated molecules, which were sensitive to various ions, *e.g.*, Ca^{2+}, Zn^{2+} and H^+ [101]. F-quene, a ^{19}F NMR sensitive analog of the fluorescent pH indicator quene-1, was used to measure intracellular pH in a perfused heart [101] and liver [102]. The chemotherapeutic agent difluoromethyl ornithine has a small chemical shift range, which is also temperature sensitive, but it has been tested in rat tumors [103]. Bental and Deutsch [104] reported a fluoro-iso-butyric acid derivative, which has the advantage of a single ^1H decoupled-^{19}F NMR resonance, improving the signal to noise ratio (SNR). Taylor and Deutsch [105] showed that N-methyl methoxyisopropyl fluoroaniline had a chemical shift range ~17 ppm, but the pKa (5.8) was less suitable for *in vivo* investigations. Modification to methoxyisopropyl fluoroaniline [105] retained a substantial chemical shift range (Δδ 12 ppm) and produced a physiologically suitable pKa, however, no biological studies have been reported. N-ethylaminophenol (NEAP) has been

[7] Cui, C., Ma, Z., He, S., Peschke, P., and Mason, R. P., 8th Int. Conf. Tumor Microenvironment and Its Impact on Cancer Therapies, Miami (South Beach), Fl, 2003, p. II-5.

[8] Yu, J., Otten, P., Cui, W., and Mason, R. P., 38th National Organic Symp., Bloomington, IN, 2003, p. B2.

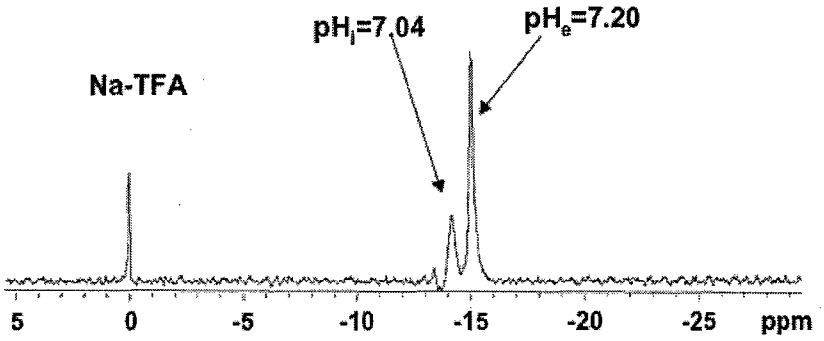

Fig. (8). ^{19}F NMR (9.4 T) of a suspension of 10^7 Morris hepatoma MH-Tk cells in buffer following addition of FPAM (58.3 mM) showed two signals attributed to intra and extra cellular compartments at -14.16 ppm and –15.04 ppm, corresponding to pHi = 7.04 and pHe = 7.20. (data obtained in collaboration with Drs. Peter Peschke and Uwe Haberkorn, DKFZ, Heidelberg, Germany).

described with various analogs to detect pH or metal ions [106]. Frenzel *et al.* [107] have described a fluoroaniline sulfonamide (ZK 150471) and its use has been demonstrated in mice and rats to investigate tumor pH [108, 109]. This molecule is restricted to the extracellular compartment only [107, 110], but combination with ^{31}P NMR of P_i to determine pHi has been used to reveal the transmembrane pH gradient in mouse tumors [111]. A distinct problem with ZK150471 is that the pKa differs in saline and plasma [110]. Both NEAP [106] and ZK150471 [107] have non-titrating intramolecular chemical shift references.

Wherever a difference exists between normal tissue and cancer there is an opportunity for selective therapy. For instance, molecular partitioning into cells is influenced by the pH gradient and many drugs are weak acids or bases [112-116]. However, the pH gradient (ΔpH) is often small and distinctly variable, and thus, the tumor microenvironment may need to be manipulated to further enhance cytotoxicity, *e.g.*, infusion of glucose or ionophores may cause tumor acidification [113, 117-120]. Inhalation of carbogen ($5\%CO_2/95\%O_2$) was reported to reduce pHe and generate a pH gradient ~0.1 units in large murine RIF-1 tumors [111]. This corresponded with the typical pH gradient found in small RIF-1 tumors, though they apparently did not respond to carbogen. Dietary alkaline load is reported to produce extracellular alkalization leading to pHe > pHi in nude mice bearing a xenografted breast tumor [115].

PH may be measured using ^{31}P NMR of endogenous Pi, though intra and extra cellular concentrations are variable and may not always be resolved [121, 122]. ^{19}F NMR agents can provide a much wider chemical shift range and in some cases report transmembrane pH gradient, though further development is needed for widespread application. Often, only a single global pH value is obtained, though chemical shift imaging (CSI) has been used to map pH based on ^{1}H and ^{31}P NMR [123, 124] and new ^{1}H pH sensitive relaxation contrast agents have been reported and reviewed [10, 32, 125, 126].

3.3. Metal Ions

Several metal ions are thought to play key roles in cellular physiological processes. Thus, there has been much interest in developing specific reporter molecules. The greatest availability is in the realm of fluorescent indicators, specifically, agents incorporating extended aromatic and conjugated structures, where the wavelength of fluorescence depends upon specific binding of a metal ion. Indeed, many agents are now commercially available (*e.g.*, Molecular Probes). The addition of fluorine atoms has yielded ^{19}F NMR reporters (Table **5**).

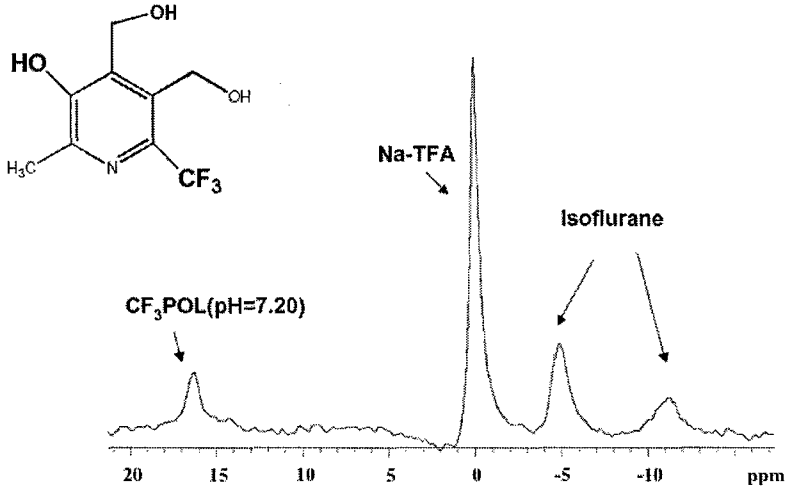

Fig. (9). 188 MHz ^{19}F NMR of Dunning prostate R3327-AT1 rat tumor (~ 1 cm^3) following administration of CF_3POL (320 mg/kg) with 17 min acquisition. NaTFA was used as chemical shift reference at 0 ppm and isoflurane anesthetic signals are also observed.

Table 5. ^{19}F NMR Metal Ions Indicators

Detected Ion	Agent	Structure	Application
$[Mg^{2+}]$	F-APTRA	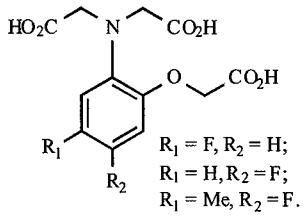	Erythrocytes [36, 142]
$[Ca^{2+}]$	5F-BAPTA	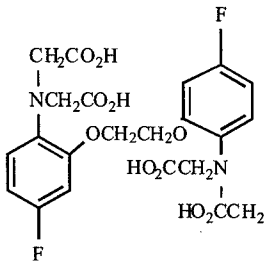	Tumors, cells, heart [36, 101, 130, 366, 367]
$[Na^{+}]$	F-cryp-1	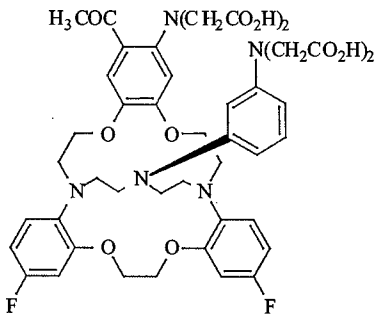	Tumors, cells, heart [145]
$[Ni^{2+}]$	F-Cyclam	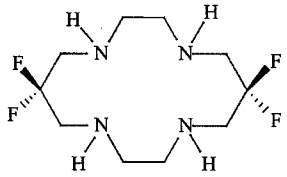	[368]
$[Cu^{2+}]$	F-Dioxocyclam	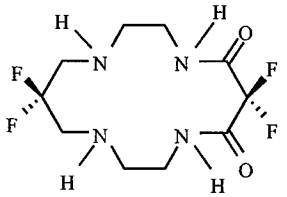	[368]
$[Li^{+}]$	FN_2O_3	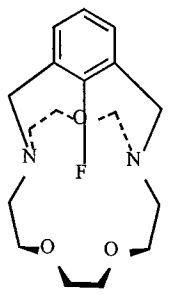	[136]

(Table 3). contd..

Detected Ion	Agent	Structure	Application
$[K^+]$	FN_2O_4	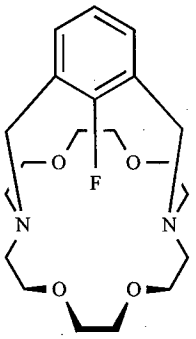	[136]
$[Sr^{2+}]$	FO_5	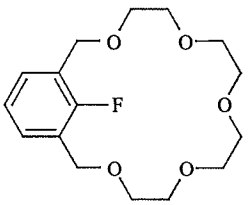	[136]
$[Ba^{2+}]$	FO_6	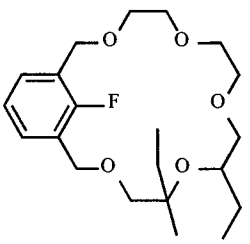	[136]
Membrane/ Chloride Potential	TFA	$CF_3CO_2^-$	Cells, perfused heart [349, 350]

3.3.1 Detection of Calcium Ions

A fundamental development was that of Tsien, *et al.* [127], who proposed loading fluorescent metal ion chelators into cells using acetoxymethyl esters and demonstrated 1,2-bis(o-amino-phenoxy)ethane-N,N,N',N'-tetraacetic acid (BAPTA) for detecting intracellular calcium ions. Metcalfe, *et al.* [101] added para-fluoro atoms to the aromatic ring yielding a ^{19}F NMR responsive agent (5,5-difluoro-1,2-bis(o-amino-phenoxy)ethane-N,N,N',N'-tetraacetic acid (5FBAPTA)) (Table **5**). Upon binding calcium, there is a change in chemical shift. Ideally, such a reporter molecule would have high specificity for the metal ion of interest. In fact, the F-BAPTA agents are found to bind several divalent metal ions, including Ca^{2+}, Zn^{2+}, Pb^{2+}, Fe^{2+}, and Mn^{2+} [128, 129]. However, there is a very low affinity for Mg^{2+}. Fortunately, each metal ion chelate has an individual chemical shift, so that they can be detected simultaneously [130] and do not directly interfere with measurements.

5FBAPTA includes two fluorine atoms symmetrically placed to provide a single signal. Upon binding there is slow exchange of Ca^{2+}, on and off the indicator, on the NMR time scale, so that separate signals are seen for the free and metal ion bound moieties, with chemical shifts of several ppm. Calcium concentration may be calculated from the formula [130].

$$[Ca^{2+}] = K_D[Ca\text{-}FBAPTA]/[FBAPTA].$$

Typical calcium concentrations detected in cells, have been independently verified using fluorescence [130]. However, it is important to recognize that the dissociation constant (K_D) does depend on pH, ionic strength, and the concentration of free Mg^{2+}, which need to be estimated independently. In many cases, pH can be estimated from the chemical shift of inorganic phosphate using ^{31}P NMR. Of course, it can also be estimated using fluorinated pH indicators, as discussed above (Section 3.2). Magnesium ion concentrations may be estimated from the chemical shifts of the resonances of ATP, which vary upon binding magnesium [131, 132]. Signals from both bound and unbound forms allow ready identification of the moieties, avoiding the need for incorporation of a chemical shift reference. 5FBAPTA has been used extensively [130] in studies of tumor cells [133], osteoblastic cells [134] thymocytes [129], blood, and the perfused beating heart, where studies of calcium transients during the myocardial cycle have been reported [135]. A variant is 4F-BAPTA, which has a somewhat lower binding constant K_D =0.7 μM, but more significantly at 94 MHz is found to be in fast exchange [130]. Thus, the signals from the bound and unbound forms are averaged, and it is the absolute chemical shift, which is related to the ratio of the two components. Plenio and Diodone have also reported fluorocrown ethers,

which exhibit chemical shift response upon binding Ca^{2+} [136]. Of course, calcium could potentially be analyzed directly by ^{43}Ca NMR, however, its natural abundance is <0.2%, its sensitivity is <1% that of ^{1}H, and being quadrupolar, it is liable to extensive line broadening [44]. Thus, the application of ^{19}F NMR with appropriately designed reporter molecules gives insight into cytosolic $[Ca^{2+}]$.

A critical issue for intracellular interrogation is loading the reporter molecule into cells. The tetra-carboxylates do not penetrate cells, however, derivatization as acetoxymethyl esters, which has been very widely used in association with analogous fluorescent indicators provides a more lipophilic entity, which can equilibrate across cell membranes [127]. These esters are specifically designed so that intra-cellular esterases cleave the acetoxy methyl ester, releasing the charged reporter molecule, which is then essentially trapped in the intracellular compartment. The release of acetic acid and formaldehyde are considered to be relatively innocuous.

3.3.2 Detection of Magnesium Ions

Magnesium ions can occur in tissues and cells at millimolar concentrations and play an important role in many physiological processes [137, 138]. There are many fluorescent indicators for detection, together with ion selective electrodes [139]. Magnesium can also be estimated based on the chemical shift difference of the resonances of ATP using ^{31}P NMR [131, 132]. However, ^{31}P NMR has intrinsically low signal to noise, exacerbated under many pathophysiological conditions, such as ischemia. Thus, there has been considerable interest in developing fluorinated NMR reporter molecules for detecting $[Mg^{2+}]$. The simplest is, perhaps, fluorocitrate [140]. Upon binding Mg^{2+} there is a change in chemical shift. However, fluorocitrate can be incorporated into the tri-carboxylic acid cycle as a potent highly toxic suicide inhibitor. Thus, it is critical that the reporter molecule be used as the plus isomer only, which shows little toxicity [141]. Given the difficulties in synthesis, and specifically isomeric isolation, alternative indicators have been sought. Levy, *et al.* [36, 142] developed classes of indicators based on the APTRA structure, both for fluorescent application and by incorporation of fluorine atoms for ^{19}F NMR. APTRA agents must be derivatized as acetoxymethyl esters in order to load tissues, and they have been reported for use in the perfused rat heart [143].

3.3.3 Other Biological Relevant Ligands

As described in 3.3.1, F-BAPTA provides a unique chemical shift with many divalent metal ions [128, 129] and has been used to estimate $[Zn^{2+}]$ [128], $[Pb^{2+}]$ [144], and $[Cd^{2+}]$ [128]. Other investigators have designed molecules to specifically interact with sodium ions. F-Cryp-1 was used to show that the total ^{23}Na NMR signal visible is less than 100% [145]. London and Gabel [146] reported fluorobenzene boronic acid, which interacted with specific sugars. Plenio and Diodone [147] reported fluorine containing cryptands, which interact with perchlorate. These investigators have also reported a series of fluorocyclophanes and fluoro crown ethers to explore specific cation binding (*e.g.*, K^+, Li^+, Na^+, Ba^{2+}, Sr^{2+}, Ca^{2+}, and associated chemical shifts [136, 148]. Takamure [149] reported macrocycles designed to bind K^+, NH_4^+, and Ag^+.

3.3.4 Reporter Molecules for Detection of Ions

In considering reporter molecules, a number of criteria are pertinent. The reporter molecule must in some way reach the cellular compartment of interest. Some molecules penetrate cells directly, for others it is facilitated by acetoxymethyl esters. In other cases specific cellular exclusion is important, so that any signal can unambiguously be attributed to the extra-cellular or interstitial compartment in a tissue. Such measurements would be analogous to electrode measurements. It is critical that the reporter molecule not perturb the system under investigation. For ions, there is inevitably some binding and complexation. Provided there is sufficient reservoir of the ions, there can be rapid re-equilibration, and the concentration may give a realistic indication of the free concentration. In unregulated systems, this may be less reliable. The fluorine NMR spectrum must be perturbed upon interaction with the ion of interest. This may be through the formation of a second signal, as in the slow exchange regime, or chemical shift in a fast exchange regime. Changes may be observed in coupling constants or relaxation times. For many ions, agents should be water soluble, although a degree of lipophilicity may help in transport. Signals should be narrow to enhance both the signal to noise and spectral resolution. The binding constant must be compatible with the typical concentration encountered *in vivo*. Ideally, the reporter ligand is highly selective for the ion of interest and of course the molecule should exhibit minimal toxicity. Further criteria are that the reporter molecule be readily available, particularly when complex synthesis is required. Reporter molecules, which are described in the literature, may not be readily available to other investigators.

3.4. Tissue Oxygenation and Hypoxia

While reporter molecules for enzyme activity and ions (Sections 3.1-3, above) are based almost exclusively on chemical shift response, measurement of pO_2 is based on variations of relaxation rates, as reviewed recently [27]. Hypoxia sensing agents rely on enzyme activated trapping [150]. It has long been appreciated that hypoxic tumor cells are more resistant to radiotherapy [151]. Indeed, a three fold increase in radio resistance may occur when cells are irradiated under hypoxic conditions compared with $pO_2 > 15$ torr for a given single radiation dose. However, recent modeling has indicated that the proportion of cells in the range 0 - 20 torr may be most significant in terms of surviving a course of fractionated radiotherapy [152]. Certain chemotherapeutic drugs also present differential efficacy depending on hypoxia [153, 154]. Increasingly, there is evidence that hypoxia also influences such critical characteristics as angiogenesis, tumor invasion and metastasis [155-158]. Given that hypoxic tumors are more resistant to certain therapies, it becomes important to assess tumor oxygenation as part of therapeutic planning. Patients could be stratified according to baseline hypoxia to receive adjuvant interventions designed to modulate pO_2, or more intense therapy as facilitated by IMRT (Intensity Modulated Radiation Therapy). Tumors, which do not respond to

Table 6. ^{19}F NMR Characteristics and Applications of PFCs for Tissue Oximetry

Name	Structure	Sensitivity to pO_2 [a]	Temp. Sensitivity (torr/^{0}C) [b]	Applications
HFB	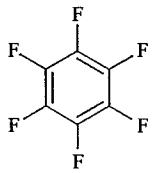	A=0.0835 B=0.001876	0.13	Rat breast and prostate tumors, human lymphoma xenograft [27, 169, 173, 199-202, 215, 218]
Perfluoro-15-crown-5-ether	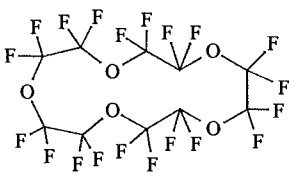	A=0.345 B=0.0034	0.94	Tumor cells, mouse tumor, spleen, liver, human glioma tumor in mice, rat breast tumor, rat brain [150, 170, 191, 194, 197, 198, 210]
FC-43	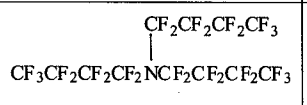	A=1.09 B=0.00623	4.43	Rodent liver, spleen, lung, eye, tumors, heart and human eye[168, 184, 189, 207, 214, 369, 370]
PFTP	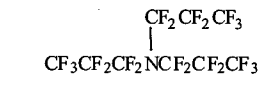	A=0.314 B=0.002760^{-3}		Rat subcutaneous tumor, spleen, lung, tumors, cells [46, 195]
F-44E	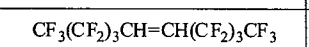	A=0.2525 B=0.16527	0.59	Alginate capsules, rodent spleen, liver, tumors [186, 196, 205]
PFOB	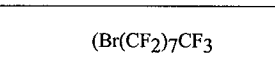	A=0.2677 B=0.12259	1.26	Rat heart, prostate tumor, rabbit liver, [162, 171, 172, 190, 371]
PTBD	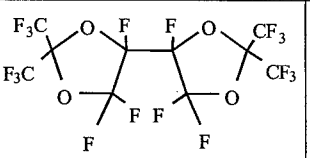	A=0.50104 B=0.1672		phantom [372]

[a] R1 (s^{-1}) = A+B*pO_2 (torr)

[b] variation in pO_2 per ^{0}C error in temperature estimate

interventions, may be ideal candidates for hypoxia selective cytotoxins (*e.g.*, tirapazamine [159]).

3.4.1. Fluorinated pO_2 Reporter Molecules

The ^{19}F NMR spin lattice relaxation rate R_1 of a perfluorocarbon varies linearly with pO_2 [27, 33, 160] and may be sensitive to temperature, and magnetic field. Importantly, R1 of PFCs is essentially unresponsive to pH, CO_2, charged paramagnetic ions, mixing with blood, or emulsification [46, 160-166]. For an emulsion of perfluorotributylamine, we have shown that the calibration curves obtained in solution are valid for PFC sequestered in tissue [167]. At any given magnetic field (B_o) and temperature (T), sensitivity of R_1 to changes in pO_2 is given by the linear relationship

$$R_1 = A + B*pO_2.$$

The value of the intercept A represents the anoxic relaxation rate and the slope B represents the sensitivity of the reporter molecule to the paramagnetic contribution of oxygen to the relaxation rate. The ratio $\eta = B/A$ has been proposed as a sensitivity index [168]. Small A, and hence long T_1, potentially creates long imaging cycles, but this is readily overcome by applying single shot (echo planar) imaging techniques [169-171]. A particular PFC molecule may have multiple resonances, and each resonance has a characteristic R_1 response to pO_2 and temperature due to steric effects of O_2, as it approaches the molecule [37, 50]. Characteristics of many reported PFCs are summarized in (Table **6**).

R1 is sensitive to temperature, although the response varies greatly between PFCs and between individual resonances of each individual PFC. Over small temperature ranges, a linear correction to calibration curves is appropriate, but over larger temperature ranges the response can be complex [50]. Differential sensitivity of pairs of resonances to pO_2 and temperature allowed Mason, *et al.* [167] to simultaneously determine both parameters by solving simultaneous equations. However, generally it is preferable for a pO_2 sensor to exhibit minimal response to

Fig. (10). ^{19}F MRI of Novikoff hepatoma in thigh of rat. Oxypherol emulsion was administered (4x4 ml over two days) and allowed to clear from the vasculature. ^{1}H MRI shows the tumor (~ 1 cm diameter) and thigh muscle. The corresponding ^{19}F MRI shows sequestered PFC in the bone marrow and around the periphery of this multi nodular tumor (image resolution 470 x 300 μm with 5 mm slice thickness) (From R. P. Mason, P. Peschke, E. W. Hahn, A. Constantinescu and P. P. Antich, Proc. *1st SMR*, Dallas, S12-059, 1994).

temperature, since this is not always known precisely *in vivo* and temperature gradients may occur across tumors. Even a relatively small error in temperature estimate can introduce a sizable discrepancy into the apparent pO_2 based on some PFCs, *e.g.*, the relative error introduced into a pO_2 determination by a 1 °C error in temperature estimate ranges from 8 torr/°C for perfluorotributylamine [167], to 3 torr/°C for PFOB (perflubron) [172] or 15-Crown-5-ether [170], when pO_2 is actually 5 torr. HFB exhibits remarkable lack of temperature dependence and the comparative error would be 0.1 torr/°C [173].

Thomas, *et al.* [33], pioneered the application of ^{19}F NMR relaxometry to measure pO_2 in tissues, *in vivo*, including lung, liver, and spleen with investigations relative to various interventions. PFCs are extremely hydrophobic and do not dissolve in blood directly, but may be formulated as biocompatible emulsions for intravenous (IV) infusion. Emulsion stability is critically dependent on the vapor pressure of the PFC and the emulsifying components, such as surfactants, and phospholipids. PFC emulsions have been developed commercially both as potential synthetic blood substitutes (*e.g.*, Oxygent®, Fluosol®, Therox®, Oxypherol®) [174-177] and as ultrasound contrast agents (*e.g.*, Optison®, Definity®, Sonovue®, Imagent® [178, 179]. Following IV infusion, a typical blood substitute emulsion (*e.g.*, Oxypherol®, Imagent®) circulates in the vasculature with a half-life of 12 h providing substantial clearance within two days [175]. Primary clearance is by macrophage activity leading to extensive accumulation in the liver, spleen, and bone marrow [180, 181]. Indeed, this is a major shortcoming of IV delivery, since animals may exhibit extensive hepatomegaly or splenomegaly [175, 180, 182]. The emulsions are not toxic, and other than causing swelling, appear not to cause health problems [175]. PFC is retained in the liver with a typical half-life of 60 days for perfluorotripropylamine and 3 days for perflubron, with primary clearance by migration to the lungs and exhalation [181]. Some investigators have examined pO_2 of tissues, while PFC remained in the blood, providing a vascular pO_2 measurement [163, 183-186]. Flow can generate artifacts and correction algorithms have been proposed [9]. More extensive pO_2 measurements have been reported following clearance from the blood, in liver, spleen, abscess, perfused heart, and tumors [169, 170, 186-202].

Uptake and deposition of PFC emulsions in tumors is highly variable and heterogeneous (Fig. **10**) typically, accounting for 1-5% of sequestered material [180]. Most signal occurs in well perfused regions, and indeed pO_2 values measured soon after intravenous infusion, but following vascular clearance, are generally high, approaching arterial pO_2 [187]. PFC does not seem to redistribute within tissue, but remains associated with specific locations. It has been shown that new tumor tissue grew around initially labeled tissue [187]. Peripheral distribution was also observed in a Novikoff hepatoma implanted in a rat (Fig. **10**). Intriguingly, this tumor showed spontaneous regression following administration of PFC emulsion, but the tumor periphery remained labeled and signal coincided with tumor shrinkage (Fig. **11**). The location of the tumor could still be identified even after the tumor had shrunken below palpable size. Such long term tissue marking has been proposed as a form of non-invasive histology and might have new applications for tracing stem cell grafts and cell migration [10]. Recently, cell labeling has been developed based on cellular retention of superparamagnetic iron oxide particles

[9] Higuchi, T., Naruse, S., Horikawa, Y., Hirakawa, K., and Tanaka, C. Proc. *7th SMRM* (1988) p435

[10] Antich, P. P., Mason, R. P., Constantinescu, A., Peschke, P., and Hahn, E. W. *Proc. Soc. Nucl. Med. 35(5),* (1994) p216

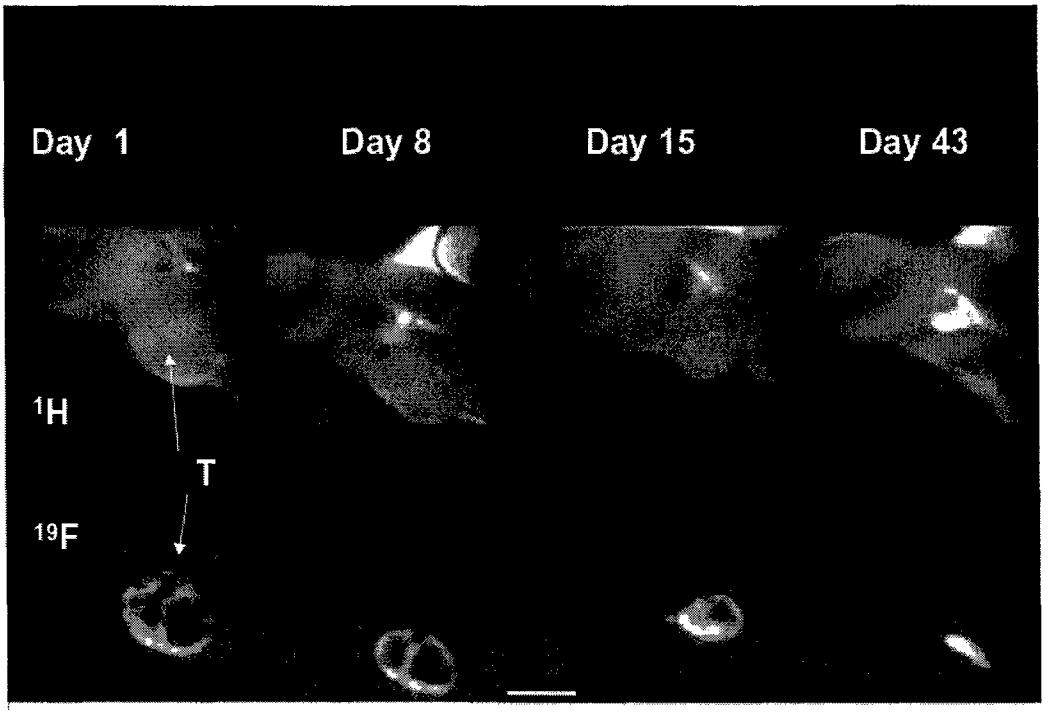

Fig. (11). ^{19}F MRI of Novikoff hepatoma in thigh of rat. The tumor in Fig. (**10**) regressed spontaneously over the next 43 days and residual PFC showed location.

[203]. Long tissue retention has the advantage of facilitating chronic studies during tumor development and progressive tumor hypoxiation has been observed over many days [187, 192].

Two approaches have been applied to circumvent reticuloendothelial uptake. PFC has been incorporated in polyalginate beads for direct implantation at a site of interest [204, 205]. We favor direct intratumoral (IT) injection of neat PFC allowing any region of interest in a tumor to be interrogated immediately. Use of a fine needle ensures minimal tissue damage. Others have used direct injection of emulsions into tumors, but this increases the volume considerably making it more invasive [206]. Investigators have suggested that emulsification improves retention at the site of injection. Direct injection of neat PFC has also been used to investigate retinal oxygenation [207-209] and cerebral oxygenation in the interstitial and ventricular spaces [210].

Choice of PFC may be governed by practical considerations, such as cost and availability, since several products, particularly, proprietary emulsions may be difficult to obtain. Many PFCs (*e.g.*, perfluorotributylamine (PFTB), perflubron (formerly referred to as perfluorooctyl bromide; PFOB), Therox^{TM} (F44-E)) have several ^{19}F NMR resonances, which can be exploited to provide additional information in spectroscopic studies, but seriously hamper effective imaging. Multiple resonances can lead to chemical shift artifacts in images, which compromise the integrity of relaxation time measurements, though they can be avoided by selective excitation, or detection, chemical shift imaging, deconvolution or sophisticated tricks of NMR spin physics [52, 171, 190, 211-214]. These approaches add to experimental complexity and are generally associated with lost signal to noise ratio (SNR). PFCs with a single resonance provide optimal SNR and simplify imaging: two agents hexafluorobenzene (HFB) [199-202, 215-218], and perfluoro-15-crown-5-ether (15C5) [170, 193, 206, 210] have found extensive use. HFB and 15C5 offer the immediate advantage of a high symmetry and a single ^{19}F NMR resonance. While 15C5 has 20 equivalent fluorine atoms per molecule and HFB has only 6, the difference in molecular weight (580 vs. 186) provides only 6% extra ^{19}F signal per unit volume (*i.e.*, µl administered dose) assuming equal density (1.62 g/ml).

Hexafluorobenzene has many virtues as a pO_2 reporter [173]. Symmetry provides a single narrow ^{19}F NMR signal and the spin lattice relaxation rate is highly sensitive to changes in pO_2, yet minimally responsive to temperature [173]. Prior to our applications of HFB to tumor oximetry *in vivo*, several studies had examined the interaction of oxygen and HFB by NMR [219-221]. HFB also has a long spin spin relaxation time (T2), which is particularly important for imaging investigations. From a practical perspective HFB is cheap (<$2/g) and readily available commercially in high purity (>99%). HFB is well characterized in terms of lack of toxicity [222, 223], exhibiting no mutagenicity [224], teratogenicity or fetotoxicity [225] and the manufacturer's material data safety sheet indicates LD_{50} > 25 g/kg (oral- rat) and LC_{50} 95 g/m^3/2 hours (inhalation-mouse). HFB had been proposed as a veterinary anesthetic and has been used in many species including ponies, sheep, cats, dogs, rats and mice, but was abandoned due to its high volatility (b.p. 81 °C) and low flash point (10 °C) [226]. It is not a problem in our studies, where small quantities of liquid (typically, 50 µl) are injected directly into the tumor. HFB requires no special storage, other than a sealed bottle to prevent evaporation.

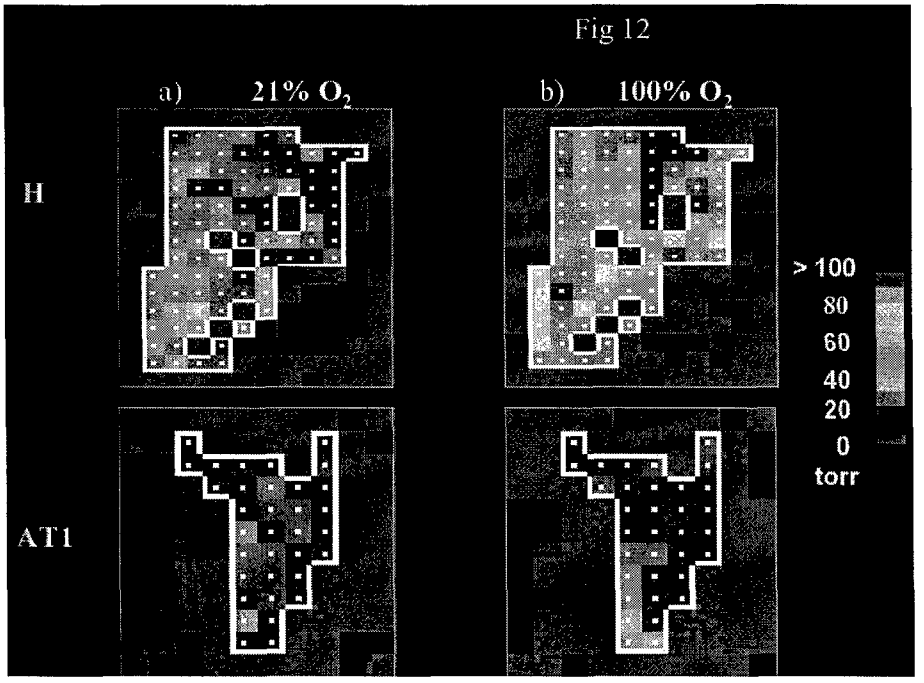

Fig. (12). pO_2 maps of Dunning prostate R3327 tumors in pedicles of Copenhagen rats obtained using *FREDOM* based on interrogation of the reporter molecule hexafluorobenzene. The H tumor (1.1 cm^3; baseline median pO_2 = 26.7 torr) was better oxygenated than the AT1 tumor (2.6 cm^3; baseline median pO_2 = 12.5 torr). In response to oxygen inhalation, pO_2 increased in both the H (median pO_2 = 96.4 torr) and the AT1 tumors (median pO_2 = 29.5 torr) and the largest response was observed in those areas initially well oxygenated. This approach allows oxygen dynamics to be observed in tissues in response to interventions based on small amounts of reporter molecule (50 µl HFB, introduced i.t.) (Data obtained in collaboration with Dr. Dawen Zhao).

For initial studies, HFB (10-20 µl) was injected directly into the center or periphery of a tumor using a very fine sharp tipped needle (32 gauge). Local pO_2 measurements indicated tumor heterogeneity [169, 173]. The insertion of a needle is reminiscent of electrode studies, but importantly the HFB remains localized in the tumor for many hours (typical half life ~ 600 mins) allowing repeat measurements from an individual location with respect to acute interventions, *e.g.*, hyperoxic gas challenge. To overcome any potential artifacts from HFB clearance during a data acquisition, we instituted the *ARDVARC* (Alternating Relaxation Delays with Variable Acquisitions to Reduce Clearance effects) protocol, which improves SNR and reduces overall data acquisition time [169, 227]. *FREDOM* (Fluorocarbon Relaxometry using Echo planar imaging for Dynamic Oxygen Mapping) can provide 50 to 150 individual pO_2 measurements across a tumor simultaneously in about 6.5 mins with a local precision of 1 to 3 torr in relatively hypoxic regions based on 50 µl injected dose (Fig. **12**) [27, 169]. NMR is also compatible with optical measurements and we have explored simultaneous NIR and MR approaches to measure vascular oxygenation in combination with pO_2 [11,12]. Other studies have examined the effects of vascular targeting agents [218], vasoactive agents [215] and hyperoxic gases [27, 169, 199-202, 215, 216, 228]. Results are consistent with hypoxia estimates using the histological marker pimonidazole [199]. Most significantly, estimates of pO_2 and modulation of tumor hypoxia are found to be consistent with modified tumor response to irradiation [201][13]. Such prognostic capability could be important in the clinic, since it is known that relatively hypoxic tumors tend to be more aggressive and respond less well to radiation therapy [155, 157, 159, 229, 230].

We have shown that measurements are consistent with sequential determinations made using electrodes [231, 232] and fiber optic systems (FOXY™ and OxyLite®) [216, 233]. Repeat measurements are highly reproducible and generally quite stable in tumors under baseline conditions. For PFCs, we believe that calibration curves determined in solution are valid *in vivo* and for an emulsion of perfluorotributylamine (Oxypherol®) measured in perfused rat heart, we have rigorously validated the measurements independently [167]. Others have shown that R1 of various PFCs was independent of emulsification [160, 161]. ^{19}F R1 of the emulsions was independent of dilution [162] and changes in pH [46, 163], common proteins [46, 163, 165] or blood [164]. R1 is unaffected by the presence of paramagnetic ions [165, 234], although certain lipophilic spin labels such as doxylsterate nitroxide did cause perturbation[14]. In essence the PFCs form droplets and are essentially immune to the influence of materials in the

[11] Xia, M.; Kodibagkar, V.D.; Constantinescu , A.; Gu, Y.; Liu, H.; Mason, R.P., Proc. 12th ISMRM, Kyoto, Japan, 2004, p. 2004.

[12] Gu, Y.; Xia, M.; Liu, H.; Kodibagkar, V.; Constantinescu, A.; Mason, R.P., Biomedical Topical Meetings, Washington, DC, 2004, p. FB6.

[13] Bourke, V., Gilio, J., Zhao, D., Constantinescu, A., Kodibagkar, V., Jiang, L., Hahn, E. W., and Mason, R. P., Radiat. Res. Meeting, St. Louis, MO, 2004.

[14] Muller, R.N.; Brown, R.D.; Koenig, S.H., Society of Magnetic Resonance in Medicine 5th Annual Meeting, Montreal, 1986, p. 327

Table 7. ^{19}F NMR Hypoxia Indicators

Name	Structure	References
CCI 103F	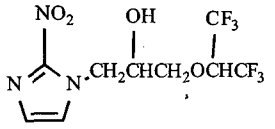	[248-252]
RO 070741	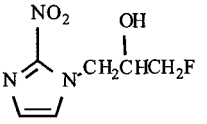	[249, 253]
SR 4554	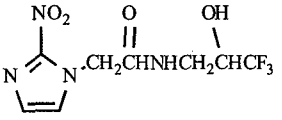	[254-259]
NLTQ-1	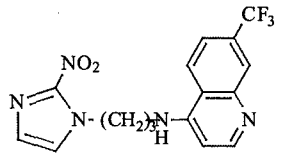	[373]

accompanying aqueous phase due to $1/r^6$ dipole effect. However, materials that dissolve in the PFC itself do alter the relaxation properties, hence, the strong effect of the highly soluble gas oxygen. For fluorohydrocarbons (not fully perfluorinated), the relaxation curves may be altered by additional environmental effects, since they may interact with lipids. For Therox F44E, we had problems achieving standard calibration curves [235] and others have also experienced unexpected values [205]. Specifically, Nöth *et al.* [205], found different calibration curves for the fluorohydrocarbon F44E in the pure state or when incorporated into polyalginate beads. This is likely a function of the partial fluorocarbon nature. Indeed, certain fluorohydrocarbons have been specifically designed to incorporate asymmetrically into membranes in order to explore micro regional pO_2 gradients [216].

3.4.2 Hypoxia

Nitroimidazoles are bioreductive agents that are reduced by intracellular reductases to generate reactive intermediates. In the presence of oxygen, the intermediates are rapidly reoxidised and may clear from cells. Under hypoxic conditions they become covalently bound to cellular constituents. These retained bioreduction products, therefore, indicate the presence of cellular hypoxia. Nitroimidazoles have been used extensively in the past as hypoxic cell radiosensitizers [236] and more recently have gained a role as markers of tumor hypoxia [237-240]. EF5 and pimonidazole are widely used to assess hypoxia in histological analysis of biopsy specimens [241-244], but non-invasive approaches would be preferable for therapeutic prognosis. Recent studies indicate that ^{18}F misonidazole and ^{64}Cu-ATSM correlate with patient survival [245, 246]. Hypoxia reporters have also been designed for PET using ^{18}F [247]. A potential problem is the relative time required for background clearance from oxygenated tissues, versus the rapid radioactive decay of ^{18}F. Non-radioactive approaches would be advantageous. By attaching a fluorine label to the nitroimidazole, it has become possible to detect the presence of hypoxic cells using *in vivo* NMR techniques [150]. Studies have reported the fluorinated nitroimidazoles CCI-103F [248-252], Ro 07-0741 [249, 253] and SR-4554 [254-259], which contain 6, 1 and 3 fluorine atoms per molecule, respectively (Table 7). Subsequent to administration, a washout period sufficient for elimination of unbound marker is required, since there is apparently no difference detectable *in vivo* in the chemical shifts of the parent molecule and the metabolites [150].

A comparative study of CCI-103F and Ro 07-0741 [249] showed similar tumor selective retention for the two agents in three different tumor types, while Ro 07-0741 had longer retention in liver. The variations in signal retention for each agent in different tumor types were consistent with known hypoxic fraction and *in vivo* nitroreductase activities. Li *et al.* [251] investigated the predictive potential of CCI-103F retention as an indicator of tumor radiosensitivity and found a weak correlation indicating that factors other than hypoxia are involved. Raleigh *et al.* [260] reported a correlation between ^{19}F MRS and scintillation counting measures of tumor-bound, tritium-labeled CCI-103F. Other studies suggest that glutathione concentration may be pertinent [150].

SR-4554 has been designed specifically for use as a noninvasive hypoxia marker detected by ^{19}F MRS and has already undergone preclinical evaluation *in vitro* [259] and *in vivo* [255, 261] and has completed a Phase I clinical trial [262]. The identification of hypoxia-dependent SR-4554 bioreduction products in tumor has been achieved in mice by comparing ^{19}F signal from retained bioreduction products acquired at a late time point (6 h), versus signal acquired at an early time point (45 min), when parent SR-4554 peaks in tumor [255, 262]. The Phase I clinical study [262] reported

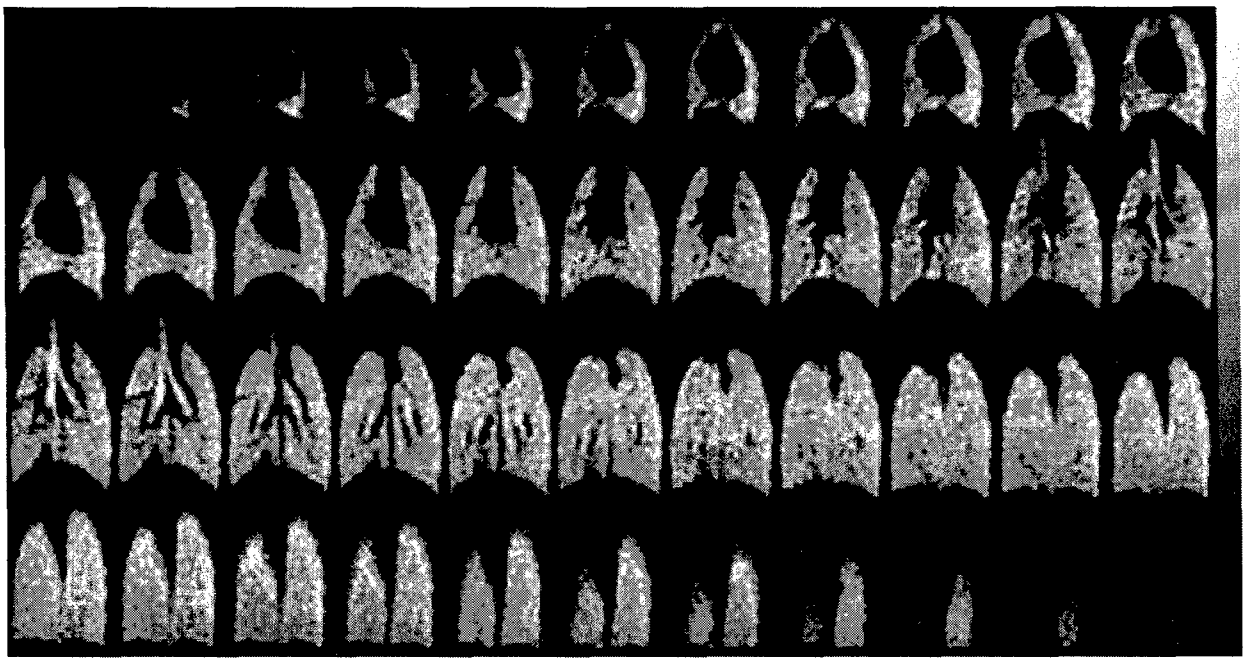

Fig. (13). Three dimensional ^{19}F MRI of SF_6 in the lungs of a large rat (594 g): 720 μm isotropic resolution obtained in 30 mins. using methods of Kuethe, *et al.*, [269, 346]. Frames, from top left to bottom right are successive planes of the image from chest to back. The large airways are brighter because the spin density of pure gas is higher than in the lungs, where 25% of the volume is occupied by tissue. Data kindly provided by Dr. Dean Kuethe *et al.*

the detection of SR-4554 by MRS in tumors immediately after infusion at doses of 400-1600 mg/m^2. The high doses of nitroimidazoles required for NMR may have adverse side effects. The biggest problem with ^{19}F hypoxia agents is that they merely provide a qualitative impression of hypoxia rather than a definitive pO_2.

Seddon *et al.* [262] reported a correlation between retention of SR4554 and pO_2. Aboagye *et al.* [254] found increased retention in hypoxic tumors, but no linear correlation with pO_2. Intriguingly administration of SR4554 was reported to reduce the hypoxic fraction in several tumor types, as determine polarographically [254]. Lack of correlation with pO_2 measurements [254, 262] and pimonidazole uptake [150] suggest that additional factors influence hypoxia marker retention and indeed flow has been implicated [150]. One must also consider the potential diversity of trapped adducts, and metabolites may exhibit multiple chemical shifts, each at very low concentration. There is also concern that polymeric adducts may have exceedingly short T2, so that they become essentially invisible for many NMR sequences.

4. PASSIVE REPORTER MOLECULES

While many active ^{19}F NMR reporter molecules have been designed, developed, and exploited, as described in Section 3, above, other methods use a passive approach, whereby fluorinated molecules occupy a space and a signal magnitude provides an indication of anatomical properties such as lung volume, bowel function, vascular volume or flow.

4.1 Lung Volume

Perfluorocarbons exhibit remarkable gas solubility, and based on the high carrying capacity for oxygen and carbon dioxide, have been developed in emulsion form as synthetic blood substitutes [179]. PFCs may also be relevant as pure liquids. In a classic experiment, Clark and Gollan [263] submersed a living mouse in PFC liquid and far from drowning, it inhaled the PFC facilitating effective oxygen transport to the lungs. Thus, PFCs have potential application as surfactants to aid breathing in extremely premature infants, as explored in clinical trials [264]. PFC may be administered as liquid or aerosols. Thomas, *et al.*, applied ^{19}F MRI to show the extent of lung filling. Further, by applying relaxation measurements (as described in Section 3.4, above) to estimate regional pO_2 in the lungs, while animals breathed various gases. Such measurements have been performed in mice, rats, dogs and pigs [168, 265]. Various perfluorocarbons and perfluorocarbon emulsions have been introduced into the lung as aerosols, sometimes with animals under forced ventilation, following thorochotomy [265]. The ^{19}F signal provides an opportunity to image lungs. By contrast ^{1}H MRI is handicapped by lack of water signal. In a novel approach, Huang, *et al.* [266] applied ^{1}H MRI to the water in a perfluorocarbon emulsion and found considerably enhanced structural information. Liquid and aerosol ventilation can be stressful, whereas inhalation of inert gas, may be more practical, as shown by proof of principal[15] using CF_4 or C_2F_6. More recent studies used SF_6 (Fig. **13**) with potential application for detection

[15] Heidelberger, E.; Lauterbur, P.C., 1st Meeting Soc. Magn. Reson. Med., Boston, MA, 1982, p. 70

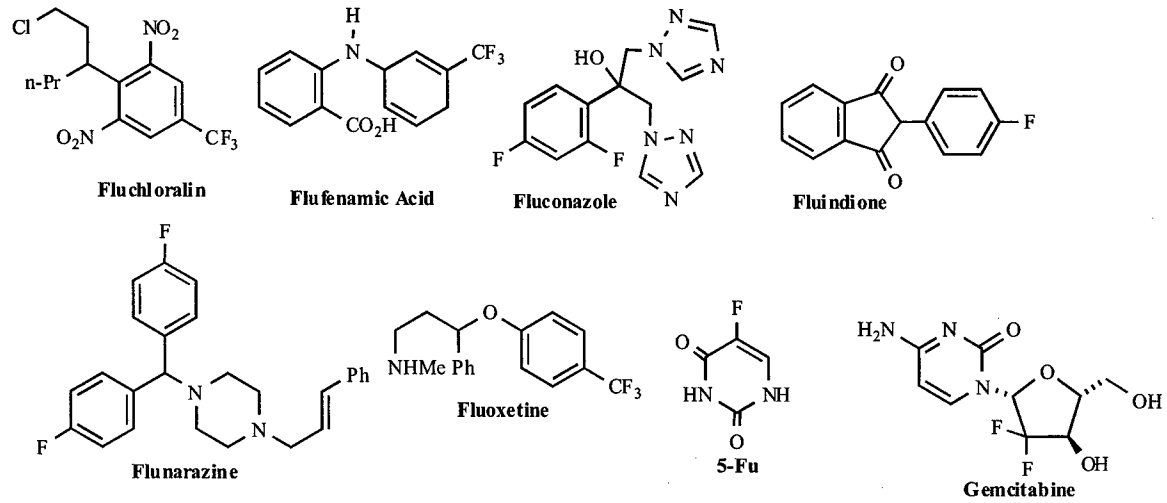

Fig. (14). Representative pharmaceuticals and industrial chemicals incorporating fluorine atoms.

of lung cancer, emphysema, or allograft rejection [267-269]. Gas detection does require special MR instrumentation, due to the exceedingly short T1 and T2 relaxation. ^{19}F MRI of lungs, has, to some extent, been superseded by inert gas approaches exploiting hyperpolarized gases, such as xenon and helium [270-272], though this requires expensive preparatory apparatus.

4.2 GI Imaging

Increasing awareness of colon cancer demands improved screening. Traditional barium meals provide contrast in CT, and virtual colonoscopy is competing with traditional fiber optic probes [273]. MR procedures have lagged behind CT, but several potential contrast agents have been presented, ranging from paramagnetic zeolite formulations [274] and ferric ammonium citrate [275] to PFC emulsions [276]. Emulsions of perflubron (PFOB) have been applied to multiple applications and are popular in ultrasound [178, 179]. For MRI, the multi-resonance spectrum requires extensive editing. PFOB has been tested in clinical trials [276, 277] and recently images were shown in mice based on perfluorononane [278].

4.3 Tumor Blood Volume

Angiogenesis is associated with tumor development and many clinical trials have found correlations between vascular density and prognosis. Traditionally, biopsy and histology are required to examine the vasculature. CD31 antibodies can provide blood vessel counts [279], while dyes such as India ink or Hoechst 33342 may reveal perfusion [280]. Small paramagnetic proton MRI contrast agents can indicate perfusion based on a first pass kinetic analysis, but interpretation is complicated by vascular permeability surface area [281, 282]. Thus, larger particulate agents (nano-particles or USPIOs) have been developed with a view to vascular retention and definite tumor blood volume measurements [283]. Nonetheless, conflicting reports appear in the literature regarding true reliability, particularly the integrity of "vascular retention". ^{19}F NMR has provided a robust indication of vascular volume based on intravenous perfluorocarbon emulsions. These are retained in the vasculature for a period of hours, and studies have validated signal based on traditional radioisotope labeled approaches and dyes [284, 285]. Non-invasive measurements based on long term vascular retention allows acute modulation of tumor blood volume to be assessed [284-289] [16]. This approach has also been applied to other organs and tissues [290], *e.g.*, demonstrating reactive hyperemia in muscles [291].

4.4 Blood Flow

Fluorinated gases (*e.g.*, FC-23 (Tri-fluoromethane) and FC-22 (chlorofluoromethane)) have been used to examine cerebral blood flow based on inflow and outflow kinetics, sometimes with pulsed delivery to facilitate compartmental analysis [292, 293]. Such tracer studies are analogous to ^{133}Xe approaches in SPECT, but avoid radioactivity.

5. METABOLISM AND DRUG UPTAKE

The fluorine atom is exceedingly versatile for designing reporter molecules, as described above. In addition, many pharmaceuticals contain a fluorine atom allowing detection of pharmacokinetics and metabolism. Examination of the Merck Index [20] shows a range of pharmaceuticals and industrial agents containing a single fluorine atom, a trifluoromethyl group or other F-substituents with applications ranging from herbicides (*e.g.*, fluchloralin) to analgesics (*e.g.*, flufenamic acid), antifungals (*e.g.*, fluconazole), anticoagulants (*e.g.*, fluindione), vasodilators (*e.g.*, flunarazine), antidepressants (*e.g.*, fluoxetine) and several chemotherapeutics for cancer (5FU, gemcitabine) (Fig. 14). ^{19}F NMR analysis can be important both in drug development and applications. As described above, oxygen influences the relaxation of PFCs and facilitates accurate measurements of pO_2 *in vivo*. Oxygen has relatively little

[16] Song, Y., Gu, Y., Kim, J. G., Liu, H., Constantinescu, A., and Mason, R. P., Proc. OSA Biomedical Topical Meetings, Miami, FL, 2002, p. 241-243.

effect on molecules in aqueous solution, however, in this case traditional paramagnetic ions, such as Gd^{3+} or Gd-DTPA may be applied [294-296]. Indeed, this approach has been used to differentiate signals from intra and extra cellular metabolites [297].

5.1 Metabolism of Fluorodeoxyglucose

Fluorodeoxyglucose (FDG) is a fluorinated glucose analogue used in Positron Emission Tomography (PET) to measure metabolic activity [298] (see Haberkorn *et al.*, this issue). Given the high glycolytic rate associated with tumors, FDG PET is also a powerful tool for detecting tumors and monitoring metastases and was recently approved for Medicare reimbursement. Substituting an F atom for the –OH in glucose leaves the structure intact, so that cells accumulate FDG based on glucose transporters. FDG is effectively phosphorylated, trapping it intracellularly, but FDG-P is not a substrate for phosphofructose isomerase. Thus, FDG accumulates in metabolically active cells, such as tumors, brain, and myocardium. The FDG isomer 2-fluoro-2-deoxy-D-glucose (2-FDG) has been used in metabolic studies using ^{19}F NMR [299-304]. While PET can assess retention with great sensitivity, it provides no metabolic information, whereas ^{19}F NMR can be used to differentiate individual metabolites from anabolic and catabolic processes. Significant metabolism of 2-FDG via the aldose reductase sorbitol pathway to the metabolites 2-fluoro-2-deoxy-D-sorbitol, 5-fluoro-5-deoxy-L-sorbose, 5-fluoro-5-deoxy-L-sorbose-1-phosphate, 2-fluoro-2-deoxy-L-glyceraldehyde, and 2-fluoro-2-deoxyglycerol was observed [299, 305-309]. It must be remembered that NMR studies typically require mM concentrations as opposed to μM for PET, and thus, metabolic fates may differ. The 3-FDG isomer is a poor substrate for hexokinase and the binding affinity of phosphohexose isomerase is low relative to glucose. Kwee *et al.* [306] introduced 3-fluoro-3-deoxy-D-glucose (3-FDG) as a probe of aldose reductase activity in brain and demonstrated metabolism. The elimination of 3-FDG from brain is slow relative to 2-FDG [310] and it has been used to probe metabolic pathways [306, 311-313].

5.2. Metabolism of Fluoropyrimidine Drugs

5-fluorouracil (5FU) is one of the most popular drugs for chemotherapy, but it has a narrow range of efficacy/toxicity. It has been suggested that both response and toxicity may be related to pharmacokinetics and there is interest in assessing dynamics of uptake, biodistribution, and metabolism. Patients with enhanced retention of 5FU in tumors ("trappers") may be expected to exhibit better response [314]. Such trapping is apparently a requisite, though not in itself sufficient for efficacy [21].

5FU requires anabolic conversion to nucleosides (*e.g.*, FdUrd, FdUmp) and nucleotides for cytostatic activity, requiring the activity of various kinases and phosphorylases [21]. However, competing catabolic reactions convert 5FU to DHFU (5,6 dihydrofluorouracil) and FBAL (α-fluoro β-alanine), in liver in addition to several other molecules offering little toxicity [21, 42, 315]. FBAL is excreted by the kidneys. However, when pH is >7.3 further conversion may liberate fluoride ion, which is cardio- and neuro-toxic [316, 317]. Pharmacokinetics have been extensively characterized by ^{18}F Positron Emission Tomography and the metabolic processes by ^{19}F NMR [22]. Chemical shifts of characterized products have been reported together with typical T1s. Studies have ranged from cells to rodents, and clinical studies in patients. Most studies have been limited to spectroscopy, though some imaging has been reported [22, 318-320].

The pharmacokinetics of 5FU are reported to be pH sensitive, and thus measurements of tumor pH may have prognostic value for drug efficacy. In tumors with lower pH the retention of 5-fluorouracil (5-FU) is considerably enhanced [321, 322] along with the cytotoxicity of several common drugs [113, 323-325]. Indeed, this prompted investigations of modulation of tumor pH to increase activity, *e.g.*, by breathing carbogen. Relevant is also the potential to monitor 5FU and tumor physiology simultaneously, based on ^{19}F NMR signals of the drug and correlated signals from physiological reporter molecules. Intriguingly, fluoronucleotides derived *in vivo* from 5FU exhibit sensitivity to changes in pH and may be used to measure pHi, although the presence of a mixture of products may complicate interpretation [111, 326]. Administration of 5-FU causes intracellular alkalinization and an increased transmembrane ΔpH.

Given the inherent dose-limiting toxicity of 5FU, various pro-drug approaches have been explored and ^{19}F NMR has played a role in analysis and development. Pro-drug therapy has new impetus in conjunction with gene therapy, specifically the use of cytosine deaminase, to convert the relatively innocuous 5-fluorocytosine (5FC) to 5FU [73-75, 327, 328]. In this context, distribution, activity, and persistence of trans-genes is of critical importance (section 3.1). Several investigations have now reported ^{19}F NMR of the conversion of 5FC to 5FU based on the ^{19}F NMR chemical shift, Δδ 2 ppm [74, 75].

5.3. Other Drugs: Retention of Anesthetics

Many gaseous anesthetics are fluorinated, *e.g.*, halothane, enflurane, isoflurane, sevoflurane, and desflurane. These are listed in decreasing order of blood gas solubility, and hence, increasing wash in - wash out rates. NMR studies of fluorinated anesthetics form some of the earliest *in vivo* applications of ^{19}F NMR. Issues regarding the use of anesthetics are site of anesthetic action, duration of residence in the brain and toxicity of metabolic byproducts. The results have been a source of debate and controversy.

Wyrwicz and co-workers [329-336] addressed the issue of residence times of anesthetics in the brain and observed signals for the anesthetics for prolonged durations after cessation of anesthesia. Both halothane [330] and isoflurane [331] showed bi-compartmental elimination from the rabbit brain with half-lives ($t_{1/2}$ of 25 and 320 mins for halothane and 26 and 174 mins for isoflurane). In the case of halothane, the findings were further supported with accompanying high resolution *in vitro* data, which showed two separate resonances with different relaxation times T_1 and T_2. One of the two resonances corresponded to

halothane, while the other was ascribed to a non-volatile metabolite possibly trifluoroacetate.

While global spectroscopy can be straightforward (Fig. **9**), anesthetics have a short transverse relaxation time (T2*) and signals may be lost in localized spectroscopy or imaging approaches. Chew *et al.* [337], James *et al.* [24, 25], and Hashimoto *et al.* [338] failed to detect anesthetics in brain tissues presumably due to the short T_2s. Lockhart *et al.* [339] reported a correlation between cerebral uptake and solubility, with desflurane (most soluble) having fastest uptake followed by isoflurane and halothane.

Very few clinical studies have been reported ^{19}F MR of anesthetics in the brain. Menon *et al.* [39] demonstrated the feasibility of such studies and found halothane signal up to 90 min after the withdrawal of anesthetic. Lockwood *et al.* [31] studied isoflurane kinetics and showed biphasic elimination with decay halftimes of 9.5 and 130 min. They also studied the relation between the cerebral kinetics of isoflurane and cerebral function [32]. Another issue of interest regarding anesthetics is the site of action of the anesthetic agent in the brain and the availability of saturable binding sites. Artificially ventilated animals showed a linear relationship between inspired concentrations of halothane and cerebral halothane levels implying the absence of binding to specific sites [340, 341]. Selinsky *et al.* and Preece *et al.* [342-345] have studied the metabolism of volatile anesthetics showing generation of potentially toxic metabolites such as methoxydifluoracetate, dichloroacetate, and fluoride ion from methoxyflurane.

4. CONCLUSIONS

Proton MRI is a mainstay of clinical Radiology. Several contrast agents are in routine use and other "smart" agents are being developed [10]. However, most investigations are limited to detection of fat and water signals, since they dominate. By contrast, there is essentially no ^{19}F NMR background signal in tissues, and thus, fluorinated reporter molecules may be assessed by changes in chemical shift and the detection ability is subject to the signal-to-noise ratio, as opposed to contrast-to-noise. Huge diversity of application has been demonstrated in the biochemical and small animal areas, with limited clinical application. To date clinical application is hindered by the lack of availability of clinical ^{19}F NMR. However, for about $200k, such a capability can be added and will be straightforward as soon as there is a proven need and opportunity for medical reimbursement. Such a situation has occurred very recently for FDG PET providing access to equipment and incentive to generate novel reporters (see reviews by McQuade and Haberkorn, this issue). ^{19}F NMR offers the potential to investigate many diverse parameters (Table 1) and with a little imagination, together with thorough development will yield further applications.

5. ACKNOWLEDGEMENTS

Supported in part by the Cancer Imaging Program, NCI Pre-ICMIC P20 CA086354 and an IDEA awards from the DOD Breast Cancer Initiative DAMD179919381 and 170310343. NMR experiments were conducted at the Mary Nell and Ralph B. Rogers NMR Center, an NIH BTRP facility #P41-RR02584. We are grateful to Drs. Peter Antich, Eric Hahn, Dawen Zhao, Uwe Haberkorn, Peter Peschke, Ken Koeneman and Dean Kuethe for collegial support and Jocelyn Chafouleas for assistance in preparing this manuscript.

ABBREVIATIONS

ARDVARC	=	Alternating Relaxation Delays with Variable Acquisitions to Reduce Clearance effects
ASL	=	Arterial Spin Labeling
ATP	=	Adenosine triphosphate
β-gal	=	β-galactosidase
BAPTA	=	1,2-bis(o-amino-phenoxy)ethane-N,N,N',-N'-tetraacetic acid
BLI	=	Bioluminescent Imaging
BOLD	=	Blood Oxygen Level Dependent
FDG	=	Fluorodeoxyglucose
15C5	=	Perfluoro-15-crown-5-ether
CD	=	Cytosine Deaminase
CSI	=	Chemical Shift Imaging
DTI	=	Diffusion Tensor Imaging
DHFU	=	5,6 Dihydrofluorouracil
FBAL	=	α-Fluoro β-alanine
5FBAPTA	=	5,5-Difluoro-1,2-bis(o-amino-phenoxy)-ethane-N,N,N',N'-tetraacetic acid
5-FC	=	5-fluorocytosine
FDG	=	Fluorodeoxyglucose
6-FPAM	=	6-Fluoropyridoxamine
6-FPOL	=	2-Fluoro-5-hydroxy-6-methyl-3,4-pyridine-dimethanol
FREDOM	=	Fluorocarbon Relaxometry using Echo planar imaging for Dynamic Oxygen Mapping
5FU	=	5-Fluorouracil
Gd-DTPA	=	Diethylenetriaminepentaacetic Acid
GDEPT	=	Gene Directed Enzyme Prodrug Therapy
GFP	=	Green Fluorescent Protein
HFB	=	Hexafluorobenzene
hNIS	=	Sodium Iodine Symporter
LETS	=	Light Emission Tomography System
MRS	=	Magnetic Resonance Spectroscopy
NaTFA	=	Sodium Trifluoroacetate
NEAP	=	N-Ethylaminophenol
NMR	=	Nuclear Magnetic Resonance

ONPG = O-Nitrophenylgalactoside

pO_2 = Partial Pressure of Oxygen

PARACEST = Paramagnetic Magnetization Transfer Contrast Agents

PFCs = Perfluorocarbons

PFOB = Perflubron; Perfluorooctyl Bromide

PFTB = Perfluorotributylamine

PFONPG = 4-Fluoro-2-nitrophenyl-β-D-galactopyranoside

pHe = Extracellular pH

pHi = Intracellular pH

R1 = Spin lattice (longitudinal) relaxation rate ($=1/T_1$)

R2 = Spin spin (transverse) relaxation rate ($=1/T2$)

SNR = Signal to Noise Ratio

REFERENCES

[1] http://www.nobel.se/physics/laureates/1952/, in 'The Nobel Prize in Physics **1952**.

[2] http://www.nobel.se/chemistry/laureates/1991/, in 'The Nobel Prize in Chemistry **1991**; http://www.nobel.se/medicine/laureates/2003/.

[3] Wright, S.M.; Wald, L.L. *NMR Biomed.* **1997**, *10,* 394.

[4] Sodickson, D.K.; Griswold, M.A.; Jakob, P.M. *Magn. Reson. Imaging Clin. North America* **1999**, *7,* 237.

[5] van den Brink, J.S.; Watanabe, Y.; Kuhl, C.K.; Chung, T.; Muthupillai, R.; Van Cauteren, M.; Yamada, K.; Dymarkowski, S.; Bogaert, J.; Maki, J.H.; Matos, C.; Casselman, J.W.; Hoogeveen, R.M. *Eur. J. Radiol.* **2003**, *46,* 3.

[6] Blumlich, B.; Kuhn, W., *Magnetic Resonance Microscopy*, VCH, Weinheim, **1992**.

[7] Barbier, E.L.; Silva, A.C.; Kim, S.G.; Koretsky, A.P. *Magn. Reson. Med.* **2001**, *45,* 1021.

[8] Fasano, F.; Capuani, S.; Hagberg, G.E.; Branca, T.; Indovina, I.; Castriota-Scanderbeg, A.; Maraviglia, B. *Magn. Reson. Imaging* **2003**, *21,* 1151.

[9] Jiang, L.; Zhao, D.; Constantinescu, A.; Mason, R.P. *Magn. Reson. Med.* **2004**, *51,* 953.

[10] Zhang, Z.; Nair, S.A.; McMurry, T.J. *Current Med. Chem.* **2004**, this issue.

[11] Gadian, D.G., NMR and its applications to living systems, OUP, Oxford, **1995**.

[12] Gillies, R.J., in 'NMR in physiology and medicine', San Diego, **1994**.

[13] Bansal, N.; Germann, M.J.; Seshan, V.; Shires III, G.T.; Malloy, C.R.; Sherry, A.D. *Biochemistry* **1993**, *32,* 5638.

[14] Seshan, V.; Bansal, N. In *In vivo ^{31}P and ^{23}Na NMR spectroscopy and Imaging*, M. Bruch, Ed.; Marcel Dekker: New York, **1996** 557.

[15] Navon, G.; Shina, R.H.; Eliav, U.; Seo, Y. *NMR Biomed.* **2001**, *14,* 112.

[16] Mason, R.P.; Sanders, J.K.M.; Gidley, M.J. *Phytochem.* **1986**, *25,* 1567.

[17] Weis, B.C.; Margolis, D.; Burgess, S.C.; Merritt, M.E.; Wise, H.; Sherry, A.D.; Malloy, C.R. *Magn. Reson. Med.* **2004**, *51,* 649.

[18] Mason, R.P.; Sanders, J.K.M. *Biochemistry* **1989**, *28,* 2160.

[19] Burgess, S.C.; Nuss, M.; Chandramouli, V.; Hardin, D.S.; Rice, M.; Landau, B.R.; Malloy, C.R.; Sherry, A.D. *Anal. Biochem.* **2003**, *318,* 321.

[20] Budavari, S. *The Merck Index*, Rahway, NJ, **1989**.

[21] Wolf, W.; Presant, C.A.; Waluch, V. *Adv. Drug Del. Rev.* **2000**, *41,* 55.

[22] Brix, G.; Bellemann, M.E.; Haberkorn, U.; Gerlach, L.; Lorenz, W.J. *Nucl. Med. Biol.* **1996**, *23,* 897.

[23] Lee, D.J.; Burt, C.T.; Koch, R.L. *J. Invest. Dermatol.* **1992**, *99,* 431.

[24] Wade, K.E.; Wilson, I.D.; Troke, J.A.; Nicholson, J.K. *J. Pharm. Biomed. Anal.* **1990**, *8,* 401.

[25] Venkatasubramanian, P.N.; Shen, Y.J.; Wyrwicz, A.M. *NMR Biomed.* **1993**, *6,* 377.

[26] Strauss, W.L.; Unis, A.S.; Cowan, C.; Dawson, G.; Dager, S.R. *Am. J. Psych.* **2002**, *159,* 755.

[27] Zhao, D.; Jiang, L.; Mason, R.P. *Methods Enzymol* **2004**, *386,* 378.

[28] Mason, R.P. *Curr. Med. Chem.* **1999**, *6,* 481.

[29] Cui, W.; Otten, P.; Li, Y.; Koeneman, K.; Yu, J.; Mason, R.P. *Magn. Reson. Med.* **2004**, *51,* 616.

[30] Golman, K.; Ardenkjaer-Larsen, J.H.; Petersson, J.S.; Mansson, S.; Leunbach, I. *PNAS USA* **2003**, *100,* 10435.

[31] Venkatesh, A.K.; Zhang, A.X.; Mansour, J.; Kubatina, L.; Oh, C.H.; Blasche, G.; Selim Unlu, M.; Balamore, D.; Jolesz, F.A.; Goldberg, B.B.; Albert, M.S. *Magn. Reson. Imaging* **2003**, *21,* 773.

[32] Zhang, S.; Merritt, M.; Woessner, D.E.; Lenkinski, R.E.; Sherry, A.D. *Acc. Chem. Res.* **2003**, *36,* 783.

[33] Thomas, S.R., In *The biomedical applications of Fluorine-19 NMR*, C. L. Partain, R. R. Price, J. A. Patton, M. V. Kulkarni, and A. E. J. James, Ed.; W.B. Saunders Co.: London, **1988**, 1536.

[34] Selinsky, B.S.; T., B.C. In *In vivo ^{19}F NMR*, L. J. Berliner and J. Reuben, Ed.; Plenum: New York, **1992**, 241.

[35] Prior, M.J.W.; Maxwell, R.J.; Griffiths, J.R., In *Fluorine-^{19}F NMR spectroscopy and imaging in-vivo*, M. Rudin, Ed.; Springer-Verlag: Berlin, **1992**, 103.

[36] London, R.E. In *In vivo NMR studies utilizing fluorinated NMR probes*, R. J. Gillies, Ed.; Academic: San Diego, **1994**, 263.

[37] Mason, R.P. Art. Cells, Blood Sub. & Immob. Biotech. 1994, 22, 1141.

[38] McSheehy, P.M.J.; Lemaire, L.P.; Griffiths, J.R., In *Fluorine-19 MRS: applications in oncology*, D. M. Grant and R. K. Harris, Ed.; Wiley: Chichester, **1996**, 2048.

[39] Menon, D.K. In *Fluorine-19 MRS: general overview and anesthesia*, R. K. Harris, Ed.; Wiley: Chichester, **1995**, 2052.

[40] Passe, T.J.; Charles, H.C.; Rajagopalan, P.; Krishnan, K.R. Prog. *Neuro-Psychopharmacol. Biol. Psych.* **1995**, *19,* 541.

[41] Martino, R.; Malet-Martino, M.; Gilard, V. *Curr. Drug Metab.* **2000**, *1,* 271.

[42] Bachert, P. *Prog. NMR Spectroscopy* **1998**, *33,* 1.

[43] Code, R.F.; Harrison, J.E.; McNeill, K.G.; Szyjkowski, M. *Mag. Reson. Med.* **1990**, *13,* 358.

[44] Bovey, F.A. *Nuclear Magnetic Resonance Spectroscopy*, Academic Press, San Diego, **1988**.

[45] Mehta, V.D.; Kulkarni, P.V.; Mason, R.P.; Constantinescu, A.; Aravind, S.; Goomer, N.; Antich, P.P. *FEBS Letters* **1994**, *349,* 234.

[46] Taylor, J.; Deutsch, C.J. *Biophys. J.* **1988**, *53,* 227.

[47] Lutz, N.W.; Hull, W.E. *NMR Biomed.* **1999**, *12,* 237.

[48] Emsley, J.W.; Feeney, J.; Sutcliffe, L.H. *High Resolution Nuclear Magnetic Resonance Spectroscopy*, Pergamon Press, Oxford, **1966**.

[49] Emsley, J.W.; Phillips, L. *Prog. in NMR Spec.* **1976**, *10,* 83.

[50] Shukla, H.P.; Mason, R.P.; Woessner, D.E.; Antich, P.P. *J. Magn. Reson. Series B* **1995**, *106,* 131.

[51] Babcock, E.E.; Mason, R.P.; Antich, P.P. *Magn. Reson. Med.* **1991**, *17,* 178.

[52] Mason, R.P.; Bansal, N.; Babcock, E.E.; Nunnally, R.L.; Antich, P.P. *Magn. Reson. Imaging* **1990**, *8,* 729.

[53] Lantum, H.B.; Baggs, R.B.; Krenitsky, D.M.; Anders, M.W. *Toxicol. Sci.* **2002**, *70,* 261.

[54] Shainyan, B.A.; Danilevich, Y.S.; Grigor'eva, A.A.; Chuvashev, Y.A. *Russian J. Org. Chem. (Trans. Zh. Organ. Khim.)* **2004**, *40,* 513.

[55] Asovich, V.S.; Kornilov, V.; Maksimov, B.N. *Russi. Zh. Prikladnoi Kh.* **1994**, *67,* 107.

[56] Olah, G.A.; Nojima, M.; Kerekes, I. *J. Am. Chem. Soc.* **1974**, *96,* 925.

[57] Haas, A.; Maciej, T. *J. Fluorine Chem.* **1982**, *20,* 581.

[58] Patrick, T.B.; Zhang, L.; Li, Q. *J. Fluorine Chem.* **2000**, *102,* 11.

[59] Belen'kii, G.G.; Petrov, V.A.; Resnick, P.R. *J. Fluorine Chem.* **2001**, *108,* 15.

[60] Rozen, S.; Brand, M. *J. Org. Chem.* **1986**, *51*, 3607.
[61] Adachi, K.; Ohira, Y.; Tomizawa, G.; Ishihara, S.; Oishi, S. *J. Fluorine Chem.* **2003**, *120*, 173.
[62] Mehta, V.; Kulkarni, P.V.; Mason, R.P.; Constantinescu, A.; Antich, P.P. *Bioorg. Med. Chem. Lett.* **1992**, *2*, 527.
[63] Joubert, J.; Roussel, S.; Christophe, C.; Billard, T.; Langlois, B.R.; Vidal, T. *Angew. Chem. Int. Ed.* **2003**, *42*, 3133.
[64] Dwek, R.A., In *The use of fluorine-19 as a detecting shift probe*, R. A. Dwek, Ed.; Clarendon: Oxford, **1975**, 158.
[65] Gerig, J.T. *Methods Enzymol.* **1989**, *177*, 3.
[66] Contag, C.H.; Ross, B.D. *JMRI* 2002, *16*, 378.
[67] Haberkorn, U.; Altmann, A.; Jiang, S.; Morr, I.; Mahmut, M.; Eisenhut, M. *Eur. J. Nucl. Med.* **2001**, *28*, 633.
[68] Tjuvajev, J.G.; Doubrovin, M.; Akhurst, T.; Cai, S.; Balatoni, J.; Alauddin, M.M.; Finn, R.; Bornmann, W.; Thaler, H.; Conti, P.S.; Blasberg, R.G. *J. Nucl. Med.* **2002**, *43*, 1072.
[69] Ichikawa, T.; Hogemann, D.; Saeki, Y.; Tyminski, E.; Terada, K.; Weissleder, R.; Chiocca, E.A.; Basilion, J.P. *Neoplasia (New York)* **2002**, *6*, 523.
[70] Paroo, Z.; Bollinger, R.A.; Braasch, D.A.; Richer, E.; Corey, D.R.; Antich, P.P.; Mason, R.P. *Molecular Imaging* **2004**, *3*, 117.
[71] Hoffman, R. *Lancet Oncol.* **2002**, *3*, 546.
[72] Herschman, H.R. *J. Cell. Biochem.* **2002**, *39*, 36.
[73] Freytag, S.O.; Khil, M.; Stricker, H.; Peabody, J.; Menon, M.; DePeralta-Venturina, M.; Nafziger, D.; Pegg, J.; Paielli, D.; Brown, S.; Barton, K.; Lu, M.; Aguilar-Cordova, E.; Kim, J.H. *Cancer Res.* **2002**, *62*, 4968.
[74] Stegman, L.D.; Rehemtulla, A.; Beattie, B.; Kievit, E.; Lawrence, T.S.; Blasberg, R.G.; Tjuvajev, J.G.; Ross, B.D. *PNAS (USA)* **1999**, *96*, 9821.
[75] Corban-Wilhelm, H.; Hull, W.E.; Becker, G.; Bauder-Wust, U.; Greulich, D.; Debus, J. *Gene Therapy* **2002**, *9*, 1564.
[76] Kruger, A.; Schirrmacher, V.; Khokha, R. *Cancer Metastasis Rev.* **1999**, *17*, 285.
[77] Serebriiskii, I.G.; Golemis, E.A. *Anal. Biochem.* **2000**, *285*, *1*.
[78] Beckwith, J.R.; Zipser, D., in 'The Lactose operon', Cold Spring Harbor, **1970**.
[79] Kawaguchi, J.; Wilson, V.; Mee, P.J. *Biotechniques* **2002**, *32*, 68.
[80] Heuermann, K.; Cosgrove, J. *Biotechniques* **2001**, *30*, 1142.
[81] Bronstein, I.; Edwards, B.; Voyta, J.C. *J. Chemilum. Biolum.* **1989**, *4*, 99–111.
[82] Louie, A.Y.; Huber, M.M.; Ahrens, E.T.; Rothbacher, U.; Moats, R.; Jacobs, R.E.; Fraser, S.E.; Meade, T.J. *Nature Biotechnol.* **2000**, *18*, 321.
[83] Yoon, S.; Kim, H.G.; Chun, K.H.; Shin, J.E.N. *Bull. Korean Chem. Soc.* **1996**, *17*, 599.
[84] Richard, J.P.; Westerfeld, J.G.; Lin, S. *Biochemistry* **1995**, *34*, 11703.
[85] Taylor, J.S.; Deutsch, C.J.; McDonald, G.G.; Wilson, D.F. *Anal. Biochem.* **1982**, *114*, 415.
[86] Deutsch, C.J.; Taylor, J.S. In *^{19}F NMR measurements of intracellular pH*, R. K. Gupta, Ed.; CRC Press: Boca Raton, **1987**, 55.
[87] Deutsch, C.J.; Taylor, J.S. *Ann. NY Acad. Sci.* **1987**, *508*, 33.
[88] Deutsch, C.; Taylor, J.S.; Wilson, D.F. *Proc. Natl. Acad. Sci. (USA)* **1982**, *79*, 7944.
[89] Deutsch, C.; Taylor, J.S.; Price, M. *J. Cell Biol.* **1984**, *98*, 885.
[90] Kashiwagura, T.; Deutsch, C.J.; Taylor, J.; Erecinska, M.; Wilson, D.F. *J. Biol. Chem.* **1984**, *259*, 237.
[91] Thoma, W.J.; Ugurbil, K. *NMR Biomed.* **1988**, *1*, 95.
[92] Taylor, J.A.; Deutsch, C.J. *Biophys. J.* **1983**, *43*, 261.
[93] Hunjan, S.; Mason, R.P.; Mehta, V.D.; Kulkarni, P.V.; Aravind, S.; Arora, V.; Antich, P.P. *Magn. Reson. Med.* **1998**, *39*, 551.
[94] He, S.; Mason, R.P.; Hunjan, S.; Mehta, V.D.; Arora, V.; Katipally, R.; Kulkarni, P.V.; Antich, P.P. *Bioorg. Med. Chem.* **1998**, *6*, 1631.
[95] Korytnyk, W.; Singh, R.P. *J. Am. Chem. Soc.* **1963**, *85*, 2813.
[96] Korytnyk, W.; Srivastava, S.C. *J. Med. Chem.* **1973**, *16*, 638.
[97] Yamada, K.; Tsuji, M. *J. Vitaminol.* **1970**, *16*, 237.
[98] Chang, Y.C.; Graves, D.J. *J. Biol. Chem.* **1985**, *260*, 2709.
[99] Scott, R.D.; Chang, Y.-C.; Graves, D.J.; Metzler, D.E. *Biochemistry* **1985**, *24*, 7668.
[100] Mantsch, H.H.; Smith, I.C.P. In Carbon-13 nuclear magnetic resonance spectroscopy of the vitamin B_6 groupEd.; Academic Press: **1979**, 422.
[101] Metcalfe, J.C.; Hesketh, T.R.; Smith, G.A. *Cell Calcium* **1985**, *6*, 183.
[102] Beech, J.S.; Iles, R.A. *Biochem. Soc. Trans.* **1987**, *15*, 871.
[103] Joseph, A.; Davenport, C.; Kwock, L.; Burt, C.T.; London, R.E. *Magn. Reson. Med.* **1987**, *4*, 137.
[104] Bental, M.; Deutsch, C. *Am. J. Physiol.* **1994**, *266*, C541.
[105] Deutsch, C.J.; Taylor, J.S. *Biophys. J.* **1989**, *55*, 799.
[106] Rhee, C.K.; Levy, L.A.; London, R.E. *Bioconj. Chem.* **1995**, *6*, 77.
[107] Frenzel, T.; Koszler, S.; Bauer, H.; Niedballa, U.; Weinmann, H.J. *Invest. Radiol.* **1994**, *29*, S220.
[108] Miyazawa, T.; Aoki, Y.; Akagi, K.; Takahashi, M.; Fritz-Zieroth, B.; Frenzel, T.; Weinmann, H.-J. *Acad. Radiol.* **1996**, *3*, S363.
[109] Ojugo, A.S.; McSheehy, P.M.; McIntyre, D.J.; McCoy, C.; Stubbs, M.; Leach, M.O.; Judson, I.R.; Griffiths, J.R. *NMR Biomed.* **1999**, *12*, 495.
[110] Aoki, Y.; Akagi, K.; Tanaka, Y.; Kawai, J.; Takahashi, M. *Invest. Radiol.* **1996**, *31*, 680.
[111] McSheehy, P.M.J.; Robinson, S.P.; Ojugo, A.S.E.; Aboagye, E.O.; Cannell, M.B.; Leach, M.O.; Judson, I.R.; Griffiths, J.R. *Cancer Res.* **1998**, *58*, 1185.
[112] Gerweck, L.E.; Seetharaman, K. *Cancer Res.* **1996**, *56*, 1194.
[113] Tannock, I.F.; Rotin, D. *Cancer Res.* **1989**, *49*, 4373.
[114] Kozin, S.V.; Gerweck, L.E. *Br. J. Cancer* **1998**, *77*, 1580.
[115] Raghunand, N.; Mahoney, B.P.; Gillies, R.J. *Biochem. Pharmacol.* **2003**, *66*, 1219.
[116] Mahoney, B.P.; Raghunand, N.; Baggett, B.; Gillies, R.J. *Biochem. Pharmacol.* **2003**, *66*, 1207.
[117] Hwang, Y.C.; Kim, S.-G.; Evelhoch, J.L.; Ackerman, J.J.H. *Cancer Res.* **1992**, *52*, 1259.
[118] Yamagata, M.; Tannock, I.F. *Br. J. Chem.* **1996**, *73*, 1328.
[119] Prescott, D.M.; Charles, H.C.; Sostman, H.D.; Page, R.L.; Thrall, D.E.; Moore, D.; Oleson, J.R.; Dewhirst, M.W. *Int. J. Hypertherm.* **1993**, *9*, 745.
[120] Jain, R.K.; Shah, S.A.; Finney, P.L. *JNCI* **1984**, *73*, 429.
[121] Stubbs, M.; Rodrigues, L.; Howe, F.A.; Wang, J.; Jeong, K.-S.; Veech, R.L.; Griffiths, J.R. *Cancer Res.* **1994**, *54*, 4011.
[122] Stubbs, M.; Bhujwalla, Z.M.; Tozer, G.M.; Rodrigues, L.M.; Maxwell, R.J.; Morgan, R.; Howe, F.A.; Griffiths, J.R. *NMR Biomed.* **1992**, *5*, 351.
[123] Bhujwalla, Z.M.; Artemov, D.; Ballesteros, P.; Cerdan, S.; Gillies, R.J.; Solaiyappan, M. *NMR Biomed.* **2002**, *15*, 114.
[124] Garcia-Martin, M.L.; Herigault, G.; Remy, C.; Farion, R.; Ballesteros, P.; Coles, J.A.; Cerdan, S.; Ziegler, A. *Cancer Res.* **2001**, *61*, 6524.
[125] Raghunand, N.; Zhang, S.; Sherry, A.; Gillies, R. *Acad. Radiol.* **2002**, *9*, S481.
[126] Raghunand, N.; Howison, C.; Sherry, A.D.; Zhang, S.; Gillies, R.J. *Magn. Reson. Med.* **2003**, *49*, 249.
[127] Tsien, R.Y. *Nature* **1981**, *290*, 527.
[128] Benters, J.; Flogel, U.; Schafer, T.; Leibfritz, D.; Hechtenberg, S.; Beyersmann, D. *Biochem. J.* **1997**, *322 (Pt 3)*, 793.
[129] Smith, G.A.; Hesketh, R.T.; Metcalfe, J.C.; Feeney, J.; Morris, P.G. *Proc. Natl. Acad. Sci. (USA)* **1983**, *80*, 7178.
[130] Gupta, R.K.; Gillies, R.J. In *^{19}F NMR measurement of intracellular free calcium ions in intact cells and tissues*, R. K. Gupta, Ed.; CRC: Boca Raton, **1987**, 45.
[131] Gupta, R.K.; Gupta, P. In *^{31}P NMR measurement of intracellular free magnesium in cells and organisms*, R. K. Gupta, Ed.; CRC: Boca Raton, **1987**, 34.
[132] Weller, E.; Bachert, P.; Meinck, H.M.; Friedmann, B.; Bartsch, P.; Mairbaurl, H. *Med. Sci. Sports Exe.* **1998**, *30*, 1584.
[133] Schanne, F.A.; Moskal, J.R.; Gupta, R.K. *Brain Res.* **1989**, *503*, 308.
[134] Schanne, F.A.; Dowd, T.L.; Gupta, R.K.; Rosen, J.F. *Proc. Nal. Acad. Sci. (USA)* **1989**, *86*, 5133.
[135] Kusuoka, H.; Backx, P.H.; Camilion de Hurtado, M.C.; Azan-Backx, M.; Marban, E.; Cingolani, H.E. *Am. J. Physiol.* **1993**, *265*, H1696.
[136] Plenio, H.; Diodone, R. *J. Am. Chem. Soc.* **1996**, *118*, 356.
[137] Romani, A.M.; Scarpa, A. *Frontiers in Biosci.* **2000**, *5*, D720.
[138] Noronha, J.L.; Matuschak, G.M. *Intensive Care Med.* **2002**, *28*, 667.
[139] Murphy, E. *Mineral & Electrolyte Metab.* **1993**, *19*, 250.
[140] Kirschenlohr, H.L.; Metcalfe, J.C.; Morris, P.G.; Rodrigo, G.C.; Smith, G.A. *Proc. Natl. Acad. Sci. (USA)* **1988**, *85*, 9017.
[141] Tecle, B.; Casida, J.E. *Chem. Res. Toxicol.* **1989**, *2*, 429.

[142] Levy, L.A.; Murphy, E.; Raju, B.; London, R.E. *Biochemistry* **1988**, *27*, 4041.
[143] Murphy, E.; Steenbergen, C.; Levy, L.A.; Raju, B.; London, R.E. *J. Biol. Chem.* **1989**, *264*, 5622.
[144] Long, G.J.; Rosen, J.F.; Schanne, F.A. *J. Biol. Chem.* **1994**, *269*, 834.
[145] Smith, G.A.; Morris, P.G.; Hesketh, T.R.; Metcalfe, J.C. *Biochim. Biophys. Acta* **1986**, *889*, 72.
[146] London, R.E.; Gabel, S.A. *J. Am. Chem. Soc.* **1994**, *116*, 2562.
[147] Plenio, H.; Diodone, R. Z. *Naturforsch. Section B-J. Chem. Sci.* **1995**, *50*, 1075.
[148] Plenio, H.; Hermann, J.; Diodone, R. *Inorg. Chem.* **1997**, *36*, 5722.
[149] Takemura, H.; Kariyazono, H.; Yasutake, M.; Kon, N.; Tani, K.; Sako, K.; Shinmyozu, T.; Inazu, T. *Eur. J. Org. Chem.* **2000**, *1*, 141.
[150] Robinson, S.P.; Griffiths, J.R. *Phil. Trans. R. Soc. London B Biol. Sci.* **2004**, *359*, 987.
[151] Gray, L.; Conger, A.; Ebert, M.; Hornsey, S.; Scott, O. *Br. J. Radiol.* **1953**, *26*, 638.
[152] Wouters, B.G.; Brown, J.M. *Radiat. Res.* **1997**, *147*, 514.
[153] Sartorelli, A.C. *Cancer Res.* **1988**, *48*, 775.
[154] Teicher, B.; Lazo, J.; Sartorelli, A. *Cancer Res.* **1981**, *41*, 73.
[155] Höckel, M.; Vaupel, P. *J. Natl. Cancer Inst.* **2001**, *93*, 266.
[156] Knowles, H.J.; Harris, A.L. *Breast Cancer Res.* **2001**, *3*, 318.
[157] Rofstad, E.K.; Sundfor, K.; Lyng, H.; Trope, C.G. *Br. J. Cancer* **2000**, *83*, 354.
[158] De Jaeger, K.; Kavanagh, M.C.; Hill, R.P. *Br. J. Cancer* **2001**, *84*, 1280.
[159] Brown, J.M. *Molec. Med. Today* **2000**, *6*, 157.
[160] Parhami, P.; Fung, B.N. *J. Phys. Chem.* **1983**, *87*, 1928.
[161] Lai, C.-S.; Stair, S.; Miziorko, H.; Hyde, J.S. *J. Magn. Reson.* **1984**, *57*, 447.
[162] Mattrey, R.F.; Schumacher, D.J.; Tran, H.T.; Guo, Q.; Buxton, R.B. *Biomat Art Cells Immob. Biotech.* **1992**, *20*, 917.
[163] Eidelberg, D.; Johnson, G.; Barnes, D.; Tofts, P.S.; Delpy, D.; Plummer, D.; McDonald, W.I. *Magn. Reson. Med.* **1988**, *6*, 344.
[164] Kong, C.F.; Holloway, G.M.; Parhami, P.; Fung, B.M. *J. Phys. Chem.* **1984**, *88*, 6308.
[165] Thomas, S.R.; Pratt, R.G.; Millard, R.W.; Samaratunga, R.C.; Shiferaw, Y.; Clark, L.C. *Radiology* **1991**, *18:*, 159.
[166] Thomas, S.R.; Pratt, R.G.; Millard, R.W.; Samaratunga, R.C.; Shiferaw, Y.; Clark Jr., L.C.; Hoffmann, R.E. *JMRI* **1994**, *4*, 631.
[167] Mason, R.P.; Shukla, H.P.; Antich, P.P. *Magn. Reson. Med.* **1993**, *29*, 296.
[168] Thomas, S.R.; Pratt, R.G.; Millard, R.W.; Samaratunga, R.C.; Shiferaw, Y.; McGoron, A.J.; Tan, K.K. *Magn. Reson. Imaging* **1996**, *14*, 103.
[169] Hunjan, S.; Zhao, D.; Constantinescu, A.; Hahn, E.W.; Antich, P.P.; Mason, R.P. *Int. J. Radiat. Oncol. Biol. Phys.* **2001**, *49*, 1097.
[170] Dardzinski, B.J.; Sotak, C.H. *Magn. Reson. Med.* **1994**, *32*, 88.
[171] Barker, B.R.; Mason, R.P.; Bansal, N.; Peshock, R.M. *JMRI* **1994**, *4*, 595.
[172] Mason, R.P.; Shukla, H.P.; Antich, P.P. *Biomater. Artif. Cells Immob. Biotechnol.* **1992**, *20*, 929.
[173] Mason, R.P.; Rodbumrung, W.; Antich, P.P. *NMR Biomed.* **1996**, *9*, 125.
[174] Riess, J.G. *Biomat. Art. Cells Immob. Biotech.* **1992**, *20*, 183.
[175] Kaufman, R.J., In *Medical oxygen transport using perfluorochemicals*, J. Goldstein, Ed.; Butterworth-Heinemann: N.Y., **1991**, 127.
[176] Zuck, T.F.; Riess, J.G. *Critical Rev. Clinical Lab. Sci.* **1994** , *31*, 295.
[177] Krafft, M.P. *Adv. Drug Delivery Rev.* **2001**, *47*, 209.
[178] Schutt, E.G.; Klein, D.H.; Mattrey, R.M.; Riess, J.G. *Angew. Chem. Int. Ed.* **2003**, *42*, 3218.
[179] Riess, J.G. *Chem. Rev.* **2001**, *101*, 2797.
[180] Mason, R.P.; Antich, P.P.; Babcock, E.E.; Gerberich, J.L.; Nunnally, R.L. *Magn. Reson. Imaging* **1989**, *7*, 475.
[181] Mattrey, R.F.; Long, D.C. *Invest. Radiol* **1988**, *23*, s298.
[182] Rosenblum, W.I.; Hadfield, M.G.; Martinez, A.J.; Schatzki, P. *Arch. Pathol. Lab. Med.* **1976**, *100*, 213.
[183] Fishman, J.E.; Joseph, P.M.; Floyd, T.F.; Mukherji, B.; Sloviter, H.S. *Magn. Reson. Imaging* **1987**, *5*, 279.
[184] Fishman, J.E.; Joseph, P.M.; Carvlin, M.J.; Saadi-Elmandjra, M.; Mukherji, B.; Sloviter, H.S. *Invest. Radiol.* **1989**, *24*, 65.
[185] Eidelberg, D.; Johnson, G.; Tofts, P.S.; Dobbin, J.; Crockard, H.A.; Plummer, D. *J. Cereb. Blood Flow Metab.* **1988**, *8*, 276.
[186] Noth, U.; Morrissey, S.P.; Deichmann, R.; Adolf, H.; Schwarzbauer, C.; Lutz, J.; Haase, A. *Magn Reson Med.* **1995**, *34*, 738.
[187] Mason, R.P.; Antich, P.P.; Babcock, E.E.; Constantinescu, A.; Peschke, P.; Hahn, E.W. *Int. J. Radiat. Oncol. Biol. Phys.* **1994**, *29*, 95.
[188] Thomas, S.R.; Millard, R.W.; Pratt, R.G.; Shiferaw, Y.; Samaratunga, R.C. *Art Cells, Blood Subst. Immob. Biotechnol.* **1994**, *22*, 1029.
[189] Mason, R.P.; Nunnally, R.L.; Antich, P.P. *Magn. Reson. Med.* **1991**, *18*, 71.
[190] Tran, H.T.; Guo, Q.; Schumacher, D.J.; Buxton, R.B.; Mattrey, R.F. *Acad. Radiol.* **1995**, *2*, 756.
[191] Helmer, K.G.; Han, S.; Sotak, C.H. *NMR Biomed.* **1998**, *11*, 120.
[192] Baldwin, N.J.; Ng, T.C. *Magn. Reson. Imaging* **1996**, *14*, 541.
[193] van der Sanden, B.J.P.; Heerschap, A.; Hoofd, L.; Simonetti, A.W.; Nicolay, K.; van der Toorn, A.; Colier, W.N.M.; van der Kogel, A.J. *Magn. Reson. Med.* **1999**, *42*, 490.
[194] Fan, X.; River, J.N.; Zamora, M.; Al-Hallaq, H.A.; Karczmar, G.S. *Int. J. Radiat. Oncol. Biol. Phys.* **2002**, *54*, 1202.
[195] Holland, S.K.; Kennan, R.P.; Schaub, M.M.; D'Angelo, M.J.; Gore, J.C. *Magn. Reson. Med.* **1993**, *29*, 446.
[196] Hees, P.S.; Sotak, C.H. *Magn. Reson. Med.* **1993**, *29*, 303.
[197] McIntyre, D.J.O.; McCoy, C.L.; Griffiths, J.R. *Curr. Sci.* **1999**, *76*, 753.
[198] van der Sanden, B.P.J.; Heerschap, A.; Simonetti, A.W.; Rijken, P.F.J.W.; Peters, H.P.W.; Stüben, G.; van der Kogel, A.J. *Int. J. Radiat. Oncol. Biol. Phys.* **1999**, *44*, 649.
[199] Zhao, D.; Ran, S.; Constantinescu, A.; Hahn, E.W.; Mason, R.P. *Neoplasia* **2003**, *5*, 308.
[200] Song, Y.; Constantinescu, A.; Mason, R.P. *Technol. Cancer Res. Treat.* **2002**, *1*, 471.
[201] Zhao, D.; Constantinescu, A.; Chang, C.-H.; Hahn, E.W.; Mason, R.P. *Radiat. Res.* **2003**, *159*, 621.
[202] Zhao, D.; Constantinescu, C.; Hahn, E.W.; Mason, R.P. *Int. J. Radiat. Oncol. Biol. Phys.* **2002**, *53*, 744.
[203] Bulte, J.W.; Arbab, A.S.; Douglas, T.; Frank, J.A. *Methods Enzymol.* **2004**, *386*, 275.
[204] Zimmermann, U.; Noth, U.; Grohn, P.; Jork, A.; Ulrichs, K.; Lutz, J.; Haase, A. *Artif. Cells, Blood Subst. Immob. Biotechnol.* **2000**, *28*, 129.
[205] Noth, U.; Grohn, P.; Jork, A.; Zimmermann, U.; Haase, A.; Lutz, J. *Magn. Reson. Med.* **1999**, *42*, 1039.
[206] Wang, Z.; Su, M.-Y.; Nalcioglu, O. *Technol. Cancer Res. Treat.* **2002**, *1*, 29.
[207] Berkowitz, B.A.; Wilson, C.A.; Hatchell, D.L. *Invest. Ophthalmol. Vis. Sci.* **1991**, *32*, 2382.
[208] Wilson, C.A.; Berkowitz, B.A.; Hatchell, D.L. *Exp. Eye Res.* **1992**, *55*, 119.
[209] Zhang, W.; Ito, Y.; Berlin, E.; Roberts, R.; Berkowitz, B.A. *Invest. Ophthalmol. Visual Sci.* **2003**, *44*, 3119.
[210] Duong, T.Q.; Iadecola, C.; Kim, S.G. *Magn. Reson. Med.* **2001**, *45*, 61.
[211] Nöth, U.; Deichmann, R.; Adolf, H.; Schwarzbauer, C.; Haase, A. *J. Magn. Reson. B.* **1994**, *105*, 233.
[212] Lee, H.K.; Nalcioglu, O. *JMRI* **1992**, *2*, 53.
[213] Busse, L.J.; Pratt, R.G.; Thomas, S.R. *J. Comp. Ast. Tomagr.* **1988**, *12*, 824.
[214] Pratt, R.G.; Zheng, J.; Stewart, B.K.; Shiferaw, Y.; McGoron, A.J.; Samaratunga, R.C.; Thomas, S.R. *Magn. Reson. Med.* **1997**, *37*, 307.
[215] Zhao, D.; Constantinescu, A.; Jiang, L.; Hahn, E.W.; Mason, R.P. *Am. J. Clin. Oncol* **2001**, *24*, 462.
[216] Prosser, R.S.; Luchette, P.A.; Westerman, P.W.; Rozek, A.; Hancock, R.E. *Biophys. J.* **2001**, *80*, 1406.
[217] Kim, J.G.; Zhao, D.; Constantinescu, A.; Mason, R.P.; Liu, H. *J. Biomed. Optics* **2003**, *8*, 53.
[218] Mason, R.P.; Ran, S.; Thorpe, P.E. *J. Cell. Biochem.* **2002**, *87S*, 45.
[219] Delpuech, J.-J.; Hamza, M.A.; Serratice, G.; Stébé, M.-J. *J. Chem. Phys.* **1979**, *70*, 2680.
[220] Hamza, M.A.; Serratice, G.; Stebe, M.-J.; Delpuech, J.-J. *J. Am. Chem. Soc.* **1981**, *103*, 3733.
[221] Hamza, M.A.; Serratice, G.; Stebe, M.-J.; Delpuech, J.-J. *J. Magn. Reson.* **1981**, *42*, 227.

[222] Rietjens, I.M.C.M.; Steensma, A.; den Besten, C.; van Tintelen, G.; Haas, J.; van Ommen, B.; van Bladeren, P.J. *Eur. J. Pharmacol.* **1995**, *293*, 292.

[223] Gorsman, Y.S.; Kapitonenko, T.A. *Izv. Estestvennonauchu. Inst. Pevinsk.* **1973**, *15*, 155.

[224] Mortelmans, K.M.; Simmon, V.F. *Gov. Rep. Announce Index (US)* **1981**, *81*, 2555.

[225] Courtney, K.D.; Andrews, J.E. *J. Environ. Sci. Health B* **1984**, *19*, 83.

[226] Hall, L.W.; Jackson, S.R.K.; Massey, G.M., In *Hexafluorobenzene in veterinary anaesthesia*, A. Arias, R. Llaurado, M. A. Nalda, and J. N. Lunn, Ed.; Excerpta Medica: Oxford, **1975**, 201.

[227] Hunjan, S.; Mason, R.P.; Constantinescu, A.; Peschke, P.; Hahn, E.W.; Antich, P.P. *Int. J. Radiat. Oncol. Biol. Phys.* **1998**, *40*, 161.

[228] Le, D.; Mason, R.P.; Hunjan, S.; Constantinescu, A.; Barker, B.R.; Antich, P.P. *Magn. Reson. Imaging* **1997**, *15*, 971.

[229] Brizel, D.M.; Sibly, G.S.; Prosmitz, L.R.; Scher, R.L.; Dewhirst, M.W. *Int. J. Radiat. Oncol. Biol. Phys.***1997**, *38*, 285.

[230] Fyles, A.W.; Milosevic, M.; Wong, R.; Kavanagh, M.-C.; Pintile, M.; Sun, A.; Chapman, W.; Levin, W.; Manchul, L.; Keane, T.J.; Hill, R.P. *Radiother. Oncol.* **1998**, *48*, 149.

[231] Mason, R.P.; Hunjan, S.; Constantinescu, A.; Song, Y.; Zhao, D.; Hahn, E.W.; Antich, P.P.; Peschke, P., In *Tumor oximetry: Comparison of ^{19}F MR EPI and electrodes*, J. F. Dunn and H. M. Swartz, Ed.; Kluwer: New York, **2003**, 19.

[232] Mason, R.P.; Constantinescu, A.; Hunjan, S.; Le, D.; Hahn, E.W.; Antich, P.P.; Blum, C.; Peschke, P. *Radiat. Res.* **1999**, *152*, 239.

[233] Gu, Y.; Bourke, V.; Kim, J.G.; Constantinescu, A.; Mason, R.P.; Liu, H. *Applied Optics* **2003**, *42*, 1.

[234] Clark Jr., L.C.; Ackerman, J.; Thomas, S.R.; Millard, R.W.; Hoffmann, R.E.; Pratt, R.G.; Ragle-Cole, H.; Kinsey, R.A.; Janakiraman, R., In *Perfluorinated organic liquids and emulsions as biocompatible NMR imaging agents for ^{19}F and dissolved oxygen*, D. Bruley, H. I. Bicher, and D. Reneau, Ed.; Plenum Press: New York, **1984**, 835.

[235] Rodbumrung, W., 'Assessment of perfluorocarbons as probes for oximetry and thermometry', UT Southwestern, Dallas TX, 1994.

[236] Stratford, I.J.; Adams, G.E., In *Radiation sensitizers and bioreductive drugs*, G. G. Steel, G. E. Adams, and A. Horwich, Ed.; Elsevier: Amsterdam, **1989**, 145.

[237] Rasey, J.S.; Casciari, J.J.; Hofstrand, P.D.; Muzi, M.; Graham, M.M.; Chin, L.K. *Radiat. Res.* **2000**, *153*, 84.

[238] Franko, A.; Koch, C.; Boisvert, D. *Cancer Res.* **1992**, *52*, 3831.

[239] Ballinger, J.R. *Semin. Nucl. Med.* **2001**, *31*, 321.

[240] Hodgkiss, R.J. *Anti-cancer Drug Design* **1998**, *13*, 687.

[241] Evans, S.M.; Hahn, S.; Pook, D.R.; Jenkins, W.T.; Chalian, A.A.; Zhang, P.; Stevens, C.; Weber, R.; Weinstein, G.; Benjamin, I.; Mirza, N.; Morgan, M.; Rubin, S.; McKenna, W.G.; Lord, E.M.; Koch, C.J. *Cancer Res.* **2000**, *60*, 2018.

[242] Koch, C.J.; Hahn, S.M.; Rockwell, K.J.; Covey, J.M.; McKenna, W.G.; Evans, S.M. *Cancer Chemother. Pharmacol.* **2001**, *48*, 177.

[243] Ljungkvist, A.S.E.; Bussink, J.; Rijken, P.F.J.W.; Raleigh, J.A.; Denekamp, J.; Van Der Kogel, A.J. *Int. J. Radiat. Oncol. Biol. Phys.* **2000**, *48*, 1529.

[244] Raleigh, J.A.; Chou, S.C.; Arteel, G.E.; Horsman, M. *Radiat. Res.* **1999**, *151*, 580.

[245] Dehdashti, F.; Mintun, M.A.; Lewis, J.S.; Bradley, J.; Govinda, R.; Laforest, R.; Welch, M.J.; Siegel, B.A. *Eur. J. Nucl. Med. Molec. Imaging* **2003**, *30*, 844.

[246] Dehdashti, F.; Grigsby, P.W.; Mintun, M.A.; Lewis, J.S.; Siegel, B.A.; Welch, M.J. *Int. J. Radiat. Oncol. Biol., Phys.* **2003**, *55*, 1233.

[247] Koch, C.J.; Evans, S.M. *Adv. Exp. Med. Biol.* **2003**, *510*, 285.

[248] Raleigh, J.A.; Franko, A.J.; Treiber, E.O.; Lunt, J.A.; Allen, P.S. *Int. J. Radiat. Oncol. Biol. Phys.* **1986**, *12*, 1243.

[249] Maxwell, R.J.; Workman, P.; Griffiths, J.R. *Int. J. Radiat. Oncol. Biol. Phys.* **1989**, *16*, 925.

[250] Jin, G.Y.; Li, S.J.; Moulder, J.E.; Raleigh, J.A. *Int. J. Radiat. Biol.* **1990**, *58*, 1025.

[251] Li, S.J.; Jin, G.Y.; Moulder, J.E. *Cancer Commun.* **1991**, *3*, 133.

[252] Kwock, L.; Gill, M.; McMurry, H.L.; Beckman, W.; Raleigh, J.A.; Joseph, A.P. *Radiat. Res.* **1992**, *129*, 71.

[253] Workman, P.; Maxwell, R.J.; Griffiths, J.R. *NMR Biomed.* **1992**, *5*, 270.

[254] Aboagye, E.O.; Maxwell, R.J.; Horsman, M.R.; Lewis, A.D.; Workman, P.; Tracy, M.; Griffiths, J.R. *Br. J. Cancer* **1998**, *77*, 65.

[255] Aboagye, E.O.; Kelson, A.B.; Tracy, M.; Workman, P. *Anticancer Drug Des.* **1998**, *13*, 703.

[256] Aboagye, E.O.; Maxwell, R.J.; Kelson, A.B.; Tracy, M.; Lewis, A.D.; Graham, M.A.; Horsman, M.R.; Griffiths, J.R.; Workman, P. *Cancer Res.* **1997**, *57*, 3314.

[257] Aboagye, E.O.; Lewis, A.D.; Johnson, A.; Workman, P.; Tracy, M.; Huxham, I.M. *Br. J. Cancer* **1995**, *72*, 312.

[258] Aboagye, E.O.; Lewis, A.D.; Graham, M.A.; Tracy, M.; Kelson, A.B.; Ryan, K.J.; Workman, P. *Anticancer Drug Des.* **1996**, *11*, 231.

[259] Aboagye, E.O.; Lewis, A.D.; Tracy, M.; Workman, P. *Biochem. Pharmacol.* **1997**, *54*, 1217.

[260] Raleigh, J.A.; Franko, A.J.; Kelly, D.A.; Trimble, L.A.; Allen, P.S. *Magn. Reson. Med.* **1991**, *22*, 451.

[261] Aboagye, E.O.; Artemov, D.; Senter, P.D.; Bhujwalla, Z.M. *Cancer Res.* **1998**, *58*, 4075.

[262] Seddon, B.M.; Maxwell, R.J.; Honess, D.J.; Grimshaw, R.; Raynaud, F.; Tozer, G.M.; Workman, P. *Clin. Cancer Res.* **2002**, *8*, 2323.

[263] Clark Jr., L.C.; Gollan, F. *Science* **1966**, 1755.

[264] Greenspan, J.S.; Fox, W.W.; Rubenstein, S.D.; Wolfson, M.R.; Spinner, S.S.; Shaffer, T.H. *Pediatrics* **1997**, *99, E2*.

[265] Thomas, S.R.; Gradon, L.; Pratsinis, S.E.; Pratt, R.G.; Fotou, G.P.; McGoron, A.J.; Podgorski, A.L.; Millard, R.W. *Invest. Radiol.* **1997**, *32*, 29.

[266] Huang, M.Q.; Ye, Q.; Williams, D.S.; Ho, C. *Magn. Reson. Med.* **2002**, *48*, 487.

[267] Schreiber, W.G.; Markstaller, K.; Weiler, N.; Eberle, B.; Laukemper-Ostendorf, S.; Scholz, A.; Burger, K.; Thelen, M.; Kauczor, H.U. *Rofo Fortschr Geb Rontgenstr Neuen Bildgeb Verfahr* **2000**, *172*, 500.

[268] Kauczor, H.U.; Heussel, C.P.; Schreiber, W.G.; Kreitner, K.F. *Radiologe* **2001**, *41*, 279.

[269] Kuethe, D.O.; Behr, V.C.; Begay, S. *Magn. Reson. Med.* **2002**, *48*, 547.

[270] Chen, X.J.; Moller, H.E.; Chawla, M.S.; Cofer, G.P.; Driehuys, B.; Hedlund, L.W.; Johnson, G.A. *Magn. Reson. Med.* **1999**, *42*, 721.

[271] Ruppert, K.; Brookeman, J.; Hagspiel, K.D.; Mugler, J.P.r. *Magn. Reson. Med.* **2000**, *44*, 349.

[272] Kauczor, H.U.; Chen, X.J.; van Beek, E.J.; Schreiber, W.G. *Eur. Respir. J.* **2001**, *17*, 1008.

[273] Remy, W.F.; Geenen, R.W.; Hussain, S.M.; Cademartiri, F.; Poley, J.W.; Siersema, P.D.; Krestin, G.P. *Radiograph.* **2004**, *24*, e18.

[274] Rubin, D.L.; Falk, K.L.; Sperling, M.J.; Ross, M.; Saini, S.; Rothman, B.; Shellock, F.; Zerhouni, E.; Stark, D.; Outwater, E.K.; Schmiedl, U.; Kirby, L.C.; Chezmar, J.; Coates, T.; Chang, M.; Silverman, J.M.; Rofsky, N.; Burnett, K.; Engel, J.; Young, S.W. *JMRI 7*, 865.

[275] Hirohashi, S.; Uchida, H.; Yoshikawa, K.; Fujita, N.; Ohtomo, K.; Yuasa, Y.; Kawamura, Y.; Matsui, O. *Magn. Reson. Imaging* **1994**, *12*, 837.

[276] Bisset, G.S.r.; Emery, K.H.; Meza, M.P.; Rollins, N.K.; Don, S.; Shorr, J.S. *Pediatric Radiol.* **1996**, *26*, 409.

[277] Mattrey, R.F.; Trambert, M.A.; Brown, J.J.; Young, S.W.; Bruneton, J.N.; Wesbey, G.E.; Balsara, Z.N. *Radiology* **1994**, *191*, 841.

[278] Schwarz, R.; Kaspar, A.; Seelig, J.; Kunnecke, B. *Magn. Reson. Med.* **2002**, *48*, 255.

[279] Uzzan, B.; Nicolas, P.; Cucherat, M.; Perret, G.Y. *Cancer Res.* **2004**, *64*, 2941.

[280] Robinson, S.P.; Rijken, P.F.; Howe, F.A.; McSheehy, P.M.; van der Sanden, B.P.; Heerschap, A.; Stubbs, M.; Van Der Kogel, A.J.; Griffiths, J.R. *J. Magn. Reson. Imaging.* **2003**, *17*, 445.

[281] Evelhoch, J.L. *JMRI* **1999**, *10*, 254.

[282] Tofts, P.S.; Brix, G.; Buckley, D.L.; Evelhoch, J.L.; Henderson, E.; Knopp, M.V.; Larsson, H.B.; Lee, T.Y.; Mayr, N.A.; Parker, G.J.; Port, R.E.; Taylor, J.; Weisskoff, R.M. *J. Magn. Reson. Imaging* **1999**, *10*, 223.

[283] Wang, Y.X.; Hussain, S.M.; Krestin, G.P. *Europ. Radiol.* **2001**, *11*, 2319.

[284] Meyer, K.L.; Joseph, P.M.; Mukherji, B.; Livolsi, V.A.; Lin, R. *Invest. Radiol.* **1993**, *28*, 710.

[285] Baldwin, N.J.; Wang, Y.; Ng, T.C. *Magn. Reson. Imaging* **1996**, *14*, 275.

[286] Thomas, C.; Counsell, C.; Wood, P.; Adams, G.E. *JNCI* **1992**, *84*, 174.
[287] Sogabe, T.; Imaizumi, T.; Mori, T.; Tominaga, M.; Koga, K.; Yabuuchi, Y. *Magn. Reson. Imaging* **1997**, *15*, 341.
[288] Joseph, P.M.; Fishman, J.E.; Mukherji, B.; Sloviter, H.A. *J. Comp. Assist. Tomogr.* **1985**, *9*, 1012.
[289] Ceckler, T.L.; Gibson, S.L.; Hilf, R.; Bryant, R.G. *Magn. Reson. Med.* **1990**, *13*, 416.
[290] Negendank, W.G.; McCoy, L.E.; Crowley, M.G.; Corbett, T.H.; Schmidt, E.L. *Biomater Artif Cells Artif Organs* **1990**, *18*, 119.
[291] Authier, B. *Magn. Reson. Med.* **1988**, *8*, 80.
[292] Ewing, J.R.; Branch, C.A.; Fagan, S.C.; Helpern, J.A.; Simkins, R.T.; Butt, S.M.; Welch, K.M.A. *Stroke* **1990**, *21*, 100.
[293] Eleff, S.M.; Schnall, M.D.; Ligetti, L.; Osbakken, M.; Subramanian, V.H.; Chance, B.; Leigh, J.S. Jr. *Magn. Reson. Med.* **1988**, *7*, 412.
[294] Ratner, A.V.; Quay, S.; Muller, H.H.; Simpson, B.B.; Hurd, R.; Young, S.W. *Invest. Radiol.* **1989**, *24*, 224.
[295] Mehta, V.D.; Mason, R.P.; Kulkarni, P.V.; Lea, P.; Constantinescu, A.; Antich, P.P., In *^{19}F MR characterization of fluorinated proteins and relaxation rate enhancement with Gd-DTPA for faster imaging*, E. H. Emram, Ed.; Plenum: New York, **1995**, 305.
[296] Lee, H.; Price, R.R.; Holburn, G.E.; Partain, C.L.; Adams, M.D.; Cacheris, W.P. *J. Magn. Reson. Imaging* **1994**, *4*, 609.
[297] Brix, G.; Bellemann, M.E.; Gerlach, L.; Haberkorn, U. *Radiology* **1998**, *209*, 259.
[298] Fowler, J.S.; Volkow, N.D.; Wang, G.J.; Ding, Y.S. *Semin. Nucl. Med.* **2004**, *34*, 112.
[299] Nakada, T.; Kwee, I.L.; Conboy, C.B. *J. Neurochem.* **1986**, *46*, 198.
[300] Nakada, T.; Kwee, I.L. *Magn. Reson. Imaging* **1987**, *5*, 259.
[301] Nakada, T.; Kwee, I.L. *Magn. Reson. Med.* **1987**, *4*, 366.
[302] Nakada, T.; Kwee, I.L.; Card, P.J.; Matwiyoff, N.A.; Griffey, B.V.; Griffey, R.H. *Magn. Reson. Med.* **1988**, *6*, 307.
[303] Nakada, T.; Kwee, I.L.; Griffey, B.V.; Griffey, R.H. *Magn. Reson. Imaging* **1988**, *6*, 633.
[304] Nakada, T.; Kwee, I.L.; Griffey, B.V.; Griffey, R.H. *Radiology* **1988**, *168*, 823.
[305] Kanazawa, Y.; Umayahara, K.; Shimmura, T.; Yamashita, T. *NMR Biomed.* **1997**, *10*, 35.
[306] Nakada, T.; Kwee, I.L. *Magn. Reson. Med.* **1993**, *29*, 543.
[307] Kanazawa, Y.; Yamane, H.; Shinohara, S.; Kuribayashi, S.; Momozono, Y.; Yamato, Y.; Kojima, M.; Masuda, K. *J. Neurochem.* **1996**, *66*, 2113.
[308] Berkowitz, B.A.; Ackerman, J.J. *Biophys. J.* **1987**, *51*, 681.
[309] O'Connell, T.M.; London, R.E. *J. Magn. Reson. B* **1995**, *109*, 264.
[310] Kwee, I.L.; Nakada, T.; Card, P.J. *J. Neurochem.* **1987**, *49*, 428.
[311] Karino, K.; Kador, P.F.; Berkowitz, B.; Balaban, R.S. *J Biol Chem* **1991**, *266*, 20970.
[312] Kwee, I.L.; Nakada, T.; Suzuki, N. *NMR Biomed.* **1991**, *4*, 38.
[313] Kwee, I.L.; Igarashi, H.; Nakada, T. *Neuroreport.* **1996**, *7*, 726.
[314] Presant, C.A.; Wolf, W.; Waluch, V.; Wiseman, C.; Kennedy, P.; Blayney, D.; Brechner, R.R. *The Lancet* **1994**, *343*, 1184.
[315] Peters, G.F.J. *J. Clin. Oncol.* **1988**, *6*, 1653.
[316] Hull, W.E.; Port, R.E.; Herrmann, R.; Britsch, B.; Kunz, W. *Cancer Res.* **1988**, *48*, 1680.
[317] Koskinen-Kainulainen, M.; Luoma, H.; Tuomisto, J. *Magn. Trace Elem.* **1990**, *9*, 15.
[318] Brix, G.; Bellemann, M.E.; Haberkorn, U.; Gerlach, L.; Lorenz, W.J. *Nucl. Med. Biol.* **1996**, *23*, 897.
[319] Brix, G.; Bellemann, M.E.; Zabel, H.J.; Bachert, P.; Lorenz, W.J. *Magn. Reson. Imaging* **1993**, *11*, 1193.
[320] Brix, G.; Bellemann, M.E.; Haberkorn, U.; Gerlach, L.; Bachert, P.; Lorenz, W.J. *Magn. Reson. Med.* **1995**, *34*, 302.
[321] Guerquin-Kern, J.-L.; Leteurtre, F.; Croisy, A.; Lhoste, J.-M. *Cancer Res.* **1991**, *51*, 5770.
[322] Ojugo, A.S.E.; McSheehy, P.M.J.; Stubbs, M.; Alder, G.; Bashford, C.L.; Maxwell, R.J.; Leach, M.O.; Judson, I.R.; Griffiths, J.R. *Br. J. Cancer* **1998**, *77*, 873.
[323] Laurencot, C.M.; Kennedy, K.A. *Oncol. Res.* **1995**, *7*, 371.
[324] Song, C.W.; Lyons, J.C.; Luo, Y., In *Intra-and extracellular pH in solid tumors: influence on therapeutic response*, B. A. Teicher, Ed.; Marcel Dekker: New York, **1993**, 25.
[325] Raghunand, N.; Gillies, R.J. *Novartis Foundation Symposium* **2001**, *240*, 199.
[326] Sijens, P.E.; Baldwin, N.J.; Ng, T.C. *Magn. Reson. Med.* **1991**, *19*, 337.
[327] Stegman, L.D.; Rehemtulla, A.; Hamstra, D.A.; Rice, D.J.; Jonas, S.J.; Stout, K.L.; Chenevert, T.L.; Ross, B.D. *Gene Ther.* **2000**, *7*, 1005.
[328] Aghi, M.; Kramm, C.M.; Chou, T.C.; Breakefield, X.O.; Chiocca, E.A. *J. Natl. Cancer Inst.* **1998**, *90*, 370.
[329] Wyrwicz, A.M.; Li, Y.E.; Schofield, J.C.; Burt, C.T. *FEBS Letters* **1983**, *162*, 334.
[330] Wyrwicz, A.M.; Conboy, C.B.; Nichols, B.G.; Ryback, K.R.; Eisele, P. *Biochim. Biophys. Acta* **1987**, *929*, 271.
[331] Wyrwicz, A.M.; Conboy, C.B.; Ryback, K.R.; Nichols, B.G.; Eisele, P. *Biochim. Biophys. Acta* **1987**, *927*, 86.
[332] Wyrwicz, A.M.; Conboy, C.B. *Magn. Reson. Med.* **1989**, *9*, 219.
[333] Wyrwicz, A.M. *Ann. NY Acad. Sci.* **1991**, *625*, 733.
[334] Venkatasubramanian, P.N.; Shen, Y.J.; Wyrwicz, A.M. *NMR Biomed.* **1993**, *6*, 377.
[335] Venkatasubramanian, P.N.; Shen, Y.J.; Wyrwicz, A.M. *Biochim. Biophys. Acta* **1995**, *1245*, 262.
[336] Venkatasubramanian, P.N.; Shen, Y.J.; Wyrwicz, A.M. *Magn. Reson. Med.* **1996**, *35*, 626.
[337] Chew, W.M.; Moseley, M.E.; Mills, P.A.; Sessler, D.; Gonzalez-Mendez, R.; James, T.L.; Litt, L. *Magn. Reson. Imaging* **1987**, *5*, 51.
[338] Hashimoto, T.; Ikehira, H.; Fukuda, H.; Ueshima, Y.; Tateno, Y. *Magn Reson Imaging* **1991**, *9*, 577.
[339] Lockhart, S.H.; Cohen, Y.; Yasuda, N.; Freire, B.; Taheri, S.; Litt, L.; Eger, E.I., 2nd *Anesthesiol.* **1991**, *74*, 575.
[340] Litt, L.; Lockhart, S.; Cohen, Y.; Yasuda, N.; Kim, F.; Freire, B.; Laster, M.; Peterson, N.; Taheri, S.; Chang, L.H.; *et al. Ann. NY Acad. Sci.* **1991**, *625*, 707.
[341] Lockhart, S.H.; Cohen, Y.; Yasuda, N.; Kim, F.; Litt, L.; Eger, E.I., 2nd; Chang, L.H.; James, T. *Anesthesiol.* **1990**, *73*, 455.
[342] Preece, N.E.; Challands, J.; Williams, S.C. *NMR Biomed.* **1992**, *5*, 101.
[343] Selinsky, B.S.; Thompson, M.; London, R.E. *Biochem. Pharmacol.* **1987**, *36*, 413.
[344] Selinsky, B.S.; Perlman, M.E.; London, R.E. *Molec. Pharmacol.* **1988**, *33*, 559.
[345] Selinsky, B.S.; Perlman, M.E.; London, R.E. *Mol. Pharmacol.* **1988**, *33*, 567.
[346] Kuethe, D.O.; Caprihan, A.; Fukushima, E.; Waggoner, R.A. *Magn. Reson. Med.* **1998**, *39*, 85.
[347] Raleigh, J.; Franko, A.; Kelly, D.; Trimble, L.; Allen, P. *Magn. Reson. Med.* **1991**, *22*, 451.
[348] Mehta, V.D.; Kulkarni, P.V.; Mason, R.P.; Constantinescu, A.; Aravind, S.; Goomer, N.; Antich, P.P. *FEBS Letters* **1994**, *349*, 234.
[349] London, R.E.; Gabel, S.A. *Biochemistry* **1989**, *28*, 2378.
[350] Ramasamy, R.; Zhao, P.; Gitomer, W.L.; Sherry, A.D.; Malloy, C.R. *Am. J. Physiol.* **1993**, *263*, H1958.
[351] Berkowitz, B.A.; Handa, J.T.; Wilson, C.A. *NMR Biomed.* **1992**, *5*, 65.
[352] Duong, T.Q.; Ackerman, J.J.; Ying, H.S.; Neil, J.J. *Magn. Reson. Med.* **1998**, *40*, 1.
[353] Daugherty, A.; Becker, N.N.; Scherrer, L.A.; Sobel, B.E.; Ackerman, J.J.; Baynes, J.W.; Thorpe, S.R. *Biochem. J.* **1989**, *264*, 829.
[354] Lanza, G.M.; Yu, X.; Winter, P.M.; Abendschein, D.R.; Karukstis, K.K.; Scott, M.J.; Chinen, L.K.; Fuhrhop, R.W.; Scherrer, D.E.; Wickline, S.A. *Circulation* **2002**, *106*, 2842.
[355] Thomas, S.R.; Gradon, L.; Pratsinis, S.E.; Pratt, R.G.; Fotou, G.P.; McGoron, A.J.; Podgorski, A.L.; Millard, R.W. *Invest. Radiol.* **1997**, *32*, 29.
[356] Robert, D.U.; Flatau, G.N.; Cambon, A.; Riess, J.G. *Tetrahedron* **1973**, *29*, 1877.
[357] Morozova, T.V.; Chuvatkin, N.N.; Panteleeva, I.Y.; Boguslavskaya, L.S. *USSR. Zh.Organ. Khim.* **1984**, *20*, 1379.
[358] Hoffmann, F.W. *J. Org. Chem.* **1949**, *14*, 105.
[359] Hu, C.; Qing, F.; Shen, C. *J. Chem. Soc., Perkin Trans. 1: Org. Bio-Org. Chem.* **1993**, *3*, 335.
[360] Kurosawa, S.; Sekiya, A.; Arimura, T.; Yamada, T. *J. Fluorine Chem.* **1993**, *62*, 69.
[361] Stepanov, I.V.; Burmakov, A.I.; Kunshenko, B.V.; Alekseeva, L.A.; Yagupol'skii, L.M. *Zhur. Organ. Khim.* **1983**, *19*, 273.
[362] Fukuhara, T.; Yoneda, N.; Sawada, T.; Suzuki, A. *Synthetic Commun.* **1987**, *17*, 685.

[363] Cacchi, S.; Fabrizi, G.; Goggiamani, A. *Organic Letters* **2003**, *5*, 4269.
[364] Prakash, G.K.S.; Yudin, A.K. *Chem. Rev.* **1997**, *97*, 757.
[365] Singh, R.P.; Shreeve, J.M. *Tetrahedron* **2000**, *56*, 7613.
[366] Marban, E.; Kitakaze, M.; Kusuoka, H.; Porterfield, J.K.; Yue, D.T.; Chacko, V.P. *Proc. Natl. Acad. Sci. (USA)* **1987**, *84*, 6005.
[367] Marban, E.; Kitakaze, M.; Chacko, V.P.; Pike, M.M. *Circ. Res.* **1988**, *63*, 673.
[368] Shionoya, M.; Kimura, E.; Iitaka, Y. *J. Am. Chem. Soc.* **1990**, *112*, 9237.
[369] Mason, R.P.; Jeffrey, F.M.H.; Malloy, C.R.; Babcock, E.E.; Antich, P.P. *Magn. Reson. Med.* **1992**, *27*, 310.
[370] Berkowitz, B.A.; Wilson, C.A.; Hatchell, D.L.; London, R.E. *Magn. Reson. Med.* **1991**, *21*, 233.
[371] Thomas, S.R.; Clark, Jr., L.C.; Ackerman, J.; Pratt, R.G.; Hoffmann, R.E.; Busse, L.J.; Kinsey, R.A.; Samaratunga, R.C. *J. Comp. Asst. Tomogr.* **1986**, *10*, 1.
[372] Sotak, C.H.; Hees, P.S.; Huang, H.N.; Hung, M.H.; Krespan, C.G.; Raynolds, S. *Magn. Reson. Med.* **1993**, *29*, 188.
[373] Papadopoulou, M.V.; Pouremad, R.; Rao, M.K.; Ji, M.; Bloomer, W.D. *In Vivo* **2001**, *15*, 365.

Submitted LDDD

Synthesis and Characterization of Novel *lacZ* Gene Reporter Molecules: Detection of β-Galactosidase Activity Using ^{19}F NMR of Polyglycosylated Fluorinated Vitamin B_6 as ^{19}F NMR Indicator

Jianxin Yu and Ralph P. Mason *

Department of Radiology, The University of Texas Southwestern, Dallas, TX

Running Title: Detection of β-galactosidase activity using ^{19}F NMR

Keywords: β-galactosidase, ^{19}F NMR, *lacZ* gene reporter, 6-fluoropyridoxol, pH

* **Author for correspondence.**
Ralph P. Mason, Ph.D., CSci., CChem.
Department of Radiology
The University of Texas Southwestern Medical Center at Dallas
5323 Harry Hines Blvd.
Dallas, Texas 75390-9058
USA
Tel: (214)-648-8926, Fax: (214)-648-4538
E-mail: Ralph.Mason@UTSouthwestern.edu

Abstract

Gene therapy has emerged as a promising strategy for treatment of various diseases. However, widespread implementation is hampered by difficulties in assessing the success of transfection, in particular, the spatial extent of expression in the target tissue and the longevity of expression. Thus, the development of non-invasive reporter techniques based on appropriate molecules and imaging modalities may help to assay gene expression. We have previously demonstrated the ability to detect β-gal activity based on ^{19}F NMR chemical shift associated with release of fluorophenyl aglycones from galactopyranoside conjugates. Use of fluoropyridoxol as the aglycone provided a potential alternative and we now report the design, synthesis and structural analysis of a series of novel polyglycosylated fluorinated vitamin B_6 derivatives as ^{19}F NMR sensitive aglycone for detection of *lacZ* gene transfection. In particular, we report the activity of the candidate molecules 3, α^4, α^5-tri-*O*-(β-D-galactopyranosyl)-6-fluoropyridoxol **4**, 3-*O*-(β-D-galactopyranosyl)-α^4, α^5-di-*O*-(β-D-glucopyranosyl)-6-fluoropyridoxol **12** and 3-*O*-(β-D-galactopyranosyl)-α^4, α^5-di-*O*-(α-D-mannopyranosyl)-6-fluoropyridoxol **13**. **12** and **13** show promising characteristics including highly sensitive ^{19}F NMR response to β-gal activity ($\Delta\delta$ = 9.0 ~ 9.4 ppm), minimal toxicity for substrate or aglycone, and good water solubility. These preliminary data show that **12** and **13** have the most promising properties for *in vivo* assessing or mapping *lacZ* gene expression.

INTRODUCTION

Gene therapy holds great promise for the treatment of diverse diseases, but widespread implementation is hindered by difficulties in assessing the success of transfection. The development of non-invasive *in vivo* reporter techniques based on appropriate molecules and imaging modalities would be of considerable value for assessing the location, magnitude, and persistence of expression.

The *lacZ* gene encoding β-galactosidase (β-gal) is widely used in molecular biology as a reporter gene to assay clonal insertion, transcriptional activation, protein expression, and protein interaction. Many *in vitro* colorimetric molecular reporter molecules have been described to detect β-gal activity [1-3]. Recently, Weissleder *et al.* [4] presented a near infrared *in vivo* approach based on 9*H*-(1, 3-dichloro-9, 9-dimethylacridin-2-one-7-yl) β-D-galactopyranoside and Lee *et al.* [5] described a radionuclide *in vivo* substrate 2-(4-[^{125}I/^{123}I]iodophenyl)ethyl-1-thio-β-D-galactopyranoside. Louie *et al.* [6] introduced an *in vivo* NMR approach using 1-[2-(β-D-galactopyranosyloxy)propyl]-4, 7, 10-tris(carboxymethyl)-1, 4, 7, 10-tetraazacyclododecane) gadolinium (III) based on proton MRI contrast. We have been developing *in vivo* reporter molecules based on ^{19}F NMR with structures exploiting fluorophenol, trifluorophenol, and fluoropyridoxol aglycones [7-10]. In a continuing effort to develop enhanced approaches for *in vivo* detection of β-gal, we now report the synthesis, and evaluation of polyglycosylated fluorinated vitamin B_6 reporter molecules, designed to enhance water solubility, cellular penetration and enzyme response.

RESULTS AND DISCUSSION

Design

We have found that 6-fluoropyridoxol (**1**, **FPOL**) readily enters red blood cells and perfused myocardium providing well resolved pH sensitive resonances reporting both intra- and extracellular pH, simultaneously [11, 12]. As an *in vivo* example, we found that following i.p. injection of a mixture of **1** and sodium trifluoroacetate (NaTFA) in aqueous dimethyl sulphoxide (DMSO) into a rat, ^{19}F NMR signals were observed from a tumor within minutes and continued to be observable for several hours. However, with the exception of a thymidine kinase transfected Morris hepatoma cell line [13], it failed to enter most tumor cells. Introduction of a D-galactose at the 3 phenolic group of FPOL, 3-*O*-(β-D-galactopyranosyl)-6-fluoropyridoxol (**GFPOL**) yielded a ^{19}F NMR gene expression reporter based on the large chemical shift response to β-gal cleavage, but with the moderate sensitivity to β-gal.[8]

We have shown that modification the 4- and 5-position hydroxymethyl moieties of **FPOL** produces modification of its pK_a with relatively minor changes in chemical shift and chemical shift range.[12,13] *Escherichia coli* (*lacZ*) β-gal catalyses the hydrolysis of galactopyranosides by cleavage of the C-O bond between D-galactose and the aglycone with overall retention of anomeric configuration, a double-displacement mechanism has been proposed, involving the formation ('glycosylation' step) and breakdown ('deglycosylation' step) of a glycosyl-enzyme intermediate *via* oxocarbonium-ion-like transition states. It has been observed that hydrogen bonding interaction between the enzyme and the glycosidic substrate is important in the formation of the enzyme-substrate complex and to the hydrolysis rate [14, 15]. The involvement of fluorine in hydrogen bonding is well documented, and in fact some of the strongest known hydrogen bonds occur in fluorine-containing systems [16]. Sufficient

evidence has suggested that the C-F fragment can act as a weak proton acceptor and may form hydrogen bonds between the enzyme and the substrate [17-20][White , 1996 #2226].

We have detected the existence ofintramolecular hydrogen bond between α^5-OH and 6-F from the ^{1}H-NMR data analysis of series **FPOL** derivatives. For example, the signal of α^5-OH in α^4-OH and α^5-OH unprotected analogues such as **FPOL** or 3-*O*-(2, 3, 4, 6-tetra-*O*-acetyl-β-D-galactopyranosyl)-6-fluoropyridoxol always appears at down-field and is coupled with 5-CH_2 as triplet due to the α^5-OH exchange-limitation by the α^5-OH and 6-F hydrogen bonding, meanwhile, the ^{1}H-NMR signal of α^4-OH at up-field as singlet. Accordingly, introduction of two additional carbohydrate residues at 4- and 5-hydroxymethyl positions of **GFPOL** can break down α^5-OH and 6-F hydrogen bonding and provide the tendency of hydrogen bonding formation between the enzyme and the new substrates. Thus, there might be net gain of hydrogen bond in this case, and additional affinity should increase, therefore, resultant efficient *in vivo* **FPOL**-related ^{19}F NMR gene expression reporters with retaining the virtues of **GFPOL**.

Syntheses

Our initial approach used a one-pot technique to introduce three D-galactose moieties at the 3 phenolic and 4, 5 hydroxymethylic sites, simultaneously. Reaction of **1** with 3.3 equivalents of 2, 3, 4, 6-tetra-*O*-acetyl-α-D-galactopyranosyl bromide **2** in a anhydrous dichloromethane catalyzed by $Hg(CN)_2$ afforded the fully galactopyranosylated 6-fluoropyridoxol (**3**) in 89% yield, which was deacetylated with NH_3/MeOH giving the free galactopyranoside **4** in quantitative yield (**Figure 1**). The ESI-MS of **3** resulted in the expected molecular ion at *m/z* 1178 and quasimolecular ion at

m/z 1179 [M+H], corresponding to the fully adorned derivative with three molecules of **2**. The identity of **3** was established using ^{1}H and ^{13}C NMR. The anomeric protons H-1', H-1" and H-1"' of D-galactoses linked to 3, 4 and 5 positions of **FPOL** at 5.24, 4.66 and 4.52 ppm, respectively, with three well resolved doublets ($J_{1,2}$ = 8.0 Hz) as well as $J_{2,3}$ (J = ~ 10 Hz) coupling constants confirmed that all D-galactoses are in the β-configuration with the $^{4}C_{1}$ chair conformation, whereas in the ^{13}C NMR spectrum, the anomeric carbons C-1', C-1" and C-1"' at 103.34 and 100.22 ppm.

The hydrolysis experiments showed that the three different β-D-galactopyranosyl $C_{1(gal)}$-O linkages in 3, α^{4}, α^{5}-tri-*O*-(β-D-galactopyranosyl)-6-fluoropyridoxol **4** have various sensitivity to β-gal and result in multiple ^{19}F signals around 3 ppm and 12 ~ 20 ppm (**Figure 2**), as we expected, the hydrolytic rate of $C_{1(gal)}$-O_3 linkage is the highest among of these three different $C_{1(gal)}$-O bonds, and increase much more than that in **GFPOL**.[8]

Inspired by these results, we designed another two new molecules 3-*O*-(β-D-galactopyranosyl)-α^{4}, α^{5}-di-*O*-(β-D-glucopyranosyl)-6-fluoropyridoxol **12** and 3-*O*-(β-D-galactopyranosyl)-α^{4}, α^{5}-di-*O*-(α-D-mannopyranosyl)-6-fluoropyridoxol **13**, in which the glycosylations take place in mixed type, galactosylation at 3 phenolic group as sensitive site to β-gal, and glucopyranosylation or mannopyranosylation at 4, 5 hydroxymethyl groups as functional parts. According to the retro-synthesis analysis, we proposed two approaches through differentially protected intermediates as key synthons for synthesis of target compounds.

6-Fluoro-α^{4}, α^{5}-isopropylidenepyrodoxol **5** was detected as a minor by-product in our previous preparation of 6-fluoro-3, α^{4}-isopropylidenepyrodoxol. Testing various

acids as catalysts showed 2% H_2SO_4 acetone solution to provide the best yield of **5** (26%). The regioselectivity of the acetonation reaction was confirmed by analyzing ^{1}H-NMR spectra of **5** and 6-fluoro-3, α^4-isopropylidenepyridoxol, in which the 5-CH_2 signal of **5** appeared at 5.03 ppm as singlet and of 6-fluoro-3, α^4-isopropylidenepyridoxol at 4.97 ppm, but as doublet ($J_{H\text{-}5,HO\text{-}5}$ = 1.2 Hz) due to the coupling of 5-OH.

Treatment of **5** with 2, 3, 4, 6-tetra-*O*-acetyl-α-D-galactopyranosyl bromide **2** using the Koenigs-Knorr glycosylation method gave rise to 3-*O*-(2, 3, 4, 6-tetra-*O*-acetyl-β-D-galactopyranosyl)-α^4, α^5-isopropylidene-6-fluoropyrodoxol **6** in 85% yield. The $\delta_{H\text{-}1'}$ at 4.64 ppm is well-resolved doublet ($J_{1,2}$ = 8.0 Hz) and $\delta_{C\text{-}1'}$ at 100.03 ppm demonstrated that the D-galactose was in the β-configuration. The correlation between 2-CH_3 and H-1' of sugar ring from the NOSEY spectrum of **6** verified that 2, 3, 4, 6-tetra-*O*-acetyl-β-D-galactopyranosyl residue connected at 3 phenolic site and, as further evidence, the acetonation reaction did occur regioselectively on 4, 5 hydroxymethyl groups.

Cleavage of acetonide **6** for synthesis of 3-*O*-(2, 3, 4, 6-tetra-*O*-acetyl-β-D-galactopyranosyl)-6-fluoropyridoxol **7** was achieved, however, the yields were quite low (≤15%), based on several hydrolysis conditions, such as 80% AcOH, 1% HCl or 90% CF_3CO_2H in MeOH, CH_2Cl_2 or 1,4-dioxane in different temperature (60 ~ 100 °C). A moderate amount of **1** was recoverable indicating that the β-D-galactopyranosyl $C_{1'(gal)}$-O_3 bond became weak and sensitive to acid hydrolysis due to the presence of the 6-fluorine atom. Condensation of **7** with 2, 3, 4, 6-tetra-*O*-acetyl-α-D-glucopyranosyl bromide **8** or 2, 3, 4, 6-tetra-*O*-acetyl-α-D-mannopyranosyl bromide **9** in dry CH_2Cl_2 with $Hg(CN)_2$ as a promoter furnished 3-*O*-(2, 3, 4, 6-tetra-*O*-acetyl-β-D-galactopyranosyl)-

α^4, α^5-di-*O*-(2, 3, 4, 6-tetra-*O*-acetyl-β-D-glucopyranosyl)-6-fluoropyrodoxol **10** or 3-*O*-(2, 3, 4, 6-tetra-*O*-acetyl-β-D-galactopyranosyl)-α^4, α^5-di-*O*-(2, 3, 4, 6-tetra-*O*-acetyl-α-D-mannopyranosyl)-6-fluoropyridoxol **11** in the yields of 80% or 78%, respectively. Deacetylation of **10** or **11** in NH_3/MeOH also from 0 °C to room temperature accomplished the target molecules **12** and **13** in quantitative yields (**Figure 3**). But, the overall yields for **12** and **13** through the five-step reactions were only of 3% with limiting steps in the α^4, α^5-isopropylidene group formation and hydrolysis procedure.

The acidic 3 phenolic group *para* to 6-fluorine atom in **FPOL** should be easily converted into the monoanion under mild base condition, [8, 12, 21] consequently, we proposed an alternate approach to selectively benzylate the 3-OH under carefully controlled conditions. Benzyl bromide (1.1 equiv.) was added dropwise over a period of 4 ~ 5 h to the well-stirred reaction mixture of compound **1** in a dichloromethane-aqueous biphasic system (pH 10 ~ 11) employing tetrabutylammonium bromide (TBAB) as the phase-transfer catalyst yielding 3-*O*-benzyl-6-fluoropyridoxol **14** in 76% yield. The structure was established on the basis of the coupling characteristics of α^4, α^5-CH_2 as doublets ($J_{H\text{-}4,HO\text{-}4}$ = 6.0 Hz, $J_{H\text{-}5,HO\text{-}5}$ = 5.4 Hz) and α^4, α^5-OH as triplets in the ^{1}H-NMR spectrum. Condensation of **14** with **8** or **9** gave 3-*O*-benzyl-α^4, α^5-di-*O*-(2, 3, 4, 6-tetra-*O*-acetyl-β-D-glucopyranosyl)-6-fluoropyridoxol **15** or 3-*O*-benzyl-α^4, α^5-di-*O*-(2, 3, 4, 6-tetra-*O*-acetyl-α-D-mannopyranosyl)-6-fluoropyridoxol **16** in satisfactory yields. Removal of the benzyl-protecting group afforded acceptors α^4, α^5-di-*O*-(2, 3, 4, 6-tetra-*O*-acetyl-β-D-glucopyranosyl)-6-fluoropyridoxol **17** or α^4, α^5-di-*O*-(2, 3, 4, 6-tetra-*O*-acetyl-α-D-mannopyranosyl)-6-fluoropyridoxol **18** in quantitative yields, which were subjected to a procedure similar to that described above for the preparation of galactosides giving **10**

or **11** in high yields (88% or 85% respectively). After work up and deacetylation, the target compounds **12** and **13** were obtained in 57% and 52% overall yields over five-step reactions (**Figure 4**).

Recognizing the differential reactivity of the 3 phenolic group over the hydroxymethyl groups, most recently, we have successfully galactopyranosylated of **1** at 3 phenolic group directly with 2, 3, 4, 6-tetra-*O*-acetyl-α-D-galactopyranosyl bromide **2** using the above phase-transfer catalysis technique.[8] Thus, **Figure 5** depicts a very efficient route to synthesize the target compounds **12** and **13** just by three-step reactions in higher overall yields (67% and 65%, respectively).

Characteristics

Before starting *in vivo* kinetic measurements, **FPOL**-related β-D-galactopyranosides **4**, **12** and **13** need to be identified by its ^{19}F NMR signal in different aqueous solutions. The chemical shifts were measured with NaTFA in a capillary as the external standard. **4**, **12** and **13** each gave a single narrow ^{19}F NMR signals between δ -2.0 ~ -3.3 ppm essentially invariant ($\Delta\delta \leq 0.06$ ppm) with pH in the range 3 to 12 and temperatures from 25 to 37 °C in rabbit whole blood, 0.9% saline or PBS solutions. Addition of β-gal (E801A) in PBS buffer (0.1 M, pH=7.4) at 37 °C, **4**, **12** and **13** were hydrolyzed rapidly as predicted releasing the aglycones α^4, α^5-di-*O*-(β-D-galactopyranosyl)-6-fluoropyridoxol, α^4, α^5-di-*O*-(β-D-glucopyranosyl)-6-fluoropyridoxol and α^4, α^5-di-*O*-(α-D-mannopyranosyl)-6-fluoropyridoxol appearing also the single narrow ^{19}F signals shifted up-field between δ -11.20 ~ -12.40 ppm. The reporter molecules **4**, **12** and **13** each exhibits a large rapid ^{19}F NMR chemical shift response to enzyme cleavage ($\Delta\delta$ = 9.0 ~ 9.4 ppm) (**Table 1**). **Figure 6** displays the relative

competition hydrolysis time courses of **4**, **12** and **13**. The β-gal hydrolytic kinetics of **4**, **12** and **13** proceed in a coherent and smooth slope indicating that the liberated aglycones have no inhibiting effects on β-gal, and the shapes of the kinetic curves suggest straightforward first-order kinetics for all substrates, which were much more rapid than for **GFPOL**. All the rate data about **4** were only measured upon the conversion of **4** direct to α^4, α^5-di-*O*-(β-D-galactopyranosyl)-6-fluoropyridoxol, but not included the changes by partially hydrolyzed derivatives from **4**. Unlike 3, α^4, α^5-tri-*O*-(β-D-galactopyranosyl)-6-fluoropyridoxol **4**, 3-*O*-(β-D-galactopyranosyl)-α^4, α^5-di-*O*-(β-D-glucopyranosyl)-6-fluoropyridoxol **12** and 3-*O*-(β-D-galactopyranosyl)-α^4, α^5-di-*O*-(α-D-mannopyranosyl)-6-fluoropyridoxol **13** were not found to exhibit the multiple ^{19}F NMR signals during enzyme cleavage, showing high potential to be as *in vivo* ^{19}F MRS and ^{19}F chemical shift imaging agents. Additionally, **12** and **13** were stable in aqueous solutions in the pH range 3 to 12 at temperatures from 25 to 37 °C during 2 days. Similarly with **GFPOL**, neither **12** nor **13** exhibited significant cytotoxicity, but **12** and **13** have much higher aqueous solubility due to the linked two more carbohydrate residues.

The aglycones α^4, α^5-di-*O*-(β-D-galactopyranosyl)-6-fluoropyridoxol (**DGFPOL**), α^4, α^5-di-*O*-(β-D-glucopyranosyl)-6-fluoropyridoxol (**DUFPOL**) and α^4, α^5-di-*O*-(α-D-mannopyranosyl)-6-fluoropyridoxol (**DMFPOL**) of **4**, **12** and **13** also exhibit the large ^{19}F NMR chemical shift in response to pH ($\Delta\delta$ = ~ 11.0 ppm) in the range of pH 1 ~ 12 (**Figure 7**). The Henderson- Hasselbalch coefficients are $pK_{a(DGFPOL)}$ = 7.95, $\delta_{acid(DGFPOL)}$ = -8.34 ppm, $\delta_{base(DGFPOL)}$ = -19.05 ppm; $pK_{a(DUFPOL)}$ = 8.08, $\delta_{acid(DUFPOL)}$ = -8.15 ppm, $\delta_{base(DUFPOL)}$ = -18.85 ppm; $pK_{a(DMFPOL)}$ = 8.18, $\delta_{acid(DMFPOL)}$ = -7.44 ppm, $\delta_{base(DMFPOL)}$ = -18.15 ppm.

Conclusion

Characterization of these three novel *in vivo* **FPOL**-related ^{19}F NMR *lacZ* gene transfection reporter molecules **4**, **12** and **13** shows *in vivo* ^{19}F NMR gene expression reporters: (a) highly sensitive to *lacZ* gene expression; (b) large chemical shift response to enzyme cleavage ($\Delta\delta$ = 9.0 ~ 9.4 ppm); (c) minimal toxicity for substrates; (d) good water solubility; (e) good blood stability; (f) pH responsiveness of aglycones. These preliminary data show that **12** and **13** have promising properties for *in vivo* assessing or mapping *lacZ* gene expression.

EXPERIMENTAL

General methods ---NMR spectra were recorded on a Varian MERCURY 400 spectrometer (400 MHz for ^{1}H, 100 MHz for ^{13}C, 376 MHz for ^{19}F) with $CDCl_3$, or DMSO-d_6 as solvents. ^{1}H and ^{13}C chemical shifts are referenced to TMS as internal standard, and ^{19}F to a dilute solution of NaTFA in a capillary as external standard (37 °C). Compounds were characterized by acquisition of ^{1}H, ^{13}C, DEPT, ^{1}H-^{1}H COSY or NOESY experiments at 25 °C. Microanalyses were performed on a Perkin-Elmer 2400CHN microanalyser. Mass spectra were obtained by positive and negative ESI-MS using a Micromass Q-TOF hybrid quadrupole/time-of-flight instrument (Micromass UK Ltd). Reactions requiring anhydrous conditions were performed under nitrogen or argon. $Hg(CN)_2$ was dried before use at 50 °C for 1h, CH_2Cl_2 was dried over Drierite, acetonitrile was dried on CaH_2 and kept over molecular sieves under N_2. Solutions in organic solvents were dried with anhydrous sodium sulfate, and concentrated *in vacuo* below 45 °C. 2, 3, 4, 6-tetra-*O*-acetyl-α-D-galactopyranosyl bromide **2**, 2, 3, 4, 6-tetra-*O*-acetyl-α-D-glucopyranosyl bromide **8** and 2, 3, 4, 6-tetra-*O*-acetyl-α-D-

mannopyranosyl bromide **9** were purchased from the Sigma Chemical Company. Column chromatography was performed on silica gel (200 ~ 300 mesh) by elution with cyclohexane-EtOAc and silica gel GF_{254} (Aldrich) used for analytical TLC. Detection was effected by spraying the plates with 5% ethanolic H_2SO_4 (followed by heating at 110 °C for ~10 min.) or by direct UV illumination of the plate.

For enzyme kinetic experiments, **4**, **12** and **13** (10.1 mg, 15 mmol) was dissolved in PBS (0.1 M, pH=7.4, 600 μL), and a PBS solution of β-gal (0.1 M, pH=7.4, 15 μL, 1 unit/μL, E801A Promega, Madison, WI, USA) was added and NMR data were acquired immediately at 37 °C.

3, α^4, α^5-tri-*O*-(2, 3, 4, 6-tetra-*O*-acetyl-β-D-galactopyranosyl)-6-fluoro-pyridoxol 3 A solution of 2, 3, 4, 6-tetra-O-acetyl-α-D-galactopyranosyl bromide **2** (1.35 g, 3.3 mmol, 1.1 equiv.) in anhydrous CH_2Cl_2 (8 mL) was added dropwise to the solution of 6-fluoropyridoxol **1** (0.18 g, 1.0 mmol) and $Hg(CN)_2$ (1.01 g, 4.0 mmol) in dry AcCN (10 mL) containing powdered molecular sieves (4 Å, 2.0 g) with vigorous stirring at r.t. under argon in the dark for 12h. The mixture was diluted with CH_2Cl_2 (30 mL), filtered through Celite, washed, dried (Na_2SO_4) and concentrated *in vacuo*. The residue was purified on a silica gel column (1:3 cyclohexane-EtOAc) to yield 3 (1.05 g, 89%) as syrup, R_f 0.30 (1:3 cyclohexane-EtOAc), NMR ($CDCl_3$), δ_H: 5.24 (1 H, d, $J_{1',2'}$ = 8.0 Hz, H-1'), 5.04 (1 H, dd, $J_{2',3'}$ = 9.8 Hz, H-2'), 4.73 (1H, dd, $J_{3',4'}$ = 3.4 Hz, H-3'), 3.98 (1 H, dd, $J_{4',5'}$ = 2.4 Hz, H-4'), 4.02~4.10 (3 H, m, H-5', H-6'), 4.66 (1 H, d, $J_{1'',2''}$ = 8.0 Hz, H-1''), 4.52 (1 H, d, $J_{1''',2'''}$ = 8.0Hz, H-1'''), 5.15 (2 H, dd, $J_{2'',3''} = J_{2''',3'''}$ = 10.0 Hz, H-2'',H-2'''), 5.07 (2 H, dd, $J_{3'',4''} = J_{3''',4'''}$ = 3.6 Hz, H-3'',H-3'''), 5.52 (2 H, dd, $J_{4'',5''} = J_{4''',5'''}$ = 3.2 Hz, H-4'', H-4'''), 3.88 (2 H, m, H-5'', H-5'''), 4.18 (2 H, dd, $J_{5'',6a''} = J_{5''',6a'''}$ = 3.6 Hz,

$J_{6a'',6b''} = J_{6a''',6b'''}$ = 9.2 Hz, H-6a'', H-6a'''), 4.11 (2 H, dd, $J_{5'',6b''} = J_{5''',6b'''}$ = 6.8 Hz, H-6b'', H-6b'''), 4.48 (2 H, d, $J_{CH2\text{-}4a,CH2\text{-}4b} = J_{CH2\text{-}5a,CH2\text{-}5b}$ = 13.2 Hz, CH_2-4a, CH_2-5a), 4.12 (2 H, d, $J_{CH2\text{-}4a,CH2\text{-}4b} = J_{CH2\text{-}5a,CH2\text{-}5b}$ = 13.2 Hz, CH_2-4b, CH_2-5b), 2.43 (3 H, s, CH_3-2), 2.18, 2.17, 2.16, 2.15, 2.12, 2.11, 2.10, 2.09, 2.08, 2.07, 2.06, 2.05 (36 H, 12s, 12×CH_3CO) ppm; δ_C: 170.84, 170.79, 170.77, 170.73, 170.68, 170.54, 170.53, 170.49, 170.45, 170.35, 170.31, 170.28 (12×CH_3**C**O), 159.73 (s, Py-C), 156.19 (s, Py-C), 148.16 (d, $J_{F\text{-}C}$ = 3.8 Hz, Py-C), 146.47 (d, $J_{F\text{-}C}$ = 14.5Hz, Py-C), 112.51 (d, $J_{F\text{-}C}$ = 31.3 Hz, Py-C), 103.34 (s, C-1'), 100.22 (s, C-1'', C-1'''), 70.75 (s, C-2'), 71.14 (s, C-3'), 70.61 (s, C-4'), 71.56 (s, C-5'), 67.03 (s, C-6'), 67.45 (s, C-2'', C-2'''), 68.39 (s, C-3'', C-3'''), 66.31 (s, C-4'', C-4'''), 68.55 (s, C-5'', C-5'''), 61.99 (s, C-6'', C-6'''), 61.54 (s, CH_2-4), 61.67 (s, CH_2-5), 21.03, 20.94, 20.90, 20.89, 20.87, 20.85, 20.83, 20.79, 20.77, 20.76, 20.74, 20.72 (12s, 12×**C**H_3CO), 18.77 (s, CH_3-3) ppm. ESIMS: *m/z* 1178 [M^+] (26%), 1179 [M+1] (14%). Anal. Calcd. for $C_{50}H_{64}NO_{30}F$(%): C, 50.96, H, 5.48, N, 1.19; Found: C, 50.93, H, 5.46, N, 1.15.

3, α^4, α^5-tri-*O*-(β-D-galactopyranosyl)-6-fluoropyridoxol 4 A solution of 3, α^4, α^5-tri-*O*-(2, 3, 4, 6-tetra-*O*-acetyl-β-D-galactopyranosyl)-6-fluoropyridoxol **3** (0.9 g) in anhydrous MeOH (20 ml) containing 0.5 M NH_3 was vigorously stirred from 0 °C to r.t. overnight until TLC showed complete reaction, evaporated to dryness *in vacuo*. Chromatography of the crude syrup on silica gel with EtOAc/MeOH (4:1) afforded **4** (0.52 g) as a syrup in quantitative yield, R_f 0.10 (1:4 MeOH-EtOAc), NMR (DMSO-d_6), δ_H: 4.95 (1 H, d, $J_{1',2'}$ = 8.2 Hz, H-1'), 4.76 (1 H, dd, $J_{2',3'}$ = 10.0 Hz, H-2'), 4.91 (1H, dd, $J_{3',4'}$ = 2.8 Hz, H-3'), 5.11 (1 H, dd, $J_{4',5'}$ = 2.3 Hz, H-4'), 3.77 (1 H, m, H-5'), 3.90 (1 H, dd, $J_{5',6a'}$ = 6.4Hz, $J_{6a',6b'}$ = 12.4 Hz, H-6a'), 3.68 (1 H, dd, $J_{5',6b'}$ = 3.6 Hz, H-6b'), 4.22 (2

H, d, $J_{1'',2''} = J_{1''',2'''}$ = 8.0 Hz, H-1'', H-1'''), 3.29 (2 H, dd, $J_{2'',3''} = J_{2''',3'''}$ = 10.6 Hz, H-2'', H-2'''), 3.51 (2 H, dd, $J_{3'',4''} = J_{3''',4'''}$ = 3.2 Hz, H-3'', H-3'''), 3.62 (2 H, dd, $J_{4'',5''} = J_{4''',5'''}$ = 2.4 Hz, H-4'', H-4'''), 3.46 (2 H, m, H-5'', H-5'''), 3.66 (2 H, dd, $J_{5'',6a''} = J_{5''',6a'''}$ = 3.6 Hz, $J_{6a'',6b''} = J_{6a''',6b'''}$ = 10.4 Hz, H-6a'', H-6a'''), 3.39 (2 H, dd, $J_{5'',6b''} = J_{5''',6b'''}$ = 6.6 Hz, H-6b'', H-6b'''), 4.48 (2 H, d, $J_{CH2\text{-}4a,CH2\text{-}4b} = J_{CH2\text{-}5a,CH2\text{-}5b}$ = 13.0 Hz, CH_2-4a, CH_2-5a), 4.44 (2 H, d, $J_{CH2\text{-}4a,CH2\text{-}4b} = J_{CH2\text{-}5a,CH2\text{-}5b}$ = 13.0 Hz, CH_2-4b, CH_2-5b), 2.32 (3H, s, CH_3-2) ppm; δ_C: 155.53 (s, Py-C), 153.18 (s, Py-C), 145.36 (d, $J_{F\text{-}C}$ = 4.6 Hz, Py-C), 136.52 (d, $J_{F\text{-}C}$ = 14.0 Hz, Py-C), 114.15 (d, $J_{F\text{-}C}$ = 32.3 Hz, Py-C), 103.19 (s, C-1'), 101.67 (s, C-1'', C-1'''), 70.36 (s, C-2'), 73.94 (s, C-3'), 69.44 (s, C-4'), 76.08 (s, C-5'), 62.88 (s, C-6'), 72.10 (s, C-2'', C-2'''), 73.50 (s, C-3'', C-3'''), 68.26 (s, C-4'', C-4'''), 75.02 (s, C-5'', C-5'''), 60.60 (s, C-6'', C-6'''), 68.77 (s, CH_2-4), 68.92 (s, CH_2-5), 19.19 (s, CH_3-3) ppm. ESIMS: *m/z* 673 [M^+] (6%), 674 [M+1] (10%). Anal. Calcd. for $C_{26}H_{40}NO_{18}F$(%): C, 46.34, H, 5.99, N, 2.08; Found: C, 46.30, H, 5.96, N, 2.05.

α^4, α^5-*O*-isopropylidene-6-fluoropyridoxol 5 The suspension of 6-fluoro-pyridoxol **1** (0.50 g, 2.67 mmol) in anhydrous acetone (40 mL) containing 2% c.H_2SO_4 was stirred for 4 ~ 5h, at the end of which time TLC (4:1 cyclohexane-EtOAc) indicated complete reaction, then cold saturated Na_2CO_3 solution was added with vigorous stirring up to pH between 8 ~ 9. The precipitate was filtered off and concentration of the reaction mixture under reduced pressure followed by purification on flash silica gel column with 4:1 cyclohexane-EtOAc as the eluent gave **5** (0.64 g, 26%) as a syrup, R_f 0.34 (4:1 cyclohexane-EtOAc), NMR ($CDCl_3$), δ_H: 7.45 (1 H, s, HO-3), 5.03 (2 H, s, CH_2-5), 4.57 (2 H, s, CH_2-4), 2.33 (3 H, s, CH_3-2), 1.55 (6 H, s, 2×CH_3) ppm; δ_C: 154.49 (s, Py-C), 152.20 (s, Py-C), 144.14 (d, $J_{F\text{-}C}$ = 14.5 Hz, Py-C), 131.37 (d, $J_{F\text{-}C}$ = 3.8 Hz, Py-

C), 114.01 (d, $J_{F\text{-}C}$ = 32.9 Hz, Py-C), 99.51 (s, **C**Me_2), 59.04 (d, $J_{F\text{-}C}$ = 3.8 Hz, CH_2-5), 54.51 (s, CH_2-4), 31.62 (s, C(**C**H_3)$_2$), 17.58 (s, CH_3-2) ppm. Anal. Calcd. for $C_{11}H_{14}NO_3F$(%): C, 58.13, H, 6.21, N, 6.17; Found: C, 58.08, H, 6.16, N, 6.11.

3-*O*-(2, 3, 4, 6-tetra-*O*-acetyl-β-D-galactopyranosyl)-α^4, α^5-*O*-isopropylidene-6-fluoropyridoxol 6 To a solution of α^4, α^5-*O*-isopropylidene-6-fluoropyridoxol **5** (0.62 g, 2.72 mmol) and $Hg(CN)_2$ (0.88 g, 3.50 mmol) in dry CH_2Cl_2 (10 mL) containing freshly activated 4Å molecular sieves (2.0 g) was added dropwise **2** (1.23 g, 3.0 mmol, 1.1 equiv.). The mixture was stirred overnight in the dark at r.t. under N_2 until TLC indicated complete reaction. Following work up as for **3** gave **6** (1.29 g, 85%), R_f 0.40 (2:3 cyclohexane-EtOAc), NMR ($CDCl_3$), δ_H: 4.64 (1 H, d, $J_{1',2'}$ = 8.0 Hz, H-1'), 5.25 (1 H, dd, $J_{2',3'}$ = 10.0 Hz, H-2'), 5.02 (1 H, dd, $J_{3',4'}$ = 3.6 Hz, H-3'), 5.41 (1 H, dd, $J_{4',5'}$ = 3.2 Hz, H-4'), 3.97 (1 H, m, H-5'), 4.21 (1 H, dd, $J_{5',6a'}$ = 4.4 Hz, $J_{6a',6b'}$ = 11.2 Hz, H-6a'), 4.13 (1 H, dd, $J_{5',6b'}$ = 7.2 Hz, H-6b'), 5.10 (1 H, d, $J_{CH2\text{-}4a,CH2\text{-}4b}$ = 8.0 Hz, CH_2-4a), 4.67 (1 H, d, $J_{CH2\text{-}4a,CH2\text{-}4b}$ = 8.0 Hz, CH_2-4b), 5.14 (1 H, d, $J_{CH2\text{-}5a,CH2\text{-}5b}$ = 9.6 Hz, CH_2-5a), 5.12 (1 H, d, $J_{CH2\text{-}5a,CH2\text{-}5b}$ = 9.6 Hz, CH_2-5b), 2.42 (3 H, s, CH_3-2), 2.17, 2.09, 2.08, 1.99 (12 H, 4s, 4xCH_3CO), 1.61, 1.59 (6 H, 2s, 2xCH_3) ppm; δ_C: 170.78, 170.39, 170.26, 170.11 (4s, 4xCH_3**C**O), 155.44 (s, Py-C), 153.15 (s, Py-C), 145.48 (d, $J_{F\text{-}C}$ = 15.2 Hz, Py-C), 133.16 (d, $J_{F\text{-}C}$ = 4.0 Hz, Py-C), 116.95 (d, $J_{F\text{-}C}$ = 32.1 Hz, Py-C), 101.41 (s, **C**Me_2), 100.03 (s, C-1'), 68.70 (s, C-2'), 70.82 (s, C-3'), 67.12 (s, C-4'), 71.53 (s, C-5'), 64.28 (s, C-6'), 55.38 (s, CH_2-4), 61.58 (s, CH_2-5), 31.88 (s, C(**C**H_3)$_2$), 20.90, 20.89, 20.82, 20.77 (4s, 4x**C**H_3CO), 18.77 (s, CH_3-2) ppm. Anal. Calcd. for $C_{25}H_{32}NO_{12}F$(%): C, 53.84, H, 5.79, N, 2.51; Found: C, 53.79, H, 5.74, N, 2.49.

3-*O*-(2, 3, 4, 6-tetra-*O*-acetyl-β-D-galactopyranosyl)-6-fluoropyridoxol 7 A mixture of 3-*O*-(2, 3, 4, 6-tetra-*O*-acetyl-β-D-galactopyranosyl)-α^4, α^5-*O*-isopropylidene-6-fluoropyridoxol **6** (1.25 g, 2.50 mmol) in 80% AcOH (40 mL) was stirred at 80 °C for 4 ~ 5h, till TLC (1:3 cyclohexane-EtOAc) showed complete reaction. The cooled mixture was neutralized with cold saturated Na_2CO_3 solution, extracted with EtOAc (4×30 mL), concentrated and purified by flash silica gel column with 1:4 cyclohexane-EtOAc giving **7** (0.17 g, 15%) as a syrup, R_f 0.18 (1:4 cyclohexane-EtOAc), NMR ($CDCl_3$), δ_H: 4.79 (1 H, d, $J_{1',2'}$ = 8.0 Hz, H-1'), 5.55 (1 H, dd, $J_{2',3'}$ = 10.6 Hz, H-2'), 5.10 (1 H, dd, $J_{3',4'}$ = 3.6 Hz, H-3'), 5.41 (1 H, dd, $J_{4',5'}$ = 3.6 Hz, H-4'), 3.88 (1 H, m, H-5'), 4.24 (1 H, dd, $J_{5',6a'}$ = 4.4 Hz, $J_{6a',6b'}$ = 12.0 Hz, H-6a'), 4.09 (1 H, dd, $J_{5',6b'}$ = 6.0 Hz, H-6b'), 5.01 (2 H, d, $J_{CH2\text{-}4a,CH2\text{-}4b} = J_{CH2\text{-}5a,CH2\text{-}5b}$ = 12.4 Hz, CH_2-4a, CH_2-5a), 4.62 (1 H, d, $J_{CH2\text{-}4a,CH2\text{-}4b}$ = 12.4 Hz, CH_2-4b), 4.66 (1 H, d, $J_{CH2\text{-}5a,CH2\text{-}5b}$ = 12.4 Hz, CH_2-5b), 3.50 (1 H, m, HO-4, exchangeable with D_2O), 3.56 (1 H, m, HO-5, exchangeable with D_2O), 2.47 (3 H, s, CH_3-2), 2.23, 2.17, 2.02, 2.00 (12 H, 4s, 4×CH_3CO)ppm; δ_C: 170.32, 170.28, 170.18, 169.48 (4×CH_3**C**O), 158.78 (s, Py-C), 156.42 (s, Py-C), 150.33 (d, $J_{F\text{-}C}$ = 15.2 Hz, Py-C), 147.62 (d, $J_{F\text{-}C}$ = 4.6 Hz, Py-C), 120.17 (d, $J_{F\text{-}C}$ = 32.0 Hz, Py-C), 102.39 (s, C-1'), 68.91 (s, C-2'), 70.74 (s, C-3'), 67.19 (s, C-4'), 71.93 (s, C-5'), 61.98 (s, C-6'), 55.91 (s, **C**H_2-4), 59.60 (s, **C**H_2-5), 20.99, 20.85, 20.70, 20.67 (4s, 4×**C**H_3CO), 19.46 (s, CH_3-2) ppm. Anal. Calcd. for $C_{22}H_{28}NO_{12}F$(%): C, 51.05, H, 5.46, N, 2.71; Found: C, 51.00, H, 5.39, N, 2.68.

Alternately **7** was synthesized from **1** directly by phase transfer catalysis: to a well stirred CH_2Cl_2 (10 mL)-H_2O (10 mL) biphasic mixture (pH 10 ~ 11) of **1** (0.5 g, 2.67 mmol) and TBAB (0.1 g, 0.31 mmol), a solution of 2, 3, 4, 6-tetra-*O*-acetyl-α-D-

galactopyranosyl bromide **2** (1.21 g, 2.94 mmol, 1.1 equiv.) in CH_2Cl_2 (10 mL) was added dropwise over a period of 4 ~ 5h at r.t., and the stirring continued for an additional hour. The products were extracted with EtOAc (4×20 mL), washed free of alkali, dried (Na_2SO_4), and concentrated. The residue was purified by column chromatography on silica gel with 1:4 cyclohexane-EtOAc as the eluent to afford **7** (1.08 g, 88%) as a syrup, which is identical in all respects to the product obtained above.

3-*O*-(2, 3, 4, 6-tetra-*O*-acetyl-β-D-galactopyranosyl)-α^4, α^5-di-*O*-(2, 3, 4, 6-tetra-*O*-acetyl-β-D-glucopyranosyl)-6-fluoropyridoxol 10 and 3-*O*-(2, 3, 4, 6-tetra-*O*-acetyl-β-D-galactopyranosyl)-α^4, α^5-di-*O*-(2, 3, 4, 6-tetra-*O*-acetyl-α-D-manno-pyranosyl)-6-fluoropyridoxol 11 Condensation of **7** (0.5 g, 1.1 mmol) with 2, 3, 4, 6-tetra-*O*-acetyl-α-D-glucopyranosyl bromide **8** or 2, 3, 4, 6-tetra-*O*-acetyl-α-D-mannopyranosyl bromide **9** (1.0 g, 2.40 mmol, 1.1 equiv.) in dry CH_2Cl_2 (10 mL) with $Hg(CN)_2$ (0.63 g, 2.50 mmol) as a promoter, according to the procedures described for the preparation of **3** and **6**, furnished 3-O-(2, 3, 4, 6-tetra-*O*-acetyl-β-D-galactopyranosyl)-α^4, α^5-di-*O*-(2, 3, 4, 6-tetra-*O*-acetyl-β-D-glucopyranosyl)-6-fluoropyridoxol **10** and 3-O-(2, 3, 4, 6-tetra-*O*-acetyl-β-D-galactopyranosyl)-α^4, α^5-di-*O*-(2, 3, 4, 6-tetra-*O*-acetyl-α-D-mannopyranosyl)-6-fluoropyridoxol **11**, respectively.

3-*O*-(2, 3, 4, 6-tetra-*O*-acetyl-β-D-galactopyranosyl)-α^4, α^5-di-*O*-(2, 3, 4, 6-tetra-*O*-acetyl-β-D-glucopyranosyl)-6-fluoropyridoxol 10 (1.04 g, 80%), syrup, R_f 0.30 (1:3 cyclohexane-EtOAc), NMR ($CDCl_3$), δ_H: 5.06 (1 H, d, $J_{1',2'}$ = 7.8 Hz, H-1'), 5.28 (1 H, dd, $J_{2',3'}$ = 8.8 Hz, H-2'), 4.98 (1 H, dd, $J_{3',4'}$ = 4.8 Hz, H-3'), 4.73 (1 H, dd, $J_{4',5'}$ = 2.8 Hz, H-4'), 3.95 (1 H, m, H-5'), 4.19 (1 H, dd, $J_{5',6a'}$ = 3.6 Hz, $J_{6a',6b'}$ = 10.8 Hz, H-6a'), 4.02 (1 H, dd, $J_{5',6b'}$ = 5.2 Hz, H-6b'), 5.36 (1 H, d, $J_{1'',2''}$ = 8.0 Hz, H-1''), 5.39 (1 H, d, $J_{1''',2'''}$ = 8.0

Hz, H-1'''), 5.12 (1 H, dd, $J_{2'',3''}$ = 7.2 Hz, H-2''), 5.15 (1 H, dd, $J_{2''',3'''}$ = 6.8 Hz, H-2'''), 5.04 (1 H, dd, $J_{3'',4''}$ = 3.2 Hz, H-3''), 5.07 (1 H, dd, $J_{3''',4'''}$ = 3.6 Hz, H-3'''), 4.76 (1 H, dd, $J_{4'',5''}$ = 2.8 Hz, H-4''), 4.78 (1 H, dd, $J_{4''',5'''}$ = 2.8 Hz, H-4'''), 3.91 (1 H, m, H-5''), 3.93 (1 H, m, H-5'''), 4.08 (1 H, dd, $J_{5'',6a''}$ = 3.2 Hz, $J_{6a'',6b''}$ = 9.4 Hz, H-6a''), 4.10 (1 H, dd, $J_{5''',6a'''}$ = 3.0 Hz, $J_{6a'',6b''}$ = 10.0 Hz, H-6a'''), 4.04 (1 H, dd, $J_{5'',6b''}$ = 7.6 Hz, H-6b''), 4.07 (1 H, dd, $J_{5''',6b'''}$ = 6.8 Hz, H-6b'''), 4.55 (2 H, d, $J_{CH2\text{-}4a,CH2\text{-}4b}$ = $J_{CH2\text{-}5a,CH2\text{-}5b}$ = 11.2 Hz, CH_2-4a, CH_2-5b), 4.49 (1 H, d, $J_{CH2\text{-}4a,CH2\text{-}4b}$ = 11.2 Hz, CH_2-4b), 4.91 (1 H, d, $J_{CH2\text{-}5a,CH2\text{-}5b}$ = 11.2 Hz, CH_2-5a), 2.34 (3 H, s, CH_3-2), 2.05, 1.98, 1.97, 1.96, 1.95, 1.94, 1.93, 1.92, 1.91, 1.90, 1.89, 1.88 (36 H, 12s, 12×CH_3CO) ppm; δ_C: 170.83, 170.80, 170.76, 170.72, 170.70, 170.56, 170.28, 170.20, 170.17, 170.00, 169.82, 169.75 (12×CH_3**C**O), 159.90 (s, Py-C), 157.56 (s, Py-C), 152.14 (d, $J_{F\text{-}C}$ = 16.0 Hz, Py-C), 138.42 (d, $J_{F\text{-}C}$ = 11.4 Hz, Py-C), 117.48 (d, $J_{F\text{-}C}$ = 32.0 Hz, Py-C), 102.66 (s, C-1'), 98.00 (s, C-1''), 98.06 (s, C-1'''), 71.09 (s, C-2'), 68.65 (s, C-2''), 68.95 (s, C-2'''), 74.46 (s, C-3'), 70.84 (s, C-3''), 71.51 (s, C-3'''), 70.05 (s, C-4'), 68.13 (s, C-4''), 68.22 (s, C-4'''), 75.10 (s, C-5'), 72.20 (s, C-5''), 74.24 (s, C-5'''), 63.75 (s, C-6'), 61.91 (s, C-6''), 63.86 (s, C-6'''), 56.77 (s, CH_2-4), 57.16 (s, CH_2-5), 21.20, 20.95, 20.93, 20.91, 20.89, 20.87, 20.85, 20.75, 20.67, 20.62, 20.58, 20.54 (12s, 12×**C**H_3CO), 19.76 (s, CH_3-3) ppm. ESIMS: *m/z* 1178 [M^+] (28%), 1179 [M+1] (12%). Anal. Calcd. for $C_{50}H_{64}NO_{30}F$(%): C, 50.96, H, 5.48, N, 1.19; Found: C, 50.92, H, 5.44, N, 1.16.

3-*O*-(2, 3, 4, 6-tetra-*O*-acetyl-β-D-galactopyranosyl)-α^4, α^5-di-*O*-(2, 3, 4, 6-tetra-*O*-acetyl-α-D-mannopyranosyl)-6-fluoropyridoxol 11 (1.01 g, 78%), syrup, R_f 0.35 (1:3 cyclohexane-EtOAc), NMR ($CDCl_3$), δ_H: 4.80 (1 H, d, $J_{1',2'}$ = 8.2 Hz, H-1'), 5.13 (1 H, dd, $J_{2',3'}$ = 9.8 Hz, H-2'), 5.36 (1 H, dd, $J_{3',4'}$ = 4.2 Hz, H-3'), 5.30 (1 H, dd, $J_{3'',4''}$ = 3.6 Hz,

H-4'), 4.01 (1 H, m, H-5'), 4.33 (1 H, dd, $J_{5',6a'}$ = 3.2 Hz, $J_{6a',6b'}$ = 10.0 Hz, H-6a'), 4.11 (1 H, dd, $J_{5',6b'}$ = 4.6 Hz, H-6b'), 4.71 (2 H, d, $J_{1'',2''} = J_{1''',2'''}$ = 2.4 Hz, H-1'', H-1'''), 4.74 (2 H, dd, $J_{2'',3''} = J_{2''',3'''}$ = 6.2 Hz, H-2'', H-2'''), 5.22 (2 H, dd, $J_{3'',4''} = J_{3''',4'''}$ = 3.8 Hz, H-3'', H-3'''), 3.95 (2 H, dd, $J_{4'',5''} = J_{4''',5'''}$ = 2.0 Hz, H-4'', H-4'''), 4.02 (2 H, m, H-5'', H-5'''), 4.11 (2 H, dd, $J_{5'',6a''} = J_{5''',6a'''}$ = 2.0 Hz, $J_{6a'',6b''} = J_{6a'',6b''}$ = 7.4 Hz, H-6a'', H-6a'''), 4.07 (2 H, dd, $J_{5'',6b''} = J_{5''',6b'''}$ = 5.6 Hz, H-6b'', H-6b'''), 4.87 (2 H, d, $J_{CH2\text{-}4a,CH2\text{-}4b} = J_{CH2\text{-}5a,CH2\text{-}5b}$ = 13.6 Hz, CH_2-4a, CH_2-5b), 4.67 (1 H, d, $J_{CH2\text{-}4a,CH2\text{-}4b} = J_{CH2\text{-}5a,CH2\text{-}5b}$ = 13.6 Hz, CH_2-4b, CH_2-5a), 2.33 (3 H, s, CH_3-2), 2.07, 2.04, 2.03, 2.00, 1.99, 1.98, 1.97, 1.96, 1.95, 1.94, 1.93, 1.92 (36 H, 12s, 12×CH_3CO); δ_C: 171.27, 171.23, 171.15, 171.06, 170.87, 170.83, 170.76, 170.63, 170.58, 170.44, 170.29, 170.25 (12×CH_3**C**O), 160.72 (s, Py-C), 158.20 (s, Py-C), 153.06 (d, $J_{F\text{-}C}$ = 16.0 Hz, Py-C), 149.41 (d, $J_{F\text{-}C}$ = 4.6 Hz, Py-C), 117.21 (d, $J_{F\text{-}C}$ = 31.3 Hz, Py-C), 103.62 (s, C-1'), 98.32 (s, C-1''), 98.61 (s, C-1'''), 70.75 (s, C-2'), 70.22 (s, C-2''), 70.26 (s, C-2'''), 71.83 (s, C-3'), 70.36 (s, C-3''), 70.39 (s, C-3'''), 69.38 (s, C-4'), 67.04 (s, C-4''), 68.60 (s, C-4'''), 72.54 (s, C-5'), 71.90 (s, C-5''), 72.45 (s, C-5'''), 61.47 (s, C-6'), 62.46 (s, C-6''), 63.53 (s, C-6'''), 56.44 (s, CH_2-4), 56.46 (s, CH_2-5), 21.29, 21.21, 21.19, 21.17, 21.13, 21.10, 21.08, 21.05, 21.00, 20.95, 20.90, 20.88 (12s, 12×**C**H_3CO), 20.35 (s, CH_3-3) ppm. ESIMS: *m/z* 1178 [M^+] (20%), 1179 [M+1] (17%). Anal. Calcd. for $C_{50}H_{64}NO_{30}F$(%): C, 50.96, H, 5.48, N, 1.19; Found: C, 50.94, H, 5.45, N, 1.16.

3-*O*-(β-D-galactopyranosyl)-α^4, α^5-di-*O*-(β-D-glucopyranosyl)-6-fluoro-pyridoxol 12 and 3-*O*-(β-D-galactopyranosyl)-α^4, α^5-di-*O*-(α-D-mannopyranosyl)-6-fluoropyridoxol 13 Compounds **10**, **11** (1.00 g, 0.85 mmol) were deacetylated as described above for **4**, to yield **12** and **13** in quantitative yields.

3-*O*-(β-D-galactopyranosyl)-α^4, α^5-di-*O*-(β-D-glucopyranosyl)-6-fluoro-pyridoxol 12 (0.57 g), foam solid, R_f 0.20 (1:4 MeOH-EtOAc), NMR (DMSO-d_6), δ_H: 5.01 (1 H, d, $J_{1',2'}$ = 8.2 Hz, H-1'), 5.22 (1 H, dd, $J_{2',3'}$ = 9.0 Hz, H-2'), 4.92 (1 H, dd, $J_{3',4'}$ = 4.6 Hz, H-3'), 4.70 (1 H, dd, $J_{4',5'}$ = 2.6 Hz, H-4'), 3.91 (1 H, m, H-5'), 4.12 (1 H, dd, $J_{5',6a'}$ = 3.2 Hz, $J_{6a',6b'}$ = 10.2 Hz, H-6a'), 4.00 (1 H, dd, $J_{5',6b'}$ = 5.6 Hz, H-6b'), 5.14 (2 H, d, $J_{1'',2''}$ = 10.0 Hz, H-1'', H-1'''), 4.82 (2 H, dd, $J_{2'',3''} = J_{2''',3'''}$ = 8.2 Hz, H-2'',H-2'''), 4.69 (2 H, dd, $J_{3'',4''} = J_{3''',4'''}$ = 3.4 Hz, H-3'', H-3'''), 4.93 (2 H, dd, $J_{4'',5''} = J_{4''',5'''}$ = 3.2 Hz, H-4'', H-4'''), 3.65 (2 H, m, H-5'', H-5'''), 3.55 (2 H, dd, $J_{5'',6a''} = J_{5''',6a'''}$ = 4.8 Hz, $J_{6a'',6b''} = J_{6a''',6b'''}$ = 12.0 Hz, H-6a'', H-6a'''), 3.31 (2 H, dd, $J_{5'',6b''} = J_{5''',6b'''}$ = 5.6 Hz, H-6b'', H-6b'''), 4.29 (1 H, d, $J_{CH2\text{-}4a,CH2\text{-}4b}$ = 7.6 Hz, CH_2-4a), 4.36 (1 H, d, $J_{CH2\text{-}4a,CH2\text{-}4b}$ = 7.6 Hz, CH_2-5a), 4.20 (2 H, d, $J_{CH2\text{-}4a,CH2\text{-}4b} = J_{CH2\text{-}5a,CH2\text{-}5b}$ = 7.6 Hz, CH_2-4b, CH_2-5b), 4.18 ~ 3.65 (12 H, br, HO-2', 3', 4', 6', 2'', 3'', 4'', 6'', 2''', 3''', 4''', 6''', exchangeable with D_2O), 2.42 (3 H, s, CH_3-2); δ_C: 157.16 (s, Py-C), 152.77 (s, Py-C), 149.47 (d, $J_{F\text{-}C}$ = 3.8 Hz, Py-C), 146.55 (d, $J_{F\text{-}C}$ = 15.0 Hz, Py-C), 137.38 (d, $J_{F\text{-}C}$ = 3.8 Hz, Py-C), 103.65 (s, C-1'), 101.76 (s, C-1'', C-1'''), 72.34 (s, C-2'), 71.28 (s, C-2'', C-2'''), 74.55 (s, C-3'), 73.88 (s, C-3'', C-3'''), 69.82 (s, C-4'), 68.89 (s, C-4'', C-4'''), 76.62 (s, C-5'), 77.29 (s, C-5'', C-5'''), 61.36 (s, C-6'), 60.95 (s, C-6'', C-6'''), 60.54 (s, CH_2-4), 60.78 (s, CH_2-5), 19.88 (s, CH_3-3) ppm. ESIMS: *m/z* 673 [M^+] (8%), 674 [M+1] (14%). Anal. Calcd. for $C_{26}H_{40}NO_{18}F$(%): C, 46.34, H, 5.99, N, 2.08; Found: C, 46.32, H, 5.97, N, 2.07.

3-*O*-(β-D-galactopyranosyl)-α^4, α^5-di-*O*-(α-D-mannopyranosyl)-6-fluoropyridoxol 13 (0.57 g), foam solid, R_f 0.26 (1:4 MeOH-EtOAc), NMR (DMSO-d_6), δ_H: 5.00 (1 H, d, $J_{1',2'}$ = 8.0 Hz, H-1'), 5.23 (1 H, dd, $J_{2',3'}$ = 10.0 Hz, H-2'), 5.16 (1 H, dd, $J_{3',4'}$ = 3.8 Hz, H-3'), 5.08 (1 H, dd, $J_{3'',4''}$ = 3.2 Hz, H-4'), 4.21 (1 H, m, H-5'), 4.51 (1 H,

dd, $J_{5',6a'}$ = 3.6 Hz, $J_{6a',6b'}$ = 10.2 Hz, H-6a'), 4.31 (1 H, dd, $J_{5',6b'}$ = 4.8 Hz, H-6b'), 4.84 (2 H, d, $J_{1'',2''} = J_{1''',2'''}$ = 2.6 Hz, H-1'', H-1'''), 4.68 (2 H, dd, $J_{2'',3''} = J_{2''',3'''}$ = 6.0 Hz, H-2'', H-2'''), 5.02 (2 H, dd, $J_{3'',4''} = J_{3''',4'''}$ = 3.6 Hz, H-3'', H-3'''), 4.05 (2 H, dd, $J_{4'',5''} = J_{4''',5'''}$ = 2.2 Hz, H-4'', H-4'''), 3.94 (2 H, m, H-5'', H-5'''), 4.21 (2 H, dd, $J_{5'',6a''} = J_{5''',6a'''}$ = 2.4Hz, $J_{6a'',6b''} = J_{6a'',6b''}$ = 8.4 Hz, H-6a'', H-6a'''), 4.17 (2 H, dd, $J_{5'',6b''} = J_{5''',6b'''}$ = 6.5 Hz, H-6b'', H-6b'''), 4.77 (2 H, d, $J_{CH2\text{-}4a,CH2\text{-}4b} = J_{CH2\text{-}5a,CH2\text{-}5b}$ = 11.6 Hz, CH_2-4a, CH_2-5b), 4.57 (1 H, d, $J_{CH2\text{-}4a,CH2\text{-}4b} = J_{CH2\text{-}5a,CH2\text{-}5b}$ = 11.6 Hz, CH_2-4b, CH_2-5a), 2.45 (3 H, s, CH_3-2), 4.30 ~ 3.70 (12 H, br, HO-2', 3', 4', 6', 2'', 3'', 4'', 6'', 2''', 3''', 4''', 6''', exchangeable with D_2O); δ_C: 159.92 (s, Py-C), 157.80 (s, Py-C), 154.10 (d, $J_{F\text{-}C}$ = 15.8 Hz, Py-C), 148.61 (d, $J_{F\text{-}C}$ = 4.8 Hz, Py-C), 113.21 (d, $J_{F\text{-}C}$ = 32.0 Hz, Py-C), 103.68 (s, C-1'), 98.56 (s, C-1''), 98.68 (s, C-1'''), 71.76 (s, C-2'), 70.66 (s, C-2''), 70.86 (s, C-2'''), 72.38 (s, C-3'), 71.46 (s, C-3''), 71.32 (s, C-3'''), 70.48 (s, C-4'), 66.87 (s, C-4''), 67.90 (s, C-4'''), 73.64 (s, C-5'), 72.20 (s, C-5''), 72.65 (s, C-5'''), 62.77 (s, C-6'), 63.56 (s, C-6''), 64.83 (s, C-6'''), 57.54 (s, CH_2-4), 58.41 (s, CH_2-5), 20.12 (s, CH_3-3) ppm. ESIMS: *m/z* 673 [M^+] (5%), 674 [M+1] (9%). Anal. Calcd. for $C_{26}H_{40}NO_{18}F$(%): C, 46.34, H, 5.99, N, 2.08; Found: C, 46.31, H, 5.97, N, 2.05.

3-*O*-Benzyl-6-fluoropyridoxol 14 To a well stirred CH_2Cl_2 (10 mL)-H_2O (10 mL) biphasic mixture (pH 10 ~ 11) of **1** (0.50 g, 2.67 mmol) and TBAB (0.10 g, 0.31 mmol), a solution of benzyl bromide (0.51 g, 2.94 mmol, 1.1 equiv.) in CH_2Cl_2 (10 mL) was added dropwise over a period of 4 ~ 5h, while the reaction temperature was maintained at 50 °C, and the stirring continued for an additional hour. Products were extracted (CH_2Cl_2, 4x20 mL), washed free of alkali, dried (Na_2SO_4), and concentrated, the residue was purified by column chromatography on silica gel with 1:2 cyclohexane-EtOAc to

afford major product **14** (0.56 g, 76%), white crystalline, R_f 0.38 (1:2 cyclohexane-EtOAc), NMR ($CDCl_3$), δ_H: 7.39 (5 H, m, Ar-H), 4.90 (2 H, s, $PhCH_2$), 4.75 (2 H, d, $J_{H-5,HO-5}$ = 5.4 Hz, CH_2-5), 4.72 (2 H, d, $J_{H-4,HO-4}$ = 6.0 Hz, CH_2-4), 3.57 (1 H, t, $J_{H-5,HO-5}$ = 5.4 Hz, HO-5, exchangeable with D_2O), 3.49 (1 H, t, $J_{H-4,HO-4}$ = 6.0 Hz, HO-4, exchangeable with D_2O), 2.44 (3 H, s, CH_3-2); δ_C: 157.38 (s, Py-C), 155.82 (s, Py-C), 149.55 (d, J_{F-C} = 4.7Hz, Py-C), 146.97 (d, J_{F-C} = 4.0Hz, Py-C), 119.09 (d, J_{F-C} = 31.2 Hz, Py-C), 136.33, 128.96, 128.88, 128.57 (Ph-C), 55.99 (s, $PhCH_2$, CH_2-4), 56.76 (s, CH_2-5), 19.31 (s, CH_3-2) ppm. Anal. Calcd. for $C_{15}H_{16}NO_3F$(%): C, 64.96, H, 5.82, N, 5.05; Found: C, 64.95, H, 5.79, N, 5.04.

3-*O*-Benzyl-α^4, α^5-di-*O*-(2, 3, 4, 6-tetra-*O*-acetyl-β-D-glucopyranosyl)-6-fluoro-pyridoxol 15 and 3-*O*-Benzyl-α^4, α^5-di-*O*-(2, 3, 4, 6-tetra-*O*-acetyl-α-D-manno-pyranosyl)-6-fluoropyridoxol 16 Glycosylation of **14** (0.46 g, 2.0 mmol) with **8** or **9** (1.83 g, 4.45 mmol, 1.1 equiv.) was carried out as for **3**, **10** and **11** to give **15** and **16**, respectively.

3-*O*-Benzyl-α^4, α^5-di-*O*-(2, 3, 4, 6-tetra-*O*-acetyl-β-D-glucopyranosyl)-6-fluoropyridoxol 15 (0.32 g, 95%), syrup, R_f 0.35 (3:2 cyclohexane-EtOAc), NMR ($CDCl_3$), δ_H: 7.41 (5 H, m, Ar-H), 5.36 (1 H, d, $J_{1',2'}$ = 8.2 Hz, H-1'), 5.41 (1 H, d, $J_{1'',2''}$ = 8.2 Hz, H-1''), 5.14 (2 H, dd, $J_{2',3'} = J_{2'',3''}$ = 7.4 Hz, H-2',H-2''), 4.45 (2 H, dd, $J_{3',4'} = J_{3'',4''}$ = 3.3 Hz, H-3', H-3''), 4.84 (2 H, dd, $J_{4',5'} = J_{4'',5''}$ = 3.8 Hz, H-4', H-4''), 3.96 (2 H, m, H-5', H-5''), 4.80 (2 H, dd, $J_{5',6a'} = J_{5'',6a''}$ = 2.6 Hz, $J_{6a',6b'} = J_{6a'',6b''}$ =10.1 Hz, H-6a', H-6a''), 4.10 (2 H, dd, $J_{5',6b'} = J_{5'',6b''}$ = 3.0 Hz, H-6b', H-6b''), 4.94 (2 H, s, $PhCH_2$), 4.55 (1 H, d, $J_{CH2-4a,CH2-4b}$ = 10.4 Hz, CH_2-4a), 4.48 (1 H, d, $J_{CH2-4a,CH2-4b}$ = 10.4 Hz, CH_2-4b), 4.60 (1 H, d, $J_{CH2-5a,CH2-5b}$ = 11.0 Hz, CH_2-5a), 4.52 (1 H, d, $J_{CH2-5a,CH2-5b}$ = 11.0 Hz, CH_2-5b), 2.37 (3

H, s, CH_3-2), 2.00, 1.99, 1.98, 1.97, 1.96, 1.95, 1.94, 1.93 (24 H, 8s, 8xCH_3CO); δ_C: 170.84, 170.76, 170.31, 170.29, 170.26, 169.95, 169.92, 169.84 (8xCH_3**C**O), 158.57 (s, Py-C), 156.23 (s, Py-C), 152.18 (d, $J_{F\text{-}C}$ = 14.5 Hz, Py-C), 142.64 (d, $J_{F\text{-}C}$ = 4.6 Hz, Py-C), 116.20 (d, $J_{F\text{-}C}$ = 32.0 Hz, Py-C), 136.37, 129.00, 128.94, 128.87, 128.16, 127.77 (Ph-C), 100.23 (s, C-1'), 100.41 (s, C-1"), 71.41 (s, C-2', C-2"), 72.08 (s, C-3'), 72.19 (s, C-3"), 68.34 (s, C-4'), 68.51 (s, C-4"), 72.86 (s, C-5'), 72.93 (s, C-5"), 61.86 (s, C-6'), 61.98 (s, C-6"), 60.98 (s, CH_2-4), 61.28 (s, CH_2-5), 20.88, 20.85, 20.82, 20.75, 20.73, 20.60, 20.59, 20.58 (8s, 8x**C**H_3CO), 19.43 (s, CH_3-3) ppm. ESIMS: *m/z* 937 [M^+] (35%), 938 [M+1] (25%). Anal. Calcd. for $C_{43}H_{52}NO_{21}F$(%): C, 55.05, H, 5.59, N, 1.49; Found: C, 55.03, H, 5.57, N, 1.48.

3-*O*-Benzyl-α^4, α^5-di-*O*-(2, 3, 4, 6-tetra-*O*-acetyl-α-D-mannopyranosyl)-6-fluoropyridoxol 16 (0.30 g, 90%), syrup, R_f 0.40 (3:2 cyclohexane-EtOAc), NMR ($CDCl_3$), δ_H: 7.38 (5 H, m, Ar-H), 5.38 (1 H, d, $J_{1',2'}$ = 2.6 Hz, H-1'), 5.41 (1 H, d, $J_{1",2"}$ = 2.6 Hz, H-1"), 5.36 ~ 3.95 (18 H, m, H-2', 3', 4', 5', 6', 2", 3", 4", 5", 6", $PhCH_2$, CH_2-4, CH_2-5), 2.38 (3 H, s, CH_3-2), 2.02, 2.00, 1.99, 1.98, 1.97, 1.96, 1.95, 1.94 (24 H, 8s, 8xCH_3CO); δ_C: 171.25, 171.18, 170.89, 170.85, 170.78, 170.66, 170.60, 170.48 (8xCH_3**C**O), 159.63 (s, Py-C), 158.24 (s, Py-C), 153.28 (d, $J_{F\text{-}C}$ = 15.8 Hz, Py-C), 145.48 (d, $J_{F\text{-}C}$ = 4.8Hz, Py-C), 118.10 (d, $J_{F\text{-}C}$ = 31.0 Hz, Py-C), 98.42 (s, C-1'), 100.03 (s, C-1"), 72.60 ~ 56.54 (13C, C-2', 3', 4', 5', 6', 2", 3", 4", 5", 6", Ph**C**H_2, CH_2-4, CH_2-5), 21.23, 20.94, 20.92, 20.90, 20.88, 20.86, 20.84, 20.80, 20.78 (8s, 8x**C**H_3CO), 18.37 (s, CH_3-3) ppm. ESIMS: *m/z* 937 [M^+] (32%), 938 [M+1] (20%). Anal. Calcd. for $C_{43}H_{52}NO_{21}F$(%): C, 55.05, H, 5.59, N, 1.49; Found: C, 55.01, H, 5.55, N, 1.45.

α^4, α^5-Di-*O*-(2, 3, 4, 6-tetra-*O*-acetyl-β-D-glucopyranosyl)-6-fluoropyridoxol 17 and α^4, α^5-di-*O*-(2, 3, 4, 6-tetra-*O*-acetyl-α-D-mannopyranosyl)-6-fluoropyridoxol 18

A mixture of **15** or **16** (0.29 g, 0.30 mmol) and Pd-C (5%, 300 mg) in MeOH (40 mL) was stirred for 24h at r.t. under H_2 (25 psi). Evaporated filtrate gave **17**, **18** in quantitative yields.

α^4, α^5-Di-*O*-(2, 3, 4, 6-tetra-*O*-acetyl-β-D-glucopyranosyl)-6-fluoropyridoxol 17 (0.26 g), syrup, R_f 0.28 (1:3 cyclohexane-EtOAc), NMR ($CDCl_3$), δ_H: 7.33 (1 H, s, HO-3, exchangeable with D_2O), 5.30 (1 H, d, $J_{1',2'}$ = 8.4 Hz, H-1'), 5.35 (1 H, d, $J_{1'',2''}$ = 8.4 Hz, H-1''), 5.09 (2 H, dd, $J_{2',3'} = J_{2'',3''}$ = 7.6 Hz, H-2',H-2''), 4.35 (2 H, dd, $J_{3',4'} = J_{3'',4''}$ = 3.4 Hz, H-3', H-3''), 4.80 (2 H, dd, $J_{4',5'} = J_{4'',5''}$ = 3.6 Hz, H-4', H-4''), 3.89 (2 H, m, H-5', H-5''), 4.77 (2 H, dd, $J_{5',6a'} = J_{5'',6a''}$ = 2.4 Hz, $J_{6a',6b'} = J_{6a'',6b''}$ = 10.6 Hz, H-6a', H-6a''), 4.05 (2 H, dd, $J_{5',6b'} = J_{5'',6b''}$ = 3.2 Hz, H-6b', H-6b''), 4.51 (1 H, d, $J_{CH2\text{-}4a,CH2\text{-}4b}$ = 10.3 Hz, CH_2-4a), 4.45 (1 H, d, $J_{CH2\text{-}4a,CH2\text{-}4b}$ = 10.3 Hz, CH_2-4b), 4.57 (1 H, d, $J_{CH2\text{-}5a,CH2\text{-}5b}$ = 11.1 Hz, CH_2-5a), 4.49 (1 H, d, $J_{CH2\text{-}5a,CH2\text{-}5b}$ = 11.1 Hz, CH_2-5b), 2.35 (3 H, s, CH_3-2), 1.99, 1.98, 1.97, 1.96, 1.95, 1.94, 1.93, 1.91 (24 H, 8s, 8×CH_3CO); δ_C: 170.82, 170.78, 170.65, 170.58, 170.46, 169.85, 169.82, 169.80 (8×CH_3**C**O), 158.77 (s, Py-C), 156.35 (s, Py-C), 152.28 (d, $J_{F\text{-}C}$ = 14.2 Hz, Py-C), 142.69 (d, $J_{F\text{-}C}$ = 4.8 Hz, Py-C), 116.26 (d, $J_{F\text{-}C}$ = 32.2 Hz, Py-C), 100.35 (s, C-1'), 100.54 (s, C-1''), 71.37 (s, C-2', C-2''), 72.18 (s, C-3'), 72.29 (s, C-3''), 68.38 (s, C-4'), 68.56 (s, C-4''), 72.83 (s, C-5'), 72.88 (s, C-5''), 61.82 (s, C-6'), 61.89 (s, C-6''), 60.90 (s, CH_2-4), 61.19 (s, CH_2-5), 20.85, 20.83, 20.82, 20.80, 20.78, 20.76, 20.73, 20.65 (8s, 8×**C**H_3CO), 19.32 (s, CH_3-3) ppm. ESIMS: *m/z* 847 [M^+] (30%), 848 [M+1] (21%). Anal. Calcd. for $C_{36}H_{46}NO_{21}F$(%): C, 50.99, H, 5.47, N, 1.65; Found: C, 50.96, H, 5.45, N, 1.62.

α^4, α^5-Di-*O*-(2, 3, 4, 6-tetra-*O*-acetyl-α-D-mannopyranosyl)-6-fluoropyridoxol

18 (0.26 g), syrup, R_f 0.27 (1:3 cyclohexane-EtOAc), NMR ($CDCl_3$), δ_H: 7.33 (1 H, s, HO-3, exchangeable with D_2O), 5.33 (1 H, d, $J_{1',2'}$ = 2.7 Hz, H-1'), 5.37 (1 H, d, $J_{1'',2''}$ = 2.7 Hz, H-1''), 5.45 ~ 4.07 (16 H, m, H-2', 3', 4', 5', 6', 2'', 3'', 4'', 5'', 6'', CH_2-4, CH_2-5), 2.35 (3 H, s, CH_3-2), 2.01, 2.00, 1.99, 1.98, 1.97, 1.96, 1.95, 1.94 (24 H, 8s, 8×CH_3CO); δ_C: 171.33, 171.21, 170.85, 170.83, 170.76, 170.61, 170.56, 170.53 (8×CH_3**C**O), 158.66 (s, Py-C), 157.74 (s, Py-C), 153.67 (d, J_{F-C} = 15.8 Hz, Py-C), 145.68 (d, J_{F-C} = 4.6 Hz, Py-C), 118.23 (d, J_{F-C} = 31.2 Hz, Py-C), 98.67 (s, C-1'), 100.33 (s, C-1''), 72.8 ~ 56.56 (12C, C-2', 3', 4', 5', 6', 2'', 3'', 4'', 5'', 6'', CH_2-4, CH_2-5), 20.99, 20.97, 20.93, 20.90, 20.88, 20.86, 20.84, 20.80 (8s, 8×**C**H_3CO), 18.45 (s, CH_3-3) ppm. ESIMS: *m/z* 847 [M^+] (25%), 848 [M+1] (18%). Anal. Calcd. for $C_{36}H_{46}NO_{21}F$(%): C, 50.99, H, 5.47, N, 1.65; Found: C, 50.97, H, 5.44, N, 1.63.

ACKNOWLEDGEMENTS

Supported by grants from the DOD Breast Cancer Initiative IDEA award DAMD17-03-1-0343-01, and the Cancer Imaging Program, NIH P20 CA 86354 (pre-ICMIC). NMR experiments were conducted at the Mary Nell and Ralph B. Rogers NMR Center, an NIH BTRP facility #P41-RR02584.

Table 1. ^{19}F chemical shifts [+] and hydrolytic rates *

Reporters	4	12	13	GFPOL
$\delta_{F\,(substrate)}$	-3.02	-2.85	-2.14	-3.22
$\delta_{F\,(product)}$	-12.37	-12.16	-11.22	-11.21
$\Delta\delta_F$	9.35	9.31	9.08	7.99
$v_{(\mu mol/min/unit)}$	34.0	39.0	36.0	4.3

[+] (ppm) with respect to sodium trifluoroacetate
* β-gal (E801A) added at 37°C in PBS (0.1 M, pH=7.4).

Figure legends

Figure 1. Reagents and conditions: (a) 2, 3, 4, 6-tetra-*O*-acetyl-α-D-galactopyranosyl bromide **2**, $Hg(CN)_2$, 4Å M.S., CH_2Cl_2, r.t., 12 h, 89%; (b) NH_3-MeOH, 0°C→r.t., 24 h, quantitative yields.

Figure 2. The ^{19}F-NMR spectrum of 3, α^4, α^5-tri-*O*-(β-D-galactopyranosyl)-6-fluoropyridoxol **4** and its partially hydrolyzed derivatives during hydrolysis by β-gal (E801A) in PBS (pH=7.4) at 37 °C. **(β-D-Galp = β-D-galactopyranosyl)**

Figure 3. Reagents and conditions: (a) 2% H_2SO_4, acetone, r.t. 4~5 h, 26%; (b) 2, 3, 4, 6-tetra-*O*-acetyl-α-D-galactopyranosyl bromide **2**, $Hg(CN)_2$, 4Å M.S., CH_2Cl_2, r.t., 12 h, 85%; (c) 80% AcOH, 80°C, 4~5 h, 15%; (d) 2, 3, 4, 6-tetra-*O*-acetyl-α-D-glucopyranosyl bromide **8** or 2, 3, 4, 6-tetra-*O*-acetyl-α-D-mannopyranosyl bromide **9**, $Hg(CN)_2$, 4Å M.S., CH_2Cl_2, r.t., 12 h, 80% (→**10**) or 78%(→**11**), respectively; (e) NH_3-MeOH, 0°C→r.t., 24 h, quantitative yields.

Figure 4. Reagents and conditions: (a) benzyl bromide (1.1 equiv.), CH_2Cl_2-H_2O, pH 10~11, 50°C, TBAB, 4~5 h, 76%; (b) 2, 3, 4, 6-tetra-*O*-acetyl-α-D-glucopyranosyl bromide **8** or 2, 3, 4, 6-tetra-*O*-acetyl-α-D-mannopyranosyl bromide **9**, $Hg(CN)_2$, 4Å M.S., CH_2Cl_2, r.t., 12 h, 90%(→**15**) or 85%(→**16**), respectively; (c) 25psi H_2, Pd/C, r.t., 12 h, quantitative yields; (d) 2, 3, 4, 6-tetra-*O*-acetyl-α-D-galactopyranosyl bromide **2**, $Hg(CN)_2$, 4Å M.S., CH_2Cl_2, r.t., 12 h, 88%(→**10**) or 85%(→**11**), respectively; (e) NH_3-MeOH, 0°C→r.t., 24 h, 95%(→**12**) or 94%(→**13**), respectively.

Figure 5. Reagents and conditions: (a) 2, 3, 4, 6-tetra-O-acetyl-α-D-galactopyranosyl bromide **2**, CH_2Cl_2-H_2O, pH 10~11, r.t., TBAB, 4~5 h, 88%; (b) 2, 3, 4, 6-tetra-*O*-acetyl-α-D-glucopyranosyl bromide **8** or 2, 3, 4, 6-tetra-O-acetyl-α-D-mannopyranosyl bromide **9**, $Hg(CN)_2$, 4Å M.S., CH_2Cl_2, r.t., 12 h, 80%(→**10**) or 78%(→**11**), respectively; (c) NH_3-MeOH, 0°C→r.t., 24 h, 95%(→**12**) or 94%(→**13**), respectively.

Figure 6. The kinetic hydrolysis time courses of **4**, **12**, **13** (15.0 mmol) and **GFPOL** (10.0 mmol) by β-gal (E801A, 15 units) hydrolysis in PBS buffer (0.1 M, pH=7.4, 600μL) at 37°C

Figure 7. ^{19}F NMR chemical shifts pH titration curve of **DGFPOL**, **DUFPOL** and **DMFPOL** in 0.9% saline at 37°C. (**DGFPOL:** α^4, α^5-di-*O*-(β-D-galactopyranosyl)-6-fluoropyridoxol; **DUFPOL:** α^4, α^5-di-*O*-(β-D-glucopyranosyl)-6-fluoropyridoxol; **DMFPOL:** α^4, α^5-di-*O*-(α-D-mannopyranosyl)-6-fluoropyridoxol).

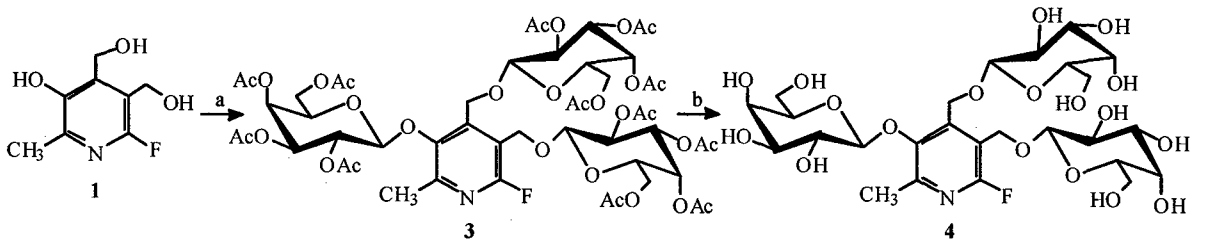

Figure 1. Reagents and conditions: (a) 2, 3, 4, 6-tetra-*O*-acetyl-α-D-galactopyranosyl bromide **2**, $Hg(CN)_2$, 4Å M.S., CH_2Cl_2, r.t., 12 h, 89%; (b) NH_3-MeOH, 0°C→r.t., 24 h, quantitative yields.

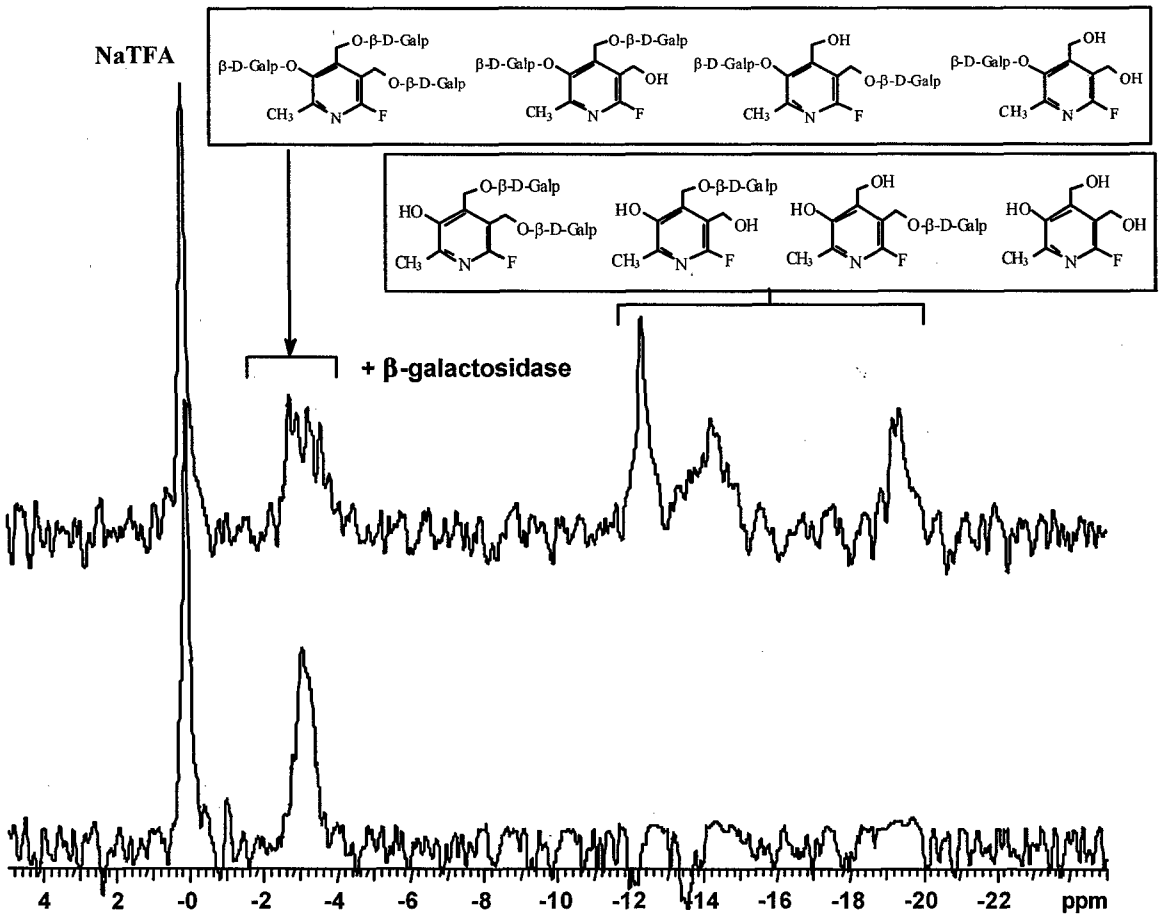

Figure 2. The ^{19}F-NMR spectrum of 3, α^4, α^5-tri-*O*-(β-D-galactopyranosyl)-6-fluoropyridoxol **4** and its partially hydrolyzed derivatives during hydrolysis by β-gal (E801A) in PBS (pH=7.4) at 37 °C. **(β-D-Galp = β-D-galactopyranosyl)**

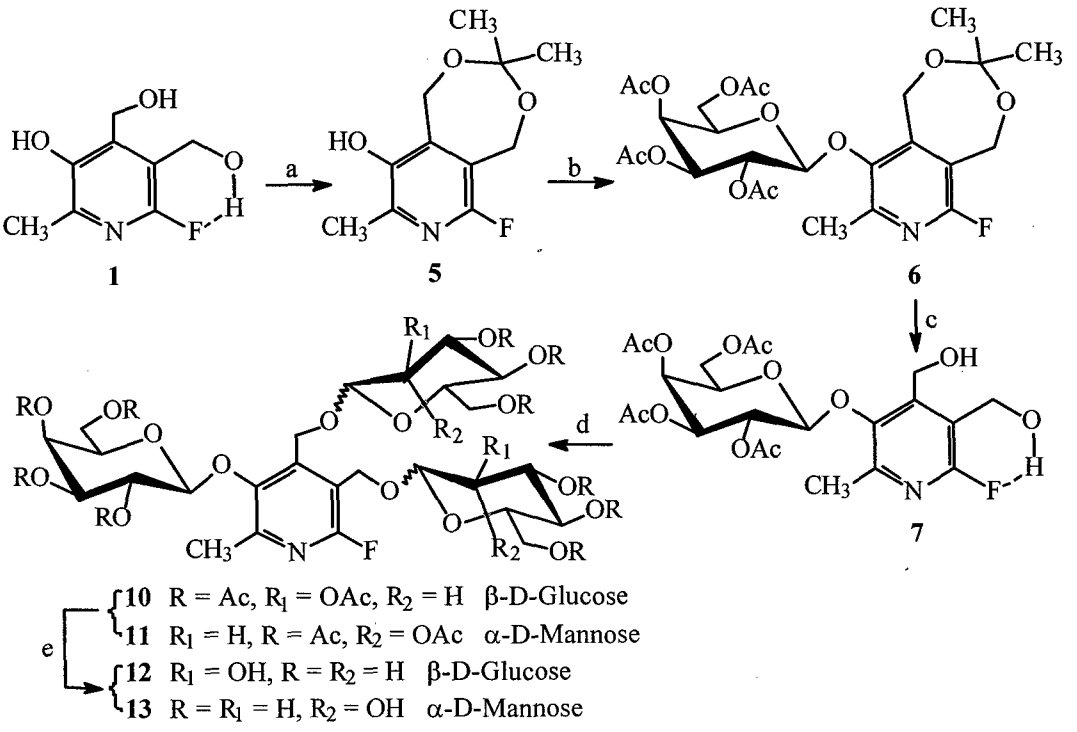

Figure 3. Reagents and conditions: (a) 2% H_2SO_4, acetone, r.t. 4~5 h, 26%; (b) 2, 3, 4, 6-tetra-O-acetyl-α-D-galactopyranosyl bromide **2**, $Hg(CN)_2$, 4Å M.S., CH_2Cl_2, r.t., 12 h, 85%; (c) 80% AcOH, 80°C, 4~5 h, 15%; (d) 2, 3, 4, 6-tetra-O-acetyl-α-D-glucopyranosyl bromide **8** or 2, 3, 4, 6-tetra-O-acetyl-α-D-mannopyranosyl bromide **9**, $Hg(CN)_2$, 4Å M.S., CH_2Cl_2, r.t., 12 h, 80% (→**10**) or 78%(→**11**), respectively; (e) NH_3-MeOH, 0°C→r.t., 24 h, quantitative yields.

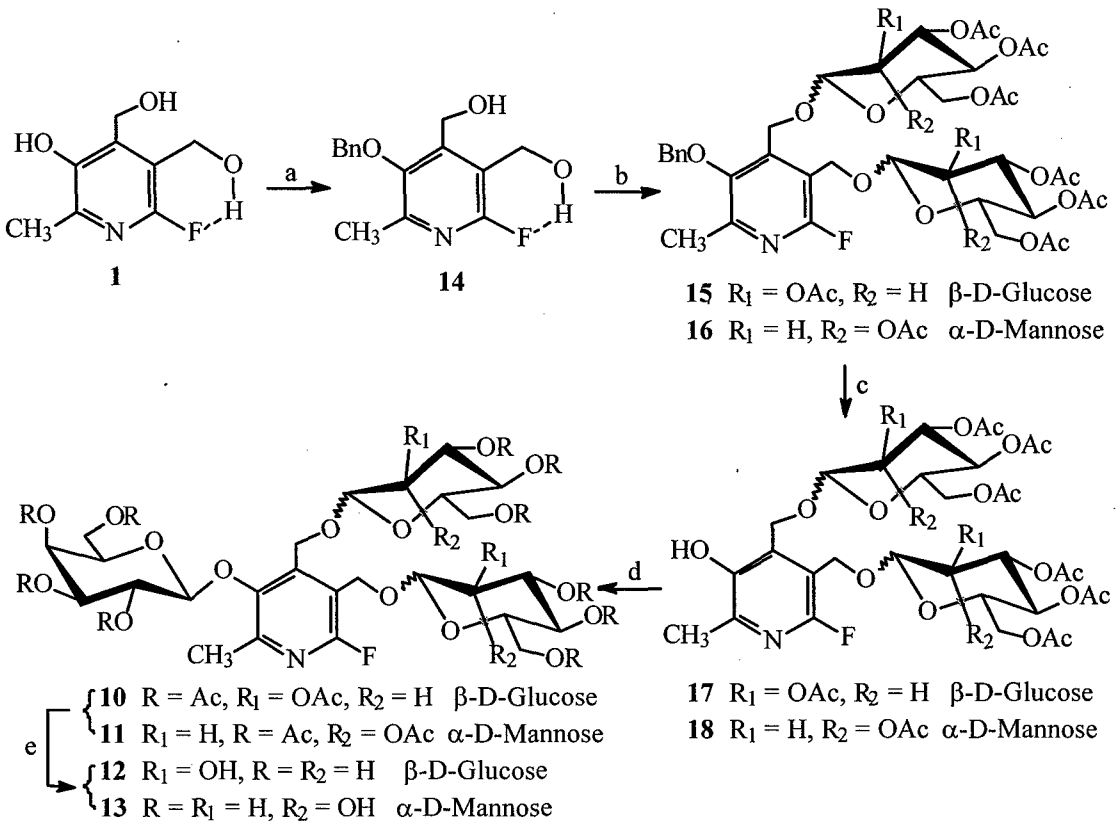

Figure 4. Reagents and conditions: (a) benzyl bromide (1.1 equiv.), CH_2Cl_2-H_2O, pH 10~11, 50°C, TBAB, 4~5 h, 76%; (b) 2, 3, 4, 6-tetra-*O*-acetyl-α-D-glucopyranosyl bromide **8** or 2, 3, 4, 6-tetra-*O*-acetyl-α-D-mannopyranosyl bromide **9**, $Hg(CN)_2$, 4Å M.S., CH_2Cl_2, r.t., 12 h, 90%(→**15**) or 85%(→**16**), respectively; (c) 25psi H_2, Pd/C, r.t., 12 h, quantitative yields; (d) 2, 3, 4, 6-tetra-*O*-acetyl-α-D-galactopyranosyl bromide **2**, $Hg(CN)_2$, 4Å M.S., CH_2Cl_2, r.t., 12 h, 88%(→**10**) or 85%(→**11**), respectively; (e) NH_3-MeOH, 0°C→r.t., 24 h, 95%(→**12**) or 94%(→**13**), respectively.

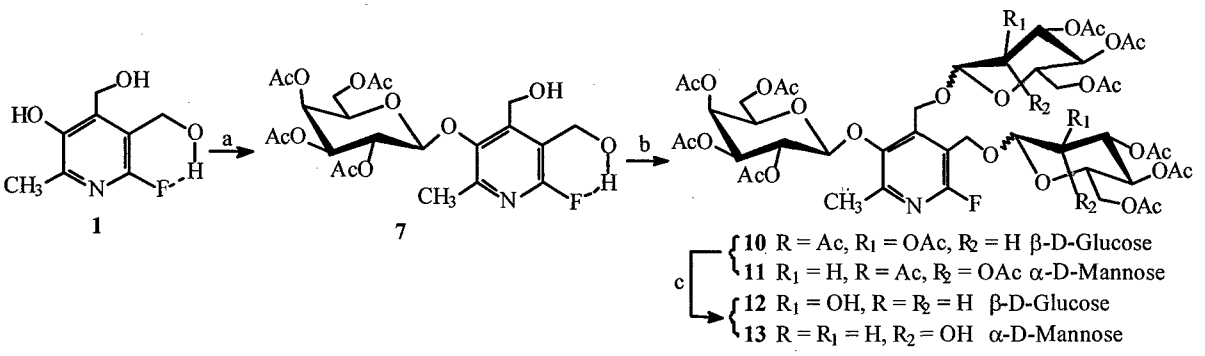

Figure 5. Reagents and conditions: (a) 2, 3, 4, 6-tetra-O-acetyl-α-D-galactopyranosyl bromide **2**, CH_2Cl_2-H_2O, pH 10~11, r.t., TBAB, 4~5 h, 88%; (b) 2, 3, 4, 6-tetra-*O*-acetyl-α-D-glucopyranosyl bromide **8** or 2, 3, 4, 6-tetra-*O*-acetyl-α-D-mannopyranosyl bromide **9**, $Hg(CN)_2$, 4Å M.S., CH_2Cl_2, r.t., 12 h, 80%(→**10**) or 78%(→**11**), respectively; (c) NH_3-MeOH, 0°C→r.t., 24 h, 95%(→**12**) or 94%(→**13**), respectively.

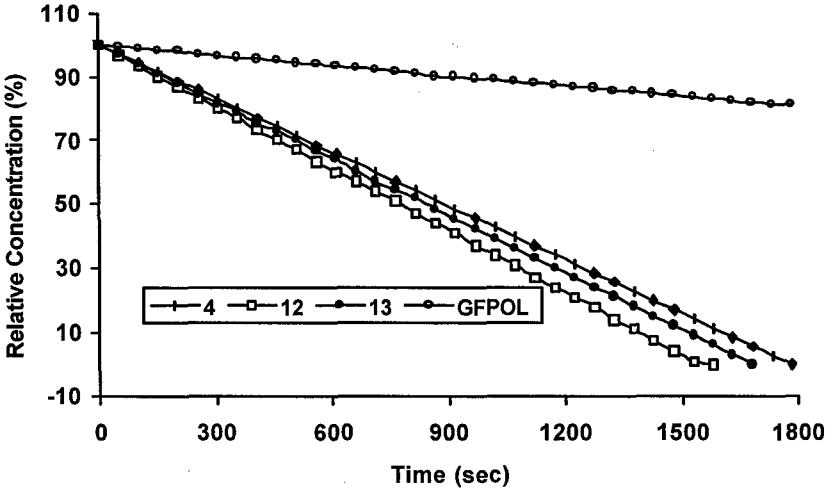

Figure 6. The kinetic hydrolysis time courses of **4**, **12**, **13** (15.0 mmol) and **GFPOL** (10.0 mmol) by β-gal (E801A, 15 units) hydrolysis in PBS (0.1 M, pH=7.4, 600 μL) at 37 °C

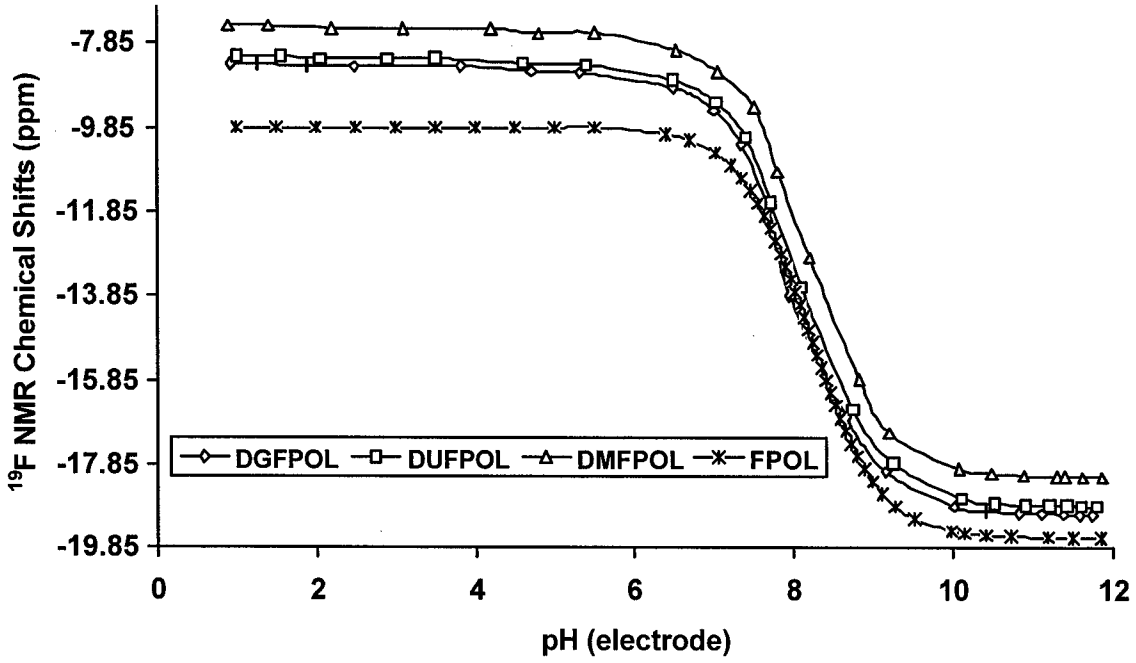

Figure 7. ^{19}F NMR chemical shifts pH titration curve of **DGFPOL**, **DUFPOL** and **DMFPOL** in 0.9% saline at 37°C. (**DGFPOL:** α^4, α^5-di-*O*-(β-D-galactopyranosyl)-6-fluoropyridoxol; **DUFPOL:** α^4, α^5-di-*O*-(β-D-glucopyranosyl)-6-fluoropyridoxol; **DMFPOL:** α^4, α^5-di-*O*-(α-D-mannopyranosyl)-6-fluoropyridoxol).

REFERENCES:

1 Pocsi, I.; Taylor, S.A.; Richardson, A.C.; Smith, B.V.; Price, R.G. *Biochim. Biophys. Acta* **1993**,*1163*,54

2 Heuermann, K.; Cosgrove, J. *Biotechniques* **2001**,*30*,1142

3 Buller, C.J.; Zang, X.P.; Howard, E.W.; Pento, J.T. *Methods & Findings in Exp. Clin. Pharmacol.* **2003**,*25*,713

4 Tung, C.H.; Zeng, Q.; Shah, K.; Kim, D.E.; Schellingerhout, D.; Weissleder, R. *Cancer Res.* **2004**,*64*,1579

5 Lee, K.H.; Byun, S.S.; Choi, J.H.; Paik, J.Y.; Choe, Y.S.; Kim, B.T. *Eur J Nucl Med Mol Imaging.* **2004**,*31*,433

6 Louie, A.Y.; Huber, M.M.; Ahrens, E.T.; Rothbacher, U.; Moats, R.; Jacobs, R.E.; Fraser, S.E.; Meade, T.J. *Nature Biotechnol.* **2000**,*18*,321

7 Cui, W.; Otten, P.; Li, Y.; Koeneman, K.; Yu, J.; Mason, R.P. *Magn. Reson. Med.* **2004**,*51*,616

8 Yu, J.; Ma, Z.; Li, Y.; Koeneman, K.S.; Liu, L.; Mason, R.P. *Med. Chem* **2005**, in the press

9 Yu, J.; Otten, P.; Ma, Z.; Cui, W.; Liu, L.; Mason, R.P. *Bioconj. Chem.* **2004**,*15*,1334

10 Yu, J.; Kodibagkar, V.; Cui, W.; Mason, R.P. *Curr. Med. Chem.* **2005**,*12*,818

11 Hunjan, S.; Mason, R.P.; Mehta, V.D.; Kulkarni, P.V.; Aravind, S.; Arora, V.; Antich, P.P. *Magn. Reson. Med.* **1998**,*39*,551

12 Mason, R.P. *Curr. Med. Chem.* **1999**,*6*,481

13 Cui, C.; Ma, Z.; He, S.; Peschke, P.; Mason, R.P., The Eighth International Conference on Tumor Microenvironment and Its Impact on Cancer Therapies, Miami (South Beach), Fl, 2003, p. II.

14 Sinnott, M.L. *Chem. Rev* **1990**,***90***,1171

15 Rye, C.S.; Withers, S.G. *Curr. Opinion Chem. Biology* **2000**,*4*,573

16 Pauling, L., *The nature of the chemical bond*, Cornell University, Ithaca, NY, **1980.**

17 McCarter, J.D.; Adam, M.J.; G., W.S. *Biochem. J.* **1992**,***286***,721

18 Street, I.P.; Armstrong, C.R.; Withers, S.G. *Biochemistry* **1986**,*25*,6021

19 Withers, S.G. *Can. J. Chem.* **1999**,*77*,1

20 Thoden, J.B.; Hegeman, A.D.; Wesenberg, G.; Chapeau, M.C.; Frey, P.A.; Holden, H.M. *Biochemistry* **1997**,***36***,6294

21 He, S.; Mason, R.P.; Hunjan, S.; Mehta, V.D.; Arora, V.; Katipally, R.; Kulkarni, P.V.; Antich, P.P. *Bioorg. Med. Chem.* **1998**,*6*,1631

Submitted Bioorg. Med. Chem. 2005

Synthesis and Evaluation of Novel Enhanced Gene Reporter Molecules: Detection of β-Galactosidase Activity Using ^{19}F NMR of Trifluoromethylated Aryl β-D-Galactopyranosides

Jianxin Yu, Li Liu, Weina Cui, Ralph P. Mason*

Department of Radiology, The University of Texas Southwestern Medical Center at Dallas, Dallas, TX

Running Title: Detection of β-galactosidase activity using ^{19}F NMR

Keywords: β-galactosidase, ^{19}F NMR, signal enhancement, *in vivo lacZ* gene reporter

* **Author for correspondence.**

Ralph P. Mason, Ph.D., CSci., CChem.

Department of Radiology

The University of Texas Southwestern Medical Center at Dallas

5323 Harry Hines Blvd

Dallas, Texas 75390-9058

USA

Tel: (214)-648-8926, Fax: (214)-648-4538

E-mail: Ralph.Mason@UTSouthwestern.edu

Abstract

Gene therapy has emerged as a promising strategy for treatment of various diseases, but there is a pressing need for the development of non-invasive reporter techniques based on appropriate molecules and imaging modalities to assay gene expression. We now report the design, synthesis, and evaluation of novel enhanced reporter molecules, which reveal *lacZ* gene transfection: trifluoromethylated aryl β-D-galactopyranosides. A series of five molecular structures was screened in solution and with stably transfected *lacZ* expressing human MCF-7 breast cancer cells *in vitro*. *p*-trifluoromethyl-*o*-nitrophenyl β-D-galactopyranoside (**PCF_3ONPG**) was found to exhibit valuable properties including a single ^{19}F NMR signal, stability in aqueous solution and with wild type cells, but a chemical shift response to enzyme cleavage ($\Delta\delta$=1.14 ppm) in breast cancer cells transfected to stably express *lacZ*.

Introduction

Strategies for identifying exogenous gene activity have been presented using radionuclide imaging [1, 2], optical imaging [3, 4], and NMR [5, 6]. In some cases natural substrates are used such as detection of fluorescent molecules or bioluminescence, but in other cases exogenous substrates have been designed to probe enzyme (*viz.* gene) activity with greatest emphasis on thymidine kinase to date. Recently, attention has turned to β-galactosidase (β-gal), the product of the lacZ gene, which have been the mainstay of molecular biology, since its characterization some 50 years ago [7]. Diverse colorimetric substrates have been developed suitable for histology [8, 9]. Tung *et al.* [10] reported a near infrared active substrate and Louie *et al.* [11] presented a proton MRI contrast agent. We have demonstrated the feasibility of using ^{19}F NMR to detect chemical shift changes accompanying enzyme induced cleavage of fluorogalactopyranosides [12-15]. We now report the synthesis of a series of trifluoromethyl (CF_3) aryl β-D-galactopyranosides designed to provide enhanced signal. We report synthesis, relevant characteristics as β-gal substrates and evaluation of their use to detect lacZ gene expression in breast cancer cells. Relative merits are compared with previous substrates.

Results and Discussion

Design and Synthesis

β-*galactosidase* (β-gal) catalyses the hydrolysis of galactopyranosides by cleavage of the C-O bond between D-galactose and the aglycone [16]. However, the enzyme shows remarkably broad substrate specificity and it appeared that introduction

of a CF_3 reporter group, in place of the fluorine atom, which we had exploited previously, could yield effective substrates with enhanced signal to noise.

Following the successful high yield phase-transfer catalysis approach to the stereoselective syntheses of fluorinated aryl β-D-galactopyranosides [13, 14] this versatile synthetic method was chosen for preparation of the target compounds **9~18** starting with commercially available trifluoromethylphenolic aglycones **2~8** (Fig. 1). The aglycones **2~8** reacted at 50 °C with 2,3,4,6-tetra-O-acetyl-α-D-galactopyranosyl bromide (**1**) in a dichloromethane-aqueous biphasic system (pH 8~9) using tetrabutylammonium bromide (TBAB) as the phase-transfer catalyst, affording trifluoromethyl aryl β-D-galactopyranoside tetraacetates **9~12** in near quantitative yield. However, **13** was obtained in poor yield (20%) and two of the trifluoromethyl phenols (3-trifluoromethylphenol **7** and 4-trifluoromethylphenol **8**) proved to be unreactive. To our knowledge molecules **9-18** are new, though we note that an isomer 4-nitro-2-(trifluoromethyl)phenyl β-D galactopyranoside has been reported previously in a patent related to CEDIA (cloned enzyme donor immunoassay) [17]. That work did not appear to exploit the ^{19}F NMR properties, but rather colorimetric changes accompanying b-gal induced cleavage. They reported a very poor yield using an alternate synthetic approach, though it may be characteristic of *o*-CF_3 groups since this was least successful in our hands.

The anomeric β-D-configuration of compounds **9~13** in the $^4C_1$ chair conformation was unambiguously established on the basis of the observed ^1H-NMR chemical shifts (δ_H 4.98~5.25ppm) of the anomeric protons and the $J_{1,2}$ (J ~8Hz) and $J_{2,3}$ (J ~10Hz) coupling constants. The signals of the ^{13}C-NMR spectra of **9~13** were

assigned by comparison with the chemical shifts of *p*-nitrophenyl β-D-galactopyranosides [14, 18]. As expected, the anomeric carbon resonances appeared at 98~101 ppm in accord with the β-D-configuration.

Deacetylation of **9~13** with NH_3/MeOH from 0°C to room temperature gave the free galactopyranosides **14~18** in quantitative yield. The signals of the ^{1}H-NMR spectra of **14~18** were assigned by ^{1}H-^{1}H COSY spectra and D_2O exchange. The ^{1}H-NMR chemical shifts (δ_H 5.00~5.15ppm) of the anomeric protons and the $J_{1,2}$ (J ~8Hz) and $J_{2,3}$ (J 9~11Hz) coupling constants showed that the free galactopyranosides **14~18** retained the anomeric β-D-configuration with the $^4C_1$ chair conformation.

^{19}F NMR

^{19}F NMR spectra of the trifluoromethylphenyl β-D-galactopyranosides **14~18** were recorded in aqueous solutions with sodium trifluoroacetate (NaTFA) as an external standard chemical shift standard. **14~18** each gave a single narrow ^{19}F NMR signal between δ 12~16 ppm essentially invariant ($\Delta\delta \leq 0.02$ppm) with pH in the range 3 to 12 and temperatures from 25 to 37 °C in whole rabbit blood, 0.9% saline, or PBS. Addition of β-gal (G-2513) to **14~17** in PBS buffer (0.1M, pH=7.4) at 37 °C led to rapid hydrolysis releasing the aglycones **2~5**, which appeared as single narrow ^{19}F signals shifted downfield. **18** was cleaved comparatively slowly. The relative efficacy of **14** and our previously reported OFPNPG as β-gal substrate is shown in **Figure 2**. As expected, **14** provides about 3 times more signal, while cleavage rates are similar. Comparison of β-gal hydrolytic kinetics of **14~18** showed that each proceeded monotonically indicating straightforward first-order kinetics for all substrates and that the liberated aglycones **2~6** did not inhibit the β-gal. The substrates **14~17** exhibited rates in excess of 33

μmol/min/unit exceeding those of *p*-fluoro-*o*-nitrophenyl β-D-galactopyranoside (**PFONPG;** 19 μmol/min/unit), *o*-fluoro-*p*-nitrophenyl β-D-galactopyranoside (**OFPNPG;** 32 μmol/min/unit) and even *o*-nitrophenyl β-D-galactopyranoside (**ONPG;** 32 μmol/min/unit), which we have reported previously [12, 14]. The low rate hydrolysis of **18** may be due to the formation of an intramolecular F···H hydrogen bond between 2-CF_3 and C_1-H or steric effects, which play an important role in the affection of the hydrolytic process [19].

As expected, trifluoromethylphenyl β-D-galactopyranosides showed enhanced ^{19}F signal intensity on a molar basis compared with analogous fluorophenyl β-D-galactopyranosides, but the ^{19}F chemical shift changes were much smaller (Fig. 2, Table 1). The chemical shift ($\Delta\delta$ 1.4 ppm) accompanying cleavage of **14** is sufficient for investigations *in vivo*, but the other substrates **15-18** give smaller values, which may be insufficient for effective studies. The aglycone *p*-trifluoromethyl-*o*-nitrophenyl (**2**, **PCF_3ONP**) also exhibits a ^{19}F NMR chemical shift in response to pH ($\Delta\delta$=~1.00 ppm) in the range of pH 4~7 (Fig. 4), but importantly they do not overlap the chemical shift of the substrate **14** (**PCF_3ONPG**).

***In Vitro* Evaluation**

CF_3- groups are often associated with increased lipophilicity. As expected, **PCF_3ONPG** has comparatively lower aqueous solubility than either **OFPNPG** or **PFONPG**. However, the higher ^{19}F signal intensity and sensitivity to β-gal allow use of lower concentrations of **PCF_3ONPG**, potentially circumventing issues of toxicity. **PCF_3ONPG** was stable in aqueous solution in the pH range 3 to 12 at temperatures from 25 to 37°C over 5 days. Toxicity was evaluated for both aglycone **PCF_3ONP** and

conjugate **PCF_3ONPG** using both wild-type and *lacZ* expressing human MCF-7 breast cancer cells. Cell viability assays [20] showed that the aglycone **PCF_3ONP** exhibited significant cytotoxicity even at 100 μM with both cell clones (Fig. 5). No toxicity was observed up to 1 mM for **14** over 96 h for wild type cells, but some toxicity was found with the *lacZ* expressing cells, presumably due to liberation of the aglycone. When **PCF_3ONPG** was incubated with MCF-7-WT cells for 5 h in PBS buffer at 37 °C under 5% CO_2 in air with 95% humidity, no changes were observed in the ^{19}F NMR spectra. However, addition of **14** to cells stably transfected to express β-gal led to cleavage in a smooth monotonic manner releasing the aglycone **2** (40.0 μmol/min per million MCF-7-*lacZ* cells, Fig. 6).

Conclusion

The phase transfer approach to synthesizing phenyl galactosides developed previously [14] was also appropriate for several of the trifluoromethyl galactosides. The substrates are stable in aqueous solution and with wild type cancer cells, but the CF_3 agents are responsive to β-gal activity with rates exceeding those of the fluorophenyl analogs. Signal to noise is enhanced and although the ^{19}F NMR chemical shift response to enzyme cleavage is smaller, it is adequate for detecting hydrolysis with **PCF_3ONPG**. Overall, the trifluoromethyl galactosides show promise as reporter molecules for β-gal activity and we are initiating investigations of *lacZ* expressing tumors in animals.

Experimental

General methods --- NMR spectra were recorded on a Varian MERCURY 400 spectrometer (400 MHz for ^1H, 100 MHz for ^{13}C, 376 MHz for ^{19}F) with $CDCl_3$, or DMSO-d_6 as solvents. ^1H and ^{13}C chemical shifts are referenced to TMS as internal

standard and ^{19}F to dil. sodium trifluoroacetate (NaTFA) in a capillary as external standard. All compounds were characterized by acquisition of ^{1}H, ^{13}C, DEPT, ^{1}H-^{1}H COSY experiments at 25 °C, ^{19}F spectra were performed at 37 °C. Microanalyses were performed on a Perkin-Elmer 2400CHN microanalyser. Solutions in organic solvents were dried with anhydrous sodium sulfate, and concentrated *in vacuo* below 45 °C. Column chromatography was performed on silica gel (200~300mesh) by elution with cyclohexane-EtOAc and silica gel GF_{254} (Aldrich) was used for analytical TLC. Detection was effected by spraying the plates with 5% ethanolic H_2SO_4 (followed by heating at 110°C for 10 min.) or by direct UV illumination of the plate.

For enzyme kinetic experiments, **PCF_3ONPG** (2.2 mg, 6 mmol) was dissolved in PBS (0.1M, pH=7.4, 573 μL) and a PBS solution of β-gal (27 μL, G-2513 (Aldrich Chemical Company) 0.22 unit/μL) was added and NMR data were acquired immediately at 37°C.

Human MCF-7 breast cancer cells were stably co-transfected with pCMVβ (Clontech, Palo Alto, CA, USA), using TransFast™ Transfection Reagent (Promega, Madison, WI, USA) comprising the *E.coli lacZ* gene located under the human cytomegalovirus (CMV) immediate-early enhancer/promoter region and pCI-neo (Promega, Madison, WI, USA) carrying the neomycin phosphotransferase gene. For MCF-7 cells, clonal selection was applied to identify those cells with highest β-gal expression. Control (wild type) and transfected (*lacZ*) cells were grown in culture dishes under standard conditions and harvested. **PCF_3ONPG** (2.2 mg) in PBS (70 μL) was added to suspension of 10^6 cells in PBS buffer (530 μL) and ^{19}F NMR spectra were acquired immediately, and again after incubation for various times up to 5 h at 37°C.

The sensitivities of MCF-7 WT and *lacZ* cells to **PCF_3ONPG** and **PCF_3ONP** were quantified using a colorimetric CellTiter 96 Aqueous Nonradioactive MTS Cell Proliferation Assay (Promega, Madison, WI, USA). Assays were performed in triplicate using 24-well plates seeded with 10^3 cells per well in 500 μL RPMI 1640 without phenol red and supplemented with 10% FCS and 2 mM glutamine. After 24 h incubation, the medium was replaced with fresh RPMI 1640 containing various concentrations (0~0.1 mM) of **PCF_3ONPG** or **PCF_3ONP** were incubated for 48 or 96 h, followed by the MTS assay.

Trifluoromethylphenyl β-D-galactopyranoside tetraacetates 9~13. ***General procedure*** --- A solution of 2,3,4,6-tetra-O-acetyl-α-D-galactopyranosyl bromide (Sigma) (**1**) (1mmol) and tetrabutyl-ammonium bromide (0.48g, 1.5mmol) in CH_2Cl_2 (5mL) was vigorously stirred at 50°C with the solution of fluorophenols (**2~8**) (1.2mmol) in H_2O (5 mL; pH 8~9) until TLC showed complete reaction (~1 h). The organic layer was separated, washed, dried (Na_2SO_4), evaporated under reduced pressure to give a syrup, which was purified by column chromatography on silica gel to give trifluoromethylphenyl β-D-galactopyranoside tetraacetates **9~13**.

2-Nitro-4-trifluoromethylphenyl 2,3,4,6-tetra-O-acetyl-β-D-galactopyranoside **9** (0.54g, 99%) as white crystals, R_f 0.38 (3:2 cyclohexane-EtOAc), δ_H: 8.07(1H, d, *J*=2.0Hz, Ar-H), 7.79(1H, dd, *J*=1.6, 7.2Hz, Ar-H), 7.48(1H, d, *J*=8.8Hz, Ar-H), 5.17(1H, d, $J_{1,2}$=7.6Hz, H-1), 5.57(1H, dd, $J_{2,3}$=10.4Hz, H-2), 5.12(1H, dd, $J_{3,4}$=3.2Hz, H-3), 5.48(1H, d, $J_{4,5}$=3.2Hz, H-4), 4.13(1H, m, H-5), 4.24(1H, dd, $J_{5,6a}$=4.4Hz, $J_{6a,6b}$=11.2Hz, H-6a), 4.18(1H, dd, $J_{5,6b}$=5.6Hz, H-6b), 2.19, 2.15, 2.10, 2.01(12H, 4s, 4×CH_3CO)ppm; δ $_C$: 170.49, 170.31, 169.45 (4×CH_3**C**O), 151.87(Ar-C), 140.96(Ar-C), 130.74(, J_{F-}

$_C$=3.9Hz), 123.10(d, J_{F-C}=3.9Hz, Ar-C), 119.59 (Ar-C), 90.83(Ar-C), 126.32(q, J_{F-C}=275.5 Hz, CF_3), 100.46(C-1), 67.80(C-2), 70.55(C-3), 66.79(C-4), 71.89(C-5), 61.55(C-6), 20.84, 20.80, 20.78, 20.73(4×**C**H_3CO)ppm.

Anal. Calcd. for $C_{21}H_{22}NO_{12}F_3$(%): C, 46.92, H, 4.13, N, 2.61; Found: C, 46.90, H, 4.10, N, 2.58.

3-Trifluoromethyl-4-nitrophenyl 2,3,4,6-tetra-O-acetyl-β-D-galactopyranoside **10** (0.54g, 99%) as syrup, R_f 0.36 (3:2 cyclohexane-EtOAc), δ_H: 7.98(1H, d, J=8.8Hz, Ar-H), 7.44(1H, s, Ar-H), 7.28(1H, d, J=9.2Hz, Ar-H), 5.25(1H, d, $J_{1,2}$=8.0Hz, H-1), 5.57(1H, dd, $J_{2,3}$=10Hz, H-2), 5.17(1H, dd, $J_{3,4}$=2.8Hz, H-3), 5.50(1H, d, $J_{4,5}$=3.2Hz, H-4), 4.15(1H, m, H-5), 4.18(2H, m, H-6), 2.20, 2.09, 2.07, 2.03(12H, 4s, 4×CH_3CO)ppm; δ_C: 170.61, 170.26, 170.16, 169.45(4× CH_3**C**O), 159.31(Ar-C), 142.91(Ar-C), 127.91(Ar-C), 120.07(Ar-C), 116.15(d, J_{F-C}=6.1Hz, Ar-C), 126.18(q, J_{F-C}=274.4 Hz, CF_3), 98.70(C-1), 68.30(C-2), 70.65(C-3), 67.01(C-4), 71.99(C-5), 61.95(C-6), 20.82, 20.79, 20.71, 20.67 (4×**C**H_3CO)ppm.

Anal. Calcd. for $C_{21}H_{22}NO_{12}F_3$(%): C, 46.92, H, 4.13, N, 2.61; Found: C, 46.89, H, 4.11, N, 2.60.

2-Chloro-3-trifluoromethylphenyl 2,3,4,6-tetra-O-acetyl-β-D-galactopyranoside **11** (0.50g, 95%) as syrup, R_f 0.61 (3:2 cyclohexane-EtOAc), δ_H: 7.46(1H, dd, J=1.2, 6.6Hz, Ar-H), 7.40(1H, d, J=8.4Hz, Ar-H), 7.32(1H, dd, J=7.8, 8.4Hz, Ar-H), 4.98(1H, d, $J_{1,2}$=8.4Hz, H-1), 5.59(1H, dd, $J_{2,3}$=10.5Hz, H-2), 5.11(1H, dd, $J_{3,4}$=3.6Hz, H-3), 5.48(1H, d, $J_{4,5}$=3.6Hz, H-4), 4.06(1H, m, H-5), 4.25(1H, dd, $J_{5,6a}$=6.6Hz, $J_{6a,6b}$=11.7Hz, H-6a), 4.16(1H, dd, $J_{5,6b}$=6.0Hz, H-6b), 2.20, 2.10, 2.06, 2.02(12H, 4s, 4×CH_3CO)ppm; δ_C: 170.45, 170.42, 170.34, 169.42(4× CH_3**C**O), 153.81(Ar-C), 130.31(Ar-C), 127.41(Ar-C),

123.48(d, J_{F-C}=14.8Hz, Ar-C), 122.35(Ar-C), 122.01(Ar-C), 121.79(Ar-C), 130.55(q, J_{F-C}=157.6Hz, CF_3), 100.83(C-1), 68.28(C-2), 70.69(C-3), 66.87(C-4), 71.47(C-5), 61.42 (C-6), 20.92, 20.77, 20.70(4×**C**H_3CO)ppm.

Anal. Calcd. for $C_{21}H_{22}O_{10}ClF_3$(%): C, 47.90, H, 4.22; Found: C, 47.89, H, 4.20.

2-Chloro-5-trifluoromethylphenyl 2,3,4,6-tetra-O-acetyl-β-D-galactopyranoside **12** (0.51g, 96%) as white crystals, R_f 0.56 (3:2 cyclohexane-EtOAc), δ_H: 7.51(1H, s, Ar-H), 7.49(1H, dd, *J*=1.8, 3.6Hz, Ar-H), 7.30(1H, dd, *J*=1.2, 7.8Hz, Ar-H), 5.02(1H, d, $J_{1,2}$=8.4Hz, H-1), 5.60(1H, dd, $J_{2,3}$=10.2Hz, H-2), 5.12(1H, dd, $J_{3,4}$=3.6Hz, H-3), 5.48(1H, d, $J_{4,5}$=3.6Hz, H-4), 4.12(1H, m, H-5), 4.22(1H, dd, $J_{5,6a}$=4.2Hz, $J_{6a,6b}$=11.4Hz, H-6a), 4.17(1H, dd, $J_{5,6b}$=7.8Hz, H-6b), 2.20, 2.10, 2.07, 2.02(12H, 4s, 4×CH_3CO)ppm; δ_C: 170.70, 170.27, 170.17, 169.40(4×CH_3**C**O), 152.97(d, J_{F-C}=1.5Hz, Ar-C), 131.03(Ar-C), 128.37(Ar-C), 122.59(Ar-C), 121.06(Ar-C), 115.13 (Ar-C), 130.34(q, J_{F-C}=158.9Hz, CF_3), 100.65(C-1), 68.13(C-2), 70.62(C-3), 67.21(C-4), 71.95 (C-5), 62.31(C-6), 20.89, 20.73, 20.50(4×**C**H_3CO)ppm.

Anal. Calcd. for $C_{21}H_{22}O_{10}ClF_3$(%): C, 47.90, H, 4.22; Found: C, 47.88, H, 4.21.

2-Trifluoromethylphenyl 2,3,4,6-tetra-O-acetyl-β-D-galactopyranoside **13** (0.30g, 20%) as white crystals, R_f 0.54 (3:2 cyclohexane-EtOAc), δ_H: 7.60(1H, dd, *J*=1.2, 7.8Hz, Ar-H), 7.50(1H, m, Ar-H), 7.27(1H, dd, *J*=1.8, 6.6Hz, Ar-H), 7.16(1H, dd, *J*=7.8Hz, Ar-H), 5.06(1H, d, $J_{1,2}$=8.4Hz, H-1), 5.58(1H, dd, $J_{2,3}$=10.5Hz, H-2), 5.12(1H, dd, $J_{3,4}$=3.6Hz, H-3), 5.47(1H, dd, $J_{4,5}$=0.6Hz, H-4), 4.11(1H, m, H-5), 4.27(1H, dd, $J_{5,6a}$=6.0Hz, $J_{6a,6b}$=11.4Hz, H-6a), 4.17(1H, dd, $J_{5,6b}$=6.0Hz, H-6b), 2.20, 2.08, 2.05, 2.01(12H, 4s, 4×CH_3CO)ppm; δ_C: 170.26, 170.20, 170.05, 169.10(4×CH_3**C**O), 154.59(Ar-C), 133.27(Ar-C), 127.03(Ar-C), 122.80(Ar-C), 116.69 (Ar-C), 120.10(q, J_{F-C}

=123.6Hz, CF_3), 99.79(C-1), 67.85(C-2), 70.73(C-3), 66.76(C-4), 71.20 (C-5), 61.40(C-6), 20.59, 20.36(4×**C**H_3CO)ppm.

Anal. Calcd. for $C_{21}H_{23}O_{10}F_3$(%): C, 51.21, H, 4.71; Found: C, 51.19, H, 4.69.

Trifluoromethylphenyl β-D-galactopyranosides 14~18. *General procedure* ---- A solution of trifluoromethylphenyl 2,3,4,6-tetra-O-acetyl-β-D-galactopyranoside (**9~13**)(0.4g) in anhydrous MeOH (15mL) containing 0.5M NH_3 was vigorously stirred from 0°C to room temperature overnight until TLC showed complete reaction and evaporated to dryness *in vacuo*. Chromatography of the crude syrup on silica gel with EtOAc-MeOH afforded the free β-D-galactopyranosides **14~18** in quantitative yield.

2-Nitro-4-trifluoromethylphenyl β-D-galactopyranoside **14** as white crystals, R_f 0.35 (1:9 MeOH-EtOAc, δ_H: 8.28(1H, d, *J*=2.0Hz, Ar-H), 7.99(1H, dd, *J*=2.0, 9.2Hz, Ar-H), 7.59(1H, d, *J*=8.8Hz, Ar-H), 5.15(1H, d, $J_{1,2}$=7.6Hz, H-1), 3.55(1H, dd, $J_{2,3}$=8.9Hz, H-2), 3.50(1H, dd, $J_{3,4}$=6.0Hz, H-3), 3.47(1H, d, $J_{4,5}$=6.0Hz, H-4), 3.42(1H, m, H-5), 3.67(1H, m, H-6), 5.24(1H, d, $J_{H\text{-}2,OH\text{-}2}$=4.8Hz, HO-2), 4.63(1H, d, $J_{H\text{-}3,OH\text{-}3}$=4.4Hz, HO-3), 4.92(1H, d, $J_{H\text{-}4,OH\text{-}4}$=6.0Hz, HO-4), 4.69(1H, t, $J_{H\text{-}6,OH\text{-}6}$=5.4, 5.6Hz, HO-6)ppm; δ_C: 152.18(Ar-C), 139.97(Ar-C), 130.82(d, $J_{F\text{-}C}$= 3.9Hz, Ar-C), 124.68(Ar-C), 122.42(Ar-C), 117.91(Ar-C), 122.22(q, $J_{F\text{-}C}$=52.7Hz, CF_3), 100.95 (C-1), 69.97(C-2), 73.29(C-3), 68.03(C-4), 76.04(C-5), 60.30(C-6)ppm.

Anal. Calcd. for $C_{13}H_{14}NO_8F_3$(%): C, 42.27, H, 3.82, N, 3.79; Found: C, 42.25, H, 3.80, N, 3.77.

3-trifluoromethyl-4-nitrophenyl β-D-galactopyranoside **15** as white crystals, R_f 0.40 (1:9 MeOH-EtOAc), δ_H: 8.16(1H, d, *J*=8.8Hz, Ar-H), 7.53(1H, d, *J*=2.8Hz, Ar-H), 7.49(1H, dd, *J*=2.8, 8.8Hz, Ar-H), 5.08(1H, d, $J_{1,2}$=7.6Hz, H-1), 3.53(1H, dd,

$J_{2,3}$=10.0Hz, H-2), 3.49(1H, dd, $J_{3,4}$=5.2Hz, H-3), 3.44(1H, d, $J_{4,5}$=2.4Hz, H-4), 3.61(1H, m, H-5), 3.68(2H, m, H-6), 5.33(1H, d, $J_{H\text{-}2,OH\text{-}2}$=4.8Hz, HO-2), 4.60(1H, d, $J_{H\text{-}3,OH\text{-}3}$=4.8Hz, HO-3), 4.96(1H, d, $J_{H\text{-}4,OH\text{-}4}$=5.6Hz, HO-4), 4.70(1H, t, $J_{H\text{-}6,OH\text{-}6}$=5.2, 5.4Hz, HO-6)ppm; δ_C: 171.73(Ar-C), 160.45(Ar-C), 141.10(Ar-C), 128.48(Ar-C), 120.45(d, $J_{F\text{-}C}$=26.7Hz, Ar-C), 115.95(d, $J_{F\text{-}C}$=11.5Hz, Ar-C), 123.84(q, $J_{F\text{-}C}$= 32.8Hz, CF_3), 100.95(C-1), 70.09(C-2), 73.11(C-3), 68.12(C-4), 75.99(C-5), 60.36(C-6)ppm.

Anal. Calcd. for $C_{13}H_{14}NO_8F_3$(%): C, 42.27, H, 3.82, N, 3.79; Found: C, 42.26, H, 3.79, N, 3.78.

2-Chloro-3-trifluoromethylphenyl β-D-galactopyranoside **16** as white crystals, R_f 0.48 (1:9 MeOH-EtOAc), δ_H: 8.28(1H, d, *J*=2.0Hz, Ar-H), 7.99(1H, dd, *J*=2.0, 9.2Hz, Ar-H), 7.59(1H, d, *J*=8.8Hz, Ar-H), 5.15(1H, d, $J_{1,2}$=7.6Hz, H-1), 3.55(1H, dd, $J_{2,3}$=8.9Hz, H-2), 3.50(1H, dd, $J_{3,4}$=6.0Hz, H-3), 3.47(1H, d, $J_{4,5}$=6.0Hz, H-4), 3.42(1H, m, H-5), 3.67(2H, m, H-6), 5.24(1H, d, $J_{H\text{-}2,OH\text{-}2}$=4.8Hz, HO-2), 4.63(1H, d, $J_{H\text{-}3,OH\text{-}3}$=4.4Hz, HO-3), 4.92(1H, d, $J_{H\text{-}4,OH\text{-}4}$=6.0Hz, HO-4), 4.69(1H, t, $J_{H\text{-}6,OH\text{-}6}$=5.4, 5.6Hz, HO-6)ppm; δ_C: 152.18(Ar-C), 139.97(Ar-C), 130.82(d, $J_{F\text{-}C}$= 3.9Hz, Ar-C), 124.68(Ar-C), 122.42(Ar-C), 117.91(Ar-C), 122.22(q, $J_{F\text{-}C}$=52.7Hz, CF_3), 100.95 (C-1), 69.97(C-2), 73.29(C-3), 68.03(C-4), 76.04(C-5), 60.30(C-6)ppm.

Anal. Calcd. for $C_{13}H_{14}ClO_6F_3$(%): C, 43.57, H, 3.94; Found: C, 43.55, H, 3.91.

2-Chloro-5-trifluoromethylphenyl β-D-galactopyranoside **17** as white crystals, R_f 0.50 (1:9 MeOH-EtOAc), δ_H: 7.69(1H, d, *J*=8.0Hz, Ar-H), 7.55(1H, d, *J*=0.6 Hz, Ar-H), 7.59(1H, dd, *J*=2,1, 8.8Hz, Ar-H), 5.11(1H, d, $J_{1,2}$=8.4Hz, H-1), 3.53(1H, dd, $J_{2,3}$=10.2Hz, H-2), 3.48(1H, dd, $J_{3,4}$=5.2Hz, H-3), 3.48(1H, d, $J_{4,5}$=6.4Hz, H-4), 3.44(1H, m, H-5), 3.69(2H, m, H-6), 5.20(1H, d, $J_{H\text{-}2,OH\text{-}2}$=3.6Hz, HO-2), 4.58(1H, d, $J_{H\text{-}3,OH\text{-}}$

$_3$=2.8Hz, HO-3), 4.91(1H, d, $J_{H\text{-}4,OH\text{-}4}$=3.6Hz, HO-4), 4.65(1H, t, $J_{H\text{-}6,OH\text{-}6}$=5.0, 6.0Hz, HO-6)ppm; δ_C: 153.01(Ar-C), 130.97(d, $J_{F\text{-}C}$=13.9Hz, Ar-C), 130.82(Ar-C), 125.86(Ar-C), 123.24(Ar-C), 112.90(Ar-C), 123.45(q, $J_{F\text{-}C}$=58.8Hz, CF_3), 100.81 (C-1), 70.02(C-2), 73.31(C-3), 68.02(C-4), 75.73(C-5), 60.18(C-6)ppm.

Anal. Calcd. for $C_{13}H_{14}ClO_6F_3$(%): C, 43.57, H, 3.94; Found: C, 43.56, H, 3.93.

2-Trifluoromethylphenyl β-D-galactopyranoside **18** as white crystals, R_f 0.52 (1:9 MeOH-EtOAc), δ_H: 7.67(1H, m, Ar-H), 7.60(1H, dd, *J*=5.2, 5.6Hz, Ar-H), 7.33(1H, d, *J*=5.6Hz, Ar-H), 7.12(1H, dd, *J*=4.8, 5.2Hz, Ar-H), 5.00(1H, d, $J_{1,2}$=7.8Hz, H-1), 3.62(1H, dd, $J_{2,3}$=10.8Hz, H-2), 3.54(1H, dd, $J_{3,4}$=4.8Hz, H-3), 3.49(1H, dd, $J_{4,5}$=5.4, 6.0Hz, H-4), 3.40(1H, m, H-5), 3.70(2H, m, H-6), 4.97(1H, d, $J_{H\text{-}2,OH\text{-}2}$=6.0Hz, HO-2), 4.57(1H, d, $J_{H\text{-}3,OH\text{-}3}$=4.2Hz, HO-3), 4.91(1H, d, $J_{H\text{-}4,OH\text{-}4}$=6.0Hz, HO-4), 4.65(1H, t, $J_{H\text{-}6,OH\text{-}6}$=5.4, 6.5Hz, HO-6)ppm; δ_C: 155.60(Ar-C), 133.95(Ar-C), 126.48(Ar-C), 121.14 (Ar-C), 115.57(Ar-C), 122.08(q, $J_{F\text{-}C}$=125.7Hz, CF_3), 100.46(C-1), 70.13(C-2), 73.58(C-3), 68.04(C-4), 75.62(C-5), 60.30(C-6)ppm.

Anal. Calcd. for $C_{13}H_{15}O_6F_3$(%): C, 48.14, H, 4.67; Found: C, 48.12, H, 4.66.

Acknowledgements

Supported by grants from the DOD Breast Cancer Initiative IDEA award DAMD17-03-1-0343-01 and the Cancer Imaging Program, NIH P20 CA 86354 (pre-ICMIC). NMR experiments were conducted at the Mary Nell and Ralph B. Rogers NMR Center, an NIH BTRP facility #P41-RR02584. We are grateful to Dr. Vikram Kodibagkar for vaalube discussions.

Table 1.

^{19}F chemical shifts[+] and hydrolytic rates by β-gal[*]

No.	14	15	16	17	18
$\delta_{F\,(substrat}$	13.40	15.23	13.24	12.70	14.11
$\delta_{F\,(product}$	14.54	15.43	13.94	12.95	14.61
$\Delta\delta_F$	1.14	0.20	0.70	0.25	0.50
$v_{(\mu mol/min/u}$	33.0	52.8	39.6	46.2	2.61

[+]ppm with respect to aq. NaTFA

* β-gal (G-2513, 11 units) at 37°C in PBS buffer (0.1M, pH=7.4).

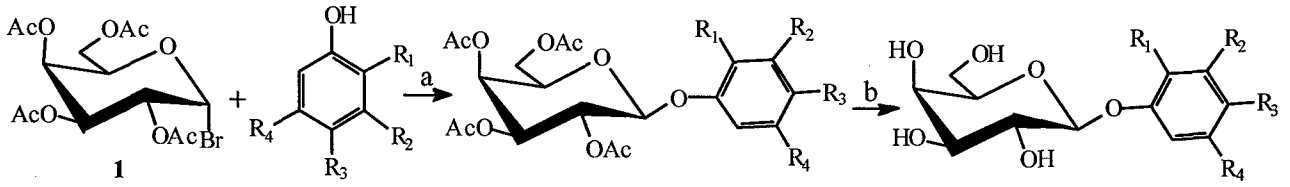

Reaction conditions: (a) CH_2Cl_2-H_2O, pH 8~9, 50 °C, TBAB, ~1 h, near quantitative yield except **13** in only 20% yield; (b) NH_3-MeOH, 0 °C→rt, 24 h, quantitative yields.

Compounds	R_1	R_2	R_3	R_4
2, 9, 14	NO_2	H	CF_3	H
3, 10, 15	H	CF_3	NO_2	H
4, 11, 16	Cl	CF_3	H	H
5, 12, 17	Cl	H	H	CF_3
6, 13, 18	CF_3	H	H	H
7	H	CF_3	H	H
8	H	H	CF_3	H

Figure 1. The reactions and the structures of **1~18**.

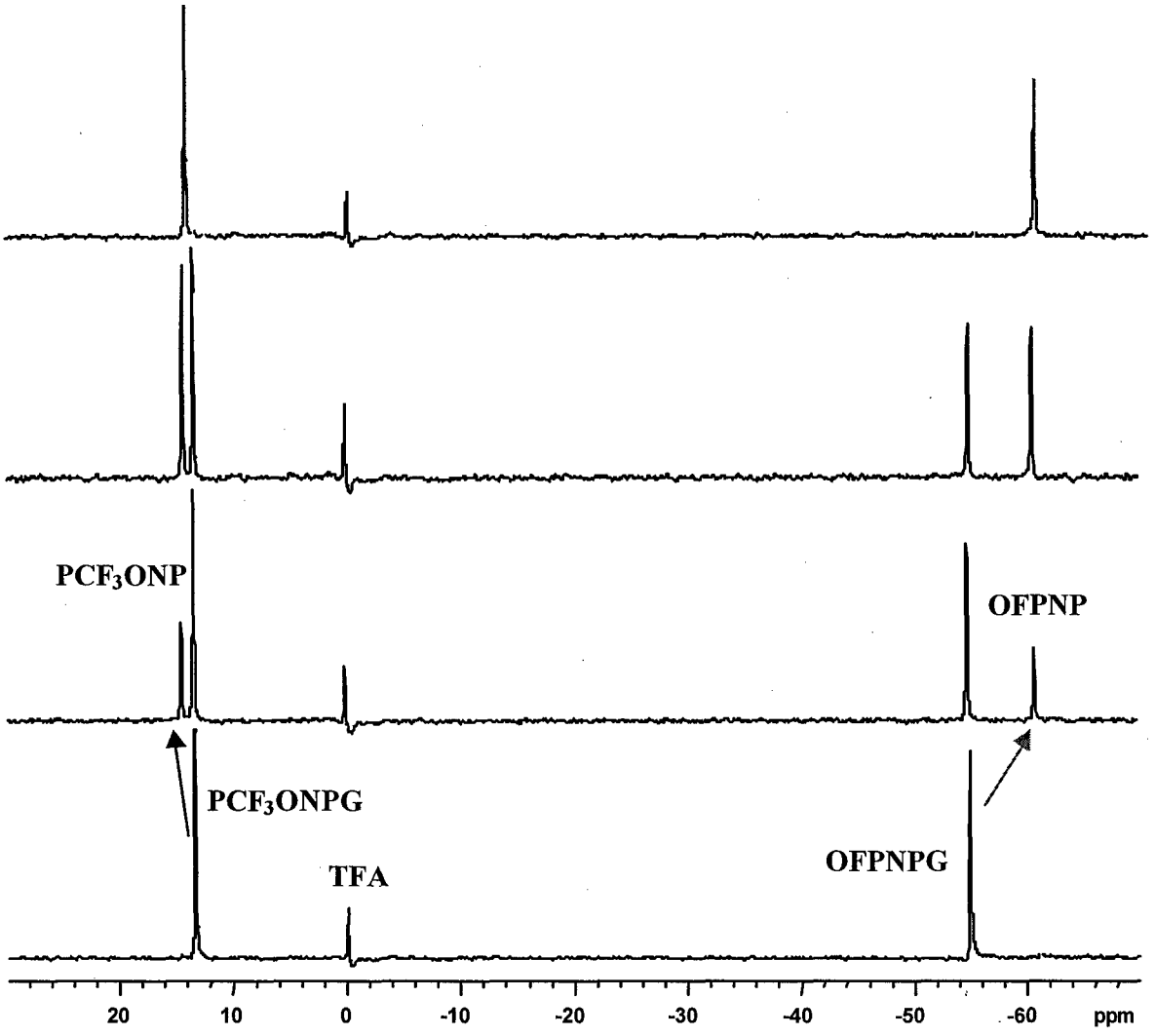

Figure 2. ^{19}F NMR spectra of **PCF_3ONPG** (1.1 mg, 3 mmol) and **OFPNPG** (2.87 mg, 9 mmol) with 1:3 molar ratios in the simultaneous hydrolysis by β-gal (11 units) in PBS (0.1M, pH=7.4, 600μL) at 37°C.

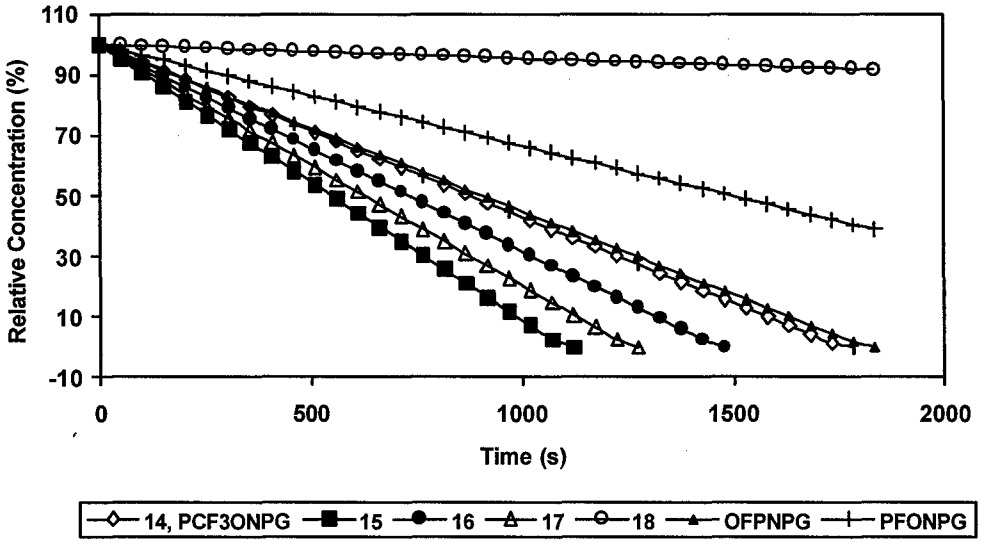

Figure 3. Relative hydrolysis time courses of **14~18** (6.0 mmol), **OFPNPG** and **PFONPG** (5.4 mmol) by β-gal (6 units) in PBS (0.1M, 600μL) at 37°C.

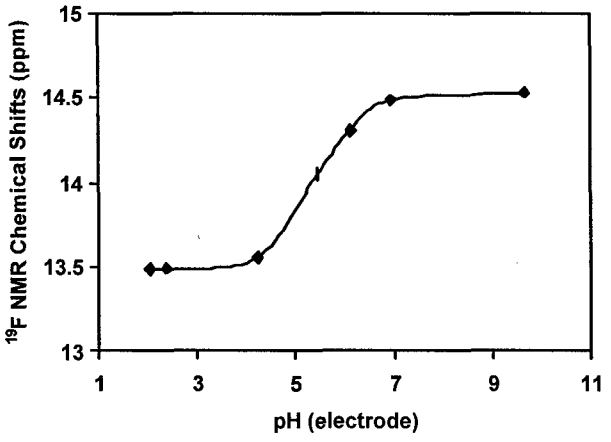

Figure 4. ^{19}F NMR chemical shift pH titration curve of **2** (**PCF_3ONP**) in saline at 37 °C.

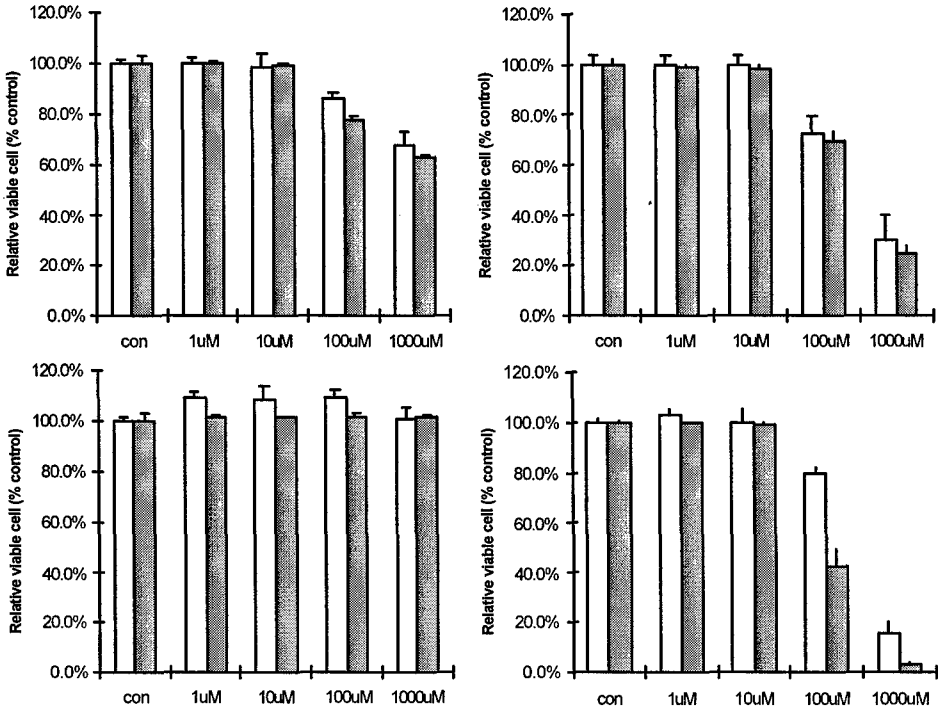

Figure 5. Cell viability of human breast cancer cells in PBS (pH=7.4) with respect to exposure to substrate **14** (left panels) or aglycone **2** (right panels). Upper panels MCF-7-lacZ cells; lower panels MCF-7-WT. Open bars 48 h exposure; hatched bars 96 h exposure.

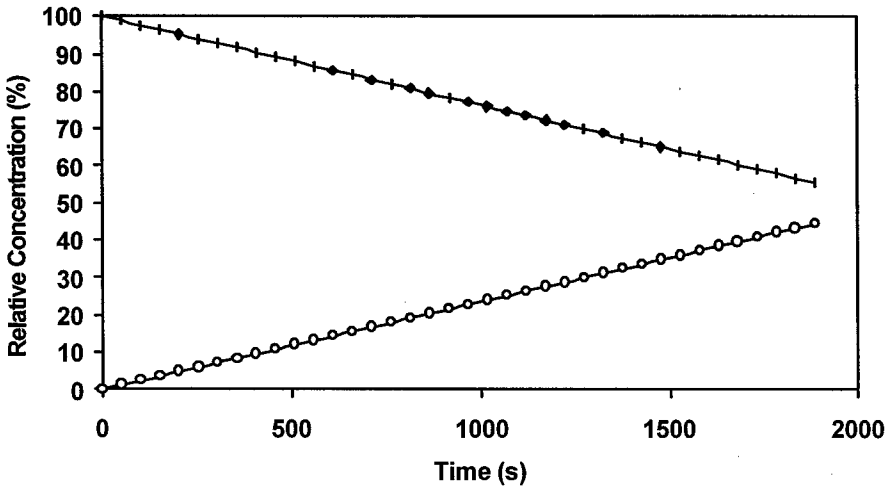

Figure 6. Hydrolysis of **14** (5.0 mmol) to **2** by stably transfected MCF-7-*lacZ* breast cancer cells (1.75×10^6) in PBS buffer at 37 °C.

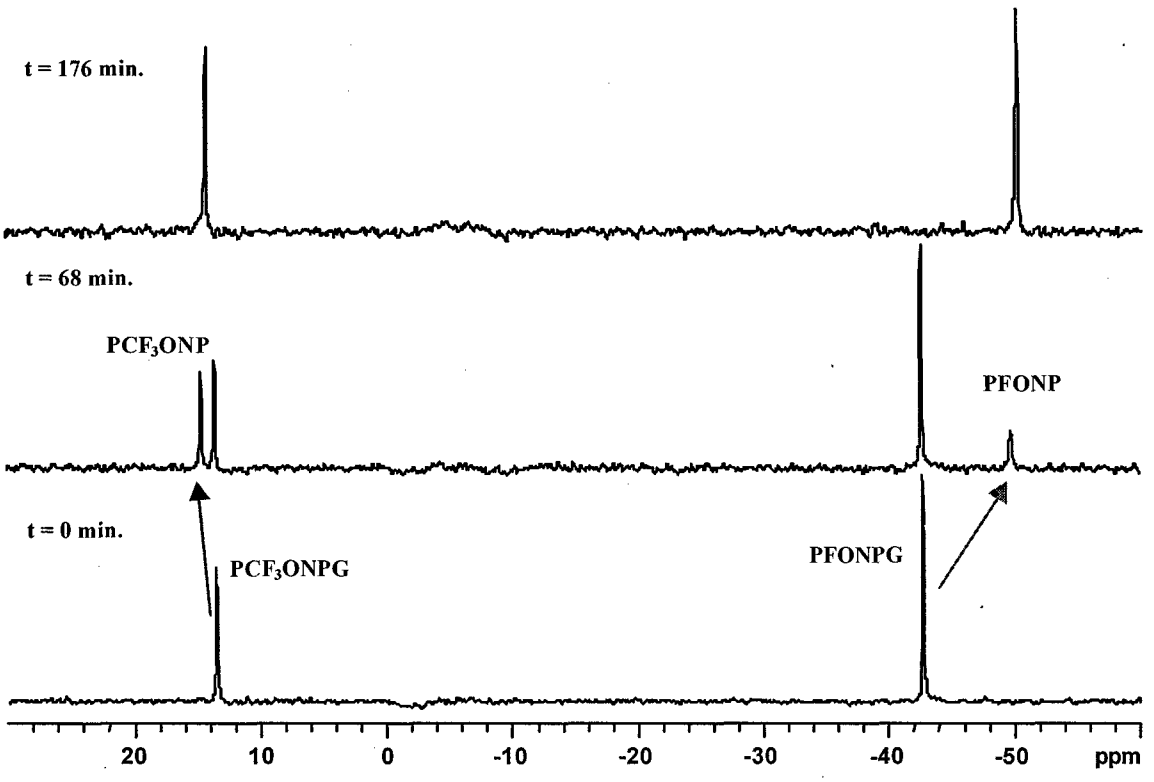

Figure 6. ^{19}F NMR spectra of **PCF_3ONPG** (1.4 mg, 4.5 mmol) and **PFONPG** (6.0 mg, 18.8 mmol) showing simultaneous hydrolysis by stably transfected MCF-7-*lacZ* cells (1.75×10^6) in PBS (0.1M, pH=7.4, 600μL) at 37°C. Each spectrum acquired in 51 s.

References:

1 Gambhir, S.S.; Herschman, H.R.; Cherry, S.R.; Barrio, J.R.; Satyamurthy, N.; Toyokuni, T.; Phelps, M.E.; Larson, S.M.; Balatoni, J.; Finn, R.; Sadelain, M.; Tjuvajev, J.; Blasberg, R. *Neoplasia (New York)* **2000**,118

2 Haberkorn, U.; Mier, W.; Eisenhut, M. *Curr. Med. Chem.* **2005**,*12*,779

3 Contag, C.H.; Ross, B.D. *JMRI* **2002**,*16*,378

4 Hoffman, R.M. *Biotechniques* **2001**,*30*,1016

5 Ichikawa, T.; Hogemann, D.; Saeki, Y.; Tyminski, E.; Terada, K.; Weissleder, R.; Chiocca, E.A.; Basilion, J.P. *Neoplasia (New York)* **2002**,*6*,523

6 Stegman, L.D.; Rehemtulla, A.; Beattie, B.; Kievit, E.; Lawrence, T.S.; Blasberg, R.G.; Tjuvajev, J.G.; Ross, B.D. *PNAS (USA)* **1999**,*96*,9821

7 Jacob, F.; Monod, J. *J. Mol. Biol.* **1961**,*3*,318

8 Pocsi, I.; Taylor, S.A.; Richardson, A.C.; Smith, B.V.; Price, R.G. *Biochim. Biophys. Acta* **1993**,*1163*,54

9 Heuermann, K.; Cosgrove, J. *Biotechniques* **2001**,*30*,1142

10 Tung, C.H.; Zeng, Q.; Shah, K.; Kim, D.E.; Schellingerhout, D.; Weissleder, R. *Cancer Res.* **2004**,*64*,1579

11 Louie, A.Y.; Huber, M.M.; Ahrens, E.T.; Rothbacher, U.; Moats, R.; Jacobs, R.E.; Fraser, S.E.; Meade, T.J. *Nature Biotechnol.* **2000**,*18*,321

12 Cui, W.; Otten, P.; Li, Y.; Koeneman, K.; Yu, J.; Mason, R.P. *Magn. Reson. Med.* **2004**,*51*,616

13 Yu, J.; Ma, Z.; Li, Y.; Koeneman, K.S.; Liu, L.; Mason, R.P. *Med. Chem* **2005**, in the press

14 Yu, J.; Otten, P.; Ma, Z.; Cui, W.; Liu, L.; Mason, R.P. *Bioconj. Chem.* **2004**,*15*,1334

15 Yu, J.; Kodibagkar, V.; Cui, W.; Mason, R.P. *Curr. Med. Chem.* **2005**,*12*,818

16 Sinnott, M.L. *Chem. Rev* **1990**,***90***,1171

17 Guder, H.J.; Herrmann, R.Z.; Zdunek, D., in 'Preparation of nitrophenyl β-D-galactopyranosides as β-galactosidase substrates for cloned enzyme donor immunoassay (CEDIA)', Germany, 1992.

18 Yoon, S.; Kim, H.G.; Chun, K.H.; Shin, J.E.N. *Bull. Korean Chem. Soc.* **1996**,*17*,599

19 McCarter, J.D.; Adam, M.J.; G., W.S. *Biochem. J.* **1992**,***286***,721

20 Mosmann, T. *Immunol. Methods* **1983**,***65***,55